

Abstracts

53. Jahrestagung der Deutschen Gesellschaft für Neuroradiologie e.V.

3.–6. Oktober 2018
Kap Europa, Frankfurt a.M.

Kongresspräsident
Prof. Dr. Martin Wiesmann
(Aachen)

Dieses Supplement wurde von der Deutschen Gesellschaft für Neuroradiologie finanziert.

Inhaltsverzeichnis

Abstracts	S##
Autorenverzeichnis	S##

Interventional Neuroradiology: Thrombectomy Studies

129

Peripheral emboli after thrombectomy commonly detectable in high resolution DWI

Michael Schönfeld^{*1}, Gabriel Brooks¹, Uta Hanning², Andreas Frölich³, Maxim Bester¹, Caspar Brekenfeld⁴, Jan-Hendrik Buhk¹, Jens Fiehler⁵

¹Klinik und Poliklinik für Neuroradiologische Diagnostik und Intervention, Universitätsklinikum Hamburg-Eppendorf, Hamburg, Deutschland

²Klinik und Poliklinik für Neuroradiologische Diagnostik und Intervention, Universitätsklinikum Hamburg-Eppendorf, Institut für Klinische Radiologie, Uniklinikum Münster, Hamburg, Deutschland

³Universitätsklinikum Hamburg-Eppendorf, Klinik und Poliklinik für Neuroradiologische Diagnostik, Klinik und Poliklinik für Neuroradiologische Diagnostik und Intervention, Hamburg, Deutschland

⁴Universitätsklinikum Hamburg-Eppendorf, Hamburg, Deutschland

⁵Diagnostikzentrum Univ.-Klinikum Hamburg-Eppendorf, Klinik und Poliklinik für Neuroradiologische Diagnostik und Intervention, Hamburg, Deutschland

Purpose: To analyse the incidence of peripheral emboli after thrombectomy.

Methods: Patients endovascularly treated for a large vessel occlusion received a 1.5T MRI including diffusion-weighted imaging (DWI) in normal and high resolution as well as susceptibility-weighted imaging (SWI) on the day following the intervention. Punctuate DWI lesions distant to a continuous core DWI lesion were counted as peripheral emboli. Peripheral emboli were related to findings on SWI and post-thrombectomy DSA.

Results: In 18 consecutive patients a total of 150 peripheral emboli were seen on DWI. 82 peripheral emboli (54.6%) were exclusively detected in high resolution DWI. 64 (42.6%) of these lesions were found in the 10 patients where thrombectomy was classified as TICI3. 2 patients did not show any peripheral emboli. 10 (6.7%) peripheral emboli in 5 patients were classified as emboli into new territory. Only 11 (7.3%) peripheral emboli were accompanied with faint SWI lesions and 55 (36.7%) peripheral emboli were seen in the 10 patients that did not show any SWI lesions associated with DWI lesions.

Conclusion: Using high resolution DWI peripheral emboli in the territory affected by a large vessel occlusion are commonly detected even after supposedly complete recanalization. These peripheral emboli are more common than emboli into new territory.

134

Thrombus enhancement is a predictor of clinical outcome in acute ischemic stroke after mechanical thrombectomy

Jonathan Kottlors^{*1}, Jan Borggrefe²

¹Universität zu Köln, Köln

²Universität zu Köln, Institut für Diagnostische und Interventionelle Radiologie, Köln, Deutschland

Purpose: Ex-vivo computed tomography (CT) studies of thrombi showed that contrast enhancement (CE) is determined by fibrin-content while unenhanced density is associated with red blood cells. Pres-

ent study investigates patient outcome in association with thrombus density measures in native and contrast-enhanced CT of ischemic stroke patients.

Methods: This study includes 137 patients with M1 occlusions treated by mechanical thrombectomy (MT). Clinical outcome was determined with modified Rankin Scale (mRS) at 90 days. Differentiation of complete and incomplete large vessel occlusion (CLVO/ILVO) was based on CT and angiography. Blinded readers classified thrombi based on native (non-enhanced) CT (NECT) as a) hypo-, b) iso-, and c) hyperdense and in contrast-enhanced CT (CECT) angio measurements as d) not-enhancing, e) intermediate and f) enhancing. Thresholds in both cases were selected in a way that all values within one standard deviation around the mean form the isodense/intermediate group. CE per se was correlated with the outcome. Tests were performed with Spearman's Rho, Pearson Chi2-test, Mann-Whitney U and one-factor ANOVA including Bonferroni correction for multiple tests.

Results: ILVO patients differed significantly from patients with CLVO in mRS at admission (and after 90 days ($p < .05$)) and thus were excluded. Classification of CLVOs according to CECT allowed an outcome prediction between the intermediate and enhancing group, and between enhancing and non-enhancing group ($p < .05$); correlation of .291 between CE and higher mRS after 90 days ($p < .005$).

Conclusion: CE of thrombi is an independent predictor of poor clinical outcome in patients undergoing MT due to acute middle cerebral artery occlusion.

136

MR versus CT for Selection of Mechanical Thrombectomy in Patients with Acute Ischemic Stroke and Anterior Circulation Large Vessel Occlusion

Stephan Meckel^{*1}, Pascal Prüllage², Lisa Forner³, Hannes Schacht², Hannah Fuhrer⁴, Lena-Alexandra Beume⁵, Karl Egger⁶, Wolf-Dirk Niesen⁷, Horst Urbach⁸

¹Klinik für Neuroradiologie, Freiburg, Deutschland

²Klinik für Neuroradiologie, Deutschland

³Klinik für Neuroradiologie, Freiburg, Deutschland

⁴Department of Neurology, University Hospital Freiburg, Freiburg, Deutschland

⁵Universitätsklinikum Freiburg, Klinik für Neurologie und Neuropsychiatrie, Klinik für Neurologie, Freiburg, Deutschland

⁶Department of Neuroradiologie, Freiburg University Medical Center, Freiburg, Deutschland

⁷Universitätsklinikum Freiburg, Klinik für Neurologie, Klinik für Neurologie, Freiburg, Deutschland

⁸Universitätsklinikum Freiburg, Klinik für Neuroradiologie, Freiburg, Deutschland

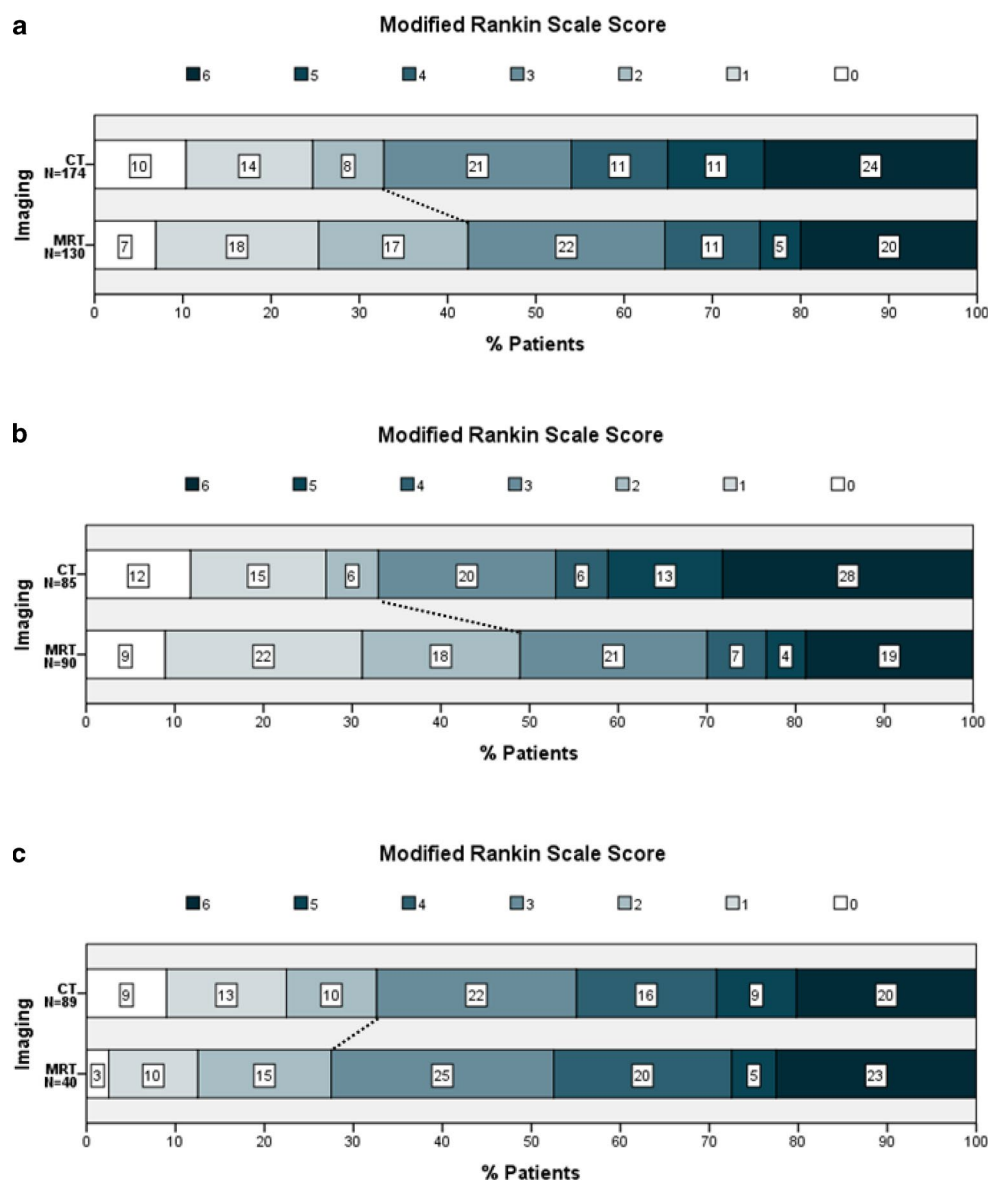
Purpose: There is an ongoing debate whether CT or MRI is the better imaging technique for patients with large vessel occlusion (LVO) stroke before mechanical thrombectomy (MT). We compared clinical outcome and workflow times between MRI and CT selection in a large LVO cohort.

Methods: All MT patients with anterior circulation LVO were selected from our prospective institutional database between 01/2014 and 06/2017. Clinical outcome at 90 days (mRS) was independently assessed. Symptom onset, NIHSS, ASPECTS, transfer mode, TICI, and workflow times were statistically compared.

Results: 304 patients were included of which 42.8% had MRI and 57.2% CT imaging. Median NIHSS was 15 in MRI and CT patients ($p=0.043$). Median ASPECTS was lower with MRI vs. CT (7 vs. 8; $p<0.001$). More MRI patients had unknown onset ($p<0.001$) and mothership transfer ($p<0.001$). Overall, TICI 2b/3 recanalization was 70.8% and 80.5% ($p=0.049$) and good clinical outcome (mRS 0–2) was 42.3% and 29.8% ($p=0.088$) in MRI and CT patients, respectively.

Die mit Sternchen (*) markierten Autoren sind die korrespondierenden Autoren.

Fig. 1 CT segmentation for quantitative image analysis. Infarct lesion was defined by CBV decrease on admission CT. **a** all patients, **b** mothership, **c** drip & ship. The infarct lesion was segmented and mirrored to obtain measurements of infarct density (Dinfarct in yellow) and contralateral normal tissue (Dnormal in blue) and further Net Water Uptake calculation as shown in the equation. (modified from Broocks et al. Investigative Radiology 2018)



In mothership patients, mRS 0–2 was 48.9% with MRI vs. 32.9% with CT ($p=0.03$) and door to angio times were minimally longer with MRI (median delay 4.5 min; $p=0.253$). In drip&ship patients, 2nd imaging after arrival did not increase favorable outcome (25.9% with 2nd MRI and 32.6% with 2nd CT vs. 31.9% without 2nd imaging; $p<0.05$), but increased door to angio times by 52.5min (MR) and 27.5min (CT).

Conclusion: In patients with mothership transfer, MRI caused only minimal delay (5 min) and marginally better outcome, the latter might relate to more patients being excluded with low DWI ASPECTS. Second CT/MRI imaging after drip&ship transfer seems not justified due to longer workflow delays without translation into a better clinical outcome.

139

Endovascular treatment in patients with large vessel occlusion and without a significant mismatch results in reduced mortality

Philip Höltner^{*1}, Manuel Schmidt², Michael F. X. Knott³, Lorenz Breuer⁴, Bernd Kallmünzer⁵, Stefan Schwab⁶, Arnd Dörfler⁷, Tobias Engelhorn³

¹Abteilung Neuroradiologie, Erlangen, D

²Universitätsklinikum Erlangen, Neuroradiologische Abteilung, Erlangen, Deutschland

³Abteilung für Neuroradiologie, Erlangen, Deutschland

⁴Universitätsklinikum Erlangen, Klinik für Neurologie, Schlaganfallnetzwerk Mit Telemedizin Steno, Erlangen, Deutschland

⁵Universitätsklinikum Erlangen, Klinik für Neurologie, Neurologische Klinik, Erlangen, Deutschland

⁶Universitätsklinikum Erlangen, Klinik für Neurologie, Erlangen, Deutschland

⁷Universitätsklinikum Erlangen, Abteilung für Neuroradiologie, Erlangen, Deutschland

Purpose: In patients with acute ischemic stroke (AIS) endovascular treatment (EVT) is highly effective for emergency revascularization. However, data on functional outcome is lacking for patients that show minimal mismatch between ischemic core and the penumbra.

Methods: 45 patients with AIS due to LVO of the anterior circulation were retrospectively analyzed. All patients received multimodal CT and subsequent CT perfusion (CTP). In all patients the relative mismatch between cerebral blood flow (CBF) and cerebral blood volume

(CBV) was $\leq 20\%$. 26/45 patients received EVT. Clinical outcome was obtained by using mRS at 30 and 90 days.

Results: NIHSS on admission (EVT:17(13–22);Non-EVT:21(19–22); $p=0.09$), NIHSS at discharge (EVT:14(7–38);Non-EVT:21(18–24); $p=0.29$) and the pre-mRS (EVT:1(0–2);Non-EVT:2(1–3); $p=0.056$) showed no significant difference between both groups. MRS at 30 days (EVT:4(3–5);Non-EVT:6(5–6); $p=0.004$), and mRS at 90 days (EVT:4(3–6); Non-EVT:6(6–6); $p=0.011$) after AIS occurrence was significantly lower in EVT-patients. There was no significant difference between both groups with regard to a good functional outcome at 30 (EVT:3/26;Non-EVT:1/18; $p=0.497$) and 90 days (EVT:4/23;Non-EVT:1/16; $p=0.306$). The mortality was significantly lower in patients undergoing EVT at 30-day follow-up (EVT: 6/26;Non-EVT:13/18; $p<0.001$) and at 90-day follow-up (EVT:8/23;Non-EVT:13/16; $p<0.001$).

Conclusion: AIS patients without a significant mismatch in CTP imaging seem to benefit from EVT in terms of reduced mortality at 30 and 90 days after AIS. However, the patients do not appear with improved functional outcome at 30 and 90 days, when compared to patients undergoing standard care.

149

Flying Interventionalists—A trial analyzing a new concept in endovascular stroke treatment

Benjamin Friedrich^{*1}, Christian Maegerlein², Frank Kraus³, Silke Wunderlich⁴, Claus Zimmer⁵, Wolfgang Gerdsmeyer-Petz⁶, Thomas Lyn Witton-Davies⁷, Christoph Degenhart⁸, Sabine Platen⁹, Roman Haberl¹⁰, Gordian Hubert¹¹

¹Klinikum Rechts der Isar der Technischen Universität, Abteilung für Diagnostische und Interventionelle Neuroradiologie, München, Deutschland

²Klinikum Rechts der Isar der Technischen Universität, Abteilung für Diagnostische und Interventionelle Neuroradiologie, München, D

³Städt. Klinikum München GmbH—Klinikum Harlaching, Klinik für Neurologie, München, Deutschland

⁴Klinikum Rechts der Isar, Technische Universität München, Neurologie, München, Deutschland

⁵Klinikum Rechts der Isar der TUM, Technische Universität München, Abteilung für Diagnostische und Interventionelle Neuroradiologie, München, Deutschland

⁶Klinikum Harlaching, Institut für Diagnostische und Interventionelle Radiologie, Neuroradiologie und Nuklearmedizin, München, Deutschland

⁷Klinikum Harlaching, Institut für Diagnostische und Interventionelle Radiologie, Neuroradiologie und Nuklearmedizin, Unteraching, Deutschland

⁸Institut für Diagnostische und Interventionelle Radiologie, Neuroradiologie und Nuklearmedizin, München, Deutschland

⁹Bezirksklinikum Regensburg, Regensburg, Deutschland

¹⁰Klinikum Harlaching, Klinik für Neurologie und Neurologische Intensivmedizin

¹¹Städtisches Klinikum München Klinikum Harlaching, Neurologie, Neurologie, München, Deutschland

Purpose: Endovascular stroke treatment is an extremely time-critical form of therapy that requires a high degree of expertise. Patients in rural areas often suffer from a lack of care for this treatment. For this reason, patients with a proven large vessel occlusion are usually transferred from a primary stroke center to a comprehensive stroke center to be treated endovascularly. Depending on the geographical and logistical conditions, this transfer process can take a very long time and thus have a negative effect on the clinical outcome of stroke patients.

Methods: A new concept in stroke care is the “Flying Interventionalist”. A team of physicians and assistants are flown by helicopter to the primary stroke center to perform the endovascular procedure on site.

We hope that this concept will significantly shorten treatment times and thus directly benefit the patients concerned. This form of treatment is carried out in a trial over 26 randomized weeks of the year within a telemedical network in Southeast Bavaria (TEMPiS) and compares process times, complication rate and clinical outcome to the patients who are transferred secondarily.

Results: We would like to present the study concept and the first experiences of the project running since 01.02.2018.

Conclusion: Already in the first patients who were approached by helicopter, there was a dramatic improvement in process times during the flight weeks with currently no increased complication rate.

178

Computer aided diagnosis for ASPECT rating: Initial experiences with the Frontier ASPECT Score software

Juliane Goebel¹, Elena Stenzel², Isabel Wanke³, Martin Köhrmann⁴, Christoph Kleinschnitz⁵, Michael Forsting⁶, Christoph Mönninghoff⁷, Alexander Radbruch^{*7}

¹Universitätsklinikum Essen, Essen, Deutschland

²Institute for Diagnostic and Interventional Radiology and Neuroradiology, University Hospital Essen, Essen, Deutschland

³Institut für Diagnostische und Interventionelle Radiologie und Neuroradiologie, Klinikum Hirslanden Zürich, Zürich, Switzerland

⁴Universitätsklinikum Essen, Klinik für Neurologie, Essen, Deutschland

⁵University Hospital Essen, Neurologie, Essen, Deutschland

⁶Institut für Diagnostische und Interventionelle Radiologie und Neuroradiologie, Essen, Deutschland

⁷Institute for Diagnostic and Interventional Radiology and Neuroradiology, Essen, Deutschland

Purpose: Early ischemic change detection computed tomography (CT) in stroke patients is a field where the application of artificial intelligence appears promising. Aim of this study was to compare the new post processing tool Frontier against a senior radiologists reading.

Methods: Retrospectively, pre-interventional CTs of 100 patients, who underwent endovascular revascularization for middle cerebral artery occlusion, were re-analyzed with respect to ASPECTS by a senior radiologist and by use of Frontier. In addition to a fully automatic Frontier reading (Frontier_1), Frontier readings adjusted for old cerebral defects (Frontier_2a), the affected side (known by CT angiography, Frontier_2b), and both (Frontier_3) were assessed. Statistical analysis was performed by intraclass correlation and Kappa statistics.

Results: Median ASPECTS was 9.5 for Frontier_1, otherwise 10. All Frontier variants significantly correlated with the radiologists reading with highest correlation for Frontier_2a ($r=0.45$; $r=0.64$; $r=0.53$; $r=0.55$; always $p<0.001$). Inter-rater agreement for each ASPECT region between Frontier_3 and the senior radiologist was fair (kappa, 0.39; $p<0.001$).

Conclusion: We found good agreement between the post processing tool Frontier and a senior radiologist in ASPECT evaluation in early stroke CT. Notably, Frontier's performance substantially improves by simple manual adjustments. It can help un-experienced readers and may be helpful even for senior radiologists.

179

Automated ASPECT rating: Comparison between the Frontier ASPECT Score software and the Brainomix software

Juliane Goebel¹, Elena Stenzel², Stefan Zülw³, Isabel Wanke⁴, Martin Köhrmann⁵, Christoph Kleinschnitz⁶, Michael Forsting⁷, Christoph Mönninghoff⁸, Alexander Radbruch^{*8}

¹Universitätsklinikum Essen, Essen, Deutschland

²Institute for Diagnostic and Interventional Radiology and Neuroradiology, University Hospital Essen, Essen, Deutschland

³Neuroradiologie, Essen, Deutschland

⁴Institut für Diagnostische und Interventionelle Radiologie und Neuroradiologie, Klinikum Hirslanden Zürich, Zürich, Switzerland

⁵Universitätsklinikum Essen, Klinik für Neurologie, Essen, Deutschland

⁶University Hospital Essen, Neurologie, Essen, Deutschland

⁷Institut für Diagnostische und Interventionelle Radiologie und Neuroradiologie, Essen, Deutschland

⁸Institute for Diagnostic and Interventional Radiology and Neuroradiology, Essen, Deutschland

Purpose: Computer aided diagnosis (CAD) appears promising in early ischemic change detection computed tomography (CT). This study aimed to compare the real life performance of two new CAD systems (Frontier and Brainomix) with two senior radiologist's readings.

Methods: Retrospectively, CTs of 150 patients suspected for acute middle cerebral artery ischemia, were analyzed with respect to ASPECTS separately by two senior radiologists and by use of Frontier and Brainomix. Beside the automatic Frontier reading (Frontier_1), a Frontier reading adjusted for the affected brain side (known by CT angiography or clinical presentation, Frontier_2) was assessed. Statistical analysis was performed by intraclass correlation and Kappa statistics.

Results: The ASPECTS readings of Brainomix and both radiologists correlated highly ($r=0.714$; $r=0.841$; $r=0.828$; always $p<0.001$), whereas Frontier_1 and Frontier_2 correlated only moderately with the radiologists and Brainomix ($r=0.471$ – 0.677 ; always $p<0.001$). Interrater agreement was fair between both radiologists ($r=0.400$), between one radiologist and Brainomix ($r=0.372$), and between the other radiologist and Frontier_2 ($r=0.212$; always $p<0.001$), otherwise interrater agreement was slight.

Conclusion: We found high agreement between both radiologists and Brainomix, but only moderate agreement to Frontier. Therefore, with respect to the current software versions, we recommend the usage of Brainomix as CAD system in acute stroke evaluation.

181

Software-based automatic ASPECTS calculation is superior in comparison to human readers.

Johanna Fischer¹, Benjamin Friedrich², Sebastian Mönch³, Maria Berndt⁴, Silke Wunderlich⁵, Christian Seifert¹, Manuel Lehm⁶, Tobias Boeckh-Behrens⁷, Claus Zimmer⁸, Christian Maegerlein⁹

¹Klinikum Rechts der Isar

²Klinikum Rechts der Isar der Technischen Universität, Abteilung für Diagnostische und Interventionelle Neuroradiologie, München, Deutschland

³Abteilung für Diagnostische und Interventionelle Neuroradiologie, Klinikum Rechts der Isar, München, Deutschland

⁴Klinikum Rechts der Isar, Technische Universität München, Abteilung für Diagnostische und Interventionelle Neuroradiologie, München, Deutschland

⁵Klinikum Rechts der Isar, Technische Universität München, Neurologie, München, Deutschland

⁶Abteilung für Diagnostische und Interventionelle Neuroradiologie, TU München, München, Deutschland

⁷Neuroradiologie, Technische Universität München, Abteilung für Diagnostische und Interventionelle Neuroradiologie, München, Deutschland

⁸Klinikum Rechts der Isar der TUM, Technische Universität München, Abteilung für Diagnostische und Interventionelle Neuroradiologie, München, Deutschland

⁹Klinikum Rechts der Isar der Technischen Universität, Abteilung für Diagnostische und Interventionelle Neuroradiologie, München, D

Purpose: The Alberta Stroke Program Early CT Score (ASPECTS) is the most widely-used measure for quantifying early signs of infarction in CT. Though interpretation is challenging and inter-rater agreement for ASPECTS is modest. By now, automatic software tools for ASPECTS analysis are available. One of these, RAPID ASPECTS (RA), is evaluated in this study.

Methods: A gold standard ASPECTS was defined by consensus reading by two board certified neuroradiologists on the basis of all available imaging data (CT, DSA, and MRI). After 6 weeks, the ASPECTS was again analyzed by the two readers unaware of follow-up imaging. ASPECTS was also automatically analyzed using RA.

Results: Human readers showed only fair agreement with the gold standard ($\kappa_1=0.574$ and $\kappa_2=0.556$). RA showed significantly better agreement ($\kappa=0.896$). If <1 h passed between symptom onset and imaging, both human readers and the software showed only minimal agreement (Reader 1 & 2: $\kappa_1=0.187$ & $\kappa_2=0.124$; RAPID-CT: $\kappa=0.169$). RA showed substantial agreement ($\kappa=0.775$) after >1 h, which increased to an almost perfect agreement ($\kappa=0.923$) >4 h. Human readers did not achieve comparable results to the software before the 4 h time interval ($\kappa_1=0.828$ and $\kappa_2=0.757$).

Conclusion: Software-based analysis of the ASPECTS using RA is more accurate than expert readers, especially for scans obtained between 1–4 hours from symptom onset.

220

A Closer Look Behind the ASPECTS Assessment -Is the Agreement Based on Identical Subregions?

Nora Jürgensen^{*1}, Thomas Lindner¹, Olav Jansen², Friederike Austein¹

¹Klinik für Radiologie und Neuroradiologie, Universitätsklinikum Schleswig-Holstein, Kiel, Deutschland

²Direktor des Instituts für Neuroradiologie, Klinik für Radiologie und Neuroradiologie, Kiel, Deutschland

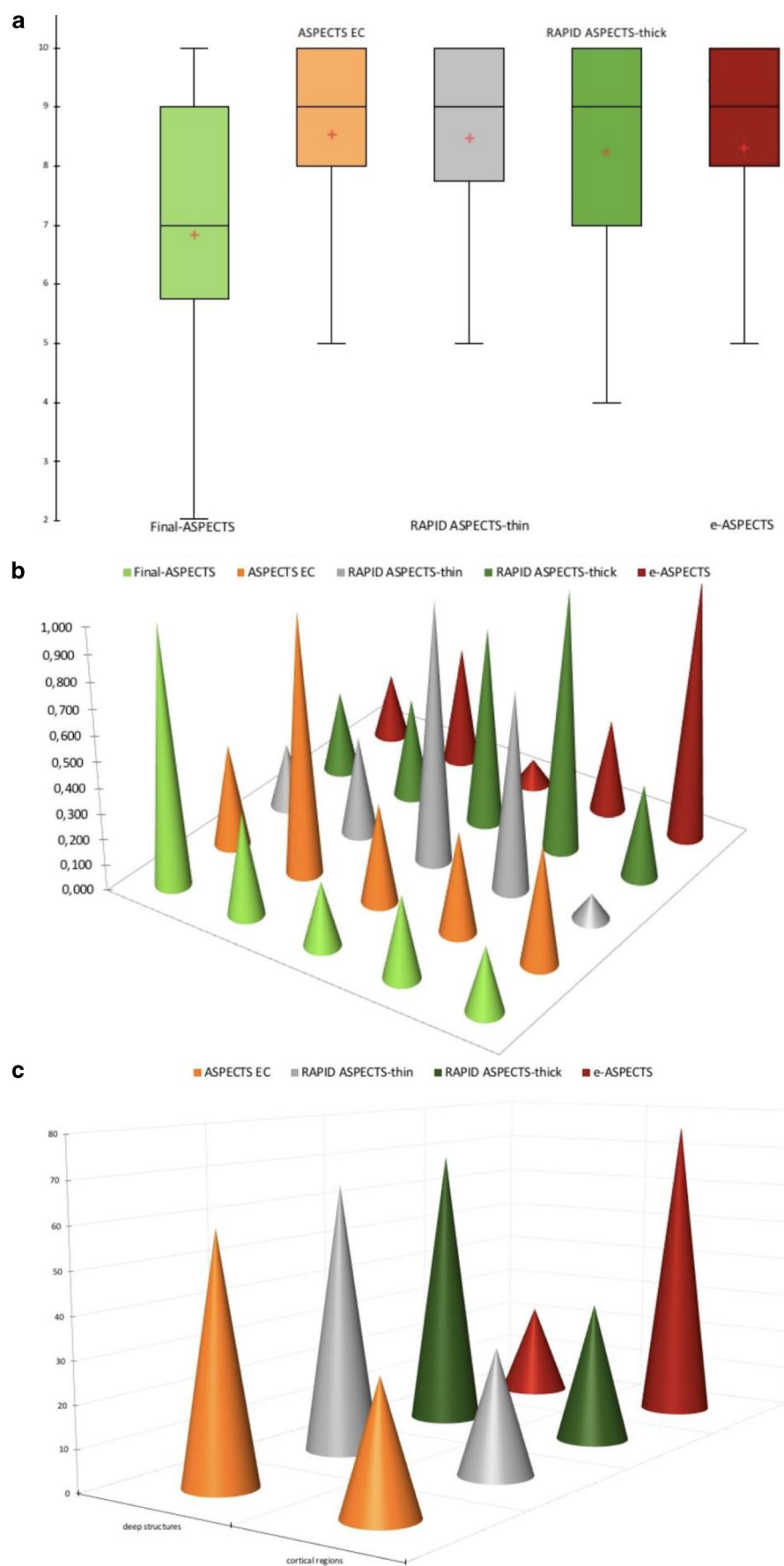
Purpose: To assess the agreement for detection of early ischemic changes between two automated ASPECTS software programs and expert consensus (EC) for both the total ASPECTS score and region-based scores.

Methods: Patients with acute anterior circulation stroke who were initially assessed with multimodal CT imaging, then treated with endovascular therapy (EVT) and achieved complete reperfusion within 100 min from NCCT were included. Total and region-based ASPECTS were evaluated on NCCT by EC (consensus of 2 expert readers). Inter-rater agreement was assessed using ICCs and Fleiss κ statistics. Sensitivity, specificity and accuracy for region-based ASPECTS was determined for each software using EC as the gold standard. Follow-up imaging was used to assess the accuracy of both EC and the software programs.

Results: Fifty-six patients met our study criteria. Median ASPECTS were 9 (IQR EC 8–10; RAPID ASPECTS-thin and RAPID ASPECTS-thick, IQR 7–10 and e-ASPECTS, IQR 8–10). Significant differences were observed in region-based analysis. Cortical areas were more often marked as positive with e-ASPECTS than EC or RAPID ASPECTS-thin and RAPID ASPECTS-thick; and deep structures less often marked with e-ASPECTS than EC, RAPID ASPECTS-thin and RAPID ASPECTS-thick; $P<0.0001$. Using the follow-up ASPECTS score as gold standard, accuracy best for deep structures with RAPID ASPECTS and EC, $P<0.0001$.

Conclusion: Good agreement was obtained between the software packages and EC for the total ASPECTS but the two software packages differed significantly with respect to regional contribution. The highest sensitivity, specificity and accuracy for region-based scoring was achieved with EC and RAPID ASPECTS, which was superior to e-ASPECTS.

Fig. 1



Systematic evaluation of different CT angiography collateral scores for estimation of long term outcome after mechanical thrombectomy in anterior circulation acute ischemic stroke

Daniel Weiß^{*1}, Marius Kaschner², Bastian Kraus³, Christian Rubbert⁴, Rebecca May⁵, John-Ih Lee⁶, Michael Gliem⁷, Sebastian Jander⁷, Carl-Albrecht Haensch⁸, Bernd Turowski¹, Julian Caspers⁹

¹Universitätsklinikum Düsseldorf, Institut für Diagnostische und Interventionelle Radiologie, Düsseldorf, Deutschland

²Universitätsklinikum Düsseldorf, Institut für Diagnostische und Interventionelle Radiologie, Neuroradiologie, Düsseldorf, Deutschland

³Uniklinik Düsseldorf, Radiologie, Neuroradiologie, Düsseldorf, Deutschland

⁴Universitätsklinikum Düsseldorf, Institut für Diagnostische und Interventionelle Radiologie, Düsseldorf, Deutschland

⁵Institut F. Diagnostische und Interventionelle Radiologie
Universitätsklinik Düsseldorf, Institut für Diagnostische und Interventionelle Radiologie, Dormagen, Deutschland

⁶Heinrich-Heine Universität, Universitätsklinikum Düsseldorf, Klinik für Neurologie, Düsseldorf, Deutschland

⁷Universitätsklinikum Düsseldorf, Klinik für Neurologie, Deutschland

⁸Kliniken Maria Hilf Mönchengladbach, Klinik für Neurologie, Deutschland

⁹Universitätsklinikum Düsseldorf, Institut für Diagnostische und Interventionelle Radiologie, Institute of Neuroscience and Medicine (INM-1), Research Centre Jülich, Düsseldorf, Deutschland

Purpose: Collateralization is a major determinant of functional outcome in acute ischemic stroke. We evaluate different CT angiography (CT-A) based collateral scores (CS) regarding their interrater reliability and predictive value for functional outcome after mechanical thrombectomy (MT).

Methods: 84 patients treated with endovascular MT in ischemic stroke from anterior circulation major vessel occlusion were prospectively en-

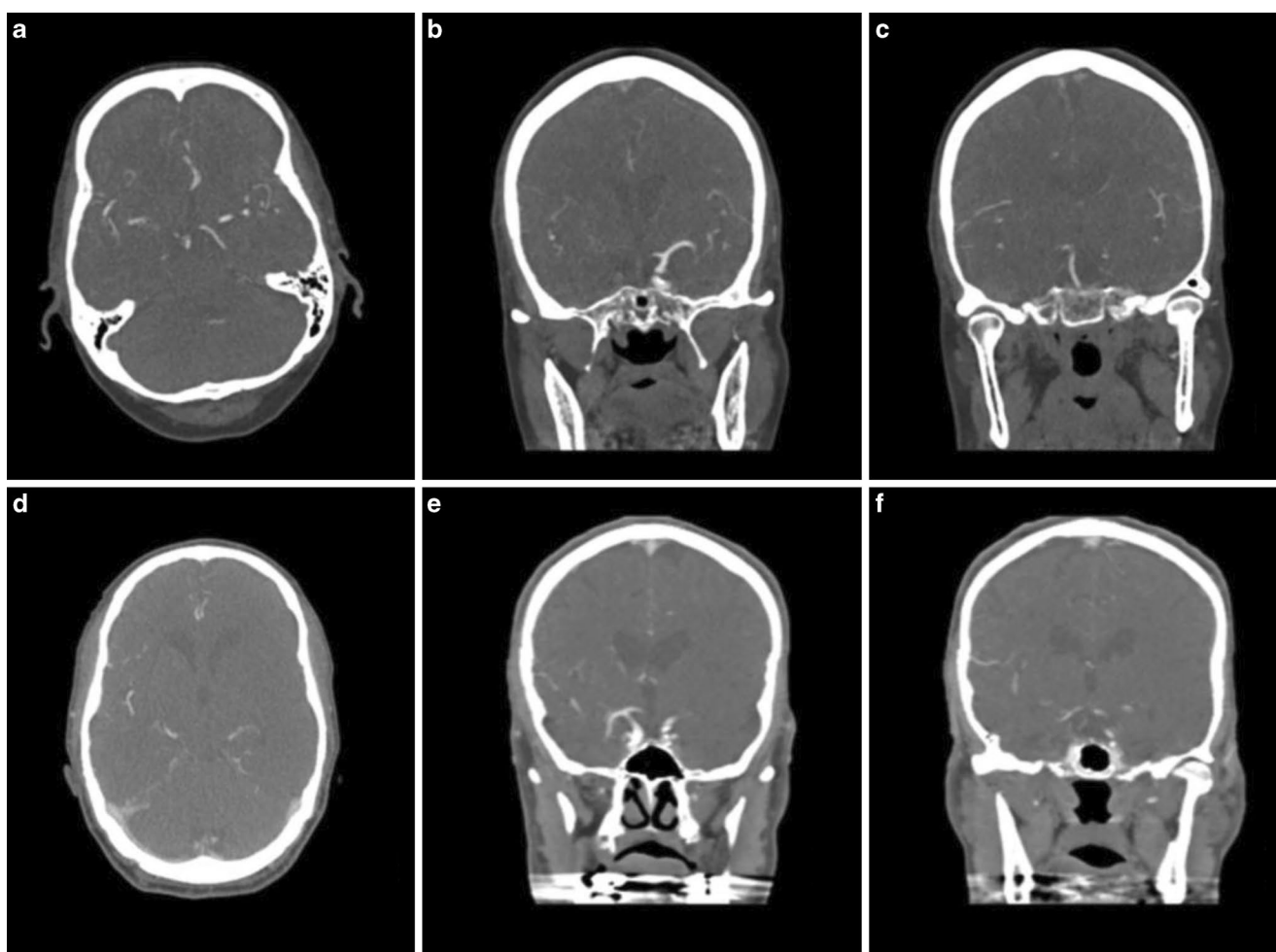


Fig. 1 CT-A scan and survey of collateral scores. **a–c** CT-A scan of a patient with occlusion of right internal carotid artery (ICA), **d–f** CT-A scan of a patient with occlusion of left middle cerebral artery (M1); **a, d** 2.25 mm axial maximum intensity projection; **b, c, e, f** 1 mm coronal maximum intensity projection. **a–c** mTan Score was 2 (more than 50% of affected MCA territory opacified in comparison to non-affected MCA territory), Miteff Score was 3 (main vessel branches and collaterals are reconstituted distal to the Sylvian fissure), Moas Score was 3 (MCA territory of affected and non-affected hemisphere are opacified similarly), Opercular Index Score Ratio was 1 (favorable OISr). **d–f** mTan Score was 1 (less than 50% of affected MCA territory opacified in comparison to non-affected MCA territory), Miteff Score was 1 (vessels and collaterals after occlusion are not reconstituted up to the Sylvian fissure), Maas Score was 1 (there is no vessel opacification in affected MCA territory), Opercular Index Score Ratio was >2 (poor OISr)

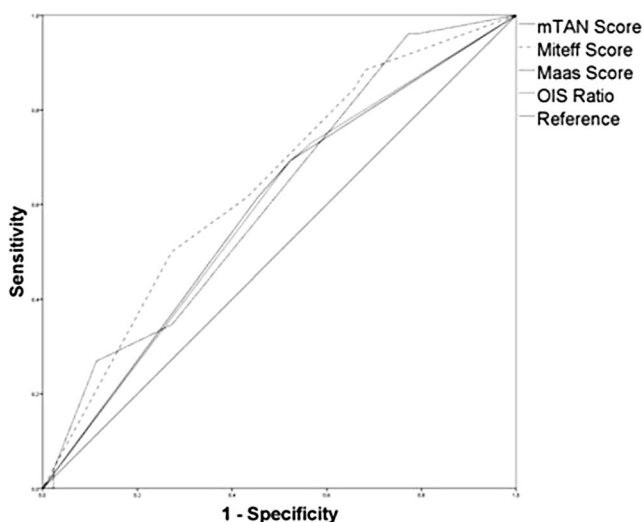


Fig. 2 Receiver operating characteristic curves analysis. mTan Score, Miteff Score, Maas Score and Opercular Index Score ration* to estimate long term functional outcome. *For illustration, reciprocal was used

rolled. Modified Tan (mTan), Miteff, Maas, and Opercular Index ratio (OISr) scores were assessed by two readers from CT-A and weighted kappa was calculated across readers. For each collateral score, Spearman correlations with three months modified Rankin Scale (mRS), Mann-Whitney U tests between patients with favorable (mRS \leq 2) and poor outcome, and ROC analyses for prediction of dichotomized mRS were performed.

Results: Very good inter-rater reliability was found for mTan ($k=0.86$), Miteff ($k=0.81$) and OISr ($k=0.91$) and good reliability for Maas ($k=0.77$). Significant group differences between patients with favorable and poor outcome were found for Maas ($p=0.03$), Miteff ($p=0.01$) and OISr ($p=0.05$), but not for mTan. ROC analysis showed AUCs of 0.59 for mTan, 0.64 for Miteff, 0.61 for Maas and 0.60 for OISr. There were no significant correlations with mRS for any CS.

Conclusion: All four evaluated CS can be reliably assessed across readers. Miteff, Maas and OISr scores seem to be more valuable for the prediction of functional outcome than mTan, whereby Miteff entails best predictions.

230

Carotid Artery Stenosis Contralateral to Cerebral Large Vessel Occlusion: a Predictor of Poor Clinical Outcome

Volker Maus^{*1}, Nuran Abdullayev², Henrik Sack³, Jan Borggrefe⁴, Anastasios Mpotsaris⁵, Daniel Behme⁶

¹University Hospital of Göttingen, Institute for Neuroradiology, Göttingen, Deutschland

²Inst. F. Diagn. U. Interv. Radiologie, Inst. F. Diagn. U. Interv. Radiologie, Köln, Deutschland

³Universitätsmedizin Göttingen

⁴Universität zu Köln, Institut für Diagnostische und Interventionelle Radiologie, Köln, Deutschland

⁵Klinik für Diagnostische und Interventionelle Neuroradiologie, Aachen, Deutschland

⁶Institut für Diagnostische und Interventionelle Neuroradiologie, Göttingen, Deutschland

Purpose: Clinical outcome in patients undergoing mechanical thrombectomy (MT) due to intracranial large vessel occlusion (LVO) in the anterior circulation is influenced by several factors. The impact

of a concomitant extracranial carotid artery stenosis (CCAS) contralateral to the intracranial lesion remains unclear.

Methods: Retrospective analysis of 392 consecutive patients treated with MT due to intracranial LVO in the anterior circulation in two comprehensive stroke centers between 2014 and 2017. Clinical (including demographics and NIHSS), imaging (including angiographic evaluation of CCAS via NASCET criteria), and procedural data were evaluated. Primary endpoint was an unfavorable clinical outcome defined as modified Rankin Scale 3–6 at 90 days.

Results: In 27/392 patients (7%) pre-interventional imaging exhibited a CCAS (>50%) contralateral to the intracranial lesion compared to 365 patients without relevant stenosis. Median baseline NIHSS, procedural timings, and reperfusion success did not differ between groups. Median volume of the final infarct core was larger in CCAS patients (176 cm³, IQR 32–213 vs. 11 cm³, 1–65; $p<0.001$). At 90 days, unfavorable outcome was documented in 25/27 CCAS patients (93%) vs. 211/326 (65%; $p=0.003$) with a mortality of 63% vs. 19% ($p=0.001$), respectively. Presence of CCAS was associated with an unfavorable outcome at 90 days independent of age and baseline NIHSS in multivariate logistic regression (OR 2.2, CI 1.1–4.7; $p<0.05$).

Conclusion: For patients undergoing MT due to intracranial vessel occlusion in the anterior circulation, the presence of a contralateral CCAS >50% is a predictor of unfavorable clinical outcome at 90 days.

231

Does the Presence of Posterior Communicating Arteries Influence Clinical Outcome in Basilar Artery Occlusion?

Volker Maus^{*1}, Alev Kalkan², Christoph Kabbasch³, Nuran Abdullayev⁴, Henning Stetefeld², Utako Barnikol², Thomas Liebig⁵, Christian Dohmen⁶, Gereon R. Fink⁷, Jan Borggrefe⁸, Anastasios Mpotsaris⁹

¹University Hospital of Göttingen, Institute for Neuroradiology, Göttingen, Deutschland

²Universitätsklinik Köln

³Uniklinik Köln, Abteilung für Radiologie und Neuroradiologie, Institut für Diagnostische und Interventionelle Radiologie, Köln, Deutschland

⁴Inst. F. Diagn. U. Interv. Radiologie, Inst. F. Diagn. U. Interv. Radiologie, Köln, Deutschland

⁵Ludwig-Maximilians-Universität München, University Hospital, Institute of Neuroradiology, München, Deutschland

⁶Lvr Klinik Bonn, Neurologie, Köln, Deutschland

⁷Universitätsklinikum Köln, Klinik und Poliklinik für Neurologie, Forschungszentrum Jülich, Institut für Neurowissenschaften und Medizin (Inm³), Köln/Jülich, Deutschland

⁸Universität zu Köln, Institut für Diagnostische und Interventionelle Radiologie, Köln, Deutschland

⁹Klinik für Diagnostische und Interventionelle Neuroradiologie, Aachen, Deutschland

Purpose: Mechanical thrombectomy (MT) in basilar artery occlusion (BAO) is a subject of debate. We investigated clinical outcome of MT in BAO and predictors of a favorable outcome.

Methods: 104 MTs in BAO (carried out between 2010 and 2016) were analyzed. Favorable outcome (modified Rankin Scale (mRS) \leq 2) at 90 days was the primary endpoint; influence of following variables on outcome was investigated: number of detectable posterior communicating arteries (PcoAs), patency of basilar tip, completeness of BAO, and posterior circulation Alberta Stroke Program Early CT Score (PC-ASPECTS). Secondary endpoints were technical periprocedural parameters including symptomatic intracranial hemorrhage (sICH).

Results: Favorable clinical outcome at 90 days was 25% and mortality was 43%. Rate of successful reperfusion (modified Thrombolysis In Cerebral Infarction (mTICI) \geq 2b) was 82%. Presence of bi-

lateral PcoAs (AUC: 0.81, $p < 0.0001$), lower National Institute of Health Stroke Scale (NIHSS) on admission (AUC: 0.74, $p < 0.01$), PC-ASPECTS ≥ 9 (AUC: 0.72, $p < 0.01$), incomplete BAO (AUC: 0.66, $p < 0.001$), and basilar tip patency (AUC: 0.66, $p < 0.01$) were associated with favorable outcome. Stepwise logistic regression analysis revealed that the strongest predictors of favorable outcome at 90 days were bilateral PcoAs, low NIHSS on admission, and incomplete BAO (AUC: 0.923, $p < 0.0001$).

Conclusion: MT in BAO is safe with high rates of successful reperfusion. Aside from baseline NIHSS and incomplete vessel occlusion, both known predictors of favorable outcome in anterior circulation events, we found collateral flow based on the presence or absence of PcoAs had a decisive prognostic impact.

249

Predictors of outcome after mechanical thrombectomy in M2 occlusions: A single-center experience with 156 patients

Fatih Seker^{*1}, Johannes Pfaff², Ulf Neuberger², Simon Schieber³, Simon Nagel², Peter Ringleb², Martin Bendszus², Markus Möhlenbruch²

¹Universitätsklinikum Heidelberg, Neuroradiologie, Heidelberg, Deutschland

²Universitätsklinik Heidelberg

³Universitätsklinik Heidelberg

Purpose: Several studies have shown that mechanical thrombectomy (MT) is safe and effective in M2 occlusions. Due to the variability of M2 occlusions, this retrospective study aims at identifying predictors of clinical outcome after MT in M2 occlusions.

Methods: Between 2009 and 2017, patients treated with MT due to M2 occlusion were selected. Univariate and multivariate analyses were performed to identify predictors of good outcome defined as modified Rankin Scale (mRS) at 90 days 0–2 or return to pre-morbid elevated mRS.

Results: 156 patients with M2 occlusion were included of which 51.9% achieved good outcome. Independent predictors of good outcome were baseline ASPECTS (OR 1.46, 95% CI 1.06–2.05, $P = 0.025$), time from groin puncture to TICI (OR 0.99, 95% CI 0.98–1.0, $P = 0.012$) and TICI 2b–3 (OR 4.37, 95% CI 1.32–17.56, $P = 0.023$). Superior division occlusion was an independent predictor of poor outcome (OR 2.43, 95% CI 1.07–5.80, $P = .038$). Dominance of the occluded vessel and side of occlusion were not predictive. Time from groin puncture to TICI, recanalization success, complication rate and postinterventional hemorrhage rate were similar in superior and inferior division occlusions.

Conclusion: Patients with superior division occlusion appear to have a lower chance of achieving good outcome, however, without a significantly increased complication rate. We, therefore, suggest treating M2 occlusions independent of the localization of the occlusion.

250

Clinical outcome after thrombectomy in stroke patients with pre-morbid modified Rankin Scale score of 3 and 4: A cohort study with 136 patients

Fatih Seker^{*1}, Johannes Pfaff², Silvia Schönerberger³, Christian Herweh⁴, Simon Nagel³, Peter Arthur Ringleb⁵, Martin Bendszus⁶, Markus Möhlenbruch⁷

¹Universitätsklinikum Heidelberg, Neuroradiologie, Heidelberg, Deutschland

²Universitätsklinikum Heidelberg, Abteilung für Neuroradiologie, Abteilung für Neuroradiologie, Heidelberg, Deutschland

³Universitätsklinikum Heidelberg, Neurologische Klinik, Neurologie, Heidelberg, Deutschland

⁴Neurologische Klinik/Abteilung für Neuroradiologie, Abteilung für Neuroradiologie, Heidelberg, Deutschland

⁵Universitätsklinikum Heidelberg, Neurologische Klinik, Sektion Vaskuläre Neurologie, Heidelberg, Deutschland

⁶University Hospital Heidelberg, Department of Neuroradiology, Heidelberg, Deutschland

⁷Universitätsklinikum Heidelberg, Abteilung für Neuroradiologie, Heidelberg, Deutschland

Purpose: Mechanical thrombectomy (MT) is regularly performed in patients with pre-morbid mRS 0–2. We aimed to analyze clinical outcome in patients with pre-morbid mRS 3 and 4, because there is currently no data on this patient group.

Methods: Between January 2009 and November 2017, all patients with pre-morbid mRS 3 or 4 undergoing MT due to anterior circulation stroke were selected. Good outcome was defined as a clinical recovery to the status before stroke onset, i.e. equal pre-morbid mRS and mRS at 90 days. Besides, mortality at discharge and at 90 days was analyzed.

Results: 136 patients were included, of which 81.6% presented with pre-morbid mRS 3 and 18.4% with pre-morbid mRS 4. In total, 21.3% achieved good outcome. Multivariate analysis identified low NIHSS (OR 0.92, 95% CI 0.85–0.99, $P = .040$), high ASPECTS (OR 1.45, 95% CI 1.02–2.16, $P = .049$) and TICI 2b–3 (OR 7.11, 95% CI 1.73–49.90, $P = .017$) as independent predictors of good outcome. Good outcome was non-significantly more frequent in patients with pre-morbid mRS 4 (24.0% vs. 20.7%, $P = .7877$). Proportion of hospital mortality and mortality at 90 days was non-significantly, but markedly higher in patients with pre-morbid mRS 4.

Conclusion: Good outcome in patients with pre-morbid mRS of 3 and 4 is less frequent compared to mRS 0–2. Nevertheless, about 20% of the patients return to their pre-morbid mRS, which may justify endovascular treatment. Most important predictor of good outcome is successful recanalization.

251

Image review on mobile devices for suspected stroke patients: Initial experiences with the mRay software solution

Alex Brehm^{*1}, Volker Maus², Eya Khadhraoui¹, Marios-Nikos Psychogios¹

¹Institut für Diagnostische und Interventionelle Neuroradiologie, Göttingen, Deutschland

²University Hospital of Göttingen, Institute for Neuroradiology, Göttingen, Deutschland

Purpose: Software solutions such as mRay® allow review of radiological images on handheld devices. We investigated if the quality is adequate for evaluating CT scans of patients with suspected stroke.

Methods: 50 patients were retrospectively selected. All patients had undergone multidetector CT (MDCT) angiography ± perfusion and presented with clinical signs of acute stroke. One experienced neuroradiologist and one resident scored the anonymized pictures separately on two handheld devices (Apple iPhone7 Plus®, MED-TAB®) equipped with the mRay Software® and on a PACS® workstation. Each case was reviewed on all three devices with a break in-between of at least 4 weeks. The scoring on the traditional workstation was compared with the two handheld devices, regarding detection of early ischemic signs, vessel occlusions, aneurysms, CBV/CBF-mismatch and intracranial hemorrhage.

Results: All three methods were of equal diagnostic value regarding the detection of intracranial hemorrhage, aneurysms and vessel occlusion. Regarding the detection of early ischemic signs there was a non-significant trend towards a better detection on the workstation and

on the MED-TAB®, however there was no difference in the detection of a CBV/CBF-mismatch. Both neuroradiologist rated the image quality sufficient on all three devices to base treatment decisions on.

Conclusion: Software solutions such as mRay® for handheld devices provide adequate diagnostic quality for the review of MDCT scans.

255

Intraoperative MR-Imaging: Ultra-early appearance of hyperacute brain ischemia on diffusion-weighted imaging

Simon Schön^{*1}, Benedikt Wiestler², Claus Zimmer²

¹Abteilung für Diagnostische und Interventionelle Neuroradiologie, Klinikum Rechts der Isar, TU München, Germany, München, D

²Abteilung für Diagnostische und Interventionelle Neuroradiologie, Klinikum Rechts der Isar, TU München, Germany

Introduction: With the establishment of intraoperative MR imaging during neurosurgical procedures it has become possible to depict pathological processes like brain infarction at an ultra-early timepoint. This raises the question about how reliable diffusion-weighted imaging can demonstrate ischemic events only a few minutes after onset.

Methods: Retrospective analysis of 5 cases who showed ischemic lesions adjacent to the resection area in the additionally control MR scan (3 Tesla) 72 h after neurosurgery.

Results: The ultra-early intraoperative DWI showed no or markedly smaller ischemic brain lesions than the following control-MRI. In 3 cases it turned out that a decrease of ADC values was apparent without demarkation of infarction on B1000-images.

Conclusion: At an ultra-early point, ischemic lesions might be missed by diffusion-weighted intraoperative MR-imaging. Thereby, ADC maps seem to predict later infarcts more sensitive.

258

Prediction of Acute Cerebrovascular Events in Vertigo Patients: a Substudy of the Observational 1000Plus Study

Kersten Villringer^{*1}, Alice Schneider², Ulrike Grittner³, Hans Tepe⁴, Ramanan Ganeshan⁵, Karl Georg Häusler⁶, Jochen B. Fiebach⁷

¹Center for Stroke Research, Berlin, Deutschland

²Charité-Universitätsmedizin, Department of Biostatistics and Clinical Epidemiology, Center for Stroke Research Berlin

³Charité—Universitätsmedizin Berlin, Biostatistics and Clinical Epidemiology, Berlin, Deutschland

⁴Charité-Universitätsmedizin, Department of Radiology

⁵Center for Stroke Research, Department of Neurology, Berlin, Deutschland

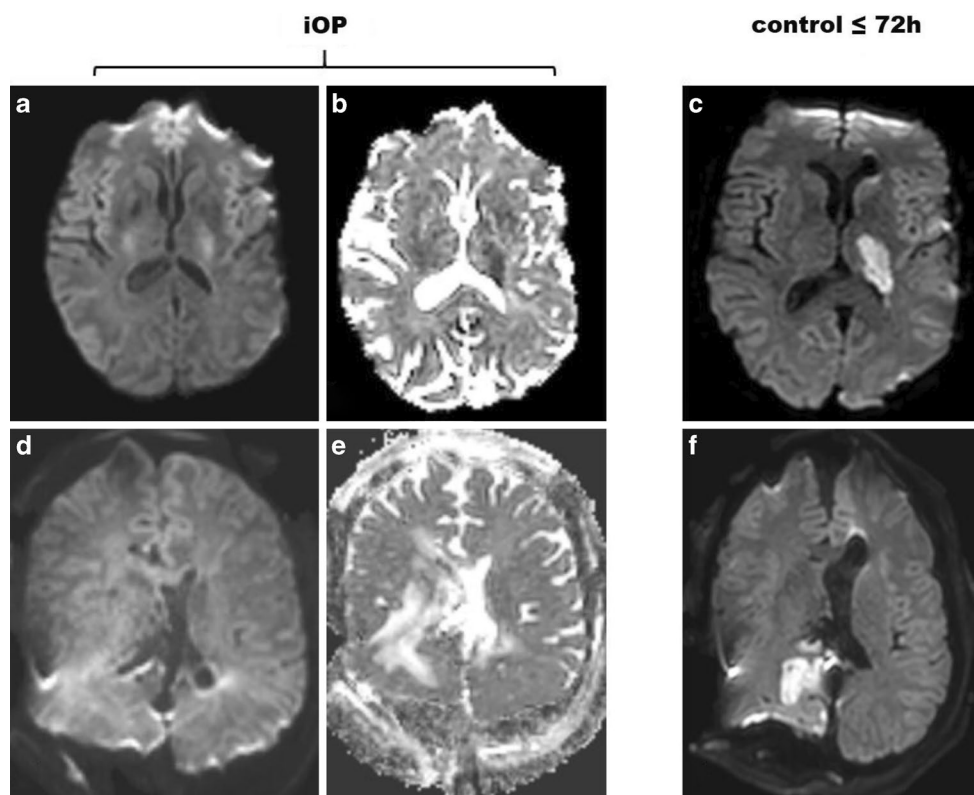
⁶Charité—Universitätsmedizin Berlin, Klinik für Neurologie, Centrum für Schlaganfallforschung Berlin, Berlin, Deutschland

⁷Charité-Universitätsmedizin, Campus Benjamin Franklin; Klinik für Neurologie, Centrum für Schlaganfallforschung, Neuroradiologie, Berlin, Deutschland

Purpose: The frequency of acute cerebrovascular events (CVE) in patients presenting with vertigo in the emergency department ranges between 0.7% and 55.3% depending on study design. In this study we not only wanted to assess the prevalence of acute CVE within 48 hours after symptom onset but also to propose a simple risk stratification approach.

Methods: Retrospective analysis of consecutive patients enrolled into the prospective observational 1000Plus study (clinicaltrials.org NCT00715533) from 2008–2013. Recursive partitioning tree analysis with 10-fold cross validation was used for prediction of CVE in patients undergoing MRI examination on a 3 T MRI scanner within 48 hours after onset of vertigo. This model is based on demographics,

Fig. 1 2 examples of perioperative ischemia. **a, b** intraoperative DWI/ADC shows only signal reduction on ADC map of the later-on thalamic infarct (**c**) but no DWI hyperintensity. **d, e** with no intraoperative signal alterations indicative of the parietooccipital infarct seen on the control MRI (**f**)



neurological symptoms, risk factors and time between symptom onset and imaging (TSI).

Results: MRI showed CVE in 185/756 patients (24.5%) with 163 (21.6%) patients having an acute ischemic stroke. Sensorimotor, cerebellar symptoms, dysarthria were more frequent in CVE patients, as well as gaze palsy and up-/down-beat nystagmus and cardiovascular risk factors. Vegetative symptoms like nausea and rotatory vertigo were more often present in non CVE patients. The prediction model reached an accuracy of 85% (sensitivity 56%, specificity 94%, PPV 75%, NPV 85%) using TSI, ABCD2 score, older age and neurological symptoms as the main parameters associated with CVE.

Conclusion: Acute CVEs were found in every fourth patient presenting with recent onset of vertigo, the vast majority caused by ischemic stroke. A combination of TSI, neurological symptoms and patients age, correctly classified 85% of vertigo patients.

261

Dynamic MRI after successful M1 thrombectomy—perfusion and permeability patterns

Matthias Mutke^{*1}, Arne Potreck², Johannes Pfaff³, Mirko Pham⁴, Markus Möhlenbruch⁵, Martin Bendszus², Sabine Heiland⁶, Angelika Hoffmann⁷

¹Abteilung für Neuroradiologie, Heidelberg

²University Hospital Heidelberg, Department of Neuroradiology, Heidelberg, Deutschland

³Universitätsklinikum Heidelberg, Abteilung für Neuroradiologie, Abteilung für Neuroradiologie, Heidelberg, Deutschland

⁴Universitätsklinikum Würzburg, Institut für Diagnostische und Interventionelle Neuroradiologie, Würzburg, Deutschland

⁵Universitätsklinikum Heidelberg, Abteilung für Neuroradiologie, Heidelberg, Deutschland

⁶Experimentelle Neuroradiologie, Experimentelle Neuroradiologie, Neuroradiologie, Heidelberg, Deutschland

⁷Universitätsklinikum Heidelberg, Abteilung für Neuroradiologie, Neuroradiologie, Heidelberg, Deutschland

Purpose: To characterize patterns of blood-brain barrier disruption and perfusion changes in patients after successful mechanical thrombectomy (MT) of M1 occlusions using multimodal MRI.

Methods: Patients underwent multimodal MR imaging within 24 hours after MT of M1 occlusions resulting in TICI 2b, 2c or 3 reperfusion. The imaging protocol included diffusion-weighted (DWI), dynamic susceptibility contrast (DSC) and dynamic contrast-enhanced (DCE) sequences. After motion correction, perfusion (CBF) and permeability maps (k_{trans} calculated by the Patlak model) were computed and then registered. Visual analysis determined infarct location and pattern. CBF pattern and k_{trans} pattern were evaluated in- and outside of the DWI lesion.

Results: 23 patients were included. All had DWI lesions, primarily inside the basal ganglia with scattered cortical lesions (15/23). 12/23 showed increased k_{trans} , 8/12 outside the DWI lesion. 10/23 showed increased CBF within the DWI lesion. Both increased k_{trans} and increased CBF was seen in 6/23. In these 6, NIHSS at admission vs discharge improved significantly (17 vs 1, median).

Conclusion: After successful mechanical thrombectomy of M1 occlusions, different imaging patterns were observed and might reflect a variable pathophysiological response: Half of the patients showed blood-brain barrier disruption. Hyperperfusion, as evidenced by increased CBF, was seen in about 40%. A combination of both was associated with excellent early neurological outcome.

277

Early Lesion Water Uptake in Acute Stroke Computed Tomography Predicts Clinical Outcome – An Observational Study

Jawed Nawabi^{*1}, Fabian Flottmann², Uta Hanning³, Helge Kniep¹, Hannes Leischner⁴, Gerhard Schoen⁵, Susanne Siemonsen⁶, Andre Kemmling⁷, Jens Fiehler⁸, Gabriel Broocks¹

¹Klinik und Poliklinik für Neuroradiologische Diagnostik und Intervention, Universitätsklinikum Hamburg-Eppendorf, Hamburg, Deutschland

²Universitätsklinikum Hamburg-Eppendorf, Klinik und Poliklinik für Neuroradiologische Diagnostik und Intervention, Klinik und Poliklinik für Neuroradiologische Diagnostik und Intervention, Hamburg, Deutschland

³Klinik und Poliklinik für Neuroradiologische Diagnostik und Intervention, Universitätsklinikum Hamburg-Eppendorf, Institut für Klinische Radiologie, Uniklinikum Münster, Hamburg, Deutschland

⁴Universitätsklinikum Hamburg-Eppendorf, Klinik und Poliklinik für Neuroradiologische Diagnostik und Intervention, Hamburg, Deutschland

⁵Universitätsklinikum Hamburg-Eppendorf, Zentrum für Experimentelle Medizin Institut für Medizinische Biometrie und Epidemiologie, Deutschland

⁶Klinik und Poliklinik für Neuroradiologische Diagnostik und Intervention, Universitätsklinikum Hamburg-Eppendorf, Hamburg, D

⁷Institut für Klinische Radiologie, Universitätsklinikum Münster, UKSH Lübeck, Hamburg, Deutschland

⁸Diagnostikzentrum Univ.-Klinikum Hamburg-Eppendorf, Klinik und Poliklinik für Neuroradiologische Diagnostik und Intervention, Hamburg, Deutschland

Purpose: Endovascular thrombectomy is of benefit to most patients with acute ischemic stroke and proximal vessel occlusion. However, clinical outcome still highly varies interindividually. Therefore, early prediction of outcome can be crucial for clinical management. Net water uptake (NWU) is a new quantitative imaging biomarker of ischemic edema, which can be measured in computed tomography (CT). Our aim was to investigate the relationship between NWU at baseline and clinical outcome compared to other established predictors.

Methods: Acute stroke patients with multimodal admission CT who received successful recanalization (TICI 2b/3) and follow-up CT were analyzed. Modified Rankin Scale (mRS) after 90 days was used to dichotomize patients into good (mRS 0–3) and poor outcome (mRS

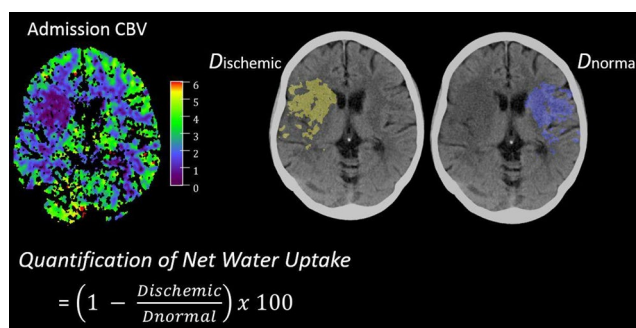


Fig. 1 CT segmentation for quantitative image analysis. Infarct lesion was defined by CBV decrease on admission CT. The infarct lesion was segmented and mirrored to obtain measurements of infarct density (Dinfarct in yellow) and contralateral normal tissue (Dnormal in blue) and further Net Water Uptake calculation as shown in the equation. (modified from Broocks et al. Investigative Radiology 2018)

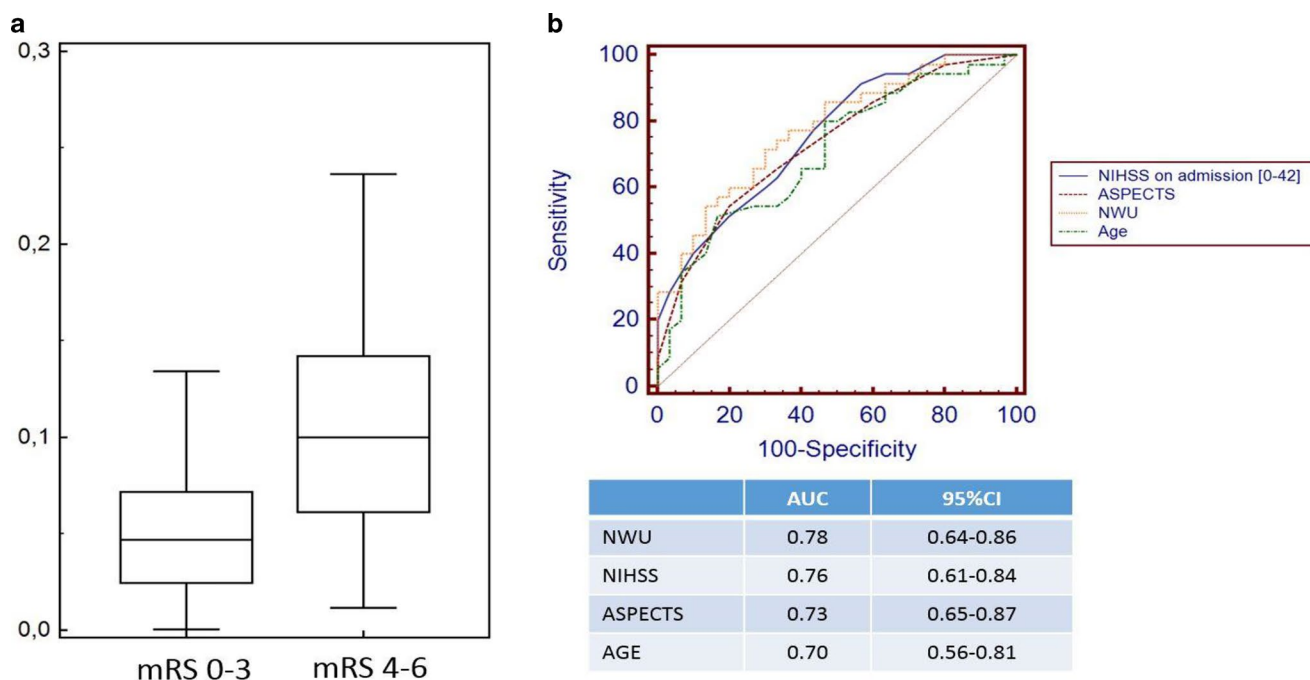


Fig. 2 **a** Comparison of Net Water Uptake (NWU) in patients with good (mRS 0-3) and poor outcome (mRS 4-6) after 90 days. **b** Receiver operating characteristics (ROC) curve comparison of NWU, ASPECTS, NIHSS on admission and age for prediction of clinical outcome. Area under the curve (AUC); 95% confidence interval (CI)

4–6). NWU was quantified by CT-Densitometry and was tested as predictor of functional outcome in univariate ROC curve and multivariate prediction analysis.

Results: A total of 72 patients were included. Admission NWU was 5.2% (± 3.8) in patients with good outcome and 10.5% (± 5.7) in patients with poor outcome ($p < 0.0001$). Based on univariate ROC curve analysis, NWU above 9% identified patients with poor outcome with good discriminative power (AUC 0.78, specificity 87%, sensitivity 55%) and was superior to NIHSS (AUC: 0.76) and ASPECTS (AUC: 0.73). In multivariate logistic regression, the probability of poor outcome was significantly associated with NWU.

Conclusion: CT-based quantitative NWU in early infarct lesions improves outcome prediction compared to other established parameters available at admission. Elevated NWU is specific for a poor outcome after ischemic stroke.

286

Mechanical Thrombectomy in very elderly patients aged 90+ with acute ischemic stroke

Lukas Meyer^{*1}, Maria Alexandrou¹, Maria Politi¹, Christian Roth¹, Andreas Kastrup², Panagiotis Papanagiotou¹

¹Diagnostische und Interventionelle Neuroradiologie, Krankenhaus Bremen-Mitte, Bremen, Deutschland

²Neurologie, Krankenhaus Bremen-Mitte, Bremen, Deutschland

Purpose: Mechanical Thrombectomy (MT) has proven itself to be a safe and effective therapy for acute ischemic stroke. Nevertheless, very elderly patients aged 90+ were excluded or underrepresented in past trials. Thus, uncertainty for this population has remained whether MT is effective or if there should be an upper age limit.

Methods: Out of our high-volume stroke center database we retrospectively analyzed patients aged 90+ years that received MT in the treatment of acute ischemic stroke. Outcome measures were the rate

of early good functional outcome (modified Rankin Scale (mRS) ≤ 2), successful recanalization (Thrombolysis In Cerebral Infarction Scale (TICI) $\geq 2b$), symptomatic intracranial hemorrhage (sICH), mortality and time of survival.

Results: Between 2013 and 2017, 29 patients aged 90+ with large arterial vessel occlusions within the anterior and posterior circulation were treated with MT at our department. Good functional outcome (mRS ≤ 2) was seen in 20.7% (6/29) at discharge. The successful recanalization rate of TICI $\geq 2b$ was 55.2% (16/29). The in-hospital mortality was 27.6% (8/29) and there were two case with sICH (6.9%) after MT. At the time of the 3-month follow-up the mortality was 69% (20/29).

Conclusion: Despite the association of higher mortality and fewer patients with good functional outcome, Mechanical Thrombectomy in very elderly patients 90+ should be considered individually as a therapy option depending especially on patient's stroke severity and pre-stroke condition.

294

Capillary Transit Time Heterogeneity predicts favorable clinical outcome and intracranial hemorrhage in acute ischemic stroke due to large vessel occlusion

Arne Potreck^{*1}, Sarah Loebel², Johannes Pfaff¹, Alexander Radbruch¹, Peter A. Ringleb², Martin Bendszus¹, Sibumundiyanapurath³

¹University Hospital Heidelberg, Department of Neuroradiology, Heidelberg, Deutschland

²University Hospital Heidelberg, Department of Neurology, Heidelberg, Deutschland

³University Hospital Heidelberg, Department of Neuroradiology" University Hospital Heidelberg, Department of Neurology, Heidelberg, Deutschland

Purpose: The DAWN and Defuse 3 trials showed that endovascular thrombectomy (ET) remains effective even in prolonged symptom-onset-to-treatment-time (OTT). However, the chance of a favorable outcome still declines over time independent from clinical-imaging mismatch. We hypothesize that microvascular changes, represented by capillary transit time heterogeneity (CTH), might explain this decline.

Methods: Using the Perfusion Graphical User Interface, we retrospectively calculated CTH-maps for 131 consecutive patients with acute ischemic stroke due to LVO of the anterior circulation who underwent MRI and subsequent ET. All patients had a relevant PWI-DWI mismatch. Multivariate logistic regressions were conducted with favorable outcome (mRS \leq 2) and the occurrence of an ICH as dependent variables and adjusted for age, successful recanalization, hypertension, diabetes, atrial fibrillation, NIHSS on admission, DWI lesion volume and OTT.

Results: A higher volume of moderately elevated CTH was a positive predictor of favorable outcome with OR 1.17 (1.03–1.33, $p=0.019$) and a negative predictor of ICH with OR 0.83 (0.73–0.96, $p=0.009$). Other predictors of favorable outcome were successful recanalization (OR 5.54 (1.8–17, $p=0.003$), NIHSS on admission (OR 0.9 (0.82–1.00, $p=0.045$), OTT (OR 0.96 (0.94–0.99, $p=0.006$)) and DWI volume (OR 0.68 (0.49–0.94, $p=0.021$)).

Conclusion: Microvascular response to hypoperfusion, represented by CTH, predicts clinical outcome and ICH in patients with acute ischemic stroke and mismatch undergoing ET.

316

Frequency and Time of Hospital Admission for Mechanical Thrombectomy in Acute Ischemic Stroke: Experiences of a High-Volume Stroke Center

Lukas Meyer^{*1}, Blanka Gemes¹, Christian Roth¹, Maria Alexandrou¹, Andreas Kastrup², Panagiotis Papanagiotou¹, Maria Politi¹

¹Diagnostische und Interventionelle Neuroradiologie, Krankenhaus Bremen-Mitte, Bremen, Deutschland

²Neurologie, Krankenhaus Bremen-Mitte, Bremen, Deutschland

Purpose: Since Mechanical Thrombectomy (MT) has been acknowledged as an emergency treatment for acute ischemic stroke (AIS) neurointerventionalists have to be on call 24/7. The purpose of this study is to analyze the daily incidence of MT and discuss the consequences for hospitals.

Methods: We retrospectively searched through our prospectively collected stroke database and selected all endovascularly treated patients within a 3-year period. Primary outcome was the time and date of admission. Secondary outcome measures were procedural parameters (National Institute of Health Stroke Scale (NIHSS), modified Rankin Scale (mRS) on admission and discharge, Thrombolysis In Cerebral Infarction Scale (TICI), time from groin puncture to recanalization, mortality and complications).

Results: Between 2014 and 2017 501 patients received endovascular treatment for AIS. There was no significance ($p>0.005$) pattern of incidence regarding day or time of year. 36,5% (183/501) of all cases were treated during regular working hours (08.00–16.30). With 63,4% (318/501) a significantly ($p<0.001$) larger number of patients were admitted and treated during off-hours (16.30–08.00), including 30,5% (153/501) on weekends/national holidays and 20,6% (103/501) at night (22.00–08.00). Compared by date and time of day there were no significant ($p>0.005$) differences in main baseline characteristics and procedural outcome measures.

Conclusion: The highest workload in endovascular stroke treatment takes place during on-call hours. To guarantee high-quality care for stroke patients, hospitals have to provide sufficient neurointerventional manpower, especially during off-hours.

353

Simulation of challenging intracranial access in a patient-based neurovascular training environment

Anna Kyselyova^{*1}, Andreas Frölich¹, Johanna Spallek², Jens Fiehler¹, Jan-Hendrik Buhk¹

¹Klinik und Poliklinik für Neuroradiologische Diagnostik und Intervention, Universitätsklinikum Hamburg-Eppendorf, Hamburg, Deutschland

²Institut für Produktentwicklung und Konstruktionstechnik, Technische Universität Hamburg-Harburg, Hamburg, Deutschland

Purpose: To present a novel integrated neurointerventional training and assessment environment combining additively manufactured supra-aortic arteries with physiological circuit conditions (HANNES, Hamburg ANatomical NEurointerventional Simulator). To evaluate HANNES' suitability for evaluating device performance in challenging carotid access scenarios.

Methods: Patient-specific, semi-elastic vascular models of intermediate (2 mm) and high-grade (<1 mm) ICA stenosis as well as tortuous ICA with ≥ 1 reverse curves were manufactured using stereolithography and joined to a patient-like aortic vascular system with physiological pulsatile circulation using HANNES. Under fluoroscopic control, various neuroendovascular devices were navigated up to the carotid-T segment. Device performance and their haptic features were recorded and evaluated.

Results: Fluoroscopic recordings of navigation attempts showed that device performance in the replicated vessels was similar compared to the patient's vascular system. Difficulties in device navigation through challenging carotid anatomies, including high-grade stenosis, can be reproduced.

Conclusion: Challenging supra-aortic access scenarios can be replicated in a fully artificial setting with additively manufactured arteries. HANNES combines advantages of both virtual reality simulators and vessel models in a realistic working environment in an animal-free training setup. The modular character of the system with interchangeable intra- and extracranial arteries could provide a good basis for systematic training and assessment of neurointerventionalists.

368

Predictive factors of intracranial hemorrhages after mechanical thrombectomy of posterior circulation stroke

Ulf Neuberger¹, Johannes Pfaff^{*2}, Martin Bendszus³, Markus Möhlenbruch⁴

¹Universitätsklinikum Heidelberg, Neurologische Klinik, Neuroradiologie, Heidelberg, D

²Universitätsklinikum Heidelberg, Abteilung für Neuroradiologie, Abteilung für Neuroradiologie, Heidelberg, Deutschland

³University Hospital Heidelberg, Department of Neuroradiology, Heidelberg, Deutschland

⁴Universitätsklinikum Heidelberg, Abteilung für Neuroradiologie, Heidelberg, Deutschland

Purpose: A rare yet feared complication when treating posterior circulation stroke (PCS) with mechanical thrombectomy (MT) is intracranial hemorrhage (ICH) with consecutive clinical deterioration. The aim of the study was to investigate factors favouring ICH after MT of PCS.

Methods: We conducted a retrospective analysis of 101 consecutive cases with PCS, which were treated with MT in our centre between January 2012 and September 2017. Bleedings were categorized according to the Heidelberg Bleeding Classification. 38 possible and technical parameters were evaluated in regards to the occurrence of any ICH and symptomatic ICH with multivariate logistic regressions.

The predictive performance of parameters was further assessed using machine learning techniques.

Results: 25 of 101 treated patients (24.8%) suffered from any type of ICH, while in 7 patients (6.9%), a symptomatic ICH occurred.

Treatment with Tirofiban ($n=12$, 11.8%) was significantly associated with any ICH (OR=24.7; 95% CI 5.79–172.00). Additionally, treatment with Tirofiban was associated with an unsatisfactory clinical outcome with of mRS 3–6 after 90 days (OR=3.61; 95% CI 0.64–67.88). 6 patients treated with Tirofiban were additionally treated with stenting (50%). No predictors for occurrence of symptomatic ICH could be identified.

Machine learning models showed a good performance of predicting occurrence of any ICH with 87% accuracy after treatment with Tirofiban, while integrative predictive performance including all parameters showed moderate results for clinical prediction of ICH.

Conclusion: Perinterventional treatment with Tirofiban was associated with poor clinical outcome and showed very high accuracy as a predictor for the occurrence of ICH.

374

Impact of Endovascular Recanalization on Quantitative Lesion Water Uptake in Acute Anterior Circulation Strokes

Gabriel Broocks^{*1}, Uta Hanning², Fabian Flottmann³, Peter Sporns⁴, Jens Minnerup⁵, Hannes Leischner⁶, Susanne Siemonsen⁷, Jens Fiehler⁸, Andre Kemmling⁹

¹Klinik und Poliklinik für Neuroradiologische Diagnostik und Intervention, Universitätsklinikum Hamburg-Eppendorf, Hamburg, Deutschland

²Klinik und Poliklinik für Neuroradiologische Diagnostik und Intervention, Universitätsklinikum Hamburg-Eppendorf, Institut für Klinische Radiologie, Uniklinikum Münster, Hamburg, Deutschland

³Universitätsklinikum Hamburg-Eppendorf, Klinik und Poliklinik für Neuroradiologische Diagnostik und Intervention, Klinik und Poliklinik für Neuroradiologische Diagnostik und Intervention, Hamburg, Deutschland

⁴Institut für Klinische Radiologie, Institut für Klinische Radiologie, Münster, Deutschland

⁵Klinik für Neurologie, Münster, Deutschland

⁶Universitätsklinikum Hamburg-Eppendorf, Klinik und Poliklinik für Neuroradiologische Diagnostik und Intervention, Hamburg, Deutschland

⁷Klinik und Poliklinik für Neuroradiologische Diagnostik und Intervention, Universitätsklinikum Hamburg-Eppendorf, Hamburg, D

⁸Diagnostikzentrum Univ.-Klinikum Hamburg-Eppendorf, Klinik und Poliklinik für Neuroradiologische Diagnostik und Intervention, Hamburg, Deutschland

⁹Institut für Klinische Radiologie, Universitätsklinikum Münster, UKSH Lübeck, Hamburg, Deutschland

Purpose: Net water uptake (NWU) per brain volume is a new quantitative imaging biomarker of space-occupying ischemic edema, which can be measured in computed tomography (CT). A recent study described that successful reperfusion reduces brain edema based on mid-line shift measurements. We sought to investigate the effects of vessel recanalization on the formation of ischemic brain edema using quantitative NWU.

Methods: All patients with an acute ischemic stroke due to a large vessel occlusion (LVO) in the anterior circulation were analyzed, admitted 01/2015–08/2017 in three German Stroke centers. Two groups were assembled and compared: Vessel recanalization (TICI 2b–3) and persistent vessel occlusion (no MT, TICI 0–1). NWU was quantified based on CT densitometry in the admission and follow-up CT.

Results: Of 194 included patients, 150 patients received successful endovascular recanalization and 44 patients had a persistent LVO. The mean (SD) NWU in the admission imaging was not different between both groups: 9.2% (4.5) in patients with persistent LVO and 7.9% (4.9) in recanalized patients ($p=0.1$). In the follow-up CT, the mean (SD) NWU was 24.9% (5.7) in persistent LVO's and 17.6% in recanalized patients ($p<0.0001$). Successful reperfusion was associated with an increased likelihood of having low ischemic brain edema formation (odds ratio 7.2; 95%CI: 2.9–18.1; $p<0.0001$).

Conclusion: Successful vessel recanalization was associated with a significantly reduced formation of ischemic brain edema. Quantitative NWU may be used to compare treatment effects in acute stroke.

Fig. 1

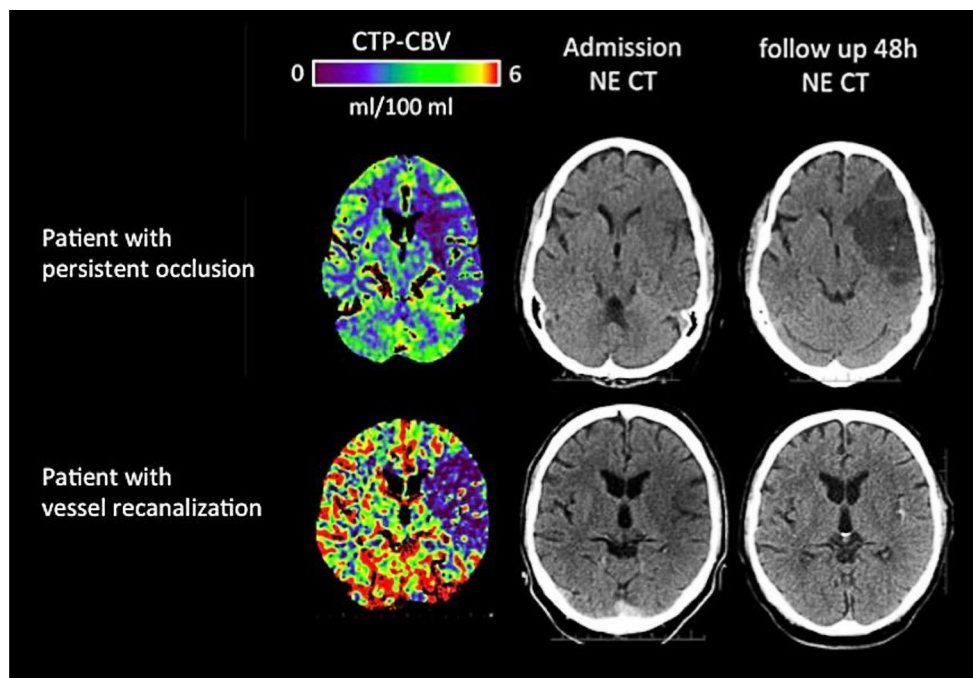
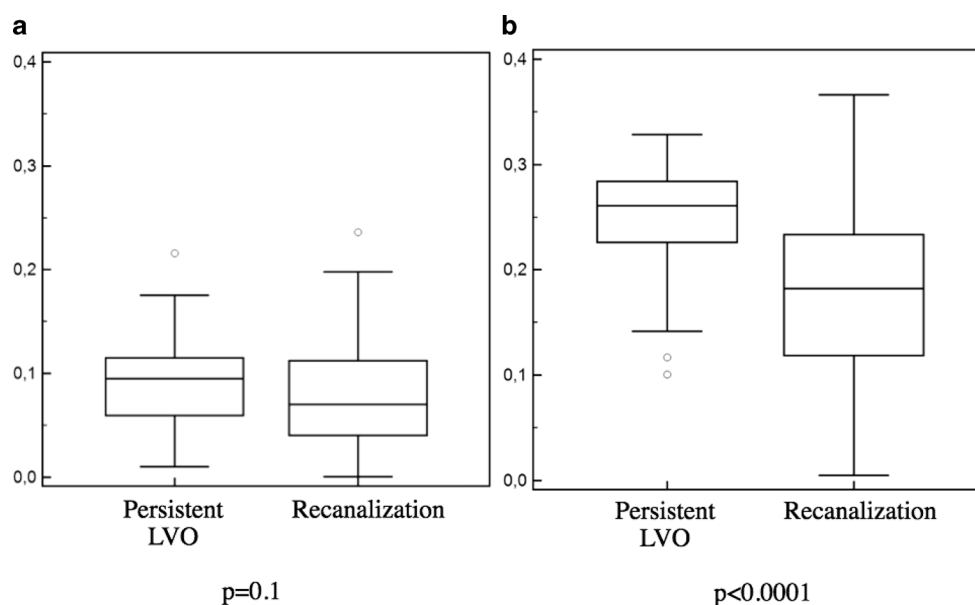


Fig. 2 **a** Netwater update at admission, **b** Netwater update at follow up



395

Systematic evaluation of stroke thrombectomy in clinical practice: The German Stroke Registry Endovascular Treatment

Anna Christina Alegiani¹, Götz Thomalla², Jens Fiehler³, Frank Arne Wollenweber⁴, Christian H. Nolte⁵, Franziska Dorn^{*6}

¹Universitätsklinikum Hamburg-Eppendorf, Neurologie, Hamburg, Deutschland

²Universitätsklinikum Hamburg-Eppendorf, Klinik und Poliklinik für Neurologie, Hamburg, Deutschland

³Diagnostikzentrum Univ.-Klinikum Hamburg-Eppendorf, Klinik und Poliklinik für Neuroradiologische Diagnostik und Intervention, Hamburg, Deutschland

⁴Ludwig-Maximilians-Universität, Klinikum der Universität München, Institut für Schlaganfall- und Demenzforschung (Isd), München, Deutschland

⁵Charité—Universitätsmedizin Berlin, Campus Benjamin Franklin, Klinik für Neurologie, Centrum für Schlaganfallforschung Berlin, Berlin, Deutschland

⁶Klinikum der Universität München—Campus Großhadern, Institut für Klinische Radiologie, Abteilung für Neuroradiologie, München, Deutschland

Purpose: Endovascular treatment has become standard of care for treatment of acute ischemic stroke with large vessel occlusion. However, patients treated in clinical practice differ from the selected populations randomized in clinical trials. The German Stroke Registry Endovascular Treatment (GSR-ET) aims at systematic evaluation of outcome, safety, and process parameters of endovascular stroke treatment in standard of care in Germany.

Methods: The GSR-ET is an academic, independent, prospective, multicenter, observational registry study. Participating stroke centers from all over of Germany consecutively enroll patients transferred with intention to be treated with endovascular stroke treatment. Patients receive regular care. Data are collected as part of clinical routine. Baseline clinical and procedural information, clinical follow-up information, and 90 days are recorded. Here, we present an analysis of baseline data of the first 1662 patients included in the GSR-ET.

Results: The registry was established 06/2015. Until 12/2017, 1662 patients were enrolled in 23 active sites. Mean age was 72 ± 13 years, 50% were female, and median NIHSS on admission was 15 (IQR 10–

19), 88% had anterior circulation occlusion. Median ASPECT score was 8 (IQR 7–10) prior to intervention. 59% of patients received iv-thrombolysis prior to thrombectomy. Mean “onset-to- groin”- time was 224 ± 176 minutes.

Conclusion: Conclusions: Baseline characteristics of stroke patients undergoing thrombectomy in clinical practice differ from those in the randomized trials. The GSR-ET will provide valuable insights into practices of endovascular treatment in routine care of acute ischemic stroke. (GSR-ET [ClinicalTrials.gov](https://clinicaltrials.gov/ct2/show/study/NCT03356392) Identifier: NCT03356392.)

406

Hemorrhagic transformation after acute ischemic stroke in the posterior circulation and endovascular therapy: frequency, risk factors and clinical significance

Nina Lummel^{*1}, David Pree¹, Silke Wunderlich², Claus Zimmer¹, Johannes Kaesmacher³, Tobias Boeckh-Behrens¹

¹Abteilung für Diagnostische und Interventionelle Neuroradiologie, München, Deutschland

²Neurologische Klinik, München, Deutschland

³Neurologische Klinik/ Neuroradiologie Inselspital Bern, Switzerland

Purpose: Hemorrhagic transformation (HT) poses a major safety concern for endovascular treatment (ET) of acute ischemic stroke. Thus, aim of this study was to determine frequency, risk factors and clinical significance of HT in patients with acute ischemic stroke in the posterior circulation undergoing ET.

Methods: We retrospectively analyzed all consecutive patients with ischemic stroke in the posterior circulation who underwent ET. We studied baseline characteristics, preinterventional imaging, periprocedural factors and clinical outcome. Postinterventional imaging was evaluated regarding HT.

Results: 113 consecutive patients were included. HT occurred in 17.7% and was significantly associated with less favorable clinical outcome ($p=0.02$). Diabetes ($p=0.05$), anticoagulation ($p=0.06$) and high baseline-NIHSS ($p=0.06$) showed a statistical trend to be associated with higher risk of HT. Furthermore, patients who were treated with stent retrieving only were less likely to develop HT ($p=0.005$). Application of iv-thrombolysis, baseline pcASPECTS and time from

symptom onset to therapy did not show significant influence on the occurrence of HT.

Conclusion: HT after acute ischemic stroke in the posterior circulation treated with ET occurs in approximately one fifth of patients and is significantly associated with less favorable clinical outcome. Diabetes, anticoagulation and high baseline-NIHSS may be risk factors. ET with stent retrievers can achieve lower rates of HT and thus better clinical outcome.

407

Is there a benefit of concomitant systemic thrombolysis during intracranial flow restoration via mechanical thrombectomy? A prospective multicenter study on behalf of the German Stroke Registry (GSR)

Manuel Lehm^{*1}, Silke Wunderlich², Claus Zimmer³, Tobias Boeckh-Behrens³

¹Abteilung für Diagnostische und Interventionelle Neuroradiologie, TU München, München, Deutschland

²Neurologische Klinik der TU München

³Abteilung für Diagnostische und Interventionelle Neuroradiologie, TU München

Purpose: Combination of systemic thrombolysis and mechanical thrombectomy (MT) currently defines the standard of care for treatment of acute ischemic stroke due to large vessel occlusion (LVO). As i. v.-administration of rt-PA usually takes place over the course of one hour, comprehensive stroke centers will increasingly be able to achieve intracranial flow restoration while i. v. rt-PA is still being administered.

Hypothesis: Concomitant administration of rt-PA during intracranial flow restoration may be associated both with better angiographic outcome as measured by a higher rate of mTICI3 recanalizations as well as better functional outcome according to mRS at day 90.

Methods: We conduct a national prospective observational multicenter cohort study on behalf of the GSR, including all patients with acute ischemic stroke due to LVO with the intention to treat via MT. In this particular study, we perform a subgroup analysis and multivariate regression for all patients that received i. v. rt-PA during intracranial flow restoration. Data release scheduled for 06/2018.

Objective: To evaluate both safety and effectiveness of the concomitant administration of rt-PA during intracranial flow restoration as measured by the rate of complications as well as angiographic and functional outcome.

409

Clinical benefit of mechanical thrombectomy in basilar artery occlusions? A prospective multicenter study on behalf of the German Stroke Registry (GSR)

Manuel Lehm^{*1}, Silke Wunderlich², Claus Zimmer³, Tobias Boeckh-Behrens³

¹Abteilung für Diagnostische und Interventionelle Neuroradiologie, TU München, München, Deutschland

²Neurologische Klinik der TU München

³Abteilung für Diagnostische und Interventionelle Neuroradiologie, TU München

Purpose: Combination of systemic thrombolysis and mechanical thrombectomy (MT) currently defines the standard of care for treatment of acute ischemic stroke due to large vessel occlusion (LVO). Although being standard of care for basilar artery occlusions in clinical routine as well, its clinical efficacy remains highly debated.

Hypothesis: MT in acute basilar artery occlusions may be safe and effective in order to achieve basilar flow restoration, the association of recanalization success and clinical outcome of patients however might be different in comparison to anterior circulation occlusions.

Methods: We conduct a national prospective observational multicenter cohort study on behalf of the GSR, including all patients with acute ischemic stroke due to LVO with the intention to treat via MT. In this particular study, we perform a subgroup analysis and multivariate regression for all patients with acute basilar artery occlusion. Data release scheduled for 06/2018.

Objective: To evaluate feasibility, safety and effectiveness of MT in acute basilar artery occlusions. We put special emphasis on the correlation of clinical outcome with recanalization success, stroke etiology and time dependency.

421

Outcome After Endovascular Thrombectomy in Acute Basilar Artery Occlusion: 206 Patients from a Single Center

Johannes Ravindren¹, Marta Aguilar Perez², Victoria Hellstern³, Muhammad AlMatter⁴, Hansjörg Bäßner⁵, Hans Henkes^{*6}

¹Neurointensiv Station Katharinen Hospital Stuttgart, Stuttgart, Deutschland

²Neuroradiologie, Neuroradiologische Klinik, Stuttgart, Deutschland

³Klinikum Stuttgart, Neuroradiologische Klinik, Stuttgart, Deutschland

⁴Klinikum Stuttgart, Neuroradiologische Klinik, Stuttgart, D

⁵Klinikum Stuttgart, Neurologische Klinik, Stuttgart, Deutschland

⁶Klinik für Neuroradiologie, Neuroradiologische Klinik, Stuttgart, Deutschland

Purpose: Acute basilar artery occlusion (aBAO) still is one of the most devastating stroke subtypes. Mortality is up to 90% if untreated. Consensus for the optimal treatment in aBAO remains unclear. Purpose of this study was to investigate the impact of procedural parameters and patient characteristics including collateral status and pathophysiological properties on functional outcome and survival within and beyond the 6 hour time window to recanalization, achieved with mTE.

Methods: 206 patients with aBAO at a single center were treated between November 2008 and November 2017 with mTE. They were dichotomized time to recanalization from stroke onset ≤ 6 h and >6 h. Univariate and bivariate analyses regarding factors on outcome (mRS 90 days) and survival were applied. Kaplan-Meier survival analysis was used. Logistic regression and Cox regression were performed to identify independent factors regarding outcome and survival.

Results: Significant difference in survival was seen in the beyond 6 h to treatment group for present collaterals and duration of treatment less than 2 h and TICI 2b-3 ($p < 0,05$). Diabetes mellitus, cholesterol, smoking status, duration of treatment and collateral status were independent factors for poor functional outcome ($p < 0,05$).

Independent factors for mortality were collateral status and duration of treatment ($p < 0,05$).

Conclusion: This might be an explanation for the ambiguous findings regarding the validity of the 6-hour time window.

Fig. 1

	IBA n=59	IMA n=28	EMA n=59
Female (%)	55	55	59
Age mean years (IQR)	74 (68-79)	68 (65-71)	78 (74-81)
Anterior circulation M1 (%)	100	100	100
IV Lysis (%)	59	75	75
NIHSS on admission, median (IQR)	15 (14-19)	15 (14-18)	15 (11-19)
TICI2b/3 (%)	73	79	71
Complications (%)	7	7	6
Number of devices used mean (SD)	1 (1)	1 (1)	1 (1)
Number of retrieval attempts mean (SD)	2 (1)	2 (1)	1 (1)
Median time groin puncture to recanalization median (IQR)	36 (24-60)	47 (37-71)	57 (46-82)
Median time first image to recanalization (IQR)	24 (20-47)	45 (33-58)	45 (35-68)

424

Endovascular treatment of stroke patients using mono- or biplane angiography systems

Hannes Leischner^{*1}, Fabian Flottmann², Uta Hanning³, Tobias D. Faizy⁴, Gabriel Broocks⁵, Milani Deb-Chatterji⁶, Götz Thomalla⁷, Christian Gerloff⁷, Jens Fiehler⁸, Caspar Brekenfeld⁹

¹Nrad Uke, Berlin, Deutschland

²Universitätsklinikum Hamburg-Eppendorf, Klinik und Poliklinik für Neuroradiologische Diagnostik und Intervention, Klinik und Poliklinik für Neuroradiologische Diagnostik und Intervention, Hamburg, Deutschland

³Klinik und Poliklinik für Neuroradiologische Diagnostik und Intervention, Universitätsklinikum Hamburg-Eppendorf, Institut für Klinische Radiologie, Uniklinikum Münster, Hamburg, Deutschland

⁴Universitätsklinikum Hamburg-Eppendorf, Klinik und Poliklinik für Interventionell und, Diagnostische Neuroradiologie, Hamburg, Deutschland

⁵Klinik und Poliklinik für Neuroradiologische Diagnostik und Intervention, Universitätsklinikum Hamburg-Eppendorf, Hamburg, Deutschland

⁶Kopf- und Neurozentrum, Klinik und Poliklinik für Neurologie, Hamburg, Deutschland

⁷Universitätsklinikum Hamburg-Eppendorf, Klinik und Poliklinik für Neurologie, Hamburg, Deutschland

⁸Diagnostikzentrum Univ.-Klinikum Hamburg-Eppendorf, Klinik und Poliklinik für Neuroradiologische Diagnostik und Intervention, Hamburg, Deutschland

⁹Universitätsklinikum Hamburg-Eppendorf, Hamburg, Deutschland

Purpose: In comprehensive stroke centers the mechanical thrombectomy (MT) of stroke patients can be carried out on bi-plane (BA) or single-plane angiography suites (SA). The aim of this study was to compare the efficacy of MT using a mono-plane or a bi-plane angiography suite.

Methods: We performed a retrospective analysis of prospectively collected patient data of stroke patients who were treated by a group of experienced interventional neuroradiologists using either an in-house bi-plane (IBA), an in-house single-plane (IMA) or a single-plane angiography system situated in an external hospital (EMA). Baseline demographics, risk factors, times from groin puncture to recanalization, time from first series of imaging to recanalization, thrombolysis in cerebral infarction scale (TICI) score, complications, number of thrombus passages and the number of devices were assessed. In further steps of the project more patients will be enrolled and clinical outcome parameters, including modified ranking scale score on day 90 (mRS90) will be analyzed.

Results: MT was performed using the IBA in 59, the IMA in 28 and the EMA in 59 cases. Time from first image until recanalization was significantly longer in the IMA (median time 51 min; IQR 37–79; $p=0.038$) or EMA (median time 57 min; IQR 46–82; $p=0.014$) group of patients compared to patients treated using the IBA (median time 37 min; IQR 26–60). The same held true for the time of groin puncture until recanalization. Regarding other parameters, there were no significant differences.

Conclusion: Conducting an MT is significantly faster if performed using a bi-plane angiography system. Therefore, the endovascular therapy of stroke patients should ideally be conducted on a bi-plane angiography system.

457

Interventional stroke treatment in patients with tandem lesions: What factors influence the clinical Outcome?

Rachid Elmouden¹, Gernot Reimann², Stefan Rohde^{*1}

¹Klinik für Radiologie und Neuroradiologie, Dortmund, Deutschland

²Klinikum Dortmund gGmbH, Klinik für Neurologie, Dortmund, Deutschland

Purpose: Endovascular treatment of acute stroke-patients with tandem lesions is challenging. We sought to evaluate the factors that influence the clinical outcome in these patients.

Methods: We retrospectively evaluated the clinical, procedural and imaging data of 42 stroke-patients (mean age 65 years, 67% male, mean NIHSS on admission 11.8) with tandem lesions of the anterior circulation that received endovascular treatment at our institution from January 2012 to December 2017. All patients were treated under general anaesthesia; 34% of the patients received IV-lysis.

Results: Recanalization and stenting of the ICA was successful in all patients; TICI 2b and 3 was achieved in 13 (35%) in 28 (65%) patients, respectively. Periprocedural complications including symptomatic in-

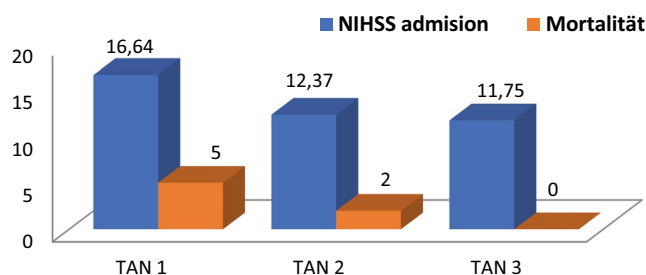


Fig. 1

tracranial haemorrhage occurred in 10% of the patients. At 90 days follow-up good clinical outcome at 90days (mRS ≤ 2) was 65%. A more favourable clinical outcome correlated with a lower NIHSS on admission, younger age, and good cerebral collaterals on CT-angiography (> Tan 2).

Conclusion: Interventional treatment of acute stroke-patients with tandem lesions is technically feasible and safe. A favourable outcome can be achieved in more than 60% of the patients and is most probable in younger patients with lower NIHSS and good intracranial collaterals.

465

Multifocal non-ischemic cerebral lesions after endovascular therapy with contrast enhancement and perifocal edema: Case reports.

Nils Dörner^{*1}, Johannes Pfaff², Markus Möhlenbruch², Martin Bendszus²

¹Abteilung für Neuroradiologie, Universitätsklinik Heidelberg, Heidelberg, Deutschland

²Universitätsklinik Heidelberg, Heidelberg, Deutschland

Purpose: Endovascular techniques for the treatment of intracranial aneurysms represent the most common therapeutic approach in the acute and elective setting. Immediate postinterventional imaging shows in a varying proportion of 15–50% mostly clinically inapparent embolic ischemia. Apart from this temporally distant lesions with contrast enhancement and perifocal edema occur.

Methods: We report two cases with similar changes.

Results: Patient 1 had a postinterventional inconspicuous MRI after flow diverter implantation. Within 5 months the patient developed bi-hemispheric lesions with contrast enhancement, perifocal edema, hemiparesis and headache. Under cortisone therapy improvement of the clinical and morphological picture within 10 months.

Patient 2 underwent complication-free coiling of an ACI aneurysm. 5 weeks postinterventional in the corresponding area supplied multiple lesions of the corona radiata and subcortical with contrast enhancement and extensive perifocal edema were seen. Clinically visual disturbances as well as headache and transient hemiparesis were noted. Under cortisone therapy significant regression of symptoms and MRI-findings.

Conclusion: Clinically and regarding MRI we interpret these very rare post-interventional complications as aseptic-inflammatory lesions. Morphologically fresh ischemia or vasculitis could be ruled out. In the literature foreign body emboli are discussed as causative by sheared polymer particles of the hydrophilic catheter coating.

467

A mandatory, prospective database for stroke patients implemented in the Clinical Information System

Johannes Gerber^{*1}, Kevin Hädrich², Andrij Abramyuk³, Angela Müller⁴, Alexandra Prakapenia⁵, Jessica Barlinn⁶, Kristian Barlinn⁶, Lars Peder Pallesen⁷, Jennifer Linn⁸, Volker Puetz⁹

¹Institut und Poliklinik für Neuroradiologie, Neuroradiologie, Dresden, Deutschland

²Institut und Poliklinik für Neuroradiologie, Universitätsklinikum Dresden, Dresden, Deutschland

³Institut und Poliklinik für Neuroradiologie, Dresden, Deutschland

⁴Universitätsklinikum Carl Gustav Carus, Dresden, Deutschland

⁵University Hospital Dresden, Neurology, Dresden, Deutschland

⁶Universitätsklinikum Carl Gustav Carus Dresden, Dresden, Deutschland

⁷Universitätsklinikum Carl Gustav Carus Dresden, Neurologie, Dresden, Deutschland

⁸Universitätsklinikum Carl Gustav Carus an der TU Dresden, Institut und Poliklinik für Diagnostische und Interventionelle Neuroradiologie, Dresden, Deutschland

⁹Universitätsklinikum Carl Gustav Carus Dresden, Klinik und Poliklinik für Neurologie, Dresden, Deutschland

Purpose: To generate good quality data for statistical analysis we designed a prospective database for stroke patients considered for endovascular therapy (EVT). To save resources and enhance data integrity we implemented the database in our Clinical Information System (CIS).

Methods: We developed a database for all stroke patients evaluated for emergency EVT. The database is fully implemented in our hospital wide CIS and shares variables of different workflows. An algorithm makes data entry mandatory for all stroke patients with a possible indication for EVT due to a suspected large vessel occlusion. Process times are gathered along the clinical pathway (admission, imaging and emergency treatment) and are pre-filled in, thus reducing manual entry and improving integrity. The relevant discipline enters clinical data and the final patient's outcome. The variables were set according to the demands of the national registries for quality control (QC) in stroke treatment (ADSR-Schlaganfallregister; DeGIR-Qualitätssicherungs-Register).

Results: Since the implementation of the database in 01/2016 until 30/04/2018 we evaluated 538 stroke patients for EVT. Of those, 330 patients (61.3%) received IV rTPA, and 314 patients (58.3%) were treated with EVT. There were 70 posterior circulation strokes (13%) and the left carotid system was affected in 237 patients (44%).

Conclusion: Implementation of a stroke database in a CIS saves resources. QC benefits from high quality data and workflow changes can readily be evaluated.

Interventional Neuroradiology: Thrombectomy Technical

140

Reperfusion with ADAPT Technique using ACE 68 and ACE 64 is safe and effective in large vessel occlusions of the anterior circulation—The PROMISE Study results

Peter Schramm^{*1}, Pedro Navia², Rosario Papa³, Joaquin Zamarro Parra⁴, Alejandro Tomasello Weitz⁵, Werner Weber⁶, Jens Fiehler⁷, Patrik Michel⁸, Vitor Pereira⁹, Laurent Pierot¹⁰, Jan Gralla¹¹, Paola Santalucia¹², Th Lo¹³

¹UKSH Universitätsklinikum Schleswig-Holstein Campus Lübeck, Institut für Neuroradiologie, Lübeck, Deutschland

²Hospital Universitario Donostia, San Sebastian, Spain

³A.O.U. Policlinico, Messina, Italy

⁴Hospital Clínico Universitario Virgen de la Arrixaca, Murcia, Spain

⁵Vall D'hebron Hospital, Barcelona, Spain

⁶Universitätsklinikum Knappschafts-Krankenhaus Bochum GmbH, Institut für Diagnostische und Interventionelle Radiologie, Neuroradiologie und Nuklearmedizin, Bochum, Deutschland

⁷Diagnostikzentrum Univ.-Klinikum Hamburg-Eppendorf, Klinik und Poliklinik für Neuroradiologische Diagnostik und Intervention, Hamburg, Deutschland

⁸Chuv, Service de Neurologie, Lausanne, Switzerland

⁹University of Toronto, Toronto Western Hospital, Joint Department of Medical Imaging, Toronto, Canada

¹⁰Hôpital Maison Blanche, Reims, France

¹¹Inselspital Universität Bern, Institut für Diagnostische und Interventionelle Neuroradiologie, Bern, Switzerland

¹²Piemonte Hospital, Messina, Italy

¹³University Medical Center Utrecht, Utrecht, Netherlands

Purpose: PROMISE aimed to observe safety and effectiveness of Penumbra System (PS) with ACE68 and ACE64 Reperfusion Catheters in patients with acute ischemic stroke from large vessel occlusion, treated with ADAPT as frontline treatment.

Methods: This was a prospective, single-arm multicenter study. Inclusion criteria were anterior circulation LVO within 6 hours of ictus; NIHSS ≥ 2 ; CT-ASPECTS ≥ 6 ; or MR-ASPECTS ≥ 5 . Primary endpoints included angiographic revascularization and clinical independence at 90 days. Secondary endpoints included safety events, functional improvement at 7–10 days, procedural metrics and quality of life.

Results: 204 patients (median age 74 ys) were enrolled in 20 European centers. 17.2% patients had occlusion of ICA, 3.9% of Carotid T, 60.8% of M1 and 18.1% of M2. Median baseline CT ASPECT score was 9. Median baseline and 7–10-day NIHSS scores were 16 and 3. IV rtPA was given in 61.8%. After PS treatment, 70.3% patients achieved TICI 2b/3. Final revascularization (TICI 2b/3) was achieved in 93.1%. Median time from stroke onset to revascularization (TICI 2b/3) was 245.5 minutes, and from puncture to TICI 2b/3 31 minutes. mRS 0–2 at 90 days was achieved in 61.0%. A reduction of ≤ 10 points or 7–10 days NIHSS of 0–1 was reported in 67.9% patients.

Safety rates were favorable (sICH=2.9%; ENT=1.5%); 90-day morbidity (mRS score 3–5), was 31.5%, 90-day all cause-mortality was 7.5%. There was no significant difference in the safety rates by treatment location. Device and procedure-related SAEs were 2.0% and 4.9%.

Conclusion: PROMISE study demonstrated safety and efficacy with latest generation of PS Reperfusion Catheters in patients with acute ischemic stroke from large vessel occlusion, using ADAPT as frontline treatment.

141

Alternative transcarotid approach for endovascular treatment of acute ischemic stroke patients: a case series

Hanna Styczen^{*1}, Marios Psychogios², Daniel Behme², Amelie Hesse²

¹Diagnostische und Interventionelle Neuroradiologie
Universitätsmedizin Göttingen, Göttingen, Deutschland

²Diagnostische und Interventionelle Neuroradiologie
Universitätsmedizin Göttingen

Purpose: Due to current studies, more patients with acute ischemic stroke including elderly with difficult vessel anatomy are treated by mechanical thrombectomy. In these patients catheterizing the internal carotid artery via the transfemoral approach can be significantly prolonged or even impossible resulting in poor neurological outcome. Therefore, in selected patients an alternative strategy is necessary in order to restore revascularization.

Methods: We report a case series of six patients undergoing mechanical thrombectomy via transfemoral and transcarotid approach. Puncture of the carotid artery was conducted using roadmap guidance after unsuccessful transfemoral attempt (Fig. 1). Technical aspects and outcomes with this alternative approach are outlined.

Results: Direct puncture of the carotid artery was achieved in 5 of 6 patients. In three patients (50%) revascularization (mTICI score $\geq 2b$) was restored. No complications related to endovascular therapy were seen. One patient showed good neurological outcome (admission mRS 5, discharge mRS 1).

Conclusion: The combination of transfemoral and transcarotid approach can be an alternative in selected patients with problematic vessel anatomy.

158

Recanalization rate per retrieval attempt in mechanical thrombectomy for acute ischemic stroke

Fabian Flottmann^{*1}, Hannes Leischner², Gabriel Broocks³, Jawed Nawabi³, Martina Bernhardt⁴, Tobias D. Faizy⁵, Milani Deb-Chatterji⁶, Götz Thomalla⁷, Jens Fiehler⁸, Caspar Brekenfeld⁹

¹Universitätsklinikum Hamburg-Eppendorf, Klinik und Poliklinik für Neuroradiologische Diagnostik und Intervention, Klinik und Poliklinik für Neuroradiologische Diagnostik und Intervention, Hamburg, Deutschland

²Universitätsklinikum Hamburg-Eppendorf, Klinik und Poliklinik für Neuroradiologische Diagnostik und Intervention, Hamburg, Deutschland

³Klinik und Poliklinik für Neuroradiologische Diagnostik und Intervention, Universitätsklinikum Hamburg-Eppendorf, Hamburg, Deutschland

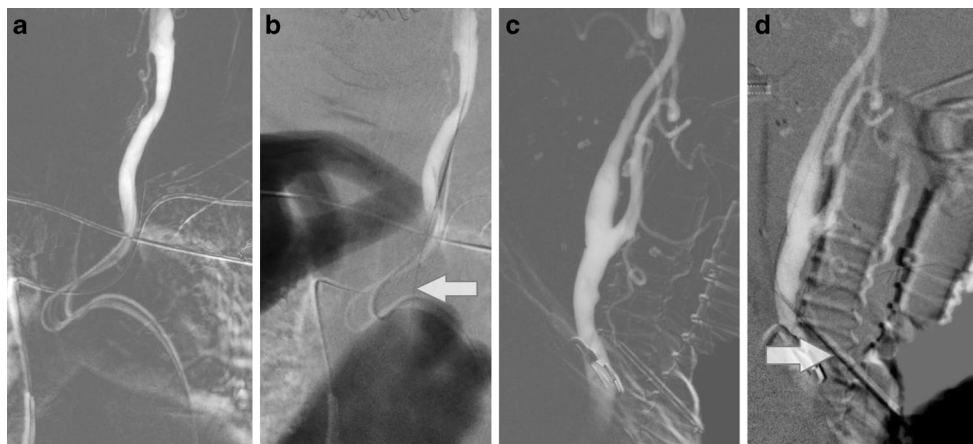
⁴Universitätsklinikum Hamburg-Eppendorf

⁵Universitätsklinikum Hamburg-Eppendorf, Klinik und Poliklinik für Interventionell und, Diagnostische Neuroradiologie, Hamburg, Deutschland

⁶Kopf- und Neurozentrum, Klinik und Poliklinik für Neurologie, Hamburg, Deutschland

⁷Universitätsklinikum Hamburg-Eppendorf, Klinik und Poliklinik für Neurologie, Hamburg, Deutschland

Fig. 1 DSA showing a biplane roadmap of the cervical carotids after injection through the SIM 2 catheter placed via transfemoral access (**a**, **c**). An 18G needle (arrow) is placed cranially to the clavicle bone and navigated in a 45° angle towards the common carotid artery on the biplane roadmap (**b**, **d**).



⁸Diagnostikzentrum Univ.-Klinikum Hamburg-Eppendorf, Klinik und Poliklinik für Neuroradiologische Diagnostik und Intervention, Hamburg, Deutschland

⁹Universitätsklinikum Hamburg-Eppendorf, Hamburg, Deutschland

Aim: Mechanical thrombectomy with stentriever devices allows flow restoration in the majority of patients with acute ischemic stroke. Nevertheless, often more than one retrieval attempt is required to achieve flow restoration. The optimal number of retrieval attempts is unknown. This study assessed the recanalization rate per retrieval maneuver.

Methods: Consecutive patients with first ever acute ischemic stroke undergoing mechanical thrombectomy in a large stroke center were retrospectively analyzed, and 338 patients treated exclusively with stentriever devices and known Thrombolysis in cerebral infarction (TICI) score were included.

Results: The median number of retrievals was 1 [IQR 1–2, max. 8]. The 1st retrieval attempt achieved flow restoration (TICI 2b/3) in 154/338 vessel occlusions (45.6%), and the following attempts had recanalization rates of 30.6% (2nd retrieval), 30.8% (3rd retrieval), 25.0% (4th

Fig. 1 Flowchart of thrombectomy attempts with Stentriever devices. Total: $n=388$

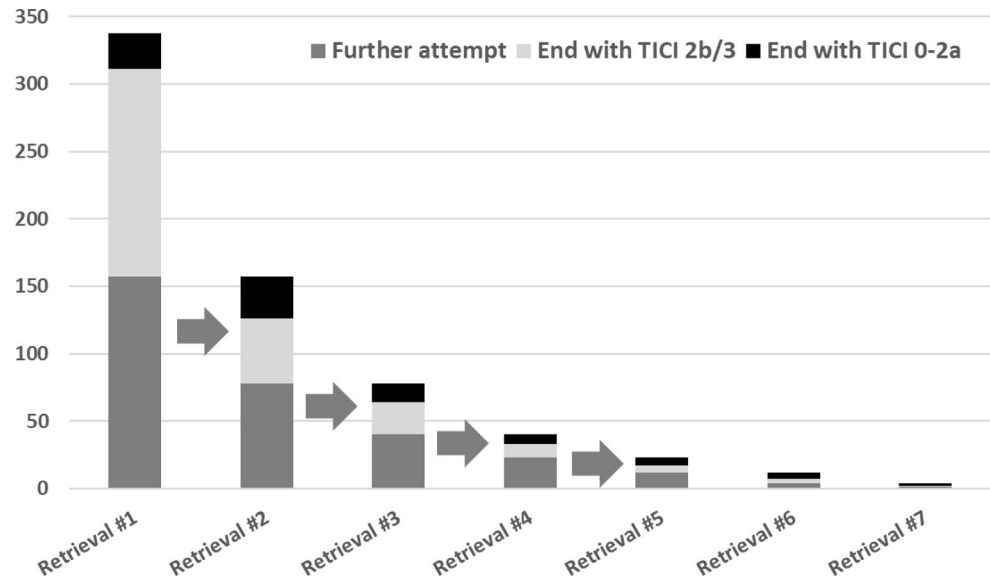


Fig. 2 Successfully recanalized vessel occlusions per retrieval attempt

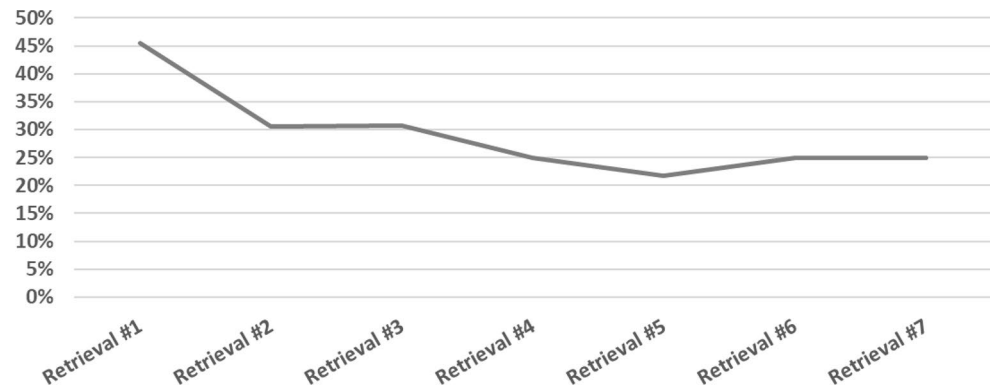
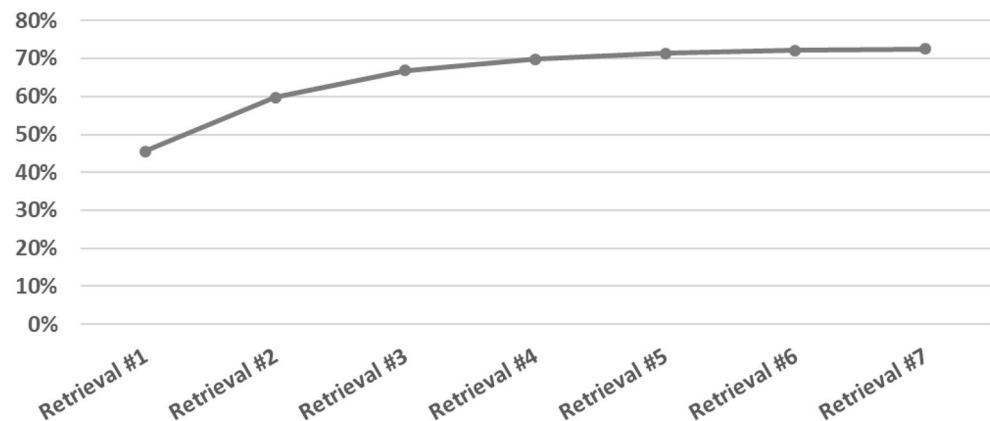


Fig. 3 Cumulative proportion of TICI 2b/3 patients after each retrieval attempt



retrieval) and 21.7% (5th retrieval). Cumulatively, flow restoration was achieved in 66.9% of all patients after three retrievals. The number of retrievals was an independent predictor for good clinical outcome (adjusted OR, 0.65; 95% CI, 0.435–0.970). Patients with up to three retrievals showed higher rates of good clinical outcome (29% vs. 7%, $p=0.018$).

Discussion: Two thirds of occlusions were successfully recanalized in the first three retrieval attempts. Subsequent retrieval maneuvers had good recanalization rates, but were associated with poor neurological outcome.

175

Pulling out all the stops to further reduce thrombus fragmentation during endovascular stroke treatment—the PROTECT PLUS technique.

Christian Maegerlein^{*1}, Maria Berndt², Sebastian Mönch³, Kornelia Kreiser⁴, Tobias Boeckh-Behrens⁵, Manuel Lehm⁶, Silke Wunderlich⁷, Claus Zimmer⁸, Benjamin Friedrich⁹

¹Klinikum Rechts der Isar der Technischen Universität, Abteilung für Diagnostische und Interventionelle Neuroradiologie, München, D

²Klinikum Rechts der Isar, Technische Universität München, Abteilung für Diagnostische und Interventionelle Neuroradiologie, München, Deutschland

³Abteilung für Diagnostische und Interventionelle Neuroradiologie, Klinikum Rechts der Isar, München, Deutschland

⁴Abteilung für Diagnostische und Interventionelle Neuroradiologie, Klinikum Rechts der Isar, München, Deutschland

⁵Neuroradiologie, Technische Universität München, Abteilung für Diagnostische und Interventionelle Neuroradiologie, München, Deutschland

⁶Abteilung für Diagnostische und Interventionelle Neuroradiologie, TU München, München, Deutschland

⁷Klinikum Rechts der Isar, Technische Universität München, Neurologie, München, Deutschland

⁸Klinikum Rechts der Isar der TUM, Technische Universität München, Abteilung für Diagnostische und Interventionelle Neuroradiologie, München, Deutschland

⁹Klinikum Rechts der Isar der Technischen Universität, Abteilung für Diagnostische und Interventionelle Neuroradiologie, München, Deutschland

Purpose: First pass complete recanalization without thrombus fragmentation must be regarded as the goal in mechanical thrombectomy (MT). We evaluate a technical modification of the previously published PROTECT approach: the PROTECT^{PLUS} technique. Under proximal flow arrest using a balloon guide catheter (BGC), a stent retriever (SR) is only partially inserted into a large-bore aspiration catheter (AC). This construction is subsequently retracted as a unit into the BGC with aspiration both at the AC and at the BGC.

Methods: We performed a case-control study comparing the PROTECT technique with the PROTECT^{PLUS} technique with respect to the technical and procedural parameters. We included 114 (84 PROTECT, 30 PROTECT^{PLUS}) patients with occlusion of either the terminus of the internal carotid artery or the proximal middle cerebral artery (M1).

Results: PROTECT^{PLUS} resulted in a higher rate of first pass complete recanalizations (56.7% vs. 30.9%, $p=0.012$) as compared with PROTECT leading to shorter procedure times (21 vs 37 minutes, $p=0.013$).

Conclusion: The PROTECT^{PLUS} technique is a promising technical modification to further optimize endovascular stroke treatment.

211

Mechanical Thrombectomy of Calcified Emboli—Case Series of a Rare and Challenging Subtype of Stroke

Christoph Maurer^{*1}, Felix Joachimski¹, Frank Runck², Philipp Zickler³, Ansgar Berlis¹

¹Klinikum Augsburg, Diagnostische und Interventionelle Radiologie und Neuroradiologie, Augsburg, Deutschland

²Klinikum Augsburg, Augsburg, Deutschland

³Klinikum Augsburg, Neurologische Klinik und Klinische Neurophysiologie, Augsburg, Deutschland

Purpose: Mechanical thrombectomy is the standard of care for intracranial large vessel occlusions. Thrombus density on unenhanced CT is known to influence the effectiveness of pharmacological and mechanical therapy of acute stroke. The purpose of this retrospective study was to evaluate the effectiveness of mechanical thrombectomy of large vessel occlusion due to calcified emboli.

Methods: A retrospective analysis of all strokes treated by endovascular means between January 2013 and February 2018 in our institution was performed and patients with intracranial vessel occlusion due to calcified emboli were identified.

Results: Seven patients received intracranial thrombectomy due to calcified emboli. Occlusion sites were carotid T ($n=2/7$), basilar artery ($n=1/7$), M1 segment of the MCA ($n=2/7$) and M2 segment of the MCA ($n=2/7$). Final angiographic result was TICI 0 in 3 Patients, TICI 2b in 3 patients and TICI 3 in one patient and Patients had an mRS between 3 and 6 at time of discharge.

Conclusion: Large vessel occlusion due to calcified emboli is a rare subtype of stroke. Unsuccessful recanalization by endovascular means might be more frequent than in large vessel occlusion due to non-calcified emboli. A more aggressive treatment strategy, for example with early use of intracranial stents, might be warranted in these cases.

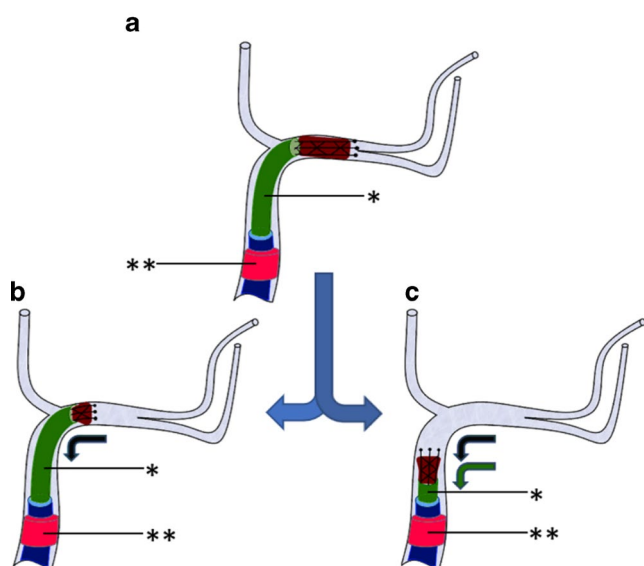


Fig. 1 PROTECT and PROTECT^{PLUS} in case of M1-occlusion. **a** Proximal flow arrest is established by BGC, **. PROTECT. **b** the SR is retracted into the AC (*) with the AC in stable position. PROTECT^{PLUS}. **c** SR is only partially retracted into AC, the clot wedged between the AC and the SR being pulled into the BGC as a unit

232

Distal Stent Retriever Placement in M1 occlusions: inferior or superior trunk?

Volker Maus^{*1}, Alex Brehm², Ioannis Tsogkas³, Silja Henkel⁴, Marios-Nikos Psychogios⁴

¹University Hospital of Göttingen, Institute for Neuroradiology, Göttingen, Deutschland

²Institut für Diagnostische und Interventionelle Neuroradiologie, Göttingen, Deutschland

³Universitätsmedizin Göttingen, Göttingen, Deutschland

⁴Universitätsmedizin Göttingen

Purpose: Embolectomy using “Stent retriever Assisted Vacuum-locked Extraction” (SAVE) is effective in intracranial large vessel occlusion. Which post-bifurcational trunk should be chosen for distal stent retriever placement in M1 occlusions is elusive.

Methods: We conducted a retrospective analysis from a comprehensive stroke center between 2015 and 2018. 89 consecutive patients with M1 occlusions were treated with SAVE. Digital subtraction angiography (DSA) series were studied to determine the anatomy of middle cerebral artery division, the position of the stent retriever, and to measure vessel diameters. Primary endpoint was first-pass complete/near-complete reperfusion, defined as a modified Thrombolysis in Cerebral Infarction (mTICI) score of 2c and 3, after distal stent retriever placement in the inferior trunk.

Results: In 76/89 (85%) patients, microcatheter-series were documented. Microcatheter was placed within the inferior trunk in 30/76 (40%) cases. First-pass near-complete/complete reperfusion was more likely achieved when the inferior trunk was used for stent retriever placement compared to superior trunk (mTICI $\geq 2c$: 22/30 (73%) vs. 22/46 (48%), $p=0.034$, and mTICI 3: 20/30 (67%) vs. 17/46 (37%), $p=0.018$). Median diameter of the inferior trunk was larger compared to superior trunk (1.4 mm (IQR 1.26–1.62) vs. 1.18 mm (IQR 0.98–1.43), $p=0.011$). The inferior trunk was dominant in 56/76 (74%) cases. Successful reperfusion was associated with placement within the dominant trunk (33/40 (83%) vs. 22/36 (61%), $p=0.044$).

Conclusion: The choice of the inferior trunk for distal stent retriever placement in M1 occlusions is associated with a high rate of first-pass near-complete/complete reperfusion when using SAVE.

233

Large-scale, Core-team Assessed Evaluation of the SAVE Technique

Volker Maus^{*1}, Silja Henkel², Alexander Riabikin³, Christian Riedel⁴, Daniel Behme², Ioannis Tsogkas², Amelie Hesse², Nuran Abdullayev⁵, Olav Jansen⁴, Martin Wiesmann³, Anastasios Mpotsaris³, Marios-Nikos Psychogios²

¹University Hospital of Göttingen, Institute for Neuroradiology, Göttingen, Deutschland

²Universitätsmedizin Göttingen

³Uniklinik Aachen

⁴UKSH Kiel

⁵Universitätsklinik Köln

Purpose: The “Stent retriever Assisted Vacuum-locked Extraction” (SAVE) technique has been introduced as an effective thrombectomy method in stroke patients suffering from intracranial large vessel occlusion (LVO).

Methods: Retrospective, core-team analysis of 200 patients undergoing mechanical thrombectomy using the SAVE technique due to intracranial LVO at 4 German centers. Primary endpoints were first-pass and overall complete/near-complete reperfusion, defined as a modified

Thrombolysis in Cerebral Infarction (mTICI) score of 2c and 3. Secondary endpoints were number of passes, time from groin puncture to reperfusion, embolization to new territories (ENT), and post-interventional symptomatic intracranial hemorrhage (sICH).

Results: Median NIHSS at admission was 16 (IQR 12–20). Occlusions sites were: ICA-T in 39/200 (19.5%), M1 in 126/200 (63%), M2 in 30/200 (15%), and others in 5/200 (2.5%) cases. The primary endpoints were documented in 114/200 (57% first-pass mTICI2c or 3) and 154/200 (77% overall mTICI2c or 3) patients, respectively. The overall median time from groin puncture to reperfusion was 34 min (IQR 25–52) with a median of 1 (IQR 1–2) attempts. ENTs were observed in 3 patients (1.5%) and the rate of sICH was 2.6%. The rate of successful reperfusion (mTICI $\geq 2b$) on final angiograms was 95%.

Conclusion: Mechanical thrombectomy using the SAVE technique is effective, fast and secure. First-line use of SAVE leads to high-rates of complete/near-complete reperfusion.

269

Stent-retriever Assisted Vacuum-locked Extraction (SAVE) versus A Direct Aspiration First Pass Technique (ADAPT) for acute stroke: Data from the real-world

Alex Brehm^{*1}, Volker Maus², Ioannis Tsogkas³, Colla Ruben¹, Amelie Carolina Hesse¹, Roland Gerard Gera⁴, Marios-Nikos Psychogios¹

¹Institut für Diagnostische und Interventionelle Neuroradiologie, Göttingen, Deutschland

²University Hospital of Göttingen, Institute for Neuroradiology, Göttingen, Deutschland

³Universitätsmedizin Göttingen, Göttingen, Deutschland

⁴Institut für Medizinische Statistik, Göttingen, Deutschland

Purpose: Embolectomy is the standard of care in acute ischemic stroke (AIS) caused by large vessel occlusion (LVO). Aim of this study was to compare two techniques: A Direct Aspiration First Pass Technique (ADAPT) and Stent-retriever Assisted Vacuum-locked Extraction (SAVE).

Methods: One hundred seventy-one patients (71 male) treated between January 2014 and September 2017 with AIS due to LVO of the anterior circulation (55 carotid T, 94 M1, 22 M2) were included. Treatment techniques were divided into two categories: ADAPT and SAVE. Primary endpoints were successful reperfusion (mTICI $\geq 2b$) and groin to reperfusion time. Secondary endpoints were the number of device-passes, first-pass reperfusion, the frequency of emboli to new territory (ENT), clinical outcome at 90 days, and the frequency of symptomatic intracranial hemorrhage (sICH). Analysis was performed on an intention to treat basis.

Results: Overall, SAVE resulted in significant higher rates of successful reperfusion (mTICI $\geq 2b$) compared to ADAPT (93.5% vs 75.0%; $p=0.002$). After stratification for the occluded vessel the carotid T remained significant (93.1% vs 65.4%; $p=0.037$), while a trend towards a higher frequency for SAVE in the M1 segment (94.8% vs 83.3%; $p=0.066$) persisted. Groin to reperfusion times were not significantly different. Secondary analysis revealed higher rates of first-pass successful reperfusion (59.6% vs 33.3%; $p=0.001$), lower frequency of ENT (12.5% vs 3%; $p=0.030$) and number of device-passes (median 1 IQR 1–2 vs 2 IQR 2–3; $p<0.001$) for SAVE. Clinical outcome and safety parameters were comparable between groups.

Conclusion: Embolectomy using SAVE appears superior to ADAPT, especially for carotid T occlusions with regard to reperfusion success.

Mechanical thrombectomy in basilar artery occlusion

Sebastian Fischer^{*1}, Werner Weber¹, Jens Altenbernd¹

¹Knappschafts Krankenhaus Bochum Langendreer, Institut für Diagnostische und Interventionelle Radiologie/Neuroradiologie U. Nuklearmedizin, Bochum, Deutschland

Purpose: Several randomized trials have been focused on patients with anterior circulation stroke, whereas few data on posterior circulation stroke are available. Thus, new mechanical thrombectomy (MT) strategies, including a direct aspiration first-pass technique (ADAPT), remain to be evaluated in basilar artery occlusion (BAO) patients. We investigated the influence of reperfusion on outcome in BAO patients.

Methods: One stroke center retrospectively collected individual data from BAO patients treated with MT. Baseline characteristics as well as radiographic and clinical outcomes were collected. The primary outcome measure was the rate of successful reperfusion, defined as a modified Thrombolysis in Cerebral Infarction (mTICI) grade of 2b–3. Favorable outcome was defined as a 90-day modified Rankin Scale score of 0–2.

Results: Among the 63 adult patients included in the study, 46 were treated with first-line ADAPT; stent-retriever rescue therapy was secondarily used in 12 and 5 were treated with a primary stent retriever. Successful reperfusion was achieved in 91% of the overall study sample. Overall, the rate of favorable outcome was 45% and 90-day all-cause mortality was 37%. Successful reperfusion positively impacted favorable outcome ($p=0.01$).

Conclusion: Among BAO patients, successful reperfusion is a strong predictor of a 90-day favorable outcome, and the choice of ADAPT as the first-line strategy achieves a significantly high rate of complete reperfusion.

Mechanical thrombectomy in posterior cerebral artery occlusion

Sebastian Fischer^{*1}, Werner Weber¹, Jens Altenbernd¹

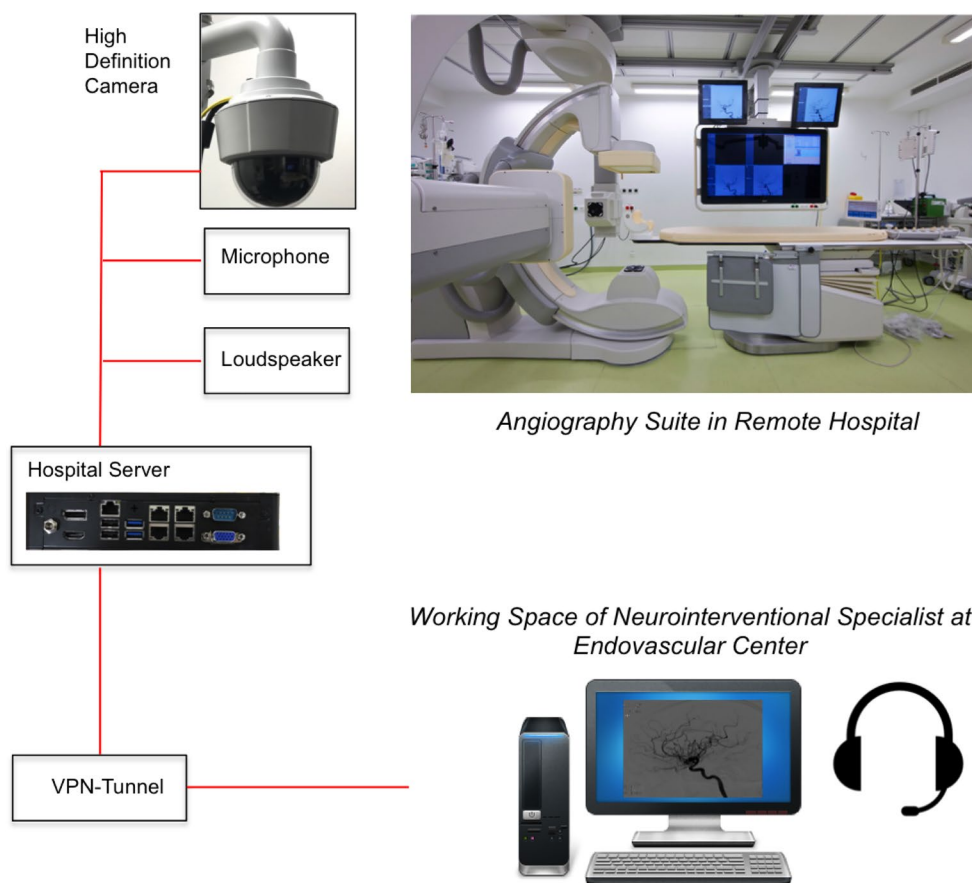
¹Knappschafts Krankenhaus Bochum Langendreer, Institut für Diagnostische und Interventionelle Radiologie/Neuroradiologie U. Nuklearmedizin, Bochum, Deutschland

Purpose: Several randomized trials have been focused on patients with anterior circulation stroke, whereas few data on posterior circulation stroke are available. Thus, new mechanical thrombectomy (MT) strategies, including a direct aspiration first-pass technique (ADAPT), remain to be evaluated in posterior cerebral occlusion (PCO) patients. We investigated the influence of reperfusion on outcome in PCO patients.

Methods: One stroke center retrospectively collected individual data from PCO patients treated with MT. Baseline characteristics as well as radiographic and clinical outcomes were collected. The primary outcome measure was the rate of successful reperfusion, defined as a modified Thrombolysis in Cerebral Infarction (mTICI) grade of 2b–3. Favorable outcome was defined as a 90-day modified Rankin Scale score of 0–2.

Results: Among the 24 adult patients included in the study, 20 were treated with first-line ADAPT; stent-retriever rescue therapy was secondarily used in 4 and 0 were treated with a primary stent retriever. Successful reperfusion was achieved in 87% of the overall study sample. Overall, the rate of favorable outcome was 56% and 90-day all-cause mortality was 21%. Successful reperfusion positively impacted favorable outcome ($p=0.005$).

Fig. 1



Conclusion: Among PCO patients, successful reperfusion is a strong predictor of a 90-day favorable outcome, and the choice of ADAPT as the first-line strategy achieves a significantly high rate of complete reperfusion.

284

Proof of Function for an Experimental Setup to Remotely Supervise and Proctor Mechanical Thrombectomy

Matthias Bechstein^{*1}, Einar Goebell², Jan-Hendrik Buhk¹, Jens Fiehler³

¹Klinik und Poliklinik für Neuroradiologische Diagnostik und Intervention, Universitätsklinikum Hamburg-Eppendorf, Hamburg, Deutschland

²Klinik und Poliklinik für Neuroradiologische Diagnostik und Intervention, Universitätsklinikum Hamburg-Eppendorf

³Diagnostikzentrum Univ.-Klinikum Hamburg-Eppendorf, Klinik und Poliklinik für Neuroradiologische Diagnostik und Intervention, Hamburg, Deutschland

Purpose: Stroke patients in areas absent of neurointerventional specialists are detained from expeditious endovascular recanalisation. We tested a remotely controlled surveillance system (*fig*), allowing a neurointerventional specialist to proctor a thrombectomy (TE) performed by a radiologist not specialized in neurointervention without being physically present (remote proctoring, REP).

Method: In total, 36 TE procedures were performed by 6 radiologists with no previous interventional experience on a Mentice endovascular simulator. Each surgeon was initially challenged with a TE under local proctoring (LOP) by a neurointerventional specialist. The following 5 procedures were randomly assigned to LOP/REP. REP was performed via a state-of-the-art online platform for visual and acoustic streaming of live content.

Results: Median number of trials for successful recanalization was 2 in each group. There was no difference in time from first catheter insertion to recanalization between LOP (median 1495s; IQR 1257–1890) and REP (1435s; IQR 1301–1723). Fluoroscopy time did not differ (LOP: 1141s; IQR 1013–1411/REP: 1191s; IQR 953–1410). The average speed when retrieving stentriever was equal in both groups (LOP: 3.7 mm/s; IQR 3.25–5.35/REP: 3.6 mm/s; IQR 2.5–4.7).

Conclusion: Our study proofs function of REP in TE procedures in a simulated environment. Further analysis is needed to verify if REP will facilitate continuous support of interventionalists with limited TE experiences in remote areas.

291

The short 115 cm SOFIA as distal access catheter

Christian Ulfert^{*1}, Martin Bendszus², Markus Möhlenbruch³

¹Universitätsklinikum Heidelberg, Abteilung für Neuroradiologie, Neuroradiologie, Heidelberg, Deutschland

²University Hospital Heidelberg, Department of Neuroradiology, Heidelberg, Deutschland

³Universitätsklinikum Heidelberg, Abteilung für Neuroradiologie, Heidelberg, Deutschland

Purpose: Stable catheter positions are essential in the endovascular treatment of intracranial pathologies. We present a series of patients that were treated using a SOFIA distal access catheter (SOFIA DAC, Microvention, Aliso Viejo, USA).

Methods: Multicenter observational study in 214 patients that were treated for a variety of intracranial pathologies (171 aneurysms, 17 AVFs, 15 AVMs, 10 intracranial stenosis und 2 other). Patient demographics were collected as well as pathology, location of the patholo-

gy, procedural details, size of the catheter used, number of turns above 90°, presence of a 360° cervical loop, the final position of the SOFIA catheter and the stability of the SOFIA during the procedure as rated by the treating interventionalist. Furthermore catheter-associated complications were gathered.

Results: Out of the 214 treatments 104 were done with the 5F SOFIA 115 cm and 110 with the 6F SOFIA 115 cm. Catheter associated complications were reported in 2 cases (1%). There was one catheter induced dissection and 1 patient with vasospasms due to the catheter.

The intended final position was reached in 98.2% of the cases. Interventionalists rated the support as adequate in 98.6%. On their way to the target position catheters negotiated an average of 2.34 90° turns.

Conclusion: We could show that the new shorter SOFIA distal access catheter provides a stable and safe foundation for endovascular treatment of intracranial vessel pathologies. The catheter can be placed further distal than previous catheters without increasing the complication rate.

321

Tempus vincit omnia—analyzing the effect of time on angiographic results after mechanical thrombectomy

Daniel Behme^{*1}, Ioannis Tsogkas², Ruben Colla³, Roland Gerard Gera⁴, Katharina Schregel⁵, Ilko Maier⁶, Jan Liman⁶, Marios-Nikos Psychogios¹

¹Institut für Diagnostische und Interventionelle Neuroradiologie, Göttingen, Deutschland

²Universitätsmedizin Göttingen, Göttingen, Deutschland

³Universitätsmedizin Göttingen, Deutschland

⁴Institut für Medizinische Statistik, Göttingen, Deutschland

⁵Department of Radiology, Brigham and Women's Hospital, Harvard Medical School, Institute of Neuroradiology, University Medical Center Goettingen, Goettingen, Deutschland

⁶Universitätsmedizin Göttingen, Neurologie, Göttingen, Deutschland

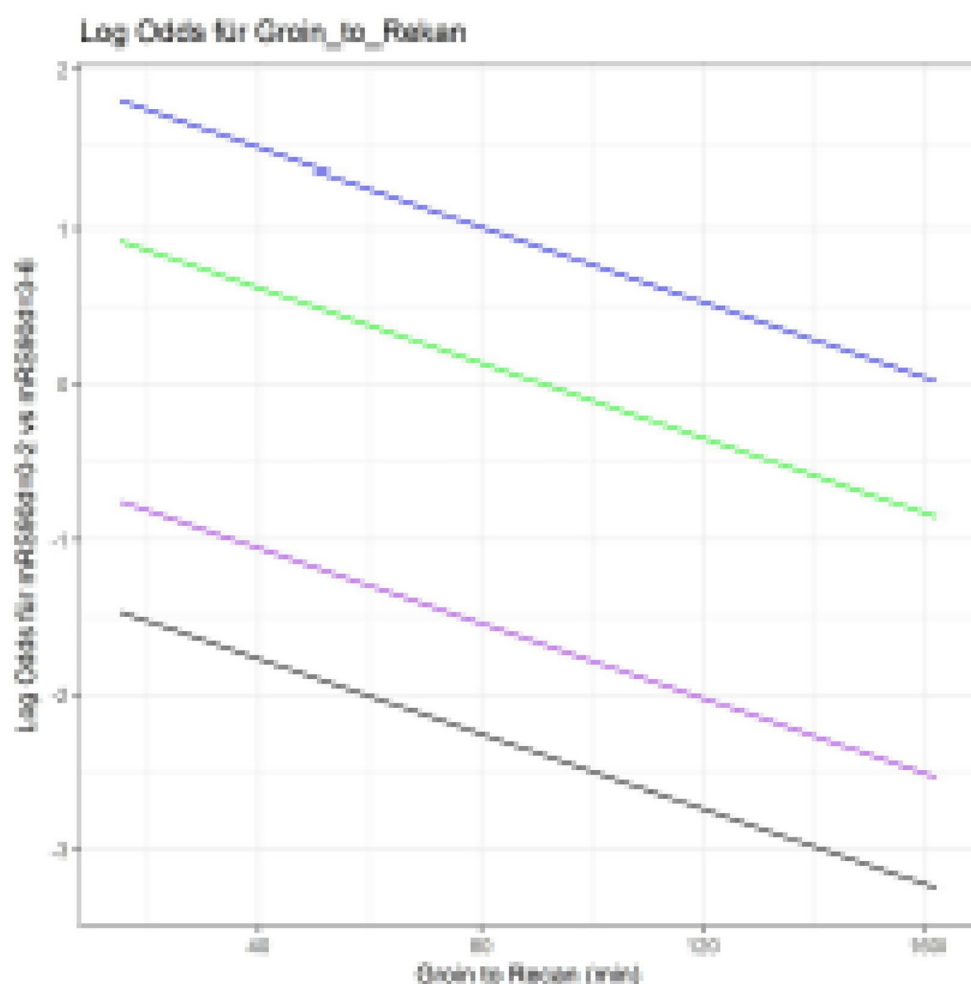
Purpose: Procedural times and angiographic results are relevant predictors of outcome after EVT. How time influences the patients' chance of achieving a favorable outcome with a distinct angiographic result is unknown. This study is the first to investigate the effect of time on different TICI scores.

Methods: Retrospective analysis of 164 patients who were successfully treated for an LVO of the anterior circulation. Clinical and angiographic data were taken from our prospective data base. Angiographic results were re-graded according to the novel expanded TICI (eTICI) score[1]. Multiple logistic regression analysis were performed calculating the effect of groin to recanalization times for different TICI scores and odds ratios as well as changes in the odds for achieving a favorable outcome per minute were calculated.

Results: For the multiple logistic regression model to predict a favorable outcome at 90d eTICI results were significant contributors ($p < 0.001$). Additionally there was a significant difference between eTICI2b67 and eTICI3 and eTICI2c and eTICI3 respectively with $p < 0.001$ (OR:0.038) and $p = 0.0297$ (OR:0.417). The change of odds over time in our model can be expressed as a formula. For example let the initial odds of achieving a favourable outcome for patients with mean age, and eTICI2b67 after 40 treatment minutes be 2.25. To see how the Probabilities would shift if the same patient got his eTICI2b67 after 80 minutes we either look into our model or calculate the new odd.

Conclusion: Achieving certain angiographic results at different time points is associated with different probabilities of favorable outcome. Understanding the correlation of time and angiographic success may help to refine endovascular treatment.

Fig. 1 Verlauf der Log Odds ratio



323

Treatment delay of MRI vs. CT admission imaging in acute stroke triage

Fabian Flottmann^{*1}, Hannes Leischner², Gabriel Brooks³, Tobias D. Faizy⁴, Milani Deb-Chatterji⁵, Götz Thomalla⁶, Jens Fiehler⁷, Caspar Brekenfeld⁸

¹Universitätsklinikum Hamburg-Eppendorf, Klinik und Poliklinik für Neuroradiologische Diagnostik und Intervention, Klinik und Poliklinik für Neuroradiologische Diagnostik und Intervention, Hamburg, Deutschland

²Universitätsklinikum Hamburg-Eppendorf, Klinik und Poliklinik für Neuroradiologische Diagnostik und Intervention, Hamburg, Deutschland

³Klinik und Poliklinik für Neuroradiologische Diagnostik und Intervention, Universitätsklinikum Hamburg-Eppendorf, Hamburg, Deutschland

⁴Universitätsklinikum Hamburg-Eppendorf, Klinik und Poliklinik für Interventionell und, Diagnostische Neuroradiologie, Hamburg, Deutschland

⁵Kopf- und Neurozentrum, Klinik und Poliklinik für Neurologie, Hamburg, Deutschland

⁶Universitätsklinikum Hamburg-Eppendorf, Klinik und Poliklinik für Neurologie, Hamburg, Deutschland

⁷Diagnostikzentrum Univ.-Klinikum Hamburg-Eppendorf, Klinik und Poliklinik für Neuroradiologische Diagnostik und Intervention, Hamburg, Deutschland

⁸Universitätsklinikum Hamburg-Eppendorf, Hamburg, Deutschland

Aim: Both computed tomography (CT) and magnet resonance imaging (MRI) are used to confirm diagnosis in acute ischemic stroke patients eligible for endovascular therapy. While CT is more readily available, MRI offers better diagnostic accuracy. The main caveat regarding usage of MRI is the possible treatment delay. This study assessed procedure times in mechanical thrombectomy patients diagnosed either with CT or MRI.

Methods: In this retrospective analysis of prospectively collected data, 286 patients with mechanical thrombectomy for first ever acute large-vessel occlusion were included. The cohort was divided in patients who received admission CT vs. MRI. Baseline demographics, risk factors, location of occlusion and times from symptom onset to admission, admission to imaging, and imaging to groin puncture were assessed, as well as clinical outcome parameters.

Results: CT was performed in 243 patients and MRI in 43 patients. MRI imaging was associated with longer times from admission to beginning of imaging (median 25 min vs. CT 15 min, 95% CI of median difference: [-14;-7]) and admission to groin puncture (median 80 min vs. CT: 65.5, 95% CI of median difference: [-22;-6]). No other significant differences were found.

Discussion: MRI imaging lead to a significant treatment delay of about 15 minutes and should be confined to difficult cases when deemed nec-

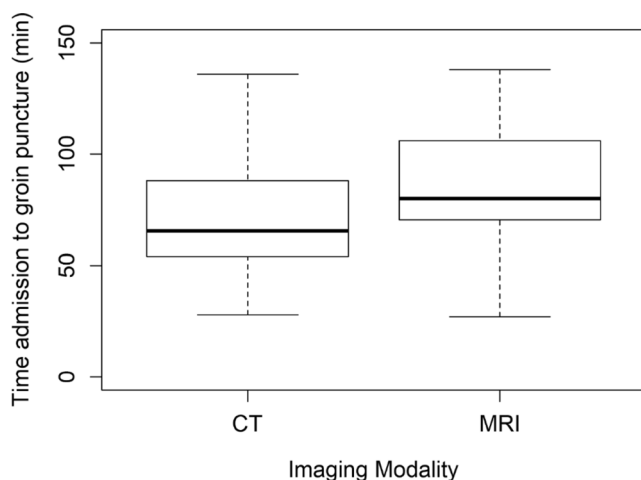


Fig. 1

essary, e.g. unknown time from symptom onset or posterior circulation occlusions. Nevertheless, due to the retrospective nature of the study, further subgroup analysis is necessary to assess a possible selection bias.

326

Influence of thrombus properties and procedural specifications on the incidence of peripheral emboli and their impact on stroke severity after thrombectomy: preliminary results

Michael Schönfeld^{*1}, Fabian Flottmann², Uta Hanning³, Gabriel Broocks¹, Andreas Frölich⁴, Maxim Bester¹, Caspar Brekenfeld⁵, Jan-Hendrik Buhk¹, Jens Fiehler⁶

¹Klinik und Poliklinik für Neuroradiologische Diagnostik und Intervention, Universitätsklinikum Hamburg-Eppendorf, Hamburg, Deutschland

²Universitätsklinikum Hamburg-Eppendorf, Klinik und Poliklinik für Neuroradiologische Diagnostik und Intervention, Klinik und Poliklinik für Neuroradiologische Diagnostik und Intervention, Hamburg, Deutschland

³Klinik und Poliklinik für Neuroradiologische Diagnostik und Intervention, Universitätsklinikum Hamburg-Eppendorf, Institut für Klinische Radiologie, Uniklinikum Münster, Hamburg, Deutschland

⁴Universitätsklinikum Hamburg-Eppendorf, Klinik und Poliklinik für Neuroradiologische Diagnostik, Klinik und Poliklinik für Neuroradiologische Diagnostik und Intervention, Hamburg, Deutschland

⁵Universitätsklinikum Hamburg-Eppendorf, Hamburg, Deutschland

⁶Diagnostikzentrum Univ.-Klinikum Hamburg-Eppendorf, Klinik und Poliklinik für Neuroradiologische Diagnostik und Intervention, Hamburg, Deutschland

Purpose: To analyse factors that might influence the number of peripheral emboli after thrombectomy and their influence on stroke severity. **Methods:** Patients endovascularly treated for a large vessel occlusion received a 1.5T MRI including a high-resolution DWI on the day following the intervention. Punctuate DWI lesions distant to a continuous core DWI lesion were counted as peripheral emboli. Thrombus location, density and length were measured on pre-interventional CT imaging. Procedural details of mechanical thrombectomy (primary aspiration or stent retrieval with or without balloon occlusion, number of passes) as well as NIHSS before thrombectomy and upon discharge

were collected. Thrombus properties, procedural details and NIHSS were correlated with the number of peripheral emboli.

Results: A total of 150 DWI lesions were seen in 18 consecutive patients. Statistical analysis revealed no influence of thrombus properties or the technique of thrombectomy on the number of peripheral emboli. The number of peripheral emboli did not correlate with stroke severity at any point or change of stroke severity over the course.

Conclusion: In this small series no factor could be found that significantly influences the number of peripheral emboli. Peripheral emboli do not seem to have a strong impact on stroke severity.

327

A competitive environment improves procedural times in endovascular stroke treatment

Jessica Mertens¹, Raveena Singh¹, Arno Reich², Johanna Leinders³, Nina Cryns³, Martin Wiesmann⁴, Omid Nikoubashmann^{*5}

¹Klinik für Diagnostische und Interventionelle Neuroradiologie, Universitätsklinikum Aachen

²Universitätsklinikum Aachen, Neurologie, Klinik für Neurologie, Aachen, Deutschland

³Klinik für Diagnostische und Interventionelle Neuroradiologie, Universitätsklinikum Aachen, Aachen, Deutschland

⁴Klinik für Diagnostische und Interventionelle Neuroradiologie, Aachen, Deutschland

⁵Klinik für Diagnostische und Interventionelle Neuroradiologie, Aachen, Deutschland

Purpose: Despite numerous optimization attempts, time delays are still a relevant problem in stroke treatment. We prospectively analyzed whether a competitive environment resulted in improvement of procedural times.

Methods: We established a competition, which lasted six months, in which the fastest neurovascular team in terms of procedural times (image to revascularization) was displayed on a public board and rewarded with public praise. We prospectively evaluated procedural times of 496 patients who received endovascular stroke treatment 0) nine months before the competition, 1) during the competition, and 2-5) during four-time periods of each six months until two years after the competition.

Results: Median image to revascularization times improved significantly from 98 minutes before the competition to 85 minutes during the competition ($p=.005$) and remained stable with a median of 81 minutes two years after the competition ($p=.837$).

Conclusion: Our stroke competition helped to improve procedural times. As extrinsic incentives were shown to have rather short-time effects, our data suggest that improvement of procedural times was rather owed to raised awareness than to extrinsic incentives.

329

Increased hemorrhage risk due to combined systemic thrombolysis and dual antiplatelet inhibition after endovascular stroke treatment

Felix Hadler¹, Arno Reich², Martin Wiesmann³, Omid Nikoubashmann^{*4}

¹Klinik für Neurologie, Universitätsklinikum Aachen

²Universitätsklinikum Aachen, Neurologie, Klinik für Neurologie, Aachen, Deutschland

³Klinik für Diagnostische und Interventionelle Neuroradiologie, Aachen, Deutschland

⁴Klinik für Diagnostische und Interventionelle Neuroradiologie, Aachen, Deutschland

Purpose: Our aim was to investigate whether the combination of systemic thrombolysis and dual platelet inhibition results in an increased hemorrhage risk, as data in the literature dealing with this issue are inconclusive.

Methods: We retrospectively analyzed data from our prospectively maintained stroke registry with regards of hemorrhage rates (symptomatic intracerebral hemorrhage, sICH) of 401 consecutive patients, who received endovascular stroke treatment in our institution.

Results: 254 of 401 (63.3%) patients received systemic thrombolysis. 63 of 401 (15.7%) patients received carotid artery stenting (CAS) with dual platelet inhibition. Systemic thrombolysis per se was no risk factor for sICH with a 6% vs. 5% sICH-rate in patients with and without systemic thrombolysis ($p=0.354$). Hemorrhage was significantly more frequent in CAS patients and consecutive dual platelet inhibition with a sICH-rate of 14% in CAS patients with dual platelet inhibition vs. 4% in patients without CAS and dual platelet inhibition ($p<0.001$). The high hemorrhage rate of patients with CAS and dual platelet inhibition was mainly owed to the high hemorrhage rate of CAS patients with dual platelet inhibition and additional systemic thrombolysis: sICH-rate was 18% for CAS patients with dual platelet inhibition and additional systemic thrombolysis. sICH-rate was 5% for CAS patients with dual antiplatelet inhibition without systemic thrombolysis, albeit this effect did not reach statistical significance ($p=0.179$).

Conclusion: Our data imply that patients, who receive a combination of systemic thrombolysis and dual platelet inhibition, have an increased hemorrhage risk. If CAS is inevitable, the administration of systemic thrombolysis should be considered carefully, and vice versa.

331

Should CT Perfusion be performed before or after CT Angiography?

Maike Jäger^{*1}, Horst Urbach²

¹University of Freiburg, Klinik für Neuroradiologie, Freiburg, Deutschland

²Universitätsklinikum Freiburg, Klinik für Neuroradiologie, Freiburg, Deutschland

Purpose: In multimodal CT stroke protocol CT perfusion (CTP) usually is performed before CT angiography (CTA) to visualize location and volume of core infarction and tissue-at-risk. Aim of this study was to analyse if CTP also can be performed after CTA.

Methods: Two groups of patients with any kind of stroke symptoms were compared, whereby group 1 ($n=25$) received CTP before CTA and group 2 ($N=33$) received CTP after CTA. Quality of perfusion maps (rCBF, rCBV and Tmax) was rated by two independent examiners for both groups on a four-point Likert scale (1–4, not adequate-very good). Furthermore concentration-time curves and histograms of density at CTP-baseline and of perfusion maps were compared.

Results: Performing CTP after CTA shifts mean concentration-time curve to about 35HU higher values and histogram of density at baseline becomes marginally wider. Relative concentration-time curves normed to a common baseline do hardly differ. Therefore perfusion maps to estimate core infarction and tissue-at-risk do not change at all (Fig. 1). Also results of qualitative analysis were comparable for all perfusion maps mentioned above (mean Likert value group 1=3,78, group 2=3,80).

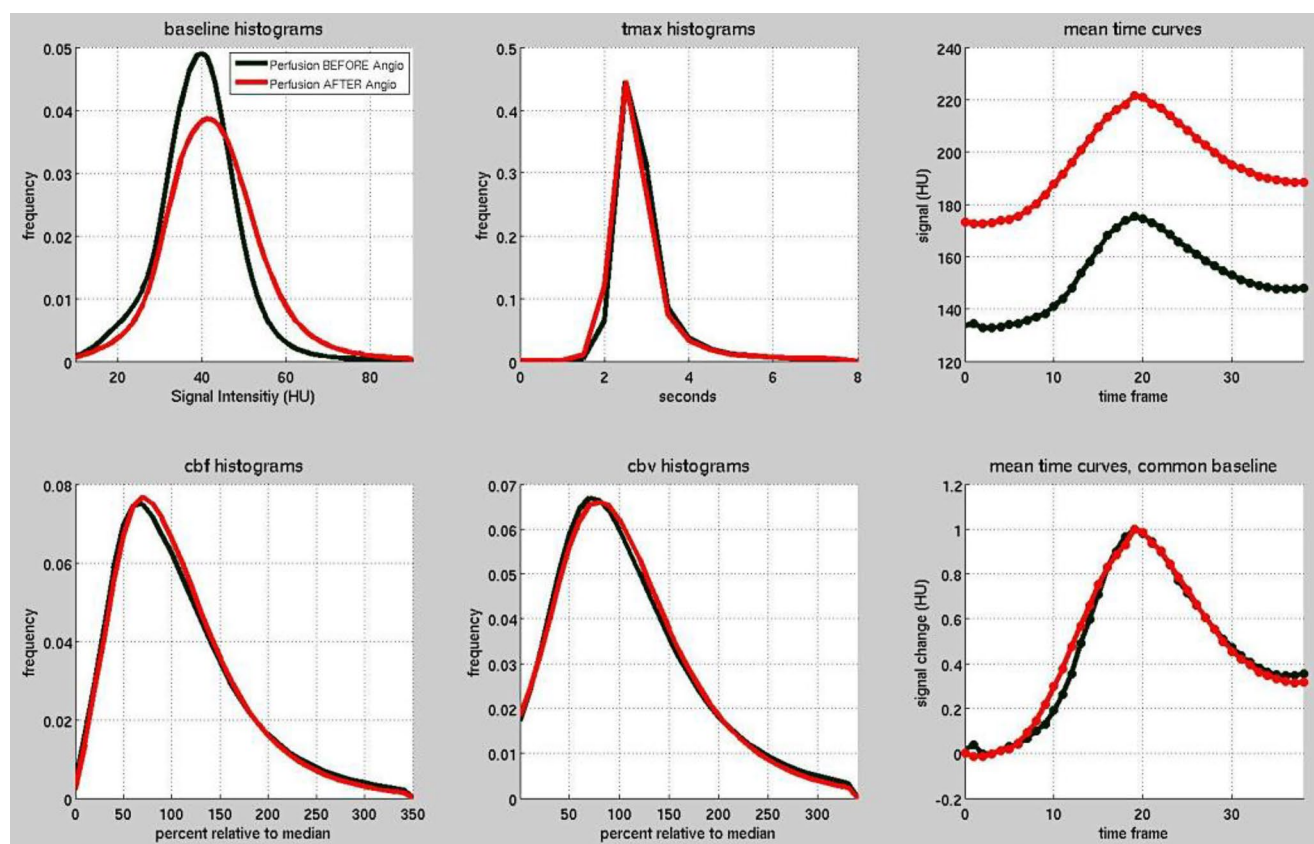


Fig. 1

Conclusion: There's no difference in performing CTP before or after CTA, so patients with suspected large vessel occlusion can receive CTA first to optimize time-management before thrombectomy.

346

Elevated Infarct Growth Rates in the Hyperacute Time Window: Why "Time is Brain" Still Matters

Gabriel Broocks¹, Furqan Rajput^{*2}, Uta Hanning³, Tobias D. Faizy⁴, Hannes Leischner⁵, Gerhard Schoen⁶, Susanne Siemonsen⁷, Peter Sporns⁸, Andre Kemmling⁹, Jens Fiehler¹⁰, Fabian Flottmann¹¹

¹Klinik und Poliklinik für Neuroradiologische Diagnostik und Intervention, Universitätsklinikum Hamburg-Eppendorf, Hamburg, Deutschland

²Radiologie, Universitätsklinikum Hamburg-Eppendorf, Klinik und Poliklinik für Neuroradiologische Diagnostik und Intervention, Universitätsklinikum Hamburg-Eppendorf, Klinik und Poliklinik für Neuroradiologische Diagnostik und Intervention, Stade, Deutschland

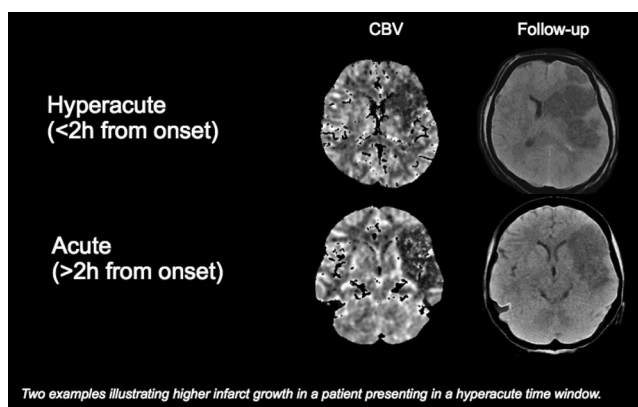


Fig. 1 Infarct growth from the early ischemic core to follow-up

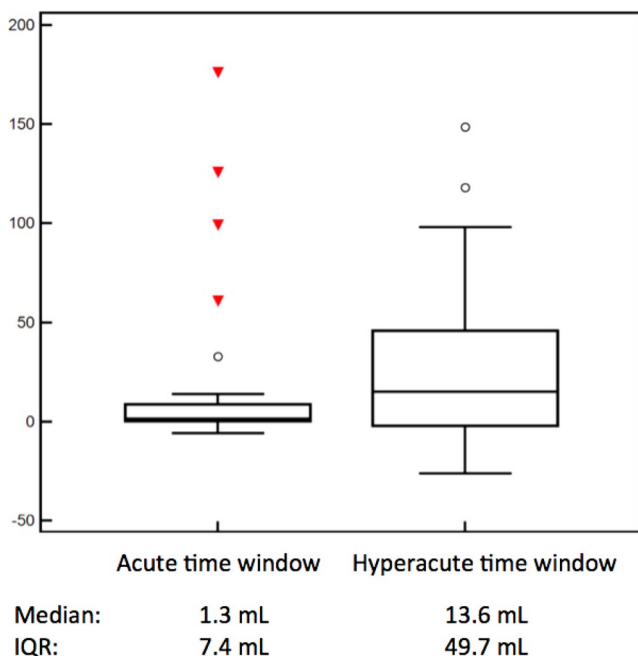


Fig. 2 Infarct growth from the early ischemic core to follow-up

³Klinik und Poliklinik für Neuroradiologische Diagnostik und Intervention, Universitätsklinikum Hamburg-Eppendorf, Institut für Klinische Radiologie, Uniklinikum Münster, Hamburg, Deutschland

⁴Universitätsklinikum Hamburg-Eppendorf, Klinik und Poliklinik für Interventionell und, Diagnostische Neuroradiologie, Hamburg, Deutschland

⁵Universitätsklinikum Hamburg-Eppendorf, Klinik und Poliklinik für Neuroradiologische Diagnostik und Intervention, Hamburg, Deutschland

⁶Universitätsklinikum Hamburg-Eppendorf, Zentrum für Experimentelle Medizin Institut für Medizinische Biometrie und Epidemiologie, Deutschland

⁷Klinik und Poliklinik für Neuroradiologische Diagnostik und Intervention, Universitätsklinikum Hamburg-Eppendorf, Hamburg, D

⁸Institut für Klinische Radiologie, Institut für Klinische Radiologie, Münster, Deutschland

⁹Institut für Klinische Radiologie, Universitätsklinikum Münster, UKSH Lübeck, Hamburg, Deutschland

¹⁰Diagnostikzentrum Univ.-Klinikum Hamburg-Eppendorf, Klinik und Poliklinik für Neuroradiologische Diagnostik und Intervention, Hamburg, Deutschland

¹¹Universitätsklinikum Hamburg-Eppendorf, Klinik und Poliklinik für Neuroradiologische Diagnostik und Intervention, Klinik und Poliklinik für Neuroradiologische Diagnostik und Intervention, Hamburg, Deutschland

Purpose: The acute growth of ischemic lesions has been described as nonlinear and lesion growth rates as highest during the earliest period after stroke onset. Therefore, we hypothesize that the time gap from imaging to revascularization results in a comparably higher infarct growth in patients presenting in a hyperacute time window.

Methods: 51 MCA-stroke patients with initial multimodal CT and follow-up-CT (FUCT) were included. All patients received successful endovascular recanalization. Two groups were assembled and distinguished according to their median time of symptom onset to imaging. To capture infarct growth the ASPECTS difference between initial CT and FUCT was assessed as well as volumetric infarct growth between lesion volume in the FUCT and volume of early ischemic core

Results: The median time from onset to imaging was 1.9 hours (interquartile range [IQR]: 1.6 hours). There was no significant difference in time from imaging to recanalization between both assembled patient groups ($p=0.3$, median 2.5 hours). The mean (SD) infarct growth by ASPECTS difference was 2.8 (2.3) in the hyperacute group and 1.6 (1.3) in the acute group ($p=0.03$). The median volumetric difference was 13.6 ml (IQR: 44 ml) in hyperacute and 1.3 ml (IQR: 7.4 ml; $p=0.3$) in acute patients, respectively.

Conclusion: The same time period from imaging to recanalization resulted in higher infarct growth in patients presenting in a hyperacute time window (<2 hours). The markedly increased range of infarct growth volume including partly reversible core lesions in the hyperacute group could be a sign of a distinctive infarct dynamic in the hyperacute time window.

350

First real-life experience with the SAVE thrombectomy technique confirms high effectiveness

Alexander Riabikin^{*1}, Omid Nikoubashman², Anastasios Mpotsaris², Daniel Behme³, Volker Maus³, Martin Wiesmann²

¹Institut für Diagnostische und Interventionelle Neuroradiologie, Aachen, Deutschland

²Uniklinikum RWTH Aachen, Aachen, Deutschland

³Universitätsklinikum Göttingen, Göttingen, Deutschland

Purpose: Various endovascular thrombectomy techniques for treatment of large vessel occlusions (LVO) in patients with acute ischemic stroke are being used. Recently, a novel approach of Stent retriever-Assisted Vacuum-locked Extraction (SAVE) has been published with promising results in a small series of patients with occlusions of the M1-segment of the middle cerebral artery (MCA). In this study we analyzed recanalization rates with the SAVE technique in a real life setting with occlusions not only of the M1 segment, but also the M2 segment and the carotid T.

Methods: We retrospectively analyzed 49 thrombectomies from two centers using the SAVE technique. Primary endpoint was successful first pass reperfusion with a modified TICI score of 3. Secondary endpoints were mTICI score at the end of the procedure, number of passes, time from groin puncture to reperfusion, embolization to new territories, postinterventional symptomatic intracranial hemorrhage, and clinical outcome at three months.

Results: First pass mTICI 3 reperfusion was achieved in 29 cases (59%), $\geq 2b$ in 38 cases (78%). A final mTICI score of 3 was achieved in 35 cases (71%), $\geq 2b$ in 48 cases (98%). Median number of passes was 1. Median time from groin puncture to recanalization was 34 minutes. No symptomatic intracranial hemorrhages were observed.

Conclusion: Our study confirms the high technical efficacy of the SAVE thrombectomy technique. We were able to achieve a considerable favorable first-pass reperfusion rate in a larger “real-life” cohort, including occlusions of the carotid T, the M1, and the M2 segment of the MCA.

358

Vascular anatomy may predict the success of primary direct aspiration

Anna Kyselyova^{*1}, Jens Fiehler¹, Jan-Hendrik Buhk¹, Andreas Frölich¹

¹Klinik und Poliklinik für Neuroradiologische Diagnostik und Intervention, Universitätsklinikum Hamburg-Eppendorf, Hamburg, Deutschland

Purpose: To evaluate factors predicting successful primary aspiration as part of the direct aspiration first pass technique (ADAPT).

Methods: 40 cases of thrombectomy in carotid-T, basilar and MCA occlusion, where ADAPT was applied as first technique were evaluated and the first pass TICI scores were assessed. TICI score $\geq 2b$ after primary aspiration was defined as “successful primary aspiration”. We evaluated the association between aortic arch type (1–3), clot perviousness (increase in HU on CTA compared with non-contrast CT), vessel diameter at the thrombus’ proximal end on CTA, access vessel tortuosity on DSA and CTA counting the number of reverse curves, clot density and clot length in non-contrast CT and patient age.

Results: Overall the successful primary aspiration was seen in 9 cases. Successful recanalization occurred significantly more frequently when vessel diameter at the thrombus’ proximal end was small (0.21 ± 0.02 mm; $p=0.04$). A trend in dependence of successful recanalization from vessel tortuosity was detected. No relation was evident for aortic arch type, clot perviousness, clot density and clot length. Patients with successful recanalization were younger (67.4 ± 15 versus 73.5 ± 11).

Conclusion: Anatomical factors such as vessel tortuosity and vessel diameter at the aspiration site appear to affect the likelihood of successful direct thrombaspiration as a first pass technique. If proven valid in a larger collective, these findings may help guide the recanalization approach.

378

Mechanical thrombectomy of M2 occlusions with distal access catheters using ADAPT

Dominik Grieb^{*1}, Martin Schlunz-Hendann¹, Katharina Melber¹, Björn Greling¹, Heinrich Lanfermann², Friedhelm Brassel¹, Dan Meila³

¹Sana Kliniken Duisburg, Klinik für Radiologie und Neuroradiologie, Duisburg, Deutschland

²Medizinische Hochschule Hannover, Institut für Diagnostische und Interventionelle Neuroradiologie, Hannover, Deutschland

³Johanna-Etienne-Krankenhaus, Department Interventionelle Neuroradiologie, Neuss, Medizinische Hochschule Hannover, Institut für Diagnostische und Interventionelle Neuroradiologie, Hannover, Deutschland

Purpose: The direct aspiration first pass technique (ADAPT) using distal access catheters (DAC) has proven to be an effective and safe endovascular treatment strategy of acute ischemic stroke with large vessel occlusions (LVO). Data about direct aspiration using DAC in M2 segment occlusions is limited. The purpose of our study is to assess the safety and efficacy of DACs in acute M2 occlusions using ADAPT with large bore (5Fr and 6Fr) aspiration catheters as the primary method for endovascular recanalization.

Methods: From January to December 2017, 24 patients with an acute ischemic stroke due to M2 occlusions underwent mechanical thrombectomy using ADAPT with DACs (SOFIA 5 French and Catalyst 6) as a frontline therapy. Of these 24 patients, 15 had an isolated M2 occlusion. Inclusion criteria were National Institutes of Health Stroke Scale (NIHSS) > 5 and modified Rankin Scale (mRS) score 3–5 at admission.

Results: Median NIHSS score was 14 at admission. Successful revascularization to mTICI 2b-3 with the ADAPT technique alone was achieved in 20 of 24 patients (83.3%) with mTICI 3 achieved in 15 of 24 (62.5%) patients. Additional stent retrievers were used in 3 patients and led to an overall successful revascularisation of the M2 thrombectomies of 87.5% (21/24). Median NIHSS at discharge was 4 and 13 of 24 (54.2%) patients had a mRS score 0–2 at three months. Symptomatic intracranial hemorrhage did not occur (0/24).

Conclusion: The results of our retrospective study suggest that DACs can safely and effectively be used for mechanical thrombectomy of acute M2 occlusions using ADAPT as a frontline therapy. High successful revascularization rates (87.5%) and good clinical outcome without symptomatic complications can be achieved.

389

Initial experience with delivery assist catheters as a new device class in mechanical thrombectomy in acute ischemic stroke

Johannes Pfaff^{*1}, Ralf Siekmann², Christian Ulfert³, Kai Koller⁴, Yogesh P. Shah⁴, Peter Arthur Ringleb⁵, Martin Bendszus⁶, Markus Möhlenbruch⁷

¹Universitätsklinikum Heidelberg, Abteilung für Neuroradiologie, Abteilung für Neuroradiologie, Heidelberg, Deutschland

²Haus 2, Ca Abt. Neuroradiologie, Haus 2, Ca Abt. Neuroradiologie, Kassel, Deutschland

³Universitätsklinikum Heidelberg, Abteilung für Neuroradiologie, Neuroradiologie, Heidelberg, Deutschland

⁴Klinikum Kassel, Kassel, Deutschland

⁵Universitätsklinikum Heidelberg, Neurologische Klinik, Sektion Vaskuläre Neurologie, Heidelberg, Deutschland

⁶Universitätsklinikum Heidelberg, Abteilung für Neuroradiologie, Heidelberg, Deutschland

⁷Universitätsklinikum Heidelberg, Abteilung für Neuroradiologie, Heidelberg, Deutschland

Purpose: To introduce a new device class “delivery assist catheter” and report first in vivo experience in acute ischemic stroke treatment.

Methods: Retrospective data collection and analysis of stroke databases of two comprehensive stroke centers focusing on technical and angiographic parameters—primary endpoint defined as reaching the occlusion with a large-bore reperfusion catheter—from patients receiving endovascular stroke treatment using an AXS Offset™ delivery assist catheter (Stryker, Fremont, CA, USA) between May 2017 and November 2017.

Results: Using the delivery assist catheter, a 6F catheter could be advanced to an intracranial occlusion for direct aspiration thrombectomy in 30 (88.2%) of a total of 34 patients (male: $n=14/34$ (41.2%), age in years: mean (SD): 75 (11), median baseline NIHSS: 16 (interquartile range (IQR): 12–21)). In 4/34 (11.7%) cases the occlusion could not be reached with the aspiration catheter because of a preceding non-occlusive arteriosclerotic plaque ($n=1$, 2.9%) or because of severe elongation and tortuosity of the arterial access route ($n=3$, 8.8%). After aspiration thrombectomy mTICI 2b–3 was reached in 14/30 (46.7%) patients. In 21/34 (61.8%) patients (additional) stent-retriever-manuevers (median: 1 (IQR: 0–2)) were needed. In 28/34 (82.3%) patients final mTICI 2b–3 could be achieved.

Conclusion: Delivery assist catheters to support large-bore reperfusion catheters for thromboaspiration in acute ischemic stroke are effective, in particular in case of vessel tortuosity and anatomic obstacles.

394

Imaging the spatio-temporal evolution of clots using an MRI compatible Chandler loop system

David Rudahl^{*1}, Olav Jansen², Christian Riedel³

¹UKSH Kiel, Klinik für Radiologie und Neuroradiologie, Kiel, Deutschland

²Direktor des Instituts für Neuroradiologie, Klinik für Radiologie und Neuroradiologie, Kiel, Deutschland

³University Medical Center Schleswig-Holstein, Department of Neuroradiology, Kiel, Deutschland

Purpose: To investigate how clots form in an in-vitro model of carotid artery blood flow.

Methods: An MRI compatible Chandler loop system was built in order to observe the formation of appositional blood clots as seen in patients suffering from acute ischemic stroke. The Chandler loop tubing used for modelling cervical arterial blood flow was filled with citrated human whole blood and recalcified immediately before starting the rotational movement of the tubing. MR imaging using thin slice T2-weighted 2D scans was repeated at constant time intervals of 10 minutes for up to 1.5 hours of Chandler loop operation. The small stack of dynamical T2-weighted images was subsequently analyzed for clot size and contrast dynamics using OsiriX.

Results: Clots in the Chandler loop system always start to form at the blood-air interfaces within the tubing. Within the first 5–10 minutes, a heterogeneously contrasted clot head forms. Within the following 20 minutes, the clot grows to maximum length. The tail of the clot constantly loses signal during this time. Clot contrast reaches a steady state after 40–50 minutes after the start of the Chandler loop.

Conclusion: To our knowledge, this is the first time that a detailed description of the spatio-temporal evolution of appositional clot models has become available. Our technique is of particular importance for studies generating experimental clots for in vitro recanalization experiments. MRI scanning of a clot under development allows for targeted clot generation.

396

Efficiency of mechanical thrombectomy depends on clot configuration

Susan Klapproth^{*1}, Olav Jansen², Christian Riedel³

¹UKSH Kiel, Klinik für Radiologie und Neuroradiologie, Kiel, Deutschland

²Direktor des Instituts für Neuroradiologie, Klinik für Radiologie und Neuroradiologie, Kiel, Deutschland

³University Medical Center Schleswig-Holstein, Department of Neuroradiology, Kiel, Deutschland

Purpose: To investigate, how the spatial configuration of clots affects the number of recanalization maneuvers.

Methods: In 105 patient suffering from acute ischemic stroke with proximal cerebral artery occlusion who underwent mechanical thrombectomy, initial thin slice NECT reconstructions were registered with CT angiography images. Clots were segmented from the NECT scans and overlaid on a 3D visualization of the brain vessels. Using these post-processed images, clots were categorized based on their spatial configuration. These categories were subsequently correlated with the numbers of mechanical thrombectomy maneuvers used in each case.

Results: In 17 patients (16%) three or more recanalization maneuvers (median: 4) were needed for the final thrombectomy result. In all of these cases, clots were either found to be long with multiple branches (7 cases), or they were either segmented with short fragments or short and particularly small in diameter. In one of the 105 thrombectomy cases, no clot could be segmented. In this case, it took 4 stent retriever maneuvers in order to recanalize the mainstem of the middle cerebral artery with a remaining stenosis.

Conclusion: Proximal cerebral artery occlusions that require multiple thrombectomy maneuvers are either characterized by very long and complex configured clots with multiple branches, or they might be caused by very tiny and often segmented clots. While in the first category fragmentation during thrombectomy might cause multiple passes, tiny and segmented clots are typical for underlying intracranial arterial stenosis.

410

Can silicone models replace animal models in hands-on training for endovascular stroke therapy?

Johanna Sandmann^{*1}, Franziska Müschenich², Alexander Riabikin³, Martin Kramer⁴, Martin Wiesmann⁵, Omid Nikoubashman⁶

¹Universitätsklinikum Aachen, Klinik für Diagnostische und Interventionelle Neuroradiologie, Aachen, Deutschland

²Klinik für Diagnostische und Interventionelle Neuroradiologie, Aachen, Deutschland

³Institut für Diagnostische und Interventionelle Neuroradiologie, Aachen, Deutschland

⁴Klinikum Veterinärmedizin Justus Liebig Universität, Gießen, Deutschland

⁵Klinik für Diagnostische und Interventionelle Neuroradiologie, Aachen, Deutschland

⁶Klinik für Diagnostische und Interventionelle Neuroradiologie, Aachen, Deutschland

Purpose: Since thrombectomy has become a standard treatment technique for stroke, there is a great demand for excellent training of interventionalists. We provide practical courses on both a silicone model and a porcine model and conducted a survey to evaluate whether ex-vivo training models could replace in-vivo models.

Methods: 92 neurointerventionalists participating in 33 trainings were included in our survey using a semi-structured questionnaire.

Results: The level of experience in thrombectomy maneuvers was almost balanced in our sample (55% experienced, 45% less experienced participants). Silicone models were regarded as useful training tools regardless of the participants' experience ($p=.455$): 85% of less experienced and 78% of experienced participants thought that a silicone model is a useful introduction to animal models. 94% of participants thought that training on animal models was helpful and necessary, regardless of their experience on humans ($p=.949$). After joining this course, 92% of all participants felt well prepared to perform thrombectomies in humans. **Conclusion:** Even experienced participants benefit from silicone models. Silicone models are a good preparation for animal models but cannot replace them. Categorizing participants depending on their experience and their individual needs before practical training may allow for an efficient endovascular training.

428

Preventing vessel perforations in endovascular thrombectomy: Feasibility and safety of passing the thrombus with a microcatheter without microwire: The wireless-microcatheter technique

Annika Keulers^{*1}, Omid Nikoubashmann², Anastasios Mpotsaris³, Martin Wiesmann⁴

¹Department of Diagnostic and Interventional Neuroradiology, University Hospital RWTH Aachen, Aachen, Deutschland

²Klinik für Diagnostische und Interventionelle Neuroradiologie, Aachen, Deutschland

³Klinik für Diagnostische und Interventionelle Neuroradiologie, Aachen, Deutschland

⁴Klinik für Diagnostische und Interventionelle Neuroradiologie, Aachen, Deutschland

Purpose: To place a stent retriever for thrombectomy the thrombus has to be passed first. For this maneuver usually a microwire is being used. As an alternative a wireless microcatheter (MC) can be used to pass the thrombus. We compared the feasibility and complication rates of both techniques.

Methods: Retrospective non-randomized analysis of 110 consecutive patients suffering from acute ischemic stroke in the anterior circulation, in whom video recordings of mechanical thrombectomies were available. In total, 203 attempts of mechanical recanalization were performed. **Results:** Successful recanalization (TICI 2b-3) was achieved in 97.3% of patients. In 71.8% of attempts the thrombus was successfully passed using a wireless MC only. When a microwire was used initially, thrombus passage was successful in 95.3% of attempts. Complication rates for angiographically visible severe subarachnoid hemorrhage were 6.1% when a microwire was used versus 0% when a wireless MC was used ($p<0.001$). Complication rates for angiographically occult, circumscribed subarachnoid contrast extravasation observed on postinterventional CT scans were 18.2% when a microwire was used versus 4.5% when a wireless MC was used ($p<0.001$).

Conclusion: In most cases of mechanical recanalization the thrombus can be passed with a wireless MC instead of a microwire. This method significantly reduces the risk for vessel perforation and subarachnoid hemorrhage and should therefore be used whenever possible.

458

Effects of intermediate catheter evolution on technical outcome of mechanical thrombectomy—a comparison of the performance of two distal access catheters in mechanical thrombectomy

Markus Le Blanc¹, Volker Maus², Christoph Kabbasch¹, Franziska Dorn³, De-Hua Chang¹, Thomas Liebig³, Anastasios Mpotsaris⁴, Jan Borggrefe¹

¹Universitätsklinik Köln, Institut für Diagnostische und Interventionelle Radiologie, Köln, Deutschland

²Universitätsmedizin Göttingen, Abteilung Neuroradiologie

³Klinikum der Universität München, Institut für Neuroradiologie

⁴Uniklinik Aachen, Klinik für Diagnostische und Interventionelle Neuroradiologie

Purpose: Fast and secure access to intracranial vessel occlusion is essential for mechanical thrombectomy (MT) in treatment of acute ischemic stroke (AIS). We compared two intermediate distal access catheters (DACâ (C1) and SOFIAâ (C2)) for procedural speed and safety of MT as well as clinical outcome at discharge and after 90 days.

Methods: 398 consecutive patients receiving MT with C1 or C2 for the treatment of AIS between 09/2010 and 06/2016 were analysed retrospectively, using a propensity score matched cohort. Baseline characteristics, clinical outcome and procedural factors were analyzed.

Results: 282 patients (70.9%) underwent MT with C1 and 116 patients (29.1%) with C2. MT with C2 was faster with an average duration of 69.8 ± 51 minutes (mean \pm SD) compared to 80.6 ± 54 minutes with C1 ($p<0.05$). The average number of necessary stent-retriever maneuvers was significantly lower with C2 (1.8 ± 1.7 vs. 3.2 ± 2.5 , $p<0.0001$). Successful TM with aspiration only yielded higher modified Thrombolysis in Cerebral Infarction rates (mTICIb/III 69.9% vs. 31.5% , $p<0.0001$) with C2. Modified Rankin Scale (mRS) at discharge was significantly lower with C2 (3.5 ± 1.9) vs. C1 (3.9 ± 1.7 , $p<0.05$). No significant differences of mRS 90 were observed.

Conclusion: The use of C2 resulted in reduced procedural times with less stent-retriever maneuvers. Clinical outcome at discharge was better for C2 catheters, without significant difference of outcome after 90 days.

459

Metric based virtual reality training—can it be applied to neurothrombectomy?

Thomas Liebig^{*1}, Markus Holtmanspoetter², Robert Crossley³, Johan Lindkvist⁴, Patrick Henn⁵, Lars Loenn⁶, Anthony Gallagher⁷

¹Ludwig-Maximilians-Universität München, University Hospital, Institute of Neuroradiology, München, Deutschland

²Rigshospitalet, University of Copenhagen, Denmark, Denmark

³North Bristol NHS Trust, Southmead Hospital, Westbury-on-Trym, Bristol

⁴Mentice AB, Gothenburg

⁵University College Cork, Cork, Ireland

⁶National Hospital, Copenhagen University, Copenhagen, Denmark

⁷School of Medicine, University College Cork, Cork, Ireland

Purpose: To evaluate the impact of metric based virtual reality training in neurothrombectomy

Methods: The authors in cooperation with MENTICE AB (Gothenburg, Sweden) have created a metric based reference approach to treat an M1-occlusion using 3D-representation of a real-patient DICOM dataset on a high-fidelity endovascular virtual reality (VR) simulator used for hands-on procedural training (VIST). The reference approach was based on recommendations of related medical societies and given accreditation by experienced INRs from 7 countries in a DELPHI-panel. As a next

step, physicians of different levels of training were asked to perform the procedure. Completed steps as well as critical errors were recorded by the VIST. The resulting datasets underwent statistical evaluation.

Results: A realistic representation of the real case was possible with the VIST. The concordance between the physical behavior of devices and visual appearance of the anatomy in the VR simulator, was felt to be sufficiently high by all operators. Statistical evaluation of the datasets of all tested operators proved that the metrics for this reference approach were able to discriminate between consultant level and trainees and demonstrated significant improvement of trainees over time and before and after training in a 2day course.

Conclusion: It is feasible and practical to take CT or MR DICOM data from a real stroke case and re-create it in VR. Metric-based simulation training can supplant parts of the learning curve for endovascular procedures. This has been shown previously for a number of surgical procedures and also applies to neurothrombectomy. This approach to training is conceptually appealing and represents a paradigm shift in education and training.

462

In vivo aspiration analysis of the ADAPT technique in relation to vessel size and catheter position.

Hannes Schwenke^{*1}, Gabriel Broocks², Uta Hanning³, Peter Sporns⁴, Peter Schramm⁵, Andre Kemmling⁶

¹UKSH Campus Lübeck, Institut für Neuroradiologie, Lübeck, Deutschland

²Klinik und Poliklinik für Neuroradiologische Diagnostik und Intervention, Universitätsklinikum Hamburg-Eppendorf, Hamburg, Deutschland

³Klinik und Poliklinik für Neuroradiologische Diagnostik und Intervention, Universitätsklinikum Hamburg-Eppendorf, Institut für Klinische Radiologie, Uniklinikum Münster, Hamburg, Deutschland

⁴Institut für Klinische Radiologie, Institut für Klinische Radiologie, Münster, Deutschland

⁵UKSH Universitätsklinikum Schleswig-Holstein Campus Lübeck, Institut für Neuroradiologie, Lübeck, Deutschland

⁶University Hospital Schleswig-Holstein, Lübeck, Neuroradiology, Lübeck, D

Purpose: ADAPT (A Direct Aspiration First Pass Technique) is a widely used thrombectomy technique, however, how frequently direct

clot aspiration occurs remains unclear. The aim was to obtain in vivo aspiration data of ADAPT in relation to catheter size and position.

Methods: In 27 consecutive patients with M1-MCA occlusion, ADAPT was performed with pump assisted aspiration (Pump MAX with -100 kPa, Penumbra) using an ACE68 reperfusion catheter with 6F long sheath (Neuron MAX, Penumbra) for distal access. During withdrawal of the clot-engaged ACE68, aspiration was measured by weight change (A&D scale, 10 datapoints per second) while recording the position of the catheter tip during road-map fluoroscopy (Fig. 1a,b). Vacuum at the tip was calculated by area and pressure.

Results: The average aspiration rate of ACE68 was 3.05 ml/s, of Neuron MAX 3.27 ml/s. During ACE68 withdrawal, free aspiration occurred with the catheter tip at the M1 segment in 4% (n=1), 11% (n=3) at the carotid T, 11% (n=3) at the level of the cavernous carotid. In 74% (n=20), free aspiration was not observed during the entire withdrawal when aspiration was then switched to Neuron Max. In 5% (n=1) free aspiration occurred with the sheath tip at the petrous ICA

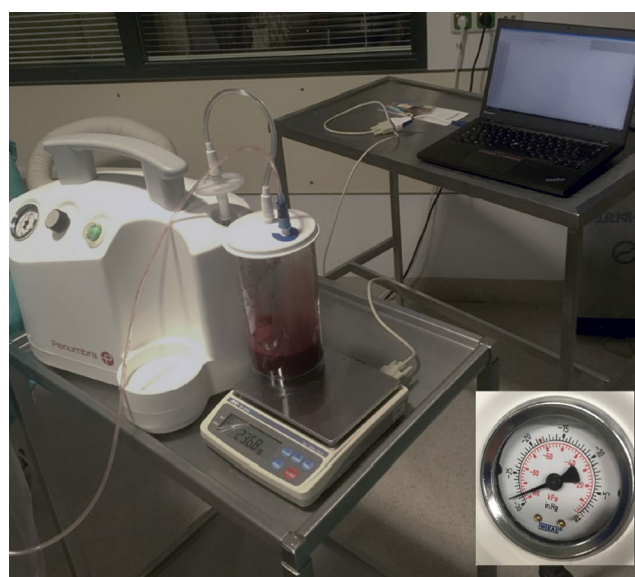
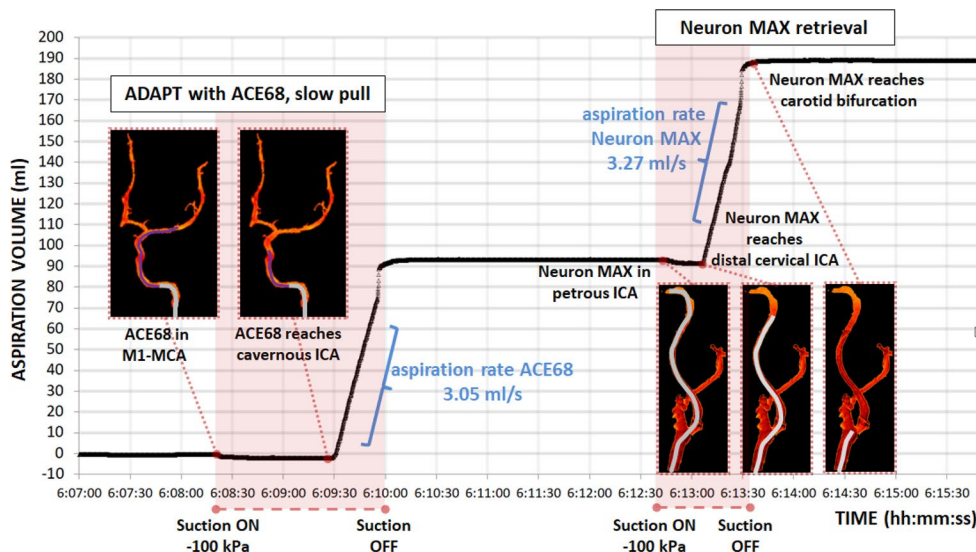


Fig 1 Experimental Setup to acquire aspiration volume per time during aspiration thrombectomy

Fig 2 Aspiration volume per time during aspiration thrombectomy in relation to catheter position within vessel



segment, 15% ($n=3$) at the distal cervical segment, 80% ($n=13$) at the middle cervical segment.

Conclusion: Clot aspiration in ADAPT rarely occurs directly. Larger vessel diameters or higher vacuum at the tip may contribute to direct clot aspiration.

463

Fast Stroke Treatment without Microcatheter and Wire—Correlation of Success and Cavernous ICA Anatomy

Joe-Iven Watkinson^{*1}, Fritz Wodarg², Friederike Austein¹

¹Klinik für Radiologie und Neuroradiologie, Universitätsklinikum Schleswig-Holstein, Kiel, Deutschland

²Klinik für Radiologie und Neuroradiologie, Klinik für Radiologie und Neuroradiologie, Kiel, Deutschland

Purpose: Due to improved devices and techniques endovascular stroke treatment becomes faster year by year. The so-called ADAPT Technique can be fast and successful in many cases. For saving time and costs it is possible to do aspiration-catheter-only (ACO) navigation without additional microcatheter and wire. The main obstacle for success of the technique is the orifice of the ophthalmic artery (OAO). The aim of this analysis was to evaluate whether the preinterventional CTA scan allows an estimation of the possible success of this approach.

Methods: We created a visual score at sagittal CTA slices of the cavernous ICA and defined 3 sectors (S1, S2, S3) where the OAO can be found. Four interventionalists tried 80 ACO approaches in 75 stroke cases with two different catheters. Approaches were rated as “easy”, “difficult” or “not-possible” and correlated with sectors.

Results: The OAO was located in S1 in 5 (6%), in S2 in 46 (58%) and in S3 in 29 (36%) cases. ACO approach was overall possible in 59% cases (S1=100%, S2=44%, S3=76%). The approaches were easy in 60% of S1, 24% of S2 and 66% of S3, and difficult in 40% of S1, 20%

Fig. 1

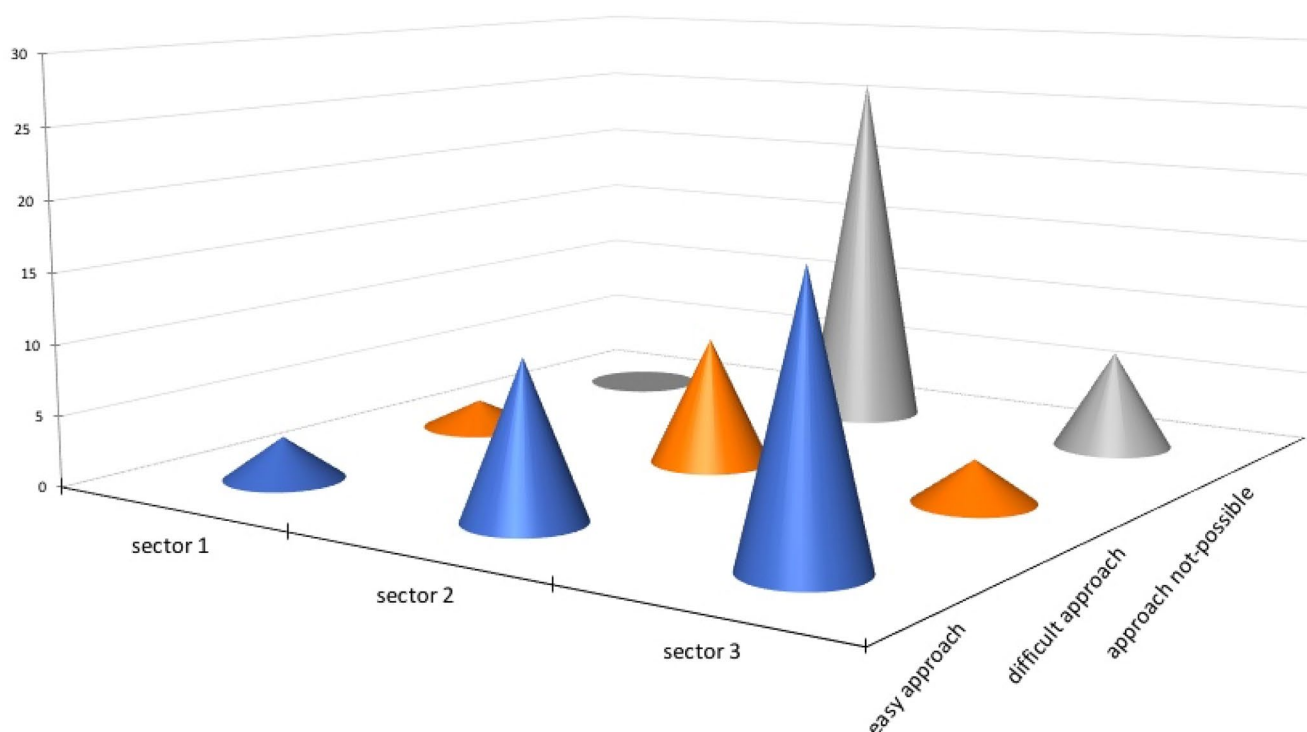
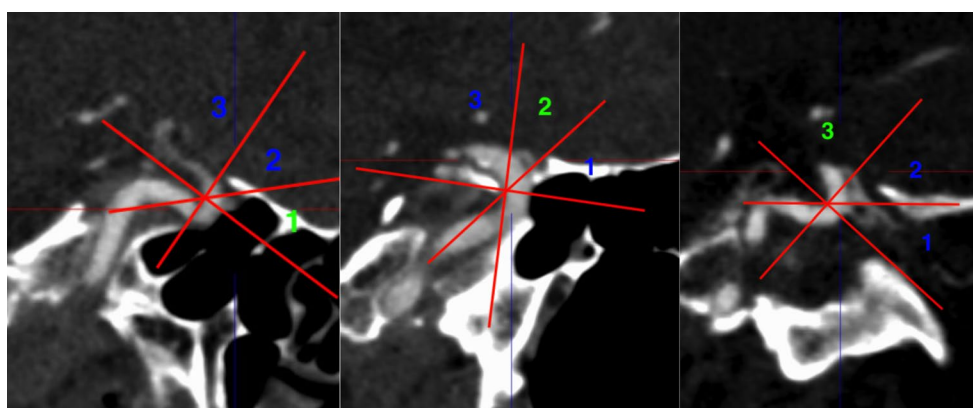


Fig. 2

of S2 and 10% of S3. Overall the correlation between approaches and defined sectors were moderate (Pearson's $\Phi=0.462$, $p=0.002$).

Conclusion: An OAO located in sector 1 or 3 seems to offer a good chance to reach the intracranial circulation with ACO. Our defined score may be helpful to decide whether to use additional microcatheter and wire for the first approach or not.

466

Intracranial stenting in the endovascular therapy of acute ischemic stroke

Maria Boutchakova^{*1}, Lukas Meyer², Maria Politi², Maria Alexandrou², Christian Roth², Andreas Kastrup³, Panagiotis Papanagiotou¹

¹Klinikum für Diagnostische und Interventionelle Neuroradiologie, Klinikum Bremen Mitte, Bremen, Deutschland

²Klinikum für Diagnostische und Interventionelle Neuroradiologie, Klinikum Bremen Mitte, Bremen, Deutschland

³Neurologische Klinik, Klinikum Bremen Mitte, Bremen, Deutschland

Purpose: The purpose of this study is to investigate the efficacy and safety in the setting of acute permanent intracranial stenting after failed mechanical thrombectomy (MT) in acute ischemic stroke.

Methods: We retrospectively reviewed records of patients treated with intracranial stents for acute ischemic stroke at our department between 2013 and 2017. Clinical, angiographic, and neuroimaging data were analyzed. Neurological status was evaluated with the NIHSS score at admission and with the mRS score at admission and discharge.

Results: 42 Patients underwent permanent intracranial stenting after MT for acute ischemic stroke. 17 of the stents were self-expanding, 25 were drug eluting. Occlusions were located either in the anterior or posterior circulation. 50% (21/42) of the Patients were started on IV tPA prior to interventional therapy. GP IIb/IIIa inhibitors were administered periprocedural to prevent in-stent-thrombosis.

Technical success and revascularization was achieved in 93% (39/42). The early good functional outcome of mRS \leq 2 at discharge was 36% (15/42). In-hospital mortality was 17% (7/42). Symptomatic intracranial hemorrhage occurred in 2,3% (1/42). Post procedural transcranial sonography and MRA revealed 20,5% stent-occlusions (7/34).

Conclusion: Acute permanent intracranial stenting after failed mechanical thrombectomy is feasible, effective and has a low risk of reperfusion-related hemorrhage.

Interventional Neuroradiology: Thrombectomy Technical

114

Comparison of endovascular device sizing based on conventional two-dimensional measurements and using numerical simulation software

Johanna Ospel^{*1}, Daniel Zumofen¹, Gregory Gascou², Vincent Costalat², Kristine Blackham¹

¹Universitätsspital Basel, Basel, Switzerland

²Chu Montpellier, Montpellier, France

Purpose: To evaluate whether use of a computer based simulation model results in selection of different device dimensions than based on conventional methods.

Methods: In a retrospective multi-center cohort study of 41 cases undergoing aneurysm treatment using the Pipeline Embolization Device

(PED), device dimensions selected by experienced neurointerventionalists based on manual 2D measurements were compared to PED dimensions calculated by the simulation model. Agreement between the different calculation methods was evaluated by calculating Cohen's Kappa.

Results: Software based measurements resulted in different device dimension suggestions in 92.7% (38/41 cases). Agreement between conventional and computer based measurements was low (Cohen's $K=0.125$ for length; $K=0.239$ for diameter, $p<0.05$).

Conclusion: The low agreement between conventional and software based calculations confirms that the choice of proper device dimensions is challenging. Virtual preimplantational simulation of multiple device sizes and prediction of their endovascular behavior potentially allows a decrease in procedure time, cost, and uncertainty related to proper device sizing by accelerating the neurointerventionalist's learning curve and confidence. This work is part of continuing evaluation of the simulation and its translation into clinical practice.

Reference

1. https://sim-and-cure.com/wp-content/uploads/2018/01/91aa70_01f-d87e567ec49e9907a061bd780c76b.pdf

125

Occlusion of a mural Vein of Galen Malformation in a 10 Month old Boy with three WEB 17 and one Coil

Frank Runck^{*1}, Christoph Maurer¹, Markus Bode², Ansgar Berlis³

¹Klinik für Diagnostische Radiologie und Neuroradiologie, Klinikum Augsburg, Augsburg, Deutschland

²Klinik für Neurochirurgie, Klinikum Augsburg, Augsburg, Deutschland

³Klinikum Augsburg, Klinik für Diagnostische Radiologie und Neuroradiologie, Augsburg, Deutschland

Case: We present a case of a 10 mo old male infant with severe motoric developmental delay first diagnosed at the age of 8 mo. Head circumference was enlarged. An MRI showed a Vein of Galen-malformation (VGAM) with a heavily dilated median proencephalic vein to a transverse diameter of 5.4 cm leading to compression of the ventricular aqueduct and consecutive internal hydrocephalus.

Angiography confirmed a mural type VGAM with three feeding arteries arising from the posterior cerebral arteries. Due to the short length of the feeding arteries occlusion of the feeding vessels with coils was not possible due to coil dislocation into the dilated vein. Embolization of the feeding vessels was then performed with WEB SL 17 (Terumo Microvention, California). The use of the new WEB SL 17 allows access with a Via 17 microcatheter (Terumo Microvention, California) even to very small arteries. In two arteries complete occlusion was accomplished with the WEB device alone, in one artery complete occlusion could only be achieved after additional deployment of one coil. A ventriculoperitoneal shunt was implanted the day after embolization. Postprocedural angiography and cerebral MRI the day after embolization showed complete occlusion.

On follow-up imaging 3 mo after embolization persistent occlusion was confirmed. MRI showed shrinkage of the aneurysmal sack with a residual transverse diameter of 4.3 cm. Neurological symptoms improved significantly.

Conclusion: Endovascular occlusion of a mural type VGAM with the new WEB SL 17 device might be a fast alternative to coil or glue embolization.

Retrieval of migrated volume coils using different clot retrievers in a porcine model.

Andreas Simgen^{*1}, toshiki tomori², Ruben Mühl-Benninghaus³, Hagen Bomberg⁴, Umut Yilmaz⁵, Heiko Körner⁵, Matthias W. Laschke⁶, Michael Menger⁷, Wolfgang Reith⁸

¹Universitätsklinikum des Saarlandes, Klinik für Neuroradiologie, Homburg, Deutschland

²Klinik für Diagnostische und Interventionelle Neuroradiologie, Universitätsklinikum des Saarlandes, Homburg/Saar, Deutschland

³Universitätsklinikum des Saarlandes, Klinik für Neuroradiologie, Homburg, D

⁴Universitätsklinikum des Saarlandes, Klinik für Anästhesiologie

⁵Klinik für Neuroradiologie, Klinik für Neuroradiologie, Homburg, Deutschland

⁶Institut für Klinisch-Experimentelle Chirurgie, Medizinische Fakultät der Universität des Saarlandes, Homburg/Saar, Homburg, Deutschland

Fig. 1 Micro-CT fluoroscopy of the applied clot retrievers transversal and longitudinal; Trevo ProVue, Solitaire FR, 3D-Separator, ERIC



Fig. 2 Roadmap images of the Trevo ProVue (2) and 3D-Separator (3). The devices are deployed so that the coil is located in the distal two-thirds. The thin arrows indicate the distal and proximal markers of the devices. The thick arrow indicates the displaced coil in a branch of the axillary artery



Devices	Retrieval rates [%]	Duration of retrieval [sec]	Retrieval attempts [n]	Vasospasm [n]	Perforation [n]	Dissection [n]	Entrapment at IC [n]	Inadvertent deployment [n]
Trevo ProVue	90	145.26 ± 35.48	1.5 ± 0.71	0	0	0	2	0
Solitaire FR	80	156.20 ± 44.70	1.4 ± 0.69	0	0	0	3	1
3D-Separator	90	148.10 ± 40.56	1.4 ± 0.69	0	0	0	3	0
ERIC	50	243.84 ± 42.57*#	2.5 ± 0.73*#	0	0	0	1	0

IC = Intermediate Catheter.

Duration of retrieval: * $p < 0.001$ vs. TREVO ProVue. # $p < 0.001$ vs. Solitaire FR. ' $p < 0.001$ vs. 3D-Separator.

Retrieval attempts: * $p = 0.02$ vs. TREVO ProVue. # $p = 0.008$ vs. Solitaire FR. ' $p \leq 0.008$ vs. 3D-Separator.

Tab. 1 Overview of results comparing the applied clot retrievers

⁷Saarland University, Institute of Clinical & Experimental Surgery, Institut für Klinische und Experimentelle Chirurgie, Homburg, Deutschland

⁸Klinik für Neuroradiologie, Neuroradiologie, Homburg, Deutschland

Purpose: During endovascular treatment of intracranial aneurysms using coils, migration is a serious complication that increases neurological morbidity. The aim of this experimental study was to assess the effectiveness and complications of retrieving volume coils with different, currently available clot retrievers in a porcine model.

Methods: Volume coils of 3-D shape and different sizes were placed in the axillary artery of pigs. By means of 4 different clot retrievers (Trevor ProVue; Solitaire FR; 3D-Separator; ERIC) a total of 40 retrieval maneuvers (10 per retriever) were performed by deploying the retrievers within the migrated coils and trying to trap parts of the coils by advancing the microcatheter. Retrieval rates, retrieval duration, retrieval attempts, and complications were assessed.

Results: Overall coil retrieval was successful in 31 of 40 cases (77.5%). Retrieval rates using the Trevor ProVue (90%), Solitaire FR (80%), and the 3D-Separator (90%) were higher than when using the ERIC (50%). Duration of retrieval and retrieval attempts were significantly higher using the ERIC ($p < 0.05$). Complications like inadvertent deployment were only observed in one case using the Solitaire FR. Additional entrapment of the coil-retriever complex at the intermediate catheter was seen in 9 cases (22.5%). There was no case of vasospasm, perforation, or dissection.

Conclusion: Retrieval of migrated volume coils using new-generation clot retrievers is a feasible and effective method. Retrieval rates and duration with the Trevor ProVue, Solitaire FR, and 3D-Separator are superior when compared to the ERIC.

142

Evaluation of Acute Occlusion of Dual-Layer Stents in Clinical Routine Follow Up

Frank Runck^{*1}, Christoph Maurer¹, Ansgar Berlis²

¹Klinik für Diagnostische Radiologie und Neuroradiologie, Klinikum Augsburg, Augsburg, Deutschland

²Klinikum Augsburg, Klinik für Diagnostische Radiologie und Neuroradiologie, Augsburg, Deutschland

Background: A recent work by Yilmaz et al. (Stroke 2017) reports occlusion rates of 50% within 72 hours after emergency treatment of tandem lesions with the Casper dual layer stent.

Methods: 106 patients (43 acute stroke, 63 elective stenting) were retrospectively analysed. Ultrasound examinations (CDDI) were available for 38 with acute stroke and 40 patients with elective carotid artery stenting. Inclusion of more patients is planned.

Results: In the subgroup with elective stenting no early stent occlusion or significant in stent thrombosis occurred. In the subgroup with emergency stenting 2 intraprocedural and 1 early stent occlusion 4 hrs after stent placement occurred. All of these were successfully recanalised. 7 emergency patients showed intraprocedural in stent-thrombosis higher than 50%. Of these patients 4 had initially received rtPA, Tirofiban was administered in 2 patients after stent deployment and 4 patients received a combination of both. In all patients follow up-CDDI documented no stent occlusion. In 4 emergency patients symptomatic intracranial hemorrhage (sICH) occurred (one receiving rtPA and 3 tirofiban). Tirofiban was used in 21 of all emergency patients. 13 emergency patients (30%) received intracranial thrombectomy, as well. Tirofiban was used in 21 of all emergency patients.

Conclusion: In our institution after emergency placement of dual layer stents in 43 patients intra- or early postprocedural stent occlusion occurred in only 3 patients (7%) and is significantly lower than previously

reported, most likely due to more aggressive antiplatelet therapy. The rate of symptomatic ICH is not higher than in previous reported.

182

Treating high flow direct carotid cavernous fistula using covered stent grafts

Bashir A. Husain^{*1}, Sebastian Arnold², Sebastian Herbert¹

¹Städtisches Klinikum Karlsruhe, Karlsruhe, Deutschland

²Städtisches Klinikum Karlsruhe, Landau, Deutschland

Purpose: reporting on case series of high flow direct carotid cavernous fistulas (DCCFs) treated successfully using covered stent grafts (CSGs), three of them as a first choice option.

Methods: case series of 4 patients. 2 patients with a traumatic DCCF, one with spontaneous DCCF and one with an iatrogenic DCCF. In 3 of 4 patients the CSG was used as a first choice to occlude the fistula. We deployed a balloon expandable covered stent Begraft (Bentley Innomed GmbH). Mid-term results available on 3 of 4 patients both MRI and DSA.

Results: the stent deployment was technically successful in 4 of 4 patients. The midterm results of 3 of 4 patients who were treated using a CSG as a first choice demonstrate a persistent occlusion of the fistula while preserving the internal carotid artery (ICA) with no evidence of relevant restenosis or endoleak. The stiffness and rigidity of the Begraft were suitable for controlled and proper navigating through elongated vessels to reach the cavernous segment of the ICA.

Conclusion: covered stent grafts can be considered as safe and feasible in treating high flow DCCFs. Furthermore, we support the idea that the device can be deployed as a first choice of treatment.

194

Treatment strategies for recurrent aneurysms after Woven Endobridge embolization: a multicentric study with mid-term follow-up

Lukas Görtz^{*1}, Eberhard Siebert², Franziska Dorn³, Jan Borggreve⁴, Thomas Liebig⁵, Christoph Kabbasch⁶

¹Universitätsklinikum Köln, Zentrum für Neurochirurgie, Köln, Deutschland

²Charite Berlin, Institut für Neuroradiologie, Klinik für Neuroradiologie, Berlin, Deutschland

³Klinikum der Universität München—Campus Großhadern, Institut für Klinische Radiologie, Abteilung für Neuroradiologie, München, Deutschland

⁴Universität zu Köln, Institut für Diagnostische und Interventionelle Radiologie, Köln, Deutschland

⁵Ludwig-Maximilians-Universität München, University Hospital, Institute of Neuroradiology, München, Deutschland

⁶Uniklinik Köln, Abteilung für Radiologie und Neuroradiologie, Institut für Diagnostische und Interventionelle Radiologie, Köln, Deutschland

Purpose: Woven Endobridge (WEB) embolization is a safe and efficient technique for endovascular treatment of wide-necked intracranial aneurysms. However, aneurysm recurrence can occur and its management is not well defined. We present our multicentric experience with retreatment of recurrent or residual aneurysms after initial WEB implantation.

Methods: This is a retrospective analysis of consecutive patients treated with the WEB device at three German neurovascular centers. Treatment strategies, clinical outcome and angiographic results were retrospectively assessed.

Results: We identified 15 patients (median age: 60 years) that underwent retreatment after initial WEB embolization. The aneurysms (10 unruptured, 5 ruptured) were located at the anterior communicating artery (6), internal carotid artery (5) and the basilar tip (4). There were 10 aneurysm remnants and 5 neck remnants. The reasons for retreatment were WEB compression (5), device migration (5), initial incomplete occlusion (4) and aneurysm regrowth (1). Retreatment strategies included coiling (4), stent-assisted coiling (7), flow-diversion (3) and implantation of an additional WEB (1). All procedures were technically successful and there were no procedure-related complications. Among 11 retreated aneurysms available for follow-up, 3 were retreated again. At last angiographic follow-up (median: 23 months), all retreated aneurysms showed adequate aneurysm occlusion (complete occlusion: 7, neck remnant: 4).

Conclusion: This pilot study demonstrates that endovascular retreatment after WEB implantation is safe and feasible and not limited by the previously placed WEB.

210

Safety and efficacy of the Derivo Embolization Device for the treatment of enrapured intracranial aneurysms: a multicentric study

Franziska Dorn^{*1}, Lukas Görtz², Bastian Kraus³, Bernd Turowski⁴, Jan Borggreffe⁵, Christoph Kabbasch⁶

¹Klinikum der Universität München—Campus Großhadern, Institut für Klinische Radiologie, Abteilung für Neuroradiologie, München, Deutschland

²Universitätsklinikum Köln, Zentrum für Neurochirurgie, Köln, Deutschland

³Uniklinik Düsseldorf, Radiologie, Neuroradiologie, Düsseldorf, Deutschland

⁴Heinrich-Heine-Universität Düsseldorf, Institut für Diagnostische und Interventionelle Radiologie, Neuroradiologie, Duisburg, Deutschland

⁵Uniklinik Köln

⁶Uniklinik Köln, Abteilung für Radiologie und Neuroradiologie, Institut für Diagnostische und Interventionelle Radiologie, Köln, Deutschland

Purpose: The Derivo embolization Device (DeD) is a novel flow diverter stent that provides increased x-ray visibility, an improved delivery system, and potentially reduced thrombogenicity. The aim of this study was to evaluate the early safety and efficacy of the second-generation DeD.

Methods: We retrospectively analyzed all patients with unruptured intracranial aneurysms (UIAs) who were treated with the DeD between 11/2015 and 12/2017 in three tertiary care centers. Procedural details, complications, and morbidity within 30d after treatment, as well as the aneurysm occlusion rates after 6 months (O'Kelly–Marotta scale, OKM), were evaluated.

Results: Forty-two patients with 42 aneurysms were treated with the DeD. All procedures were technically successful. Multiple DeDs were used in 3 aneurysms (7.2%) and adjunctive coiling in 11 (26.2%). Procedure-related complications occurred in 4 cases (9.5%) including 3 thromboembolic events and one aneurysm perforation. Morbidity was 2.4% and mortality was 0.0%. One patient suffered from a thromboembolic stroke at 30d follow-up (mRS 1). Among 33 patients (78.6%) available for angiographic follow-up, complete (OKM D) and favorable (OKM C+D) aneurysm occlusion was obtained in 72.7% (24/33) and 87.9% (29/33).

Conclusion: Endovascular treatment of UIAs with the DeD is associated with high procedural safety and adequate occlusion rates. Follow-up data will be necessary to confirm the long-term safety and angiographic outcomes of the device.

265

Multicenter experience in the endovascular treatment of ruptured and unruptured intracranial aneurysms using the Low-Profile WEB 17(Woven Endobridge) device

Sebastian Fischer^{*1}, Ansgar Berlitz², Werner Weber³, Jens Altenbernd³

¹Knappschafts Krankenhaus Bochum Langendreer, Institut für Diagnostische und Interventionelle Radiologie/Neuroradiologie U. Nuklearmedizin, Bochum, Deutschland

²Klinikum Augsburg

³Knappschafts Krankenhaus Bochum, Institut für Diagnostische und Interventionelle Radiologie, Neuroradiologie und Nuklearmedizin

Purpose: The safety and efficacy of the Woven Endobridge (WEB) device for the treatment of cerebral aneurysms has been investigated in several studies. Our objective was to report the experience of two neurovascular centers with the Low-Profile WEB 17 device in the treatment of broad based intracranial aneurysms, including technical feasibility and safety as well as angiographic and clinical follow-up-results.

Methods: We performed a retrospective analysis of all ruptured and unruptured aneurysms that were treated with the Low-Profile WEB 17 device (WEB SL and SLS) between July 2017 and February 2018. Primary outcome measures included the feasibility of implantation and the angiographic outcome. Secondary outcome measures included the clinical outcome at discharge and procedural complications.

Results: Forty-five (45) aneurysms in 44 patients, including 11 ruptured aneurysms/patients, were treated with the Low-Profile WEB 17 device. Implantation was successful in 44 cases. Additional devices (stents/coils) were necessary in 3/44 cases (6.8%). Procedural complications occurred in 3/44 (6.8%). Of these 2 were thromboembolic events and to 1 was an intraprocedural rupture. Angiographic follow-up at 3 months was available for 23/44 (52.3%) of all aneurysms to date, showing an adequate aneurysm occlusion in 19/23 (82.6%). Delayed aneurysm ruptures were not observed during the follow-up period to date.

Conclusion: The Low-Profile WEB 17 device offers a safe and effective treatment option for otherwise difficult to treat broad based small ruptured and unruptured intracranial aneurysms without the need of a dual antiplatelet therapy.

270

Elective aneurysm Treatment in the anterior and posterior circulation using Fred Junior Stent

Sebastian Fischer^{*1}, Werner Weber¹, Jens Altenbernd¹

¹Knappschafts Krankenhaus Bochum Langendreer, Institut für Diagnostische und Interventionelle Radiologie/Neuroradiologie U. Nuklearmedizin, Bochum, Deutschland

Purpose: Retrospective monocentric evaluation of elective aneurysm treatments in the anterior and posterior circulation using Fred Junior stent.

Methods: Retrospective evaluation of all intracranial aneurysms treated electively using Fred Junior stent. Assessment of aneurysmal localization, post-interventional aneurysm occlusion, complications and neurological status pre- and postinterventional.

Results: From 4/2016 to 5/2017, a total of 14 aneurysms (14 patients) were treated with Fred Junior stent. 13/14 aneurysms showed complete occlusion after 3 and 12 months, 1/14 aneurysms was constantly perfused at the base. Following aneurysmal localizations: 7/14 ACA, 4/14 PCA, 2/14 BA, 1/14 MCA. Symptomatic complication: 1 in-stent thrombosis 24 h after intervention, MRS-shift from 0 pre-interventional 4 post-interventional. Non-symptomatic complications: Stent stenosis: 3/14 aneurysms PCA, 1/14 aneurysms ACA.

Conclusion: The aneurysm treatment with the Fred Junior stent is safe and effective. Postinterventional stent-thrombosis and -stenosis should be further investigated.

273

New MicroNet covered Carotid-Stent: Vessel Diameter Conforming System with Stable Radial Force—Experimental data and first clinical results

Christian Wissgott^{*1}, Christoph Brandt-Wunderlich², Christoph Kopetsch³, Wolfram Schmidt⁴, Reimer Andresen⁵

¹Institute of Diagnostic and Interventional Radiology/Neuroradiology, Westkuestenkrankenhaus Heide, Heide, Deutschland

²Institute for Biomedical Engineering, University Rostock

³Institute of Diagnostic and Interventional Radiology/Neuroradiology, Westkuestenkrankenhaus Heide

⁴Institute for Biomedical Engineering, University of Rostock

⁵Institute of Diagnostic and Interventional Radiology/Neuroradiology, Department of Neurosurgery and Spine Surgery, Westkuestenkrankenhaus Heide, Academic Teaching Hospital of the Universities of Kiel, Luebeck and Hamburg, Heide, Deutschland

Purpose: Evaluation of a new self-adjusting to vessel diameter MicroNet covered stent for the carotid artery in respect to the mechanical behavior, and clinical safety and effectiveness.

Methods: 20 patients with high-grade stenosis of the internal carotid artery (ICA) were treated using a self-adjusting to vessel diameter carotid stent and the technical success and clinical follow-up were analyzed. The stent consists of self-expanding to vessel diameter an inner open-cell nitinol design covered by an outer MicroNet conformable layer. Stents were used with a diameter of 10 mm and a length of 30 or 40 mm, these stents would fit in vessels between 5 and 10 mm in diameter. The chronic outward force of a 10×40 mm stent was determined with a segmented head radial force test device (Blockwise Engineering LCC, USA). The stent was expanded directly into the test device at a diameter of 5 mm. The chronic outward force was measured up to complete expansion.

Results: The average stenosis rate of the treated arteries was $82.3 \pm 8.1\%$ (NASCET). In all 20 patients the stent was successfully implanted. No peri- or postinterventional minor or major stroke occurred until 30 days. The chronic outward force normalized by stent length was at 9 mm 0.195 N/mm and showed only a slight increasing force up to 0.330 N/mm at 5.5 mm.

Conclusion: The new self-expanding MicroNet covered stent is characterized due to its structure by a high conformability combined with a nearly similar radial force between 5.5 to 9 mm expansion diameter. Our first clinical results demonstrate that the 10 mm stent can be implanted to vessels from 5.5 to 9 mm with a very safe and effective implantation behavior with comparable respect to the vessel architecture.

293

A retrospective unicenter study towards endovascular therapy results of cranial dural arteriovenous fistulas

Christoph Mönninghoff^{*1}, Ewelina Pohl², Cornelius Deuschl³, Elena Stenzel⁴, Juliane Goebel², Karsten H. Wrede⁵, Alexander Radbruch¹, Michael Forsting⁶, Isabel Wanke⁷

¹Institute for Diagnostic and Interventional Radiology and Neuroradiology, Essen, Deutschland

²Universitätsklinikum Essen, Essen, Deutschland

³Institut für Diagnostische und Interventionelle Radiologie und Neuroradiologie, Universitätsklinikum Essen, Universität Duisburg-

Essen, Institut für Diagnostische und Interventionelle Radiologie und Neuroradiologie, Essen, Deutschland

⁴Institute for Diagnostic and Interventional Radiology and Neuroradiology, University Hospital Essen, Essen, Deutschland

⁵Universitätsklinikum Essen der Universität Duisburg-Essen, Klinik und Poliklinik für Neurochirurgie, Klinik für Neurochirurgie, Essen, Deutschland

⁶Universitätsklinikum Essen, Inst. F. Diagn. U. Interv. Radiologie U. Neuroradiologie, Essen, Deutschland

⁷Institut für Diagnostische und Interventionelle Radiologie und Neuroradiologie, Klinikum Hirslanden Zürich, Zürich, Switzerland

Purpose: Purpose of this retrospective unicenter study is the evaluation of endovascular therapy (EVT) of dural arteriovenous fistulas (dAVF) regarding the occlusion rate, recurrences, and complications.

Methods: Seventy-six consecutive patients with dAVF were included (42 men, 34 women, mean age 57.3 y) after EVT between 2008 and 2018. Patient records and angiograms of all patients were assessed towards demographic data, symptoms, type and size of the dAVF, number of EVTs and catheter positions, amount of embolic material, recurrences, and occlusion rate.

Results: According to the classification of Cognard/Merland 23 (30%) patients were diagnosed with a dAVF type 1 to 2a and 53 (70%) with a dAVF type 2b to 5. The latter group included 31 (41%) type 4 fistulas. 42 (55%) patients presented with pulsatile ear noise and 9 (12%) patients with intracranial bleeding (all > type 2b). All patients were primarily treated with EVT, 9% additionally underwent neurosurgical therapy. EVT reached complete occlusion of dAVFs in 59/76 (78%) patients. Partial occlusion with residual dAVF type 1–2a was achieved in 14/76 (18%) patients, and recurrence after complete occlusion occurred in 3 (3.9%) patients. Periprocedural complications were registered in 6/76 (8%) patients, 4 (5%) intracranial bleedings, one (1%) cerebral ischemia, and one (1%) temporary cranial nerve palsy. The length of the dAVF zone positively correlated with the number of arterial feeders (Pearson's correlation; $p=0.001$) and the amount of injected embolic material ($p<0.001$), but not with the number of needed catheter positions ($p=0.778$).

Conclusion: Endovascular treatment is the mainstay of therapy for cranial dAVFs with a low rate of complications and recurrences.

310

Risk factors for aneurysm recurrence after Woven Endobridge embolization determined by multiple logistic regression analysis

Lukas Görtz^{*1}, Eberhard Siebert², Franziska Dorn³, Jan Borggrefe⁴, Thomas Liebig⁵, Christoph Kabbasch⁶

¹Universitätsklinikum Köln, Zentrum für Neurochirurgie, Köln, Deutschland

²Charité Berlin, Institut für Neuroradiologie, Klinik für Neuroradiologie, Berlin, Deutschland

³Klinikum der Universität München—Campus Großhadern, Institut für Klinische Radiologie, Abteilung für Neuroradiologie, München, Deutschland

⁴Universität zu Köln, Institut für Diagnostische und Interventionelle Radiologie, Köln, Deutschland

⁵Ludwig-Maximilians-Universität München, University Hospital, Institute of Neuroradiology, München, Deutschland

⁶Uniklinik Köln, Abteilung für Radiologie und Neuroradiologie, Institut für Diagnostische und Interventionelle Radiologie, Köln, Deutschland

Purpose: The Woven Endobridge (WEB) device is a novel endovascular tool for treatment of wide-necked intracranial aneurysms. We aimed

to evaluate the risk factors of aneurysm recurrence after WEB embolization.

Methods: This is a retrospective study of consecutive patients with successful WEB implantation performed at three German tertiary care centers. Aneurysm recurrence was evaluated using the Raymond-Roy occlusion classification. The following variables were assessed: patient demographics, aneurysm location, bifurcation location, previous aneurysm treatment, ruptured aneurysm status, aneurysm size and combined treatment with additional devices. Predictive factors in the univariate analysis ($p < 0.05$) were entered into a binary logistic stepwise regression model to identify independent risk factors for aneurysm recurrence.

Results: A total of 86 patients (mean age: 59.2 ± 12.7 years) with 88 aneurysms (mean size: 9.2 ± 5.6 mm) were included. Seventeen aneurysms (19.3%) recurred. Aneurysm recurrence was significantly associated with location at the anterior communicating artery ($p = 0.029$), larger aneurysm height ($p < 0.001$) and adjunctive coiling ($p = 0.009$). The impact of bifurcation location on aneurysm recurrence was tendentially significant ($p = 0.084$). Previous aneurysm treatment ($p = 0.128$), neck width ($p = 0.138$) and ruptured aneurysm status ($p = 0.261$) were not significantly associated with aneurysm recurrence. In the multivariate analysis, aneurysm height remained as an independent prognostic factor for WEB recurrence ($p = 0.024$; odds ratio: 1.2, 95% confidence interval: 1.0–1.4).

Conclusion: Aneurysm height is an independent risk factor for aneurysm recurrence after WEB embolization.

312

Expanding the indication of Woven Endobridge (WEB) embolization to internal carotid artery aneurysms: a multicentric safety and feasibility study

Eberhard Siebert^{*1}, Lukas Görtz², Franziska Dorn³, Jan Borggrefe⁴, Thomas Liebig⁵, Christoph Kabbasch⁶

¹Charite Berlin, Institut für Neuroradiologie, Klinik für Neuroradiologie, Berlin, Deutschland

²Universitätsklinikum Köln, Zentrum für Neurochirurgie, Köln, Deutschland

³Klinikum der Universität München—Campus Großhadern, Institut für Klinische Radiologie, Abteilung für Neuroradiologie, München, Deutschland

⁴Universität zu Köln, Institut für Diagnostische und Interventionelle Radiologie, Köln, Deutschland

⁵Ludwig-Maximilians-Universität München, University Hospital, Institute of Neuroradiology, München, Deutschland

⁶Uniklinik Köln, Abteilung für Radiologie und Neuroradiologie, Institut für Diagnostische und Interventionelle Radiologie, Köln, Deutschland

Purpose: Woven Endobridge (WEB) embolization is an approved technique for endovascular treatment of wide-necked and bifurcation aneurysms. However, the WEB is not yet routinely used for internal carotid artery (ICA) aneurysms, especially at the paraophthalmic and posterior communicating segments. We present our multicentric experience with treatment of ICA aneurysms with the WEB device.

Methods: We reviewed all patients with ICA aneurysms that underwent WEB embolization at three German neurovascular centers. Technical success, complication rates and angiographic outcome at 6-months follow-up were retrospectively assessed.

Results: Twenty patients (mean age: 55.5 ± 14.0 years) with 20 ICA aneurysms were identified. The aneurysms were located at the paraophthalmic segment (8), posterior communicating segment (9), anterior choroidal segment (1) and at the ICA terminus (2). The mean aneurysm size was 9.1 ± 6.2 mm with a mean neck width of 3.9 ± 1.5 mm. Thirteen aneurysms (65%) were wide-necked (neck width > 4 mm and/

or dome-to-neck ratio < 2) and 6 (30%) were ruptured. The aneurysms were treated with a single WEB (12) or in combination with coiling (2), stenting (3) or flow diversion (3). All procedures were technically successful. There were one hemorrhagic and one ischemic event that resolved without permanent clinical sequelae, respectively. Among 19 aneurysms available for angiographic follow-up, 12 showed complete occlusion (63.2%), 4 had neck remnants (21.0%) and 3 aneurysm remnants (15.8%). The patients with aneurysm remnants were retreated.

Conclusion: The WEB device can be used for treatment of ICA aneurysms with a high level of procedural safety and a high degree of technical success.

313

Treatment of ruptured intracranial aneurysms with the Derivo Embolization Device: a multicentric study

Lukas Görtz^{*1}, Franziska Dorn², Bastian Kraus³, Bernd Turowski⁴, Marc Schlamann⁵, Robert Forbrig⁶, Jan Borggrefe⁷, Christoph Kabbasch⁸

¹Universitätsklinikum Köln, Zentrum für Neurochirurgie, Köln, Deutschland

²Klinikum der Universität München—Campus Großhadern, Institut für Klinische Radiologie, Abteilung für Neuroradiologie, München, Deutschland

³Uniklinik Düsseldorf, Radiologie, Neuroradiologie, Düsseldorf, Deutschland

⁴Heinrich-Heine-Universität Düsseldorf, Institut für Diagnostische und Interventionelle Radiologie, Neuroradiologie, Duisburg, Deutschland

⁵Uniklinik Köln, Institut für Diagnostische und Interventionelle Radiologie, Köln, Deutschland

⁶University Hospital, Institute of Neuroradiology, Munich, Deutschland

⁷Universität zu Köln, Institut für Diagnostische und Interventionelle Radiologie, Köln, Deutschland

⁸Uniklinik Köln, Abteilung für Radiologie und Neuroradiologie, Institut für Diagnostische und Interventionelle Radiologie, Köln, Deutschland

Purpose: The Derivo Embolization Device (DED) is a novel flow-diverter with increased x-ray visibility, reduced thrombogenicity and an advanced delivery system. We assessed the safety and efficacy of the DED for treatment of patients with ruptured intracranial aneurysms.

Methods: Eleven patients (median age: 53 years; 7 females) were treated with the DED in the acute phase of subarachnoid hemorrhage at three German neurovascular centers. We retrospectively assessed procedural details, complications, morbidity (modified Rankin Scale, mRS) and aneurysm occlusion (O'Kelly-Marotta scale, OKM).

Results: Of 11 treated aneurysms, 8 were located in the anterior circulation and 3 in the posterior circulation. Aneurysm morphology was classified as saccular (4), dissecting (3), blister-like (2), fusiform (1) and mycotic (1). All procedures were technically successful with one single DED used. Additional coiling was employed for two aneurysms. There was one in-stent thrombosis that occurred due to low clopidogrel response 4 days after the procedure. After aspiration-thrombectomy, the patient remained with a mild hemiparesis (mRS 1). We did not observe any further thromboembolic or hemorrhagic events. Ten patients (90.9%) achieved a favorable outcome (mRS ≤ 2) at last follow-up. The patient with a mycotic aneurysm died as consequence of severe subarachnoid hemorrhage itself. At angiographic control, complete aneurysm occlusion (OKM D) was achieved in 8 of 9 cases (88.9%).

Conclusion: In this pilot study, endovascular treatment of ruptured intracranial aneurysms with the DED was reasonably safe and efficient. Larger series are warranted to provide a definite conclusion in the setting of acute subarachnoid hemorrhage for this device.

Conclusions about the Medina Embolic Device after a single center experience in 65 aneurysms. Has this concept still a future in the treatment of intracranial aneurysms?

Marta Aguilar Perez^{*1}, Victoria Hellstern², Mohammed AlMatter², Paul Bhogal², Oliver Ganslandt³, Hansjörg Bänzner⁴, Hans Henkes²

¹Neuroradiologie, Neuroradiologische Klinik, Stuttgart, Deutschland

²Neuroradiologie, Klinikum Stuttgart

³Neurochirurgie, Klinikum Stuttgart

⁴Neurologie, Klinikum Stuttgart

Purpose: The Medina Embolic Device (MED) represented a novel device for the treatment of intracranial aneurysms by combining flow-diverting technology and the familiarity of standard coils. We describe our final experience with this device in intracranial aneurysms both as a solitary treatment strategy or in conjunction with additional devices, our reasoning behind the treatment strategies, as well as the potential advantages and disadvantages of this design concept.

Methods: 62 consecutive patients (39 females) with a total of 65 aneurysms (6 ruptured) were treated between September 2015 and January 2018. We retrospectively evaluated the angiographic results at the end of the procedure and at follow-up, the clinical status, complications, and requirement for adjunctive devices

Results: The MED was successfully deployed in all but one case and adjunctive devices, including standard coils, were required in 56 aneurysms at the first treatment. Seven of the 9 aneurysms initially treated with MED alone required retreatment, most of them with intraluminal flow diversion. Eight patients had complications although none could be attributed to the MED. Delayed angiographic follow-up (median 284 days) was available in 55 aneurysms, with 29 showing complete aneurysm exclusion (53%), 18 showing neck remnants (33%) and 8 patients showing persistent but subtotal filling of the aneurysm fundus (14%).

Conclusion: The MED represented a novel device for the treatment of intracranial aneurysms, which is actually retired from the market. We believe that the true value of this concept will be in combining its use with adjunctive devices such as endoluminal flow diverters that will result in rapid aneurysm exclusion.

Flow Diverter Treatment of Saccular Sidewall Aneurysms using p64: The Stuttgart Series

Marta Aguilar Perez¹, Elina Henkes², Muhammad AlMatter³, Victoria Hellstern⁴, Hansjörg Bänzner⁵, Oliver Ganslandt⁶, Hans Henkes^{*7}

¹Neuroradiologie, Neuroradiologische Klinik, Stuttgart, Deutschland

²Neuroradiologie, Klinikum Stuttgart

³Klinikum Stuttgart, Neuroradiologische Klinik, Stuttgart, D

⁴Klinikum Stuttgart, Neuroradiologische Klinik, Stuttgart, Deutschland

⁵Klinikum Stuttgart, Neurologische Klinik, Stuttgart, Deutschland

⁶Klinikum Stuttgart, Neurochirurgische Klinik, Stuttgart, Deutschland

⁷Klinik für Neuroradiologie, Neuroradiologische Klinik, Stuttgart, Deutschland

Purpose: To evaluate the occlusion rate and safety margins of the endovascular treatment of intracranial saccular sidewall aneurysms using the p64 flow diverter.

Methods: Retrospective data collection and analysis by aneurysm location was performed. Only unruptured saccular sidewall aneurysms without previous treatment were included, if no other stent was in the parent artery. The below given numbers indicate: occurrence of complications (procedural/day 1–30/beyond day 30), % adequate occlusion

(complete occlusion or neck remnant) at 3, 9 and 24 months, based on follow-up DSA.

Results: N=336 aneurysms of consecutive patients were enrolled. Cavernous ICA (*n*=24) 1/0/0, 91/95/100 (i. e., 1 procedural complication, no complication 1–30 days or beyond, 91%, 95%, 100% occlusion at 3, 9 and 24 months). Paraophthalmic ICA (*n*=94) 4/2/3, 82/86/98. Superior hypophyseal artery (*n*=74) 1/0/2, 81/93/100. Supracaloid ICA (*n*=21) 0/0/0, 70/89/90. PcomA (*n*=47) 1/1/1, 61/80/80. AcoA (*n*=26) 1/0/0, 71/82/100. ACA and AcomA (23) 0/0/0, 70/94/94. MCA/M1 (*n*=16) 0/0/0, 88/85/73. VA/BA (*n*=11) 1/2/0, 70/88/100.

Conclusion: Flow diversion using p64 yields high occlusion rates and low complication rates if used in untreated sidewall saccular aneurysms. Platelet inhibition verification and accurate vessel diameter measurement are mandatory.

Stent-assisted coiling of intracranial aneurysms using a low-profile stent (LEO Baby): A single-center retrospective study of 49 Cases

Michael Tepper^{*1}, Maria Alexandrou², Maria Politi³, Panagiotis Papanagiotou⁴, Christian Roth⁵

¹Klinikum Bremen-Mitte, Klinik für Diagnostische und Interventionelle Neuroradiologie, Bremen, Deutschland

²Klinikverbund Bremen, Radiologie, Bremen, Deutschland

³Klinikum Bremen-Mitte, Klinik für Diagnostische und Interventionelle Neuroradiologie, Bremen

⁴Klinikum Bremen-Mitte, Bremen, Deutschland

⁵Klinikum Bremen Mitte, Bremen

Purpose: The aim of this study was to investigate the clinical and angiographic results of stent-assisted coiling (SAC) of intracranial aneurysms using low-profile intracranial stents.

Methods: A retrospective analysis was performed including patients who were treated with LEO Baby intracranial stent-assisted coiling between 2014–2017. Forty-nine patients were included in this study. Forty-three patients attended angiographic and clinical follow-up for a mean duration of 13.0 ± 7.8 months.

Results: Initial complete occlusion of the aneurysm was achieved in 83.7% (41/49) of patients. The last follow-up angiograms showed complete occlusion of the aneurysm in 76.7% (33/43) of patients and a residual neck of the aneurysm was observed in 20.9% (9/43) of patients. Two (4.6%) of the 43 patients with a follow-up showed an increase in the filling status of the aneurysm and one patient required restenting after 5 months. Thrombus formation was seen in 5 cases 10.2% (5/49), including one patient who failed to take aspirin and clopidogrel followed by an in-stent occlusion 5 days after SAC with no relevant clinical consequences. No further device-related complications were observed.

Conclusion: The results of this study demonstrate the safety and efficacy of LEO Baby stent-assisted coiling of intracranial aneurysms.

Interventional Neuroradiology: Embolisation Others

Clinical course of patients with dolichoectasia or fusiform aneurysms of the basilar artery

Philipp Müller^{*1}

¹Medizinische Universität Graz, Stockdorf, Deutschland

Background: Dolichoectasia and fusiform aneurysms of the basilar artery (VBD) are rare vascular diseases related to a significant increase

of the risk of hemorrhagic or ischemic infarctions. Treatment options are not curative and rarely successful.

Objective: By grading the radiological findings, a better understanding of the clinical relevance of the disease should be achieved. The hypotheses that a higher-grading is associated with increased neurological complications and occurs with accumulated cardiovascular risk factors are evaluated. Additionally, the used grading system was tested for feasibility.

Methods: In a retrospective data analysis, MR studies of patients examined between 2005 and 2015, and who were diagnosed with VBD have been evaluated and graded at the Department of Radiology of the University of Graz. Dolichoectasia was graded and the two groups (severe versus moderate) were statistically compared using the Chi-Square or Fisher-Exact-Test.

Results: A total of 50 patients were analyzed, of which three were classified as “mild”, 32 as “moderate” and 15 as “severe”. The severe dolichoectasia has a significantly higher probability of causing neurological symptoms due to ischemia ($p=0.031$) or cerebral nerve palsy ($p=0.003$). The basilar artery thrombosed in 95% of cases only in the “severe” grading stage above 10 mm. The reference groups did not significantly differ with regard to the vascular risk factors. The grading system used proves to be feasible and its defined limits are in a comprehensible range of values.

Conclusion: The presence of neurological symptoms is significantly related to a vessel diameter >10 mm. The radiological grading of VBD is a relevant prognostic factor and should be included in future trials.

130

Treatment recommendations for incidental intracranial aneurysms: real-world experience from a neurovascular board

Michael Schönfeld*¹, Matthias Stöckmann², Gabriel Broocks¹, Uta Hanning³, Marielle Sophie Ernst⁴, Andreas Frölich⁵, Lasse Dührsen⁶, Nils Ole Schmidt⁷, Jan Regelsberger⁸, Jens Fiehler⁹, Maxim Bester¹

¹Klinik und Poliklinik für Neuroradiologische Diagnostik und Intervention, Universitätsklinikum Hamburg-Eppendorf, Hamburg, Deutschland

²Klinik und Poliklinik für Neuroradiologische Diagnostik und Intervention, Universitätsklinikum Hamburg-Eppendorf

³Klinik und Poliklinik für Neuroradiologische Diagnostik und Intervention, Universitätsklinikum Hamburg-Eppendorf, Institut für Klinische Radiologie, Uniklinikum Münster, Hamburg, Deutschland

⁴Klinik und Poliklinik für Neuroradiologische Diagnostik und Intervention, Hamburg, Deutschland

⁵Universitätsklinikum Hamburg-Eppendorf, Klinik und Poliklinik für Neuroradiologische Diagnostik, Klinik und Poliklinik für Neuroradiologische Diagnostik und Intervention, Hamburg, Deutschland

⁶Department of Neurosurgery, University Medical Center Hamburg-Eppendorf, Hamburg, Deutschland

⁷Klinik und Poliklinik für Neurochirurgie, Universitätsklinikum Hamburg-Eppendorf, Hamburg, Deutschland

⁸Universitätsklinikum Hamburg-Eppendorf, Klinik und Poliklinik für Neurochirurgie, Klinik und Poliklinik für Neurochirurgie, Hamburg, Deutschland

⁹Diagnostikzentrum Univ.-Klinikum Hamburg-Eppendorf, Klinik und Poliklinik für Neuroradiologische Diagnostik und Intervention, Hamburg, Deutschland

Purpose: To describe our experience with a neurovascular board for consensus-based treatment recommendations in incidental intracranial aneurysms.

Methods: Aneurysm characteristics and treatment recommendations from a weekly neurovascular board meeting from 4/2017 to 4/2018 were compared.

Results: 190 patients harboring 254 untreated or recurrent intracranial aneurysms were discussed. 25 patients (13.1%) were re-evaluations after a previous board meeting and 23 patients (12.1%) evaluations of follow-up DSAs without a previous board meeting. Recommendations were endovascular treatment for 82 aneurysms (32.2%), neurosurgery for 72 aneurysms (28.3%) and follow-up imaging alone for 79 aneurysms (31.1%). In absence of a clear recommendation it was suggested to discuss the preferred treatment option with the patient for 14 aneurysms (5.5%) and for 7 aneurysms (2.8%) no recommendation was given. Maximum aneurysm diameter was larger where treatment was recommended compared to where follow-up imaging was recommended (median 5.0 mm vs. 2.7 mm; $p<0.001$). Aneurysm location differed significantly between type of recommended treatment (ratio endovascular/surgery: ACI 36/16, ACM 2/34, ACA 11/21, posterior circulation 33/1; $p<0.001$).

Conclusion: The neurovascular board is a helpful and transparent tool to provide consensus-based individualized recommendations for treatment strategies in the absence of unambiguous evidence.

146

Trends and Differences in Endovascular and Neurosurgical Treatment of Ruptured and Unruptured Intracranial Aneurysms between 2010 and 2016: Secondary use of Billing Codes in the MIRACUM (Medical Informatics for Research and Care in University Medicine) Consortium

Stephan Meckel*¹, Martin Boeker², Jennifer Linn³, Gabriele Schackert⁴, Christoph Groden⁵, Daniel Hänggi⁶, Siegfried Bien⁷, Christopher Nimsky⁸, Martin Skalej⁹, Raimund Firsching¹⁰, Jürgen Konczalla¹¹, Joachim Berkefeld¹², Arnd Dörfler¹³, Michael Buchfelder¹⁴, Marc A. Brockmann¹⁵, Florian Ringel¹⁶, Mukesh Shah¹⁷, Jürgen Beck¹⁸, Horst Urbach¹⁹, Christian Haverkamp²⁰

¹Klinik für Neuroradiologie, Freiburg, Deutschland

²Faculty of Medicine and Medical Center, University of Freiburg, Freiburg, Deutschland

³Universitätsklinikum Carl Gustav Carus an der TU Dresden, Institut und Poliklinik für Diagnostische und Interventionelle Neuroradiologie, Dresden, Deutschland

⁴Klinikum Carl Gustav Carus, Klinik und Poliklinik für Neurochirurgie, Carl-Gustav-Carus Universitätsklinikum an der Technischen Universität Dresden, Dresden, Deutschland

⁵Universitätsmedizin Mannheim, Abteilung für Neuroradiologie, Mannheim, Deutschland

⁶Universitätsklinikum Mannheim, Neurochirurgische Klinik, Universitätsmedizin Mannheim, Medizinischen Fakultät Mannheim der Universität Heidelberg, Mannheim, Deutschland

⁷Universitätsklinikum Gießen und Marburg GmbH, Abteilung für Neuroradiologie, Meizinisches Zentrum für Nervenheilkunde, Marburg, Deutschland

⁸Universitätsklinikum Gießen und Marburg GmbH, Standort Marburg, Klinik für Neurochirurgie, Marburg, Deutschland

⁹Institut für Neuroradiologie, Institut für Neuroradiologie, Institut für Neuroradiologie, Universitätsklinikum Magdeburg, Magdeburg, Deutschland

¹⁰Otto-von-Guericke-Universität, Universitätsklinik für Neurochirurgie, Magdeburg, Deutschland

¹¹Klinik für Neurochirurgie, Frankfurt, Deutschland

¹²Neuroradiologie, Kelkheim, Deutschland

¹³Universitätsklinikum Erlangen, Abteilung für Neuroradiologie, Erlangen, Deutschland

¹⁴Universitätsklinikum Erlangen, Klinik für Neurochirurgie, Erlangen, Deutschland

¹⁵Department of Neuroradiology, Deutschland

¹⁶Universitätsmedizin der Johannes Gutenberg-Universität Mainz, Mainz, Deutschland

¹⁷Universitätsklinikum Freiburg, Klinik für Neurochirurgie, Klinik für Neurochirurgie, Freiburg, Deutschland

¹⁸Department of Neurosurgery, Medical Center, University of Freiburg, Deutschland

¹⁹Universitätsklinikum Freiburg, Klinik für Neuroradiologie, Freiburg, Deutschland

²⁰Staff Unit IT-Processes, Deutschland

Purpose: Intracranial aneurysms (IA) are treated by neurosurgical clipping and various endovascular embolization treatments (EVT). We performed a multicenter analysis using shared hospital data from the MIRACUM consortium of 8 university hospitals to discover trends in the treatment of IAs.

Methods: Anonymized billing data were loaded into a local i2b2 data warehouse. A locally executed uniform SQL (structured query language) query delivered aggregated site data for all inpatients with a discharge diagnosis of ruptured (ICD-10 I60) and unruptured IAs (I67.10). Type of treatment including different EVT techniques and length of hospital stay were centrally analyzed with R.

Results: From 2010 to 2016, 2729 ruptured and 2635 unruptured IAs were treated at 8 centers. EVT vs. clipping ratio was slightly higher in ruptured (64% vs. 36%) than unruptured IAs (62.9% vs. 37.1%). Overall, a temporal decline in clipping rates of ruptured IAs was noted from 42% to 33.5%. Simple coiling showed a declining trend (ruptured IAs: 48% to 42.6%). Whereas, complex treatment techniques increased over time such as balloon assisted coiling (2.9% to 12.8%) in ruptured and stent-assisted coiling and flow-diversion in unruptured IAs (7.2% to 25.7%). Median hospital stay was significantly shorter in EVT vs. clipping in unruptured (6 vs. 13 days) but not in ruptured IAs (17 vs. 21 days) IAs.

Conclusion: The observed trends show an increased utilization of EVT in ruptured IAs and use of more complex EVT techniques for both ruptured and unruptured IAs. EVT of unruptured IAs is associated with shorter length of hospitalization. Gross outcome measures (discharge home and in-hospital death) are currently evaluated.

213

Symptomatic cerebral vasospasm after aneurysmal subarachnoid hemorrhage: comparison of single and multiple intra-arterial treatments with regard to the outcome

Alexander Neumann^{*1}, Jan Küchler², Thomas Eckey¹, Tobias Boppel¹, Claudia Ditz², Peter Schramm¹

¹Institut für Neuroradiologie, UKSH—Campus Lübeck, Lübeck, Deutschland

²Klinik für Neurochirurgie, UKSH—Campus Lübeck, Lübeck, Deutschland

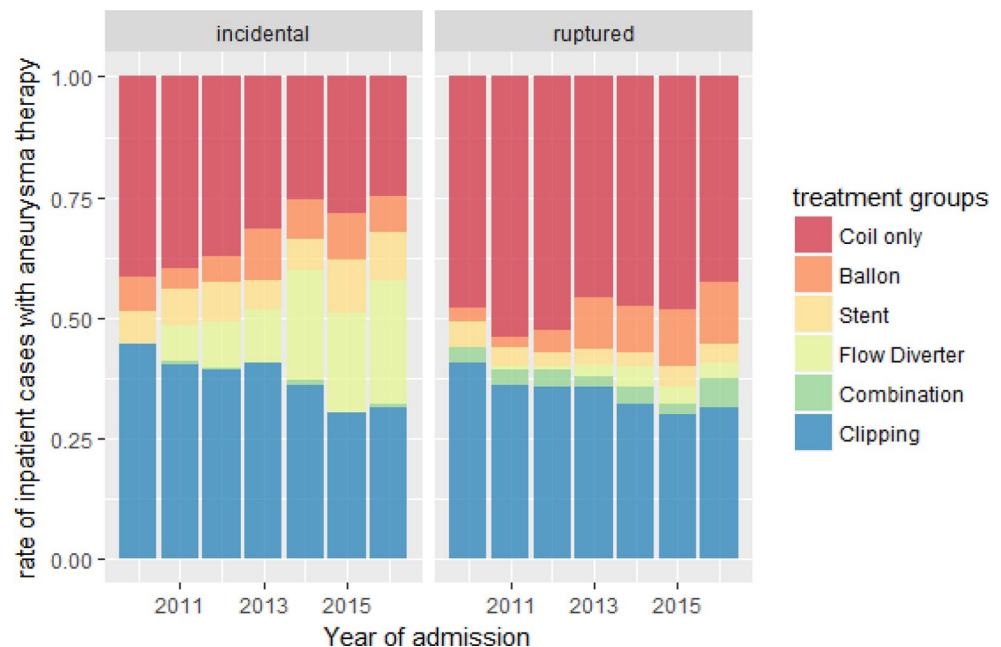
Purpose: In the case of aneurysmal subarachnoid hemorrhage (aSAH) and symptomatic cerebral vasospasm (sCVS), multiple intra-arterial treatments (IAT) can be regarded as potentially useful for the outcome, in spite of the extensive effort and expense involved, even if the prognosis is initially poor. At the same time it must be kept in mind that the precise influence of the number of IAT has yet to be clarified. We wanted to assess, if multiple IAT are disadvantageous for the outcome.

Methods: In a single center study 258 consecutive patients with non-traumatic SAH were analyzed over a period of 6 years. 76 of them developed sCVS, of whom, in turn, 25 received singular and 29 multiple (i.e. >1) IAT (Nimodipin/+ PTA). 22/76 patients did not receive IAT for various reasons. The statistical evaluation of the comparison of both groups was carried out using Fisher's exact test.

Results: In the group with single IAT 17/25 patients developed cerebral infarcts in the CT whereas we found this in 15/29 cases in connection with multiple IAT ($p > 0.05$). Initially an unfavorable outcome (mRS 3–5) resulted for 22/25 with a single IAT and for 27/29 patients with multiple IAT, after 3 months 13/25 as compared to 18/29 (in each case $p > 0.05$). Regarding the case fatality rate, there were again no statistically significant differences between the two groups.

Conclusion: Patients, who received multiple IAT (Nimodipin/+ PTA) in connection with sCVS after aSAH showed no disadvantages in the outcome compared to patients with only a single IAT.

Fig. 1 Treatment trends



After aneurysmal subarachnoid haemorrhage—which factors influence cerebral vasospasm?

Christian Siedentopf^{*1}, Astrid E. Grams², Sarah Honold³, Ruth Steiger⁴, Raimund Helbok⁵, Bernhard Glodny⁶, Elke Ruth Gizewski⁷

¹Medical University Innsbruck, Department of Neuroradiology, Neuroimaging Research Core Facility, Patsch, Austria

²Medizinische Universität Innsbruck, Universitätsklinik für Neuroradiologie, Neuroimaging Research Core Facility, Innsbruck, Austria

³Medical University Innsbruck

⁴University Clinic of Neuroradiology, Neuroimaging Research Core Facility, Medical University of Innsbruck, Innsbruck, Austria

⁵Medical University Innsbruck, Department of Neurology, Innsbruck, Austria

⁶Department Radiologie, Department für Radiologie, Universitätsklinik für Neuroradiologie, Innsbruck, Austria

⁷Department F. Radiologie- Univ-Kliniki F. Neurorad., Department F. Radiologie- Univ-Kliniki F. Neurorad., Neuroimaging Research Core Facility, Innsbruck, Austria

Purpose: Based on the observation that older patients suffer less frequent from vasospasm due to a subarachnoid hemorrhage (SAH) compared to younger patients, the assumption was made that increased intracranial arterial calcification could be a reason.

Object of study was to find out if there is a negative correlation between intracranial calcification and the presence of cerebral vasospasm.

Methods: CT-, MRI- and DSA-scans from 103 patients with a severe SAH were investigated retrospectively. The amount of intracranial arterial calcification and of intracranial blood were calculated and the occurrence of vasospasm during clinical course were assessed.

Results: A vasospasm occurred in 54 patients. A significantly positive correlation was found between the age and the presence of a vasospasm and between age and intracranial calcification. A direct correlation between the presence of a vasospasm and intracranial calcification was not found. Nevertheless men showed higher amounts of intracranial

blood than women. A significantly positive correlation was found between the intracranial blood and the Hunt & Hess classification.

Conclusion: Correlations could be found between younger age and the presence of vasospasms after a SAH as well as between increasing age and higher intracranial arterial calcification. These findings could lead to continuous monitoring of vasospasms in younger patients with SAH. Due to the fact of increasing life expectation the mean age of patients who suffer from a SAH will increase over time. This could lead to the fact that in future the prevalence of cerebral vasospasm in the context of a SAH, which is still accompanied by a worse outcome after subarachnoid hemorrhage, will slightly decrease.

240

Flow diverter Treatment of blood Blister-like aneurysms of the posterior circulation in the acute phase of SAH is safe and efficient

Victoria Hellstern¹, Muhammad AlMatter², Marta Aguilar Perez³, Elina Henkes⁴, Oliver Ganslandt⁵, Hans Henkes^{*6}

¹Neuroradiologie Klinikum Stuttgart, Stuttgart, D

²Klinikum Stuttgart, Neuroradiologische Klinik, Stuttgart, D

³Neuroradiologie, Neuroradiologie, Stuttgart, Deutschland

⁴Klinikum Stuttgart, Neuroradiologische Klinik, Stuttgart, Deutschland

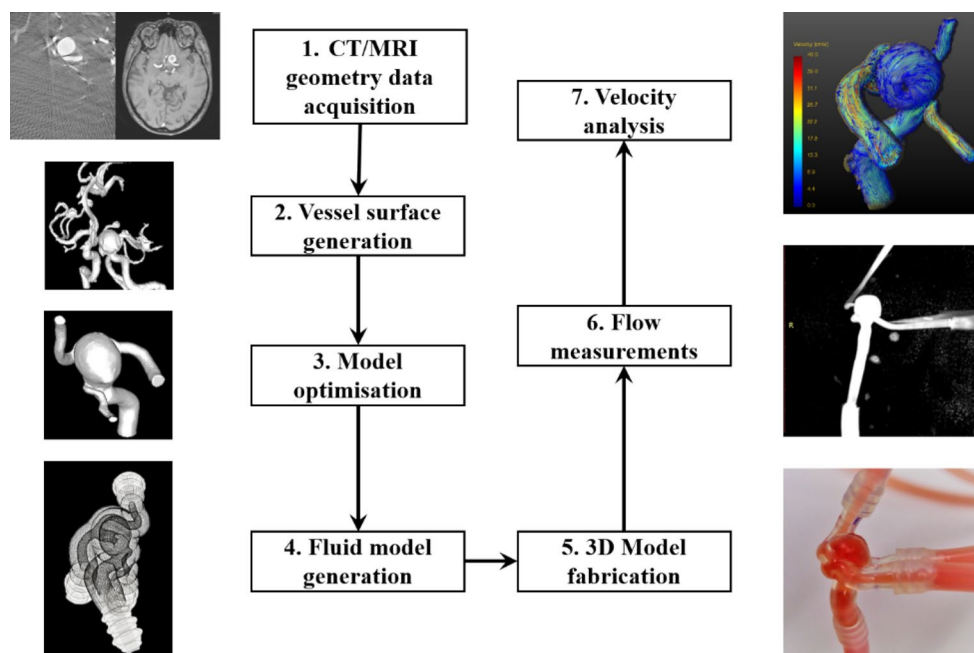
⁵Klinikum Stuttgart, Neurochirurgische Klinik, Stuttgart, Deutschland

⁶Klinik für Neuroradiologie, Neuroradiologische Klinik, Stuttgart, Deutschland

Purpose: Subarachnoidal hemorrhage (SAH) due to blood blister-like aneurysms (BBA) of the posterior circulation is very rare but can be fatal. The optimal treatment has not been identified yet. We reviewed the feasibility of flow Diverter (FD) implantation in the acute phase of SAH based on a retrospective review of 10 patients.

Methods: Between 01/2012 und 01/2018 N=10 patients with BBAs of the posterior circulation were treated within 30 days of SAH with implantation of FDs ($n=7$). Three patients were treated conservatively. Treatment was performed on average after 11 days (range 1–49 days).

Fig. 1



The localizations of the BBAs were: Vertebral artery ($n=2$), Basilar artery ($n=3$), perforating branches of the basilar artery $n=5$.

Results: In 1/7 treatments (14%) a procedural complication was observed without permanent morbidity or mortality due to the procedure. In one patient the BBA could not be detected on DSA; this patient suffered a re—bleeding and died; no patient suffered a permanent morbidity due to the treatment.

Follow-up DSAs confirmed the complete occlusion of the BBA. There were no re—bleedings. The parent vessels remained patent.

Conclusion: FD treatment of BBAs of the posterior circulation in the acute phase of SAH is safe and efficient.

244

Patient specific models for flow investigations of aneurysms

Mariya Pravdivtseva^{*1}, Eva Peschke², Thomas Lindner³, Olav Jansen⁴

¹University Hospital Schleswig-Holstein, Department of Radiology and Neuroradiology, Grk ²¹⁵⁴ Materials for Brain, Kiel, Deutschland

²Molecular Imaging North Competence Center, Kiel, Deutschland

³Klinik für Radiologie und Neuroradiologie, Universitätsklinikum Schleswig-Holstein, Kiel, Deutschland

⁴Direktor des Instituts für Neuroradiologie, Klinik für Radiologie und Neuroradiologie, Kiel, Deutschland

Purpose: Fabrication of patient-specific vascular flow models can improve neuroradiological interventions. These possibilities include realistic student practice, doctors' practice before an operation of difficult pathologic cases and the search for the best treatment solution such as a test of new treatment devices or strategies.

Methods: Numerical models were created and optimized with following software: Mevislab, Autodesk fusion, Meshmixer. Vascular models were printed with the Stereolithography 3D printing technique. The important parameters (e. g. design of the connectors, wall thickness, printing resolution) were checked using MRI (TOF, 4D flow).

Results: In the presented study the workflow of creating vascular models was established. This protocol includes following steps: patient data acquisition, vessel mask creation, surface generation, surface optimization, the creation of a fluid volume and adding the connections between the models and the flow pump. During the MRI investigation, it was found that neither printing resolution nor wall thickness plays any role in the quality of flow behavior. On the other hand, less wall thickness makes the models more fragile and transparent. The impact of four different connectors on laminar flow was considered and as a result, only one is recommended to use in flow experiments. Obtained results don't show any significant differences between flow patterns in model and patient.

Conclusion: The current work shows an accurate protocol for the fabrication of patient-specific models. The accuracy of the models was checked in comparison with patient data by the flow MRI.

276

Concept, realization and evaluation of a new pump assisted module for the physiological flow simulation of cerebral aneurysms in digital subtraction angiography and magnetic resonance angiography.

Hannes Schwenke^{*1}, Oskar Pfau², Philipp Rostalski², Peter Schramm³, Andre Kemmling⁴

¹UKSH Campus Lübeck, Institut für Neuroradiologie, Lübeck, Deutschland

²Institute for Electrical Engineering in Medicine, Universität zu Lübeck

³UKSH Universitätsklinikum Schleswig-Holstein Campus Lübeck, Institut für Neuroradiologie, Lübeck, Deutschland

⁴UKSH Lübeck, Institut für Neuroradiologie, Institut für Neuroradiologie, Hamburg, Deutschland

Purpose: In order to plan, train and evaluate endovascular treatment procedures, it has been shown that 3D printing of aneurysms combined with a water circuit allows a realistic simulation environment. However, in addition to patient specific aneurysms, the simulation of blood flow plays an important role. In this context a high precision pulsatile, self-regulating and low cost pump was developed and tested for use in DSA and MRA settings.

Methods: A pump assisted module was designed that expands a simulator for endovascular treatment procedures by a pulsatile flow which can be regulated automatically and additionally controlled externally. Internal sensor controlled algorithms keep the flow constant irrespective of pressure changes due to inserted catheters or embolization material. For evaluation purposes conventional DSA and TOF-MRA investigations were performed and compared visually and statistically.

Results: In both DSA and MRI settings the pump assisted module was easy to apply and generated a realistic flow situation. DSA and TOF-MRA revealed both an accurate anatomical precision and a good

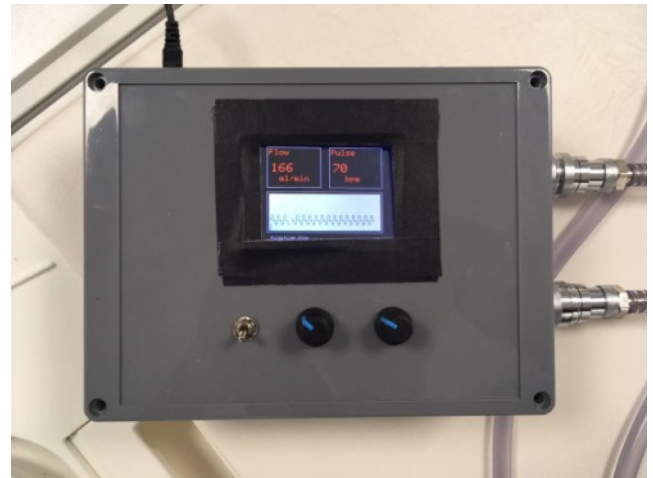


Fig. 1 Pump assisted module with graphical interface environment

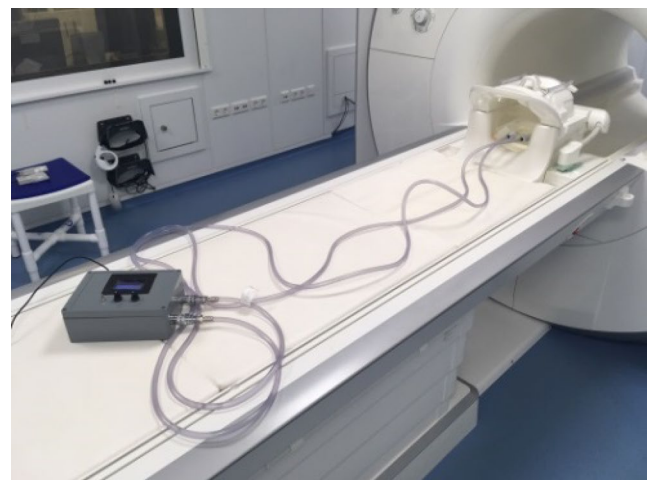


Fig. 2 Experimental setting in MRI

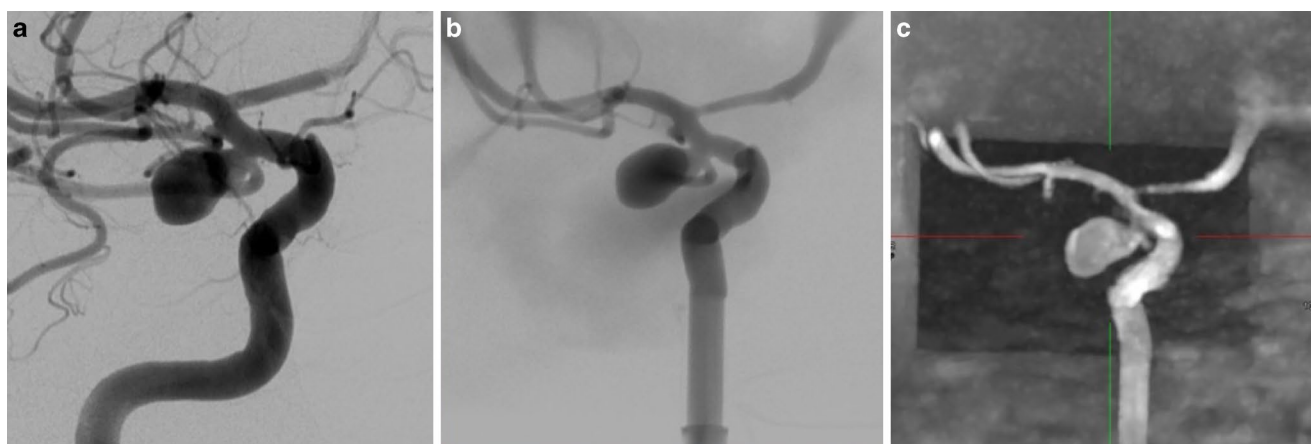


Fig. 3 Source DSA (a) and patient specific model of an aneurysm of the right PCOM assessed with DSA (b) and TOF-MRA (c)

overlap when the data was compared visually and statistically with patients' source DSA.

Conclusion: The pump assisted module is applicable both in DSA and MRA settings and leads to a more realistic flow environment in interventional training, treatment planning and evaluation of new treatment devices. Furthermore it could open the door to further investigations with other methods like 4D-Flow-MRA.

290

Stereotactic Cisternal Lavage Therapy Reduces Delayed Cerebral Ischemia and Improves Outcome in Patients with Aneurysmal Subarachnoid Hemorrhage.

Roland Rölz^{*1}, Karl Egger², Christian Scheiwe³, Wolf-Dirk Niesen⁴, Christine Steiert⁵, Volker Arnd Coenen⁶, Peter Reinacher⁷

¹Department of Neurosurgery, Freiburg University Medical Center, Deutschland

²Department of Neuroradiologie, Freiburg University Medical Center, Freiburg, Deutschland

³Department of Neurosurgery, Medical Center Freiburg, Faculty of Medicine, University of Freiburg, Department of Neurosurgery, Medical Center—University of Freiburg, Faculty of Medicine, University of Freiburg, Germany, Freiburg, Deutschland

⁴Universitätsklinikum Freiburg, Klinik für Neurologie, Klinik für Neurologie, Freiburg, Deutschland

⁵Department of Neurosurgery, Medical Center—University of Freiburg, Faculty of Medicine, University of Freiburg, Neurochirurgie Uniklinik Freiburg, Freiburg, Deutschland

⁶Universitätsklinikum Freiburg, Stereotaktische und Funktionelle Neurochirurgie, Freiburg, Deutschland

⁷Universitätsklinikum Freiburg, Abt. Stereotaktische und Funktionelle Neurochirurgie, Freiburg, Deutschland

Purpose: Delayed cerebral infarction (DCI) is a major source of morbidity and mortality after aneurysmal subarachnoid hemorrhage (aSAH). Stereotactic catheter ventriculocisternostomy (STX-VCS) and continuous fibrinolytic/spasmolytic lavage is a new method for DCI prevention. We compare aSAH patients before and after introduction of STX-VCS.

Methods: We analyzed aSAH patients admitted 2.5 years before and 2.5 years after introduction of STX-VCS. STX-VCS was performed on the basis of individual treatment decisions. Continuous fibrinolytic cisternal lavage using urokinase (100 IU/ml at a rate of 50 ml/h) was applied for 5–10 days. In case of vasospasm nimodipine was applied

via STX-VCS at a concentration of 0.005 mg/ml. Neurological outcome and DCI rating was performed according to existing guidelines and DCI volumes were determined.

Results: A total of 160 patients were included: 80 patients before implementation of STX-VCS and 80 patients after implementation of this technique. Baseline and treatment characteristics of both groups were highly comparable. 40 of 80 patients were selected for STX-VCS. The DCI rate was 28% before and 13% after STX-VCS was introduced ($p=0.029$). The total DCI volume was reduced by 78%. Poor neurological outcome at 6 months occurred in 66% vs. 39% of patients, respectively ($p=0.039$). In the 40 STX-VCS patients the DCI incidence was 10%, and poor neurological outcome at 6 months was 28%.

Conclusion: STX-VCS was feasible and safe in patients with severe aSAH. Performing STX-VCS in high-risk patients reduced the DCI incidence from 28% to 13% and the total DCI volume by 78%. Poor neurological outcome was significantly reduced from 66% to 39%.

315

Evaluation of an integrated patient-based neurovascular training environment for intracranial aneurysm treatment

Marie Teresa Nawka^{*1}, Johanna Spallek², Jan-Hendrik Buhk³, Jens Fiehler⁴, Andreas Frölich⁵

¹Klinik und Poliklinik für Neuroradiologische Diagnostik und Intervention Universitätsklinikum Hamburg-Eppendorf, Hamburg, Deutschland

²Institut für Produktentwicklung und Konstruktionstechnik, Technische Universität Hamburg-Harburg, Hamburg, Deutschland

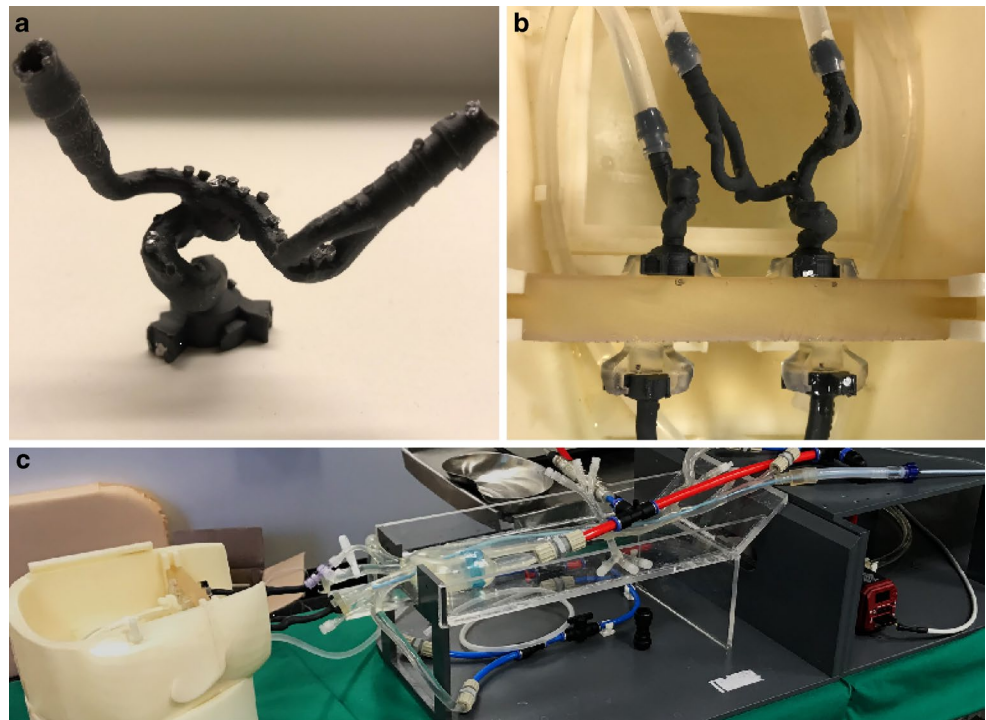
³Klinik und Poliklinik für Neuroradiologische Diagnostik und Intervention, Universitätsklinikum Hamburg-Eppendorf, Hamburg, Deutschland

⁴Diagnostikzentrum Univ.-Klinikum Hamburg-Eppendorf, Klinik und Poliklinik für Neuroradiologische Diagnostik und Intervention, Hamburg, Deutschland

⁵Universitätsklinikum Hamburg-Eppendorf, Klinik und Poliklinik für Neuroradiologische Diagnostik, Klinik und Poliklinik für Neuroradiologische Diagnostik und Intervention, Hamburg, Deutschland

Purpose: Developments in endovascular aneurysm therapy continuously drive the demand for neurointerventional training. We aimed to investigate the value of an integrated neurovascular training environment for aneurysm embolization using additively manufactured intracranial aneurysm models.

Fig. 1 **a** 3D-printed model of an incidental Carotid-T-Aneurysm, **b** Two different aneurysm models connected to the skull base of 'HANNES', **c** 'HANNES' in the angiographic research laboratory



Methods: A portfolio of 22 patient-specific aneurysm models derived from different treatment settings was fabricated. Models were integrated into a customizable neurointerventional simulator with interchangeable intracranial and cervical vessel segments applying physiological circuit conditions ('HANNES'; Hamburg ANatomical NEurointerventional Simulator). Multiple training courses were performed and participant feedback was obtained using a questionnaire.

Results: Case-specific clinical difficulties can be reproduced using HANNES. Due to standardized connectors, models can be exchanged easily during a training session in order to switch to a different treatment scenario. Among 15 participants evaluating hands-on courses using a 5-point scale from 1 (strongly agree) to 5 (strongly disagree), HANNES was rated as highly suitable ('1' and '2') for practicing aneurysm coil embolization (2.0 ± 0.82 ; 67%).

Conclusion: In its current state, HANNES offers a wide variability and flexibility for case-specific hands-on training of intracranial aneurysm treatment and may reduce the need for animal experiments. The high level of standardization might be of value for practical assessment of neurointerventionalists.

325

Comparison of Rupture Rates of Paraophthalmic Aneurysms and Anterior Communicating Artery Aneurysms

Elena Stenzel^{*1}, Daniel Paech², Juliane Göbel¹, Christoph Mönninghoff¹, Isabel Wanke³, Michael Forsting¹, Alexander Radbruch¹

¹Institute for Diagnostic and Interventional Radiology and Neuroradiology, University Hospital Essen, Essen, Deutschland

²German Cancer Research Center, Heidelberg, Deutschland

³Institute for Diagnostic and Interventional Radiology and Neuroradiology, University Hospital Essen, Center for Neuroradiology, Clinic Hirslanden, Zurich, Switzerland

Purpose: A widely accepted recommendation for treatment is provided for incidental aneurysms of the anterior circulation with a diameter

≥ 7 mm depending on patient age, health condition and treatment risk without differentiating between different anatomical locations within the anterior circulation. In the current study we compared the rupture rate of paraophthalmic aneurysms of the internal carotid artery (ICA) and aneurysms of the anterior communicating artery (ACA).

Methods: Two cohorts of 77 consecutively treated (clipping or coiling) patients with paraophthalmic and anterior communicating artery aneurysms were retrospectively analyzed in this single center study.

Results: Rupture rate was 21% in paraophthalmic ICA aneurysms (group 1) compared to 53% in anterior communicating artery aneurysms (group 2) (OR=4.4132 (95% CI: 2.1722–8.9661)). Irregularity of aneurysm shape was associated with a significantly higher rupture rate in both groups (group 1: OR=13.1818 (95% CI: 1.6388–106.026); group 2: OR=2.3315 (95% CI: 0.8331–6.5251)). Notably, a relatively high proportion of regular-shaped aneurysms caused SAH in group 2 (39%) compared to group 1 (3%). In group 1, maximum and medium aneurysm diameter were significantly associated with the rupture rate whereas in group 2, no correlation was found.

Conclusion: The current study revealed a significantly lower rupture rate of paraophthalmic aneurysms compared to ACA aneurysms. Importantly, a subgroup of small and regular-shaped paraophthalmic aneurysms was identified that is significantly less prone to rupture than aneurysms of similar size and configuration arising from the ACA.

330

Flow Diverter For Treatment For Acutely Ruptured Intracranial Aneurysms

Maïke Jäger^{*1}, Christian Taschner¹, Michelle ten Brinck², Jeroen Boogaarts²

¹University of Freiburg, Klinik für Neuroradiologie, Freiburg, Deutschland

²Radboud University Medical Center, Nijmegen

Purpose: Subarachnoid hemorrhages (SAH) due to dissecting or blood-blister like intracranial aneurysms are therapeutically very chal-

lenging. The use of flow diverters (FD) in this situation has been discussed and several cases have been reported recently, whereby available evidence is still limited. This study aims to investigate rates of rebleed, clinical and angiographic outcome after 6–12 months in patients being treated with a FD in acutely phase of SAH. Outcomes will be compared to stent-assisted coiling.

Methods: Retrospective data-analysis of patients (≥ 18 years) of six different centers around Europe and the US, treated with any kind of FD within the first 15 days after SAH is planned. Baseline characteristics, clinical and angiographic data are collected online with an itemlist from an electronically stored database.

Results: At present, 43 patients treated since March 2012 are enrolled. Mean age at time of treatment is 55,1 years, mean time between SAH and treatment is 3 days. Most patients received Surpass FD (47,8%). Others were FRED, Pipeline, Silk and Derivo. 6 patients (14%) died within 30 days after treatment due to complications concerning treatment or SAH.

Conclusion: If the use of FD and stent-assisted coiling show comparable outcome and complication rates, the use of FD might become the preferred strategy in this patient group since it may have better durability. Patient inclusion is still ongoing. Results of the main study outcomes are expected in Sept. 2018.

335

Is there an increased haemorrhagic risk for preprocedural double antiaggregation in the treatment of unruptured MCA bifurcation aneurysms

Florian Hagen^{*1}, Christoph Maurer², Ansgar Berlis³

¹Klinikum Augsburg, Neusäß, Deutschland

²Klinikum Augsburg, Augsburg, Deutschland

³Klinikum Augsburg, Klinik für Diagnostische Radiologie und Neuroradiologie, Augsburg, Deutschland

Purpose: The antiaggregation and anticoagulation takes a major role in the treatment of cerebral aneurysm. Especially the balance between risk of the creation of thromboembolic events and hemorrhage risk

Methods: Retrospectively examination of 163 unruptured MCA bifurcation aneurysm comparing preprocedural simple antiaggregation and the double antiaggregation between May 2008 and August 2017. 85 patients received a double antiaggregation with ASS 100 mg and Clopidogrel 75 mg starting five days before treatment. Preprocedural a clopidogrel responder status was compiled. In case of non-responding they treatment was changed to ticagrelor with a loading dose of 180 mg. 78 patients were simple antiaggregated with ASS 100 mg. Both groups received procedural 5000 IU of Heparin.

Results: We find less significant postprocedural CT-Scan pathologies in the double antiaggregated group. A new hemorrhage occurred in three patients, contrast agent pooling in two and an infarction in one of the simple antiaggregated group compared to zero incidents in the other group. No differences were found in long term follow-up in both groups (mean at 30 month).

Conclusion: The preprocedural double antiaggregation with an ADP-receptor antagonist seems not to increase the haemorrhage risk and could be given to all patients preventing a thromboembolic event.

336

Antithrombotic Therapy in Acute Carotid Stenting of Tandem Lesions

Maria Boutchakova^{*1}, Lukas Meyer², Maria Politi², Maria Alexandrou², Christian Roth², Andreas Kastrup³, Panagiotis Papanagiotou²

¹Klinikum für Diagnostische und Interventionelle Neuroradiologie, Klinikum Bremen Mitte, Bremen, Deutschland

²Klinikum für Diagnostische und Interventionelle Neuroradiologie, Klinikum Bremen Mitte

³Neurologische Klinik, Klinikum Bremen Mitte

Purpose: There is no consensus regarding peri/postprocedural antithrombotic therapy (AT) in acute stenting of the extracranial carotid artery (aCAS). The aim of the this study was to investigate the rates of symptomatic intracerebral hemorrhage (sICH) and stent occlusion in correlation with different medical regimens during and after an emergency CAS in acute ischemic stroke due to tandem lesions.

Methods: We retrospectively analyzed the clinical and radiological findings of patients with acute tandem (intra- and extracranial) lesions who underwent aCAS with antithrombotics and intracranial thrombectomy at our institution. The AT that was used, included anticoagulants (heparin) and one or more antiplatelet agents such as aspirin, thienopyridines (clopidogrel or prasugrel) and glycoprotein IIb/IIIa receptor inhibitors (Eptifibatid). End points were acute stent occlusions rates and sICH

Results: 100 Patients were included to our analysis from 2013 to 2017. Successful recanalization was achieved in 90% of the patients. Forty (40)% of the patients had a good clinical outcome at discharge. In-hospital mortality was 10%. Symptomatic ICH occurred in 8 Patients (8%), postprocedural diagnostics revealed 9 patients with stent-occlusion (9%). The use of Prasugrel was associated with increased sICH risk (37%). Patients who received antiplatelet medication before admission had lower risk to revealed stent thrombosis (11% vs 89%). IV Thrombolysis was not associated with increased risk of symptomatic ICH.

Conclusion: Aspirin before admission is protective against stent-thrombosis in acute ICA-Stenting. Prasugrel is associated with a higher risk of hemorrhage after acute ICA-Stenting compared to other antiplatelet agents.

405

Rescue therapy for a stent dislocation into a wide-neck basilar tip aneurysm

Seraphine Kutschke^{*1}, Alexander Riabikin², Anastasios Mpotsaris³, Martin Wiesmann⁴

¹Institut für Diagnostische und Interventionelle Neuroradiologie, Universitätsklinikum Aachen, Aachen, Deutschland

²Institut für Diagnostische und Interventionelle Neuroradiologie, Aachen, Deutschland

³Klinik für Diagnostische und Interventionelle Neuroradiologie, Aachen, Deutschland

⁴Klinik für Diagnostische und Interventionelle Neuroradiologie, Aachen, Deutschland

Purpose: Stent dislocation is a rare, but severe and challenging complication.

We present an example of a stent dislocation into the aneurysm during an attempted Y-stenting of a wide-neck basilar tip aneurysm. The snare over stent retriever (SOS)-technique was performed successfully as rescue maneuver.

Methods: A 71 year-old man presented with temporary vision disorders. Cranial MRI showed a wide-neck basilar tip aneurysm (6×7 mm) without evidence of subarachnoid hemorrhage or acute ischemic stroke. Since both left and right PCA and SCA were part of the aneurysm base, Y-Stenting was attempted. A self-expanding stent was implanted from the basilar artery into the left PCA (Enterprise 4/30). While advancing the microcatheter over the guidewire through the previously placed stent, the stent was dislocated into the aneurysm dome.

Results: Using the SOS-technique, the stent was retracted and relocated into the basilar artery so that its distal tip protruded slightly into the aneurysm neck. Through this, the stent protected the origins of the PCAs and SCAs. Finally, coil embolization was performed using the stent for waffle-cone technique remodelling.

Conclusion: Although rarely required, neurointerventionalists should be aware of rescue maneuvers for dislocated stents. The SOS-technique, previously published by our group, showed good results in an in-vitro and an in-vivo swine model. To the best of our knowledge, this is the first example of an application of this technique in a clinical case.

442

Dural arteriovenous fistulas of the condylar vein

Christoph Mönninghoff^{*1}, Elena Stenzel¹, Alexander Radbruch¹, Daniel Rüfenacht², Isabel Wanke³

¹Institute for Diagnostic and Interventional Radiology and Neuroradiology, Essen, Deutschland

²Hirslanden Clinic, Zürich, Switzerland

³Hirslanden Clinic, Institute for Diagnostic and Interventional Radiology and Neuroradiology, University Hospital Essen, Deutschland, Zürich, Switzerland

Purpose: To evaluate risk and success of venous access when treating DAVF of the condylar vein.

Methods: Quality control measures in a consecutive series from 2017–2018 identified 6 patients with a DAVF at the condylar vein. All sought treatment for pulsatile tinnitus. Arterial supply involved in all cases branches from the ascending pharyngeal artery, with connection to branches supplying cranial nerves near the jugular foramen. Consequently, in all 6 cases, a transvenous access was chosen to deliver implants and to avoid possible complications by injecting critical arterial branches to nervous structures. For this purpose, in all cases, a combination of coils and liquid precipitating polymer were used to obliterate the AV-shunt region.

Results: In all cases, the transvenous access allowed for delivering occlusive implants and to obtain obliteration of the DAVF without damage to cranial nerves. Alleviation from pulsatile tinnitus was observed in all cases.

Conclusion: DAVF of the condylar vein presented with pulsatile tinnitus and EVT was safely performed and achieved good symptom alleviation by occluding the condylar vein and nearby tributaries with a combination of coils and precipitating polymers through a transvenous access.

Diagnostic Neuroradiology: Tumors

113

Intratumoral fiber tracking of meningiomas

Fritz Klausner^{*1}, Jürgen Steinbacher², Mark Mc Coy³

¹Christian-Doppler-Klinik, Salzburg, Austria

²Christian-Doppler Klinik

³Division für Neuroradiologie der Christian Doppler Klinik, Salzburg, Austria

Purpose: Diffusion tensor imaging (DTI) is a valuable tool in characterizing meningiomas with respect to consistency and grading. Fiber tracking can depict potential structures in areas of anisotropy. Evaluation of structures in meningiomas with fiber tracking

Methods: 14 patients with 15 meningiomas without severe calcifications were retrospectively examined with 3T MRI. We used DTI with

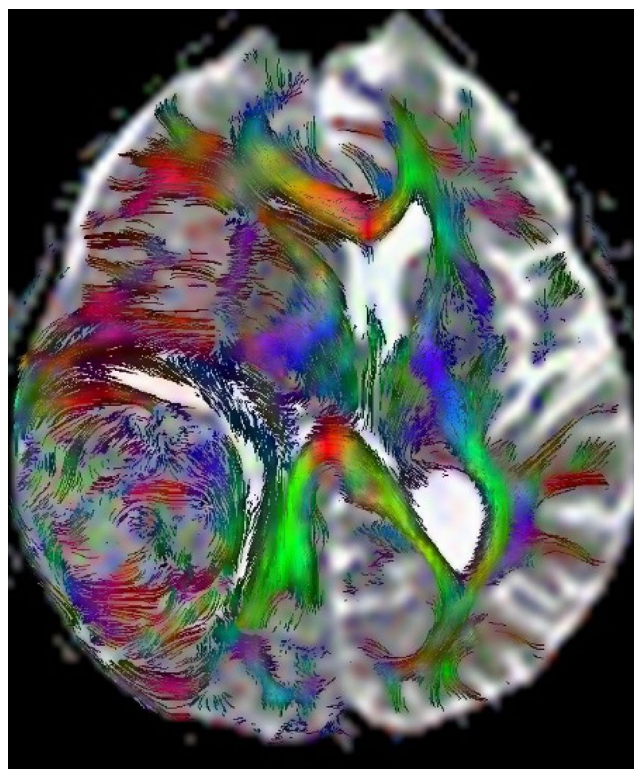


Fig. 1 Meningioma with whorls of fibers

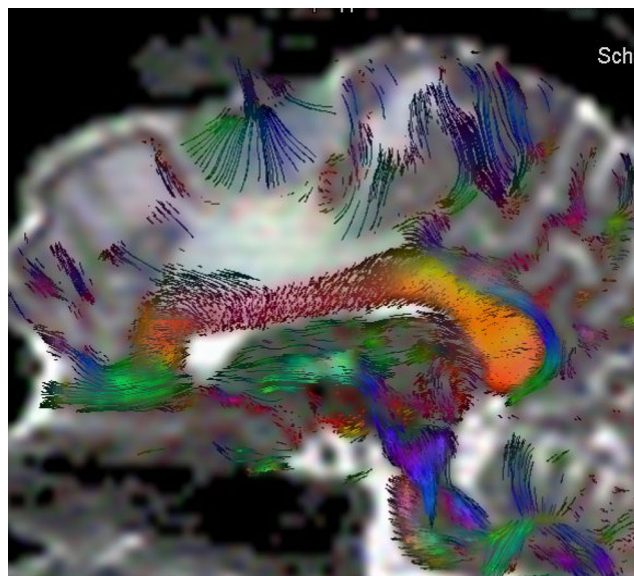


Fig. 2 Meningioma with an umbilicus and radial fibers. Peritumoral edema

deterministic tractography. Directionally- dependent color-coded fibers were superimposed on b0 images and fractional anisotropy (FA) maps with a matrix of 1024×1024. Single ROIs including the whole cranium in three orthogonal planes showed tumor area and fibers of the brain. Histologic diagnosis of meningiomas was available.

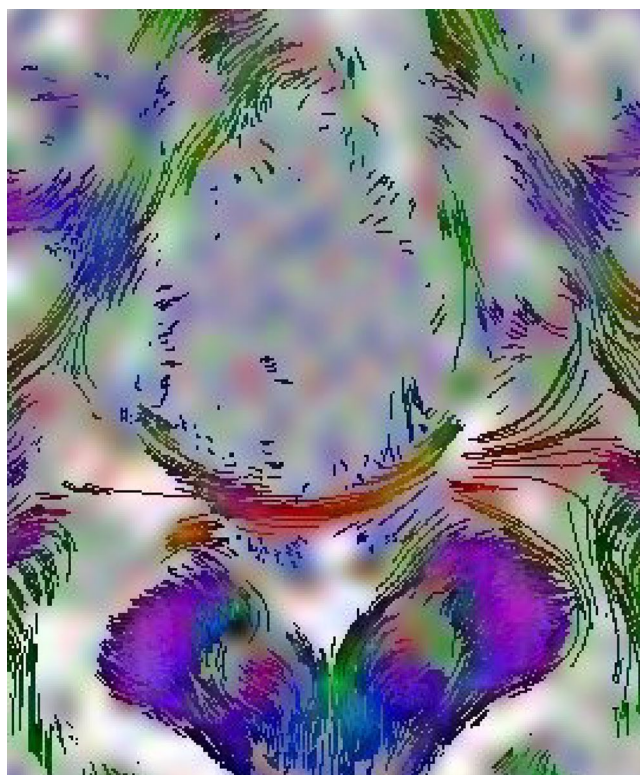


Fig. 3 Meningioma with compression of the optic chiasm. Sparse intratumoral fibers

Results: We found three patterns in meningiomas: whorls of fibers in 6 cases, radial fibers with an umbilicus-like structure in 2 cases, and meningiomas with only sparse fibers in 8 cases.

Conclusion: B0-FA maps with overlay of fibers is a feasible technique in acquiring information about the structure of meningiomas which may assist in differential diagnosis of anisotropic tumors to more isotropic lesions.

Effects of anti-angiogenic treatment on glioblastoma stiffness in an orthotopic animal model

Katharina Schregel^{*1}, Michal O. Nowicki², Miklos Palotai³, Navid Nazari⁴, Rachel Zane², Ralph Sinkus⁵, Sean E. Lawler⁶, Samuel Patz³

¹Department of Radiology, Brigham and Women's Hospital, Harvard Medical School, Institute of Neuroradiology, University Medical Center Goettingen, Goettingen, Deutschland

²Harvey Cushing Neurooncology Laboratories, Department of Neurosurgery, Brigham and Women's Hospital, Boston, United States

³Department of Radiology, Brigham and Women's Hospital, Harvard Medical School, Boston, United States

⁴Department of Biomedical Engineering, Boston University, Boston, United States

⁵Department of Radiological Imaging, Imaging Sciences & Biomedical Engineering Division, King's College London, London, United Kingdom

⁶Harvey Cushing Neurooncology Laboratories, Department of Neurosurgery, Brigham and Women's Hospital, Harvard Medical School, Boston, United States

Purpose: Glioblastoma (GBM) is the most common primary malignant brain tumor. Neuroradiological work-up of GBM is challenging and complicated by therapy-associated phenomena. We evaluated the potential of magnetic resonance elastography (MRE) to monitor GBM under anti-angiogenic therapy.

Methods: GBM was orthotopically implanted in 10 nude mice. Five animals received anti-VEGF-treatment, the other 5 served as controls. MRI and MRE were performed longitudinally. Histopathology was conducted afterwards.

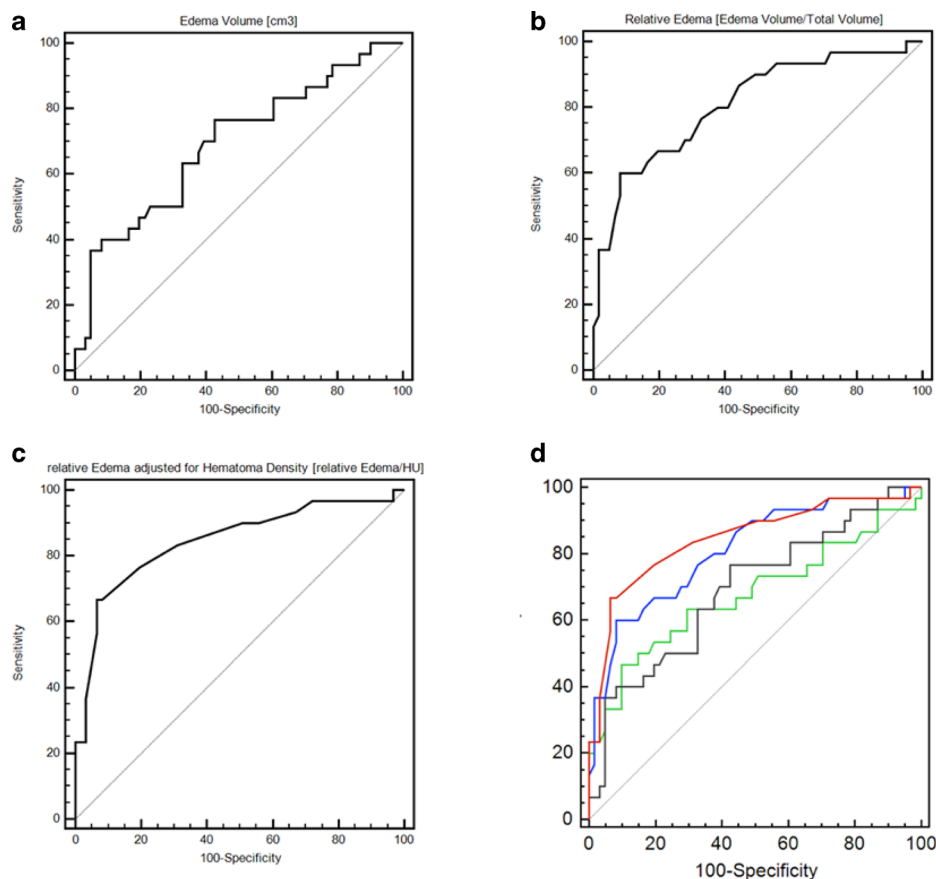
Results: Tumor volume progressively increased in untreated animals, while there was only a small increase under anti-VEGF-treatment. GBM in untreated mice were softer and had predominant elastic properties compared to tumors in treated animals. Untreated GBM exhibited a progressive softening, which did not occur under anti-angiogenic therapy. The phase angle similarly decreased in untreated animals. In treated animals, a drop in the phase angle was observed in late stages. Histology revealed that untreated GBM were more necrotic, while treated tumors were more invasive.

Conclusion: The results suggest that anti-VEGF treatment slows down tumor progression, which is in line with previous studies.¹ Moreover, it decelerates tumor softening that has been shown with progression.² The phase angle γ expressing the solid/liquid ratio appeared to indicate tumor progression.

References

1. Keunen O, et al. Anti-VEGF treatment reduces blood supply and increases tumor cell invasion in glioblastoma. *Proc. Natl. Acad. Sci.* 2011;108:3749–54.
2. Schregel K, et al. Characterization of glioblastoma in an orthotopic mouse model with magnetic resonance elastography. *NMR Biomed.* <https://doi.org/10.1002/nbm.3840>

Fig. 1 Receiver operating characteristics (ROC) analysis for prediction of tumorous intracranial hemorrhage (ICH) using different perihematomal edema (PHE) parameters: **a** PHE volume, **b** relative edema, **c** relative edema adjusted for hematoma density and **d** ROC curves comparison of PHE volume, relative edema, relative edema adjusted for hematoma density and hematoma density. Area under the curve (AUC); 95% confidence interval (CI); PPV = positive predictive value and NPV = negative predictive value



	AUC	95% CI	Optimal cut-off *	Sensitivity	Specificity	PPV	NPV
PHE [cm³]	0.691	0.586-0.784	0.3404	76.67	57.38	63.35	71.91
Relative PHE	0.810	0.714-0.885	0.5180	60	91.80	87.63	70.34
Hematoma Density [HU]	0.675	0.569-0.769	0.3683	46.67	90.16	82.11	63.60
Relative PHE corrected for Density	0.845	0.754-0.912	0.6011	66.67	93.44	90.77	74.34

150

Perihematomal edema in the discrimination of tumorous and non-tumorous causes of acute intracerebral hemorrhage on CT

Jawed Nawabi^{*1}, Gabriel Brooks¹, Uta Hanning², Gerhard Schoen³, Tanja Schneider⁴, Jens Fiehler⁵, Christian Thaler⁶, Susanne Siemonsen⁷

¹Klinik und Poliklinik für Neuroradiologische Diagnostik und Intervention, Universitätsklinikum Hamburg-Eppendorf, Hamburg, Deutschland

²Klinik und Poliklinik für Neuroradiologische Diagnostik und Intervention, Universitätsklinikum Hamburg-Eppendorf, Institut für Klinische Radiologie, Uniklinikum Münster, Hamburg, Deutschland

³Universitätsklinikum Hamburg-Eppendorf, Zentrum für Experimentelle Medizin Institut für Medizinische Biometrie und Epidemiologie, Deutschland

⁴Klinik und Poliklinik für Neuroradiologische Diagnostik und Intervention, Universitätsklinikum Hamburg-Eppendorf

⁵Diagnostikzentrum Univ.-Klinikum Hamburg-Eppendorf, Klinik und Poliklinik für Neuroradiologische Diagnostik und Intervention, Hamburg, Deutschland

⁶Diagnostikzentrum Univ.-Klinikum Hamburg-Eppendorf, Department of Radiology, Stanford University, Hamburg, Deutschland

⁷Klinik und Poliklinik für Neuroradiologische Diagnostik und Intervention, Universitätsklinikum Hamburg-Eppendorf, Hamburg, Deutschland

Background and Purpose: The etiological differentiation of intracerebral hemorrhage (ICH) is crucial as early diagnosis of the underlying

Fig. 1 This figure illustrates the integration of language mapping data by nTMS including nTMS-based DTI FT into neuronavigation (purple) during surgery

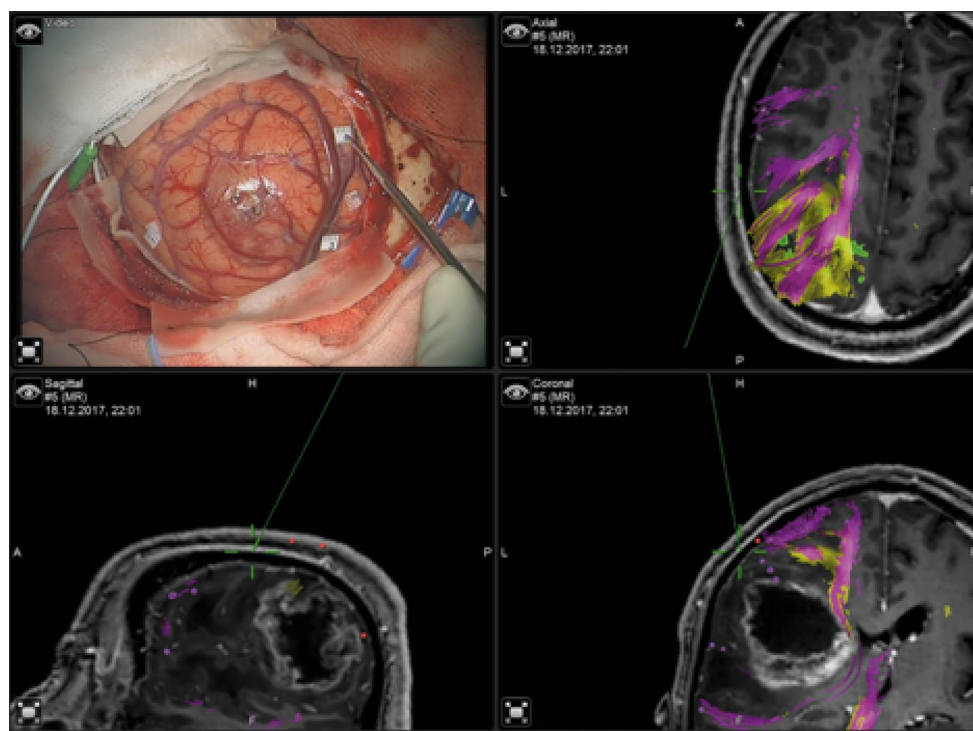
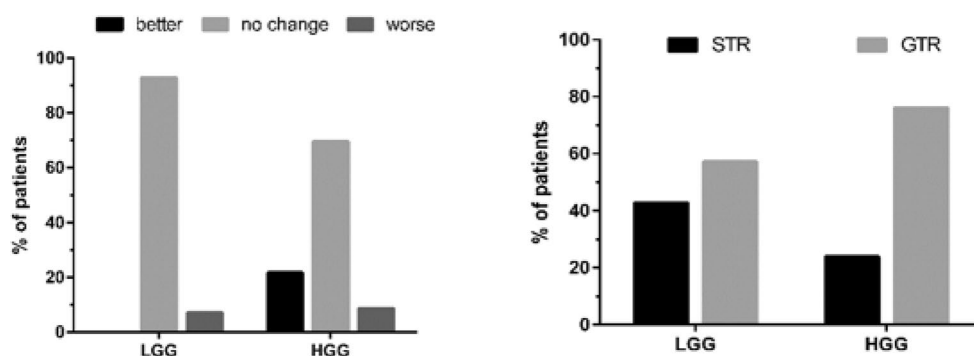


Fig. 2 These bar charts illustrate the percentage of patients who showed improved, unchanged, or worse Language performance (left graph) and the percentage of patients in whom subtotal resection (STR) or gross total resection (GTR) was achieved. The fractions were calculated in relation to the total number of patients enrolled suffering from either a low-grade (LGG, $n=14$ patients) or high-grade glioma (HGG, $n=46$ patients).



pathology can both influence clinical management and guide prognosis in acute ICH patients. The objective of this study was to investigate the diagnostic value of perihematomal edema (PHE) volume in non-enhanced CT (NECT) to discriminate tumorous and non-tumorous causes of acute ICH.

Materials and Methods: From 560 patients with acute ICH, 91 patients fulfilled the inclusion criteria and were classified into non-tumorous and tumorous ICH. For each patient, ICH and total hemorrhage volume (ICH+PHE) were segmented semiautomatically. PHE volume and relative PHE were further calculated and all parameters were compared between the different groups. Additionally, hematoma density was measured and compared between the groups.

Results: PHE volume and relative PHE on NECT was significantly higher in tumorous vs. the non-tumorous ICH ($p \leq 0.003$). Absolute ICH volume, symptom time onset to CT and ICH localization showed no significant difference between the two groups ($p > 0.1$). ROC analysis revealed a high diagnostic performance for relative PHE with an optimal optimal cut-off of 0.50 (60.0% sensitivity, 91.8% specificity).

Conclusions: Relative PHE with a cut-off of >0.50 is a specific and simple indicator for tumorous causes of acute ICH and a potential tool for clinical practice. This observation needs to be validated in an independent patient cohort.

187

Setup presentation and clinical outcome analysis of treating language-eloquent gliomas via preoperative navigated transcranial magnetic stimulation and tractography

Nico Sollmann^{*1}, Anna Kelm², Sebastian Ille², Claus Zimmer¹, Bernhard Meyer², Sandro M. Krieg²

¹Abteilung für Neuroradiologie, Klinikum Rechts der Isar, Technische Universität München, München, Deutschland

²Neurochirurgische Klinik und Poliklinik, Klinikum Rechts der Isar, Technische Universität München, München, Deutschland

Purpose: Awake surgery with intraoperative stimulation is considered the gold standard for the resection of language-eloquent tumors. Recently, navigated transcranial magnetic stimulation (nTMS) and nTMS-based diffusion tensor imaging fiber tracking (DTI FT) have been introduced as preoperative adjuncts. This study analyzes the impact of this multimodal approach on outcome.

Methods: 60 patients (47.6 ± 13.3 years) suffering from language-eloquent left-hemispheric low-grade or high-grade glioma underwent preoperative nTMS language mapping and nTMS-based DTI FT (Fig. 1). Clin-

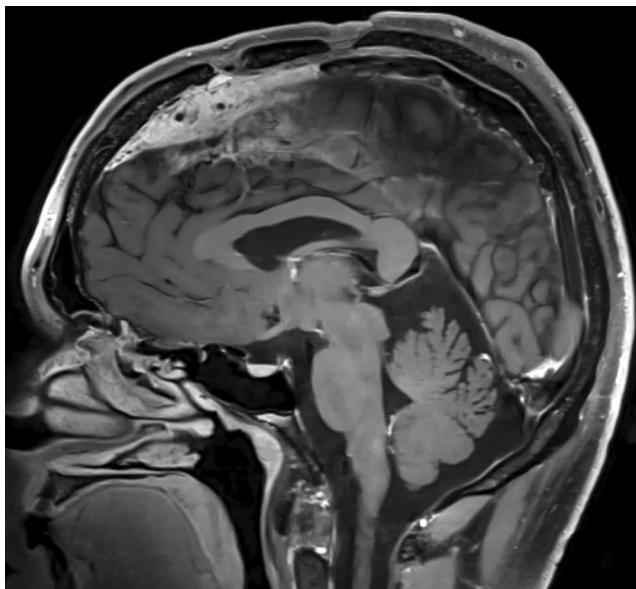


Fig 1 Sagittal T1w DB CS-SPACE image of meningioma infiltrating superior sagittal sinus

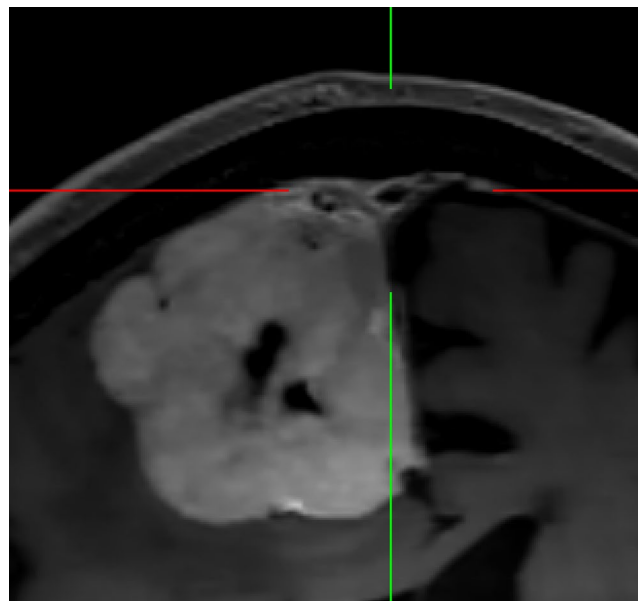


Fig. 3 Meningeoma infiltration the wall of superior sagittal sinus with open sinus lumen on T1w DB CS-SPACE

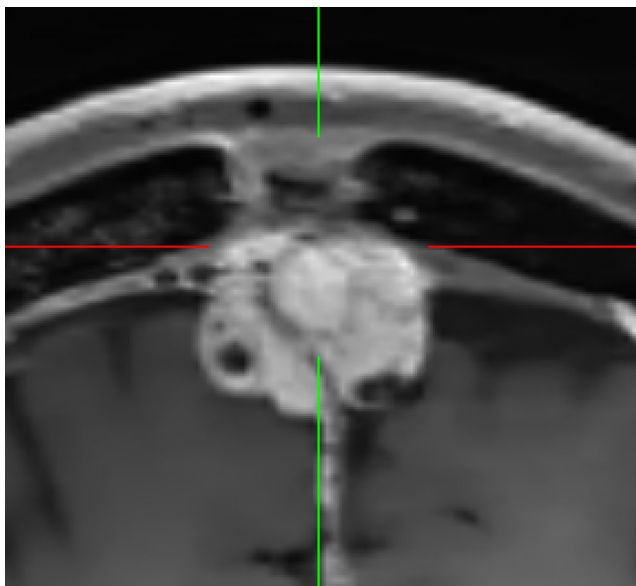


Fig 2 Complete obliteration of superior sagittal sinus by meningioma on T1w DB CS-SPACE

ical outcome parameters, including craniotomy size, extent of resection (EOR), language deficits at different time points, Karnofsky performance status (KPS) score, duration of surgery, and inpatient stay were assessed. **Results:** Regarding the EOR according to postoperative evaluation, 28.3% of patients showed tumor residuals, whereas new surgery-related permanent language deficits occurred in 8.3% of patients (Fig. 2). KPS scores remained unchanged (median preoperatively: 90; follow-up: 90).

Conclusion: This is one of the first studies to present a clinical outcome analysis of this modern approach. Despite human language function is a highly complex and dynamic network, the presented approach offers excellent functional and oncological outcome in patients undergoing surgery of lesions affecting this network.

203

Imaging cerebral venous sinus infiltration of meningiomas using a 3D T1w dark blood fast spin echo sequence with compressed sensing.

Philippe Dovi-Akue^{*1}, Axel Krafft², Oliver Schnell³, Horst Urbach⁴, Stephan Meckel⁵

¹Klinik für Neuroradiologie, Freiburg

²Albert-Ludwigs-Universität Freiburg, Universitätsklinikum Freiburg, Medizinische Fakultät, Radiologische Klinik, Medizin Physik, Freiburg, Deutschland

³Department of Neurosurgery, Medical Center—University of Freiburg, Faculty of Medicine, University of Freiburg, Freiburg, Deutschland

⁴Universitätsklinikum Freiburg, Klinik für Neuroradiologie, Freiburg, Deutschland

⁵Klinik für Neuroradiologie, Freiburg, Deutschland

Purpose: To evaluate the cerebral venous sinus infiltration of meningiomas by using a new contrast enhanced 3D T1w dark blood (DB) fast spin echo sequence using compressed sensing (CS-SPACE) and compare it to the routinely used 2D TOF and T1w MPRAGE.

Methods: 3T MR imaging was performed in 20 patients with suspected meningioma infiltrating the venous sinus. Two neuroradiologists evaluated the infiltration of the meningioma in the venous sinus using a 2D TOF venography and a contrast enhanced T1w MPRAGE together and independently the contrast enhanced T1w DB CS-SPACE. Furthermore the tumor signal was determined in the contrast enhanced sequences objectively by measuring a contrast to noise ratio (CNR) as well as subjectively by using a 4 point scale.

Results: Tumor infiltration of a venous sinus assessed on T1w DB CS-SPACE showed an excellent agreement with the combination of 2D TOF and T1w MPRAGE sequences with a kappa value of 0.857. Furthermore grading the lumen infiltration in no occlusion, partial occlusion (<50%, >50%) and complete occlusion (**Fig 1–3**) showed a very good agreement with a kappa value of 0.783. The tumor contrast in the T1w DB CS-SPACE was higher than in the T1w MPRAGE while the

differences of the CNR values ($p=0.06$) and the 4 point scale ($p=0.1$) were not significant.

Conclusion: In MRI imaging of meningiomas, 3D T1w DB CS-SPACE may replace the routinely used combination of 2D TOF venography and T1w MPRAGE for evaluating the venous sinus infiltration.

245

Radiological effect of dexamethasone use in patients with brain metastasis

Tanja Schneider^{*1}, Paul Bittrich², Hannes Leischner³, Jens Fiehler⁴, Gerhard Schoen⁵, Helge Kniep⁶, Susanne Siemonsen⁷

¹-, -, Hamburg, Deutschland

²Universitätsklinikum Hamburg-Eppendorf

³Universitätsklinikum Hamburg-Eppendorf, Klinik und Poliklinik für Neuroradiologische Diagnostik und Intervention, Hamburg, Deutschland

⁴Diagnostikzentrum Univ.-Klinikum Hamburg-Eppendorf, Klinik und Poliklinik für Neuroradiologische Diagnostik und Intervention, Hamburg, Deutschland

⁵Universitätsklinikum Hamburg-Eppendorf, Zentrum für Experimentelle Medizin Institut für Medizinische Biometrie und Epidemiologie, Deutschland

⁶Klinik und Poliklinik für Neuroradiologische Diagnostik und Intervention, Universitätsklinikum Hamburg-Eppendorf, Hamburg, Deutschland

⁷Klinik und Poliklinik für Neuroradiologische Diagnostik und Intervention, Universitätsklinikum Hamburg-Eppendorf, Hamburg, D

Purpose: Imaging studies quantifying the amount of edema reduction in patients with brain metastases (BM) treated with corticosteroids are rare. Here, we aim to determine the radiological effect of dexamethasone use in BM patients.

Methods: This monocentric retrospective study includes 299 patients first-ever diagnosed with 2759 intraaxial BM on MRI. 126/299 patients received dexamethasone prior to MRI due to mass effect of edema (D-pos) and 173 patients did not (D-neg). All BM and their respective edema were semi-manually segmented on post-contrast T1-weighted images.

Results: Edema volumes were higher in D-pos compared to D-neg ($p=0.009$). Multivariate regression analysis showed D-pos being correlated with improved edema reduction ($p<0.001$) even in case of multiple BM ($p=0.038$). The primary tumor type, the total BM volume, and corticosteroid dosage had no significant influence on edema volume.

Conclusion: Use of dexamethasone is effective for peritumoral edema reduction in BM regardless of primary tumor type, BM size, and dosage.

252

Prediction of brain invasion in patients with meningiomas using preoperative magnetic resonance imaging (MRI)

Alborz Adeli^{*1}, Katharina Hess², Christian Mawrin³, Werner Paulus², Walter Stummer⁴, André Kemmling⁵, Walter Heindel⁵, Dorothee Cäcilia Spille⁴, Peter Sporns⁵, Benjamin Brokinkel⁶

¹Institut für Klinische Radiologie, Münster, Deutschland

²Institute für Neuropathologie, Münster

³Institute für Neuropathologie, Magdeburg

⁴Klinik und Poliklinik für Neurochirurgie, Münster

⁵Institut für Klinische Radiologie, Münster

⁶Klinik und Poliklinik für Neurochirurgie, Universitätsklinikum Münster, Münster, Deutschland

Purpose: Brain invasion in meningiomas impacts WHO grading and thus adjuvant treatment and study inclusion. However, brain invasion is rare and both neurosurgical sampling and neuropathological analyses are not standardized. Moreover, associations with imaging findings are sparsely known but could distinctly improve the accuracy of the detection of brain invasion.

Methods: Correlations between brain invasion on microscopic analyses and findings on preoperative MRI were investigated in 880 meningioma patients (262 males, 30% and 618 females, 80%, median age: 58 years) in uni- and multivariate analyses.

Results: Brain invasion was found in microscopic analyses of 58 tumors (6%) and strongly correlated with other criteria of atypia/anaplasia ($p<0.001$). All contrast enhancing tumor capsule, disruption of the arachnoid layer, intratumoral calcifications and T2-intensity of the lesion were not related to high-grade histology or brain invasion ($p>0.05$, each). High-grade histology ($p<0.001$) but not brain invasion (OR: 1.66, 95%CI .88–3.06; $p=.116$) was associated with convexity or parasagittal tumor location. Irregular shape (OR: 4.74, 95%CI 1.25–18.04; $p=.022$), heterogeneous enhancement (OR: 4.14, 95%CI 1.12–15.30; $p=.033$) and, with borderline significance, peritumoral brain edema (OR: 1.00, 95%CI 1.00–1.01; $p=.063$) were identified as new predictors for brain invasive growth, independent of other histopathological criteria.

Conclusion: Several imaging characteristics were identified as predictors for brain invasion. Consideration in communication between the neuroradiologist, neurosurgeon and the neuropathologist might increase the accuracy of the detection of brain invasion during microscopic analyses.

259

Contrast enhancement predicting survival in integrated molecular subtypes of diffuse glioma: an observational cohort study

Johann-Martin Hempel^{*1}, Cornelia Brendle², Benjamin Bender², Georg Bier³, Marco Skardelly⁴, Irina Gepfner-Tuma³, Franziska Eckert⁵, Ulrike Ernemann², Jens Schittenhelm⁶

¹Uniklinik Tübingen, Abteilung für Diagnostische und Interventionelle Neuroradiologie, Tübingen, Deutschland

²Universitätsklinikum Tübingen, Radiologische Klinik, Abteilung für Diagnostische und Interventionelle Neuroradiologie, Tübingen, Deutschland

³Uniklinik Tübingen

⁴Universitätsklinik Tübingen, Klinik für Neurochirurgie, Tübingen, Deutschland

⁵Universitätsklinik für Radioonkologie, Tübingen, Deutschland

⁶Universitätsklinik Tübingen, Institut für Neuropathologie, Tübingen, Deutschland

Purpose: To assess the predictive value of MRI gadolinium enhancement as a prognostic factor in the 2016 CNS WHO integrated glioma groups.

Methods: 450 glioma patients were retrospectively assessed using gadolinium enhancement, survival, and relevant prognostic molecular data [isocitrate dehydrogenase (IDH); alpha-thalassemia/mental retardation syndrome X-linked (ATRX); chromosome 1p/19q loss of heterozygosity; and O6-methylguanine DNA methyltransferase (MGMT)]. Kaplan–Meier method was used to assess univariate survival data. Multivariate Cox proportional hazards model was performed on significant results from the univariate analysis.

Results: There were significant differences in survival between patient age ($p<0.0001$), WHO glioma grades ($p<0.0001$), and integrated molecular profiles ($p<0.0001$). Patients with IDH1/2 mutation, loss of ATRX expression, and methylated MGMT promoter showed significantly better survival than those with the IDH wild type ($p<0.0001$),

retained ATRX expression ($p < 0.0001$), and unmethylated MGMT promoter ($p = 0.019$). Survival was significantly better in patients without gadolinium enhancement ($p = 0.009$) who were in the IDH wild type glioma and glioma with retained ATRX expression groups ($p = 0.018$ and 0.030 , respectively).

Conclusion: In univariate analysis, the presence of gadolinium enhancement on preoperative MRI scans is an unfavorable factor for survival. Regarding the molecular subgroups, gadolinium enhancement is an unfavorable prognostic factor in gliomas with IDH wild type and those with ATRX retention. However, in multivariate analysis only patient age, IDH1/2 mutation status, MGMT promoter methylation status, and WHO grade IV are relevant for predicting survival.

271

MP2RAGE-based T1-relaxometry in glioblastomas

Gheorghe Jamneala^{*1}, Urs Würtemberger², Dieter Henrik Heiland³, Irina Mader⁴, Horst Urbach⁵

¹Department of Neuroradiology, University Hospital Freiburg, Freiburg, Deutschland

²Department of Neuroradiology, University Hospital Freiburg, Freiburg Im Breisgau

³Department of Neurosurgery, Medical Center—University of Freiburg, Faculty of Medicine, University of Freiburg, Freiburg, Germany, Freiburg, D

⁴Klinik für Neuroradiologie, Universitätsklinikum Freiburg, Bad Krozingen, D

⁵Universitätsklinikum Freiburg, Klinik für Neuroradiologie, Freiburg, Deutschland

Purpose: The aim of MP2RAGE-based T1-relaxometry is to test the statement that contrast uptake in glioblastomas can be predicted using native T1-relaxometry (Hattingen E et al., *Oncotarget* 2017).

Methods: 14 patients with histologically confirmed glioblastomas were preoperatively examined in addition to a standardized tumor protocol with T2* perfusion and ¹H-Spectroscopy with a MP2RAGE sequence before and after contrast administration. T1 relaxation times were calculated in contrast enhancing, necrotic and diffuse infiltrating tumor as well as in normal appearing white matter.

Results: T1 relaxation times were 1637 ± 108 , 1757 ± 93 , and 1724 ± 80 ms before and 702 ± 53 , 1506 ± 140 , and 1678 ± 86 ms after contrast administration in contrast enhancing, necrotic, and diffuse infiltrating tumor segments, respectively. In the normal appearing white matter, T1 relaxation times were 872 ± 35 ms before and 840 ± 35 ms after contrast administration.

Conclusion: T1 relaxation times derived from a MP2RAGE sequence tend to be lower in the contrast enhancing than in the non-contrast enhancing tumor portions. Only in contrast-enhanced tumor segments the T1-relaxation time after contrast administration drops significantly.

285

Selective Chemical Exchange Saturation Transfer effects in brain tumors compared to PET contrast at 3T

Anagha Deshmane¹, Kai Herz¹, Mark Schuppert¹, Tobias Lindig², Chirayu Gandhi¹, Matthias Reimold³, Ghazaleh Tabatabai⁴, Klaus Scheffler⁵, Ulrike Ernemann⁶, Moritz Zaiss⁷, Benjamin Bender^{*6}

¹Magnetic Resonance Center, Max Planck Institute for Biological Cybernetics, Tübingen, Deutschland

²Radiologische Klinik, Abteilung für Diagnostische und Interventionelle Neuroradiologie, Tübingen, Deutschland

³Nuclear Medicine and Clinical Molecular Imaging, Tübingen, Deutschland

⁴Interdisziplinäres Zentrum für Neuroonkologie, Universitätsklinik Tübingen, Tübingen, Deutschland

⁵Department of Biomedical Magnetic Resonance, University of Tübingen, Tübingen, Germany, High-Field Magnetic Resonance Center, Max-Planck-Institute for Biological Cybernetics, Tübingen, Deutschland

⁶Universitätsklinikum Tübingen, Radiologische Klinik, Abteilung für Diagnostische und Interventionelle Neuroradiologie, Tübingen, Deutschland

⁷Max Planck Institut für Biologische Kybernetik, Tübingen, Deutschland

Purpose: CEST allows for indirect detection of diluted molecules via their saturation transfer to the abundant water pool ¹⁻³. At 3T, the frequency separation of different CEST effects is difficult and many applications of CEST use MTR_{asym} evaluation. In this study, we use low-power saturation to separate the two major contributors the MTR_{asym} signal, namely APT (at +3.5 ppm) and NOE effects (at -3.5 ppm), and investigate correlations with 18F-FET PET enhancement in brain tumors.

Methods: 9 patients scanned on a 3T PET/MR system for suspected glioma or recurrent glioma were evaluated (1 radio-necrosis, 1 gliosis, 3 high grade, 4 low grade). Selective protein CEST Z-spectra were acquired with 4s saturation (100 Gaussian pulses, B1=0.6 μT, pulse duration 20ms, duty cycle 50%) at 53 frequency offsets ranging from -100 ppm to +100 ppm. CEST Z-spectra were de-noised using principle component analysis, retaining 15 principle components. Two-stage Lorentzian analysis was applied to estimate contributions from direct water saturation, magnetization transfer effects from macromolecules⁴, and selective CEST effects.

Results: Selective NOE effects were stronger than APT CEST effects in both healthy and diseased tissues. Compared to contralateral tissues, tumor regions exhibit reduced NOE signals and mixed APT signals, consistent with results from previous studies^{4,5}. There was no correlation between PET uptake and CEST signals within the tumor.

Conclusion: NOE and amide CEST separation is possible at 3T and provide additional information compared to 18F-FET PET.

Reference

1. J. Chem. Phys. 1963;39:2892–901
2. J. Magn. Reson. 2000;143:79–87
3. Nat. Med. 2003;9:1085–90
4. Neuroimage 2015;112:180–188
5. NMR Biomed. 2017;30:e3735

299

Correlated MRI and ultramicroscopy of brain tumors reveals vast heterogeneity of tumor infiltration and neoangiogenesis in preclinical models and the human disease

Michael Breckwoldt^{*1}, Julia Bode², Felix Sahn³, Gergely Solecki⁴, Artur Hahn⁵, Anna Berghoff⁴, Wolfgang Wick⁶, Christel Herold-Mende⁷, Sabine Heiland⁸, Martin Bendszus⁹, Felix Tobias Kurz¹⁰, Frank Winkler¹¹, Björn Tews²

¹Abteilung für Neuroradiologie, Universitätsklinikum Heidelberg, Heidelberg, Deutschland

²Deutsches Krebsforschungszentrum, Heidelberg

³Neuropathologie Uniklinik Heidelberg

⁴Deutsches Krebsforschungszentrum

⁵Abteilung für Neuroradiologie, Universitätsklinikum Heidelberg, D

⁶Neurologie, Uniklinik Heidelberg

⁷Neurochirurgie, Uniklinik Heidelberg

⁸Experimentelle Neuroradiologie, Experimentelle Neuroradiologie, Neuroradiologie, Heidelberg, Deutschland

⁹University Hospital Heidelberg, Department of Neuroradiology, Heidelberg, Deutschland

¹⁰Universitätsklinik Heidelberg, Uniklinikum Heidelberg, Neuroradiologie, Heidelberg, Deutschland

¹¹Universitätsklinikum Heidelberg, Neurologie, Neuroonkologie, Nationales Centrum für Tumorerkrankungen (Nct), Deutsches Konsortium für Translationale Krebsforschung (Dktk), Deutsches Krebsforschungszentrum (Dkfz), Heidelberg, Deutschland

Purpose: Diffuse tumor infiltration into the adjacent brain parenchyma is an effective dissemination mechanism of brain tumors. We use correlated magnetic resonance imaging and ultramicroscopy (MR-UM) to investigate tumor infiltration and neoangiogenesis in a translational approach in several preclinical brain tumor models and the human disease.

Methods: We compare infiltration and neoangiogenesis patterns in four brain tumor models (U87, RCAS/tva, S24, A2058) and brain tumor pathological specimen (IDH WT, IDH R132H, brain metastasis). The MRI protocol included T1w/T2w, DCE and T2*w and was performed on a small animal scanner at 9.4 Tesla (80 μ m isotropic resolution). Ultramicroscopy of entire unsectioned brains/brain tumor specimen was performed after tissue clearing (5 μ m in plane resolution). Fluorescent labeling of tumor cells and/or the microvasculature was based on the expression of fluorescent proteins (S24-tdtomato, intravital dyes (lectin-FITC) or endogenous contrasts (erythrocytes).

Results: The U87MG glioma model resembles the brain metastases model A2058 with an encapsulated growth, extensive neoangiogenesis and profound blood-brain barrier disruption on dynamic contrast enhanced MRI. In contrast S24 experimental gliomas exhibited only minimal blood-brain barrier breakdown but extensive infiltration into the adjacent parenchyma and along white matter tracts to the contralateral hemisphere mimicking *IDH* wildtype glioblastomas. MR-UM.

Conclusion: MR-UM reveals huge morphological diversity of brain tumor models regarding their infiltrative and neoangiogenic capacities and directly compares them to the human disease.

340

Diffusion and perfusion MRI in glioblastoma with gliomatosis cerebri growth pattern

Alex Förster^{*1}, Stefanie Brehmer², Marcel Seiz-Rosenhagen², Iris Mildenerberger³, Frank Giordano⁴, Holger Wenz⁵, Christoph Groden⁵

¹Abteilung für Neuroradiologie, Universitätsmedizin Mannheim, Mannheim, Deutschland

²Neurochirurgische Klinik, Universitätsmedizin Mannheim

³Neurologische Klinik, Universitätsmedizin Mannheim

⁴Klinik für Strahlentherapie und Radioonkologie, Universitätsmedizin Mannheim

⁵Abteilung für Neuroradiologie, Universitätsmedizin Mannheim

Purpose: Gliomatosis cerebri (GC) is a rare growth pattern of glioblastoma (GBM) whose diffuse nature is reflected by unspecific findings on conventional MRI. In the present study we sought to evaluate the additional value of diffusion- (DWI) and perfusion weighted (PWI) MRI for a more detailed characterization.

Methods: We analyzed the MRI findings in 8 patients with histologically proven GBM with GC growth pattern with special focus on T2 lesion pattern, volume, relative apparent diffusion coefficient (rADC), and relative cerebral blood volume (rCBV) and compared these to age-/gender-matched patients with solitary GBM.

Results: Overall, 16 patients (median age 59.5 years, 4 male) were included in the study. Of these, 8 patients had a GBM with GC growth pattern, and 8 patients a solitary GBM. While the median rADC (1.27 [IQR 1.12–1.41]) within the T2 lesion was significant lower in GBM with GC growth pattern compared to solitary GBM (1.74 [IQR 1.45–1.96]; $p=0.003$), the median T2 lesion volume and rCBV within the T2 lesion did not differ significantly. Furthermore, 6 patients with GBM with GC growth pattern showed focal areas with significantly reduced rADC ($p=0.043$), and/or increased rCBV ($p=0.028$, see Fig. 1).

Conclusion: Lower rADC in GBM with GC growth pattern might reflect the diffuse tumor cell infiltration whereas the focal areas with decreased rADC and/or increased rCBV probably indicate high tumor cell density which may be useful for biopsy guidance.

352

Ein Übersichtsvortrag von MTRA für MTRA's und lautet "Stroke-Bildgebung Heute". Der Vortrag beinhaltet einfache, jedoch aber auch interessante Physiologie und Pathologie mit vielen anschaulichen Beispielen, und damit auch das Verstehen eines Strokes und dessen Folgen mit und ohne Therapie für MTRA'S.

Tommy Bienias^{*1}

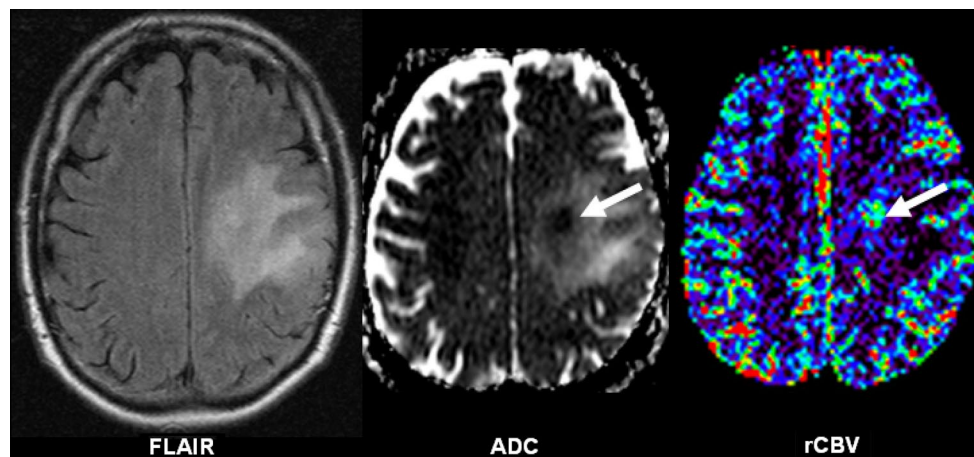
¹Ab 01.07.2018 Institut für Neuroradiologie Uniklinik-Frankfurt, Radiologische Klinik Bonn (Neuroradiologie), Frankfurt am Main, Deutschland

Purpose: A Dissertation from X-Ray-Assistant to X-Ray-Assistants.

It contains physiology, pathology in an easy way for a better understanding of (neuro-) radiological-diagnostic methods of today and shows the consequences of Strokes with, or without therapy by CT/MRI Images.

Methods: It's only a dissertation for X-Ray Assistant

Fig. 1



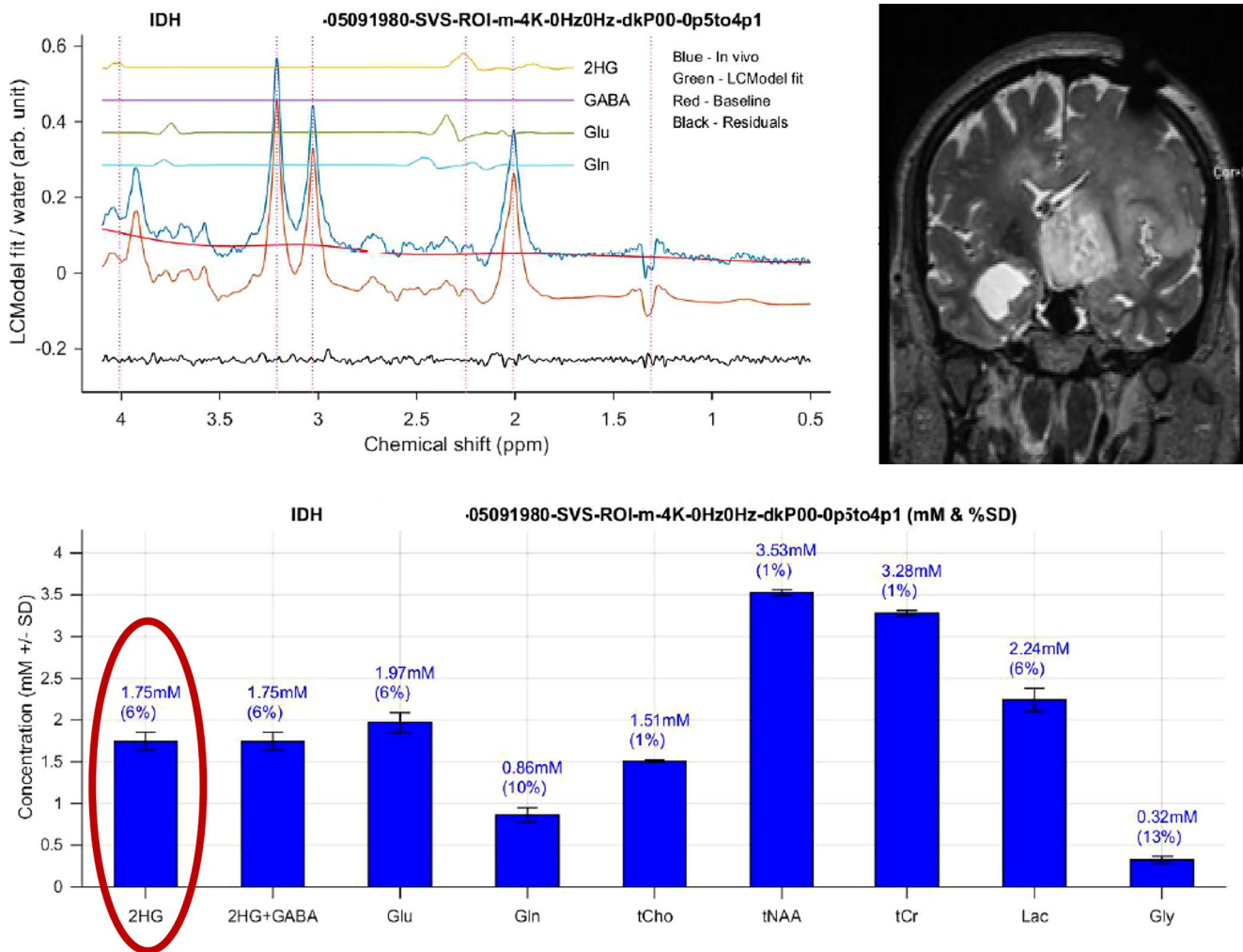


Fig. 1

354

IDH characterization of glioma using 1H MR-spectroscopy

Annett Werner^{*1}, Amir Zolal², Tareq Juratli², Gabriele Schackert², Jennifer Linn³

¹Clinic and Institute for Diagnostic and Interventional Neuroradiology, University Hospital Carl Gustav Cars Dresden, Dresden, Deutschland

²Department of Neurosurgery and Outpatient Clinic, Carl Gustav Carus Medical Faculty

³Clinic and Institute for Diagnostic and Interventional Neuroradiology, University Hospital Carl Gustav Cars Dresden

Purpose: IDH (*Isocitrate dehydrogenase*) mutation is a central and defining event in the progression of glioma and may be a key target for future therapies.

To test the accuracy and reliability of 2HG (2-Hydroxyglutarate) MR-spectroscopy for the characterization of glioma

1. preoperative identification of the mutation status
2. differentiation between tumor recurrence and therapeutically caused changes

Methods: 17 patients (Ø 42 years); MRS: 3T Siemens "Verio"; modified PRESS-sequence; metabolite quantification using LC-Model and

special MATLAB-script (C.Choi, USA [1]); analysis of IDH mutation using the *Ion Torrent NGS* (next gen sequencing) technology.

Results: Good accordance between 2HG-estimation using MRS and the molecular IDH-mutation status (13/15 cases; sensitivity: 92%, specificity: 67%); technical problems in 2 cases (metal artefacts).

Conclusion: Reliable method for the preoperative characterization of IDH-mutation in glioma within the context of this study, but larger number of cases are necessary to address the clinical significance of 2HG-MRS.

Literatur

1. Choi C, Ganji SK, De Berardinis RJ, Hatanpaa KJ, Rakheja D, Kovacs Z, et al. 2-hydroxyglutarate detection by magnetic resonance spectroscopy in IDH-mutated patients with gliomas. *Nat Med* 2012;18:624–9.

384

Non-invasive, intracranial detection of the fluoridated mutation specific IDH1-Inhibitor BAY 1436032 in an orthotopic glioma model using small animal MR spectroscopy

Katharina Wenger-Alakmeh^{*1}, Michael Burger², Christian Richter³, Joachim Steinbach², Marlies Wagner⁴, Oliver Bähr⁵, Ulrich Pilatus⁶

¹Department of Neuroradiology, University Hospital Frankfurt, Frankfurt am Main, Germany, Frankfurt am Main

²Department of Neurooncology, University Hospital Frankfurt, Frankfurt am Main, Germany

³Institute for Organic Chemistry and Chemical Biology, Goethe University, Frankfurt am Main, Germany

⁴Universitätsklinikum Frankfurt, Institut für Neuroradiologie, Frankfurt, D

⁵Universitätsklinikum Frankfurt, Dr. Senckenbergisches Institut für Neurooncologie, Frankfurt/Main, Deutschland

⁶Goethe Universität, Institut für Neuroradiologie, Frankfurt, Deutschland

Purpose: IDH mutations are the most important molecular alterations in human glioma. BAY 1436032 is a small-molecule inhibitor of IDH1 R132X mutations, inhibiting the mutation mediated generation of (D-)2-Hydroxyglutarate (2-HG), thereby reducing oncometabolic effects of 2-HG on tumor cells. BAY 1436032 has a trifluoromethoxy group and might be detectable in vivo using ¹⁹F MRS.

Methods: BAY 1436032 was solubilized in DMSO or ethanol, administered to human serum and analyzed using NMR spectrometers (500 and 600 MHz, Bruker Avance DRX) as well as a small animal MR-scanner (300 MHz, Bruker PharmaScan®). We analyzed serum samples of a patient treated with BAY 1436032 in a clinical phase I trial. Finally, we aimed to detect BAY 1436032 in glioma mouse models. Female athymic nude mice and C57BL/6 mice with orthotopic glioma xenografts (LNT-229, LNT-229 IDH1R132H, GL261) were orally treated with BAY 1436032 and examined using a 20 mm ¹H/¹⁹F transmit-receive surface coil (¹H PRESS, ¹⁹F single pulse).

Results: We were able to detect BAY 1436032 using above-mentioned in vitro and ex vivo probes. Signal shape was highly dependent on serum proteins. In our animals, a ¹⁹F signal could be identified at approximately -59 ppm to -60 ppm in the previously (in vitro and ex vivo) identified area for the BAY 1436032 fluorine signal (external reference TFA at -76.55 ppm). Signal shape varied from one to multiple broad peaks. Mass spectrometric analysis of corresponding tissue probes (brain, extracted immediately after completion of MRI scan) and signal quantitation are still ongoing, as well as the evaluation of 2-HG levels using ¹H MRS.

Conclusion: In vivo detection of BAY 1436032 using ¹⁹F MRS is technically challenging, but feasible with regard to our animal model.

413

Vessel radius mapping for realistic vascular architecture in a U87-glioblastoma xenograft model

Lukas R Buschle¹, Christian H Ziener¹, Ke Zhang¹, Volker J Sturm², Thomas Kampf³, Artur Hahn², Gergely Solecki⁴, Frank Winkler⁴, Martin Bendszus², Sabine Heiland², Heinz-Peter Schlemmer⁴, Felix Tobias Kurz⁵

¹Universitätsklinikum Heidelberg, Neuroradiologie, Deutsches Krebsforschungszentrum, Heidelberg

²Universitätsklinikum Heidelberg, Neuroradiologie

³Universitätsklinikum Würzburg, Neuroradiologie

⁴Deutsches Krebsforschungszentrum, Heidelberg

⁵Universitätsklinik Heidelberg, Uniklinikum Heidelberg, Neuroradiologie, Heidelberg, Deutschland

Purpose: To produce cerebral vessel radius maps that incorporate both susceptibility and diffusion effects in random vessel geometries to monitor and quantify microvascular changes in glioblastoma multiforme.

Methods: The cerebral microvascular arrangement is codified in the free induction decay through local differences in magnetic susceptibility between blood-filled capillaries and the surrounding tissue that

generates local magnetic field inhomogeneities. We have developed a model that considers both diffusion and susceptibility effects around randomly positioned and oriented arrangements of vessels that provides a connection between relaxation rate R2* and voxel-specific capillary radius R. The model is an extension of the strong-collision approximation (SCA) model ¹.

Results: Relaxation rates are shown versus capillary radii for a set of typical model parameters in brain tissue (Fig. 1); the model is validated against a numerically simulated signal decay on randomly positioned and oriented vessels ². Radius maps are produced in a U87-glioblastoma xenograft mouse model ³ based on a multi-gradient-echo sequence (Fig. 2) that show significantly larger radii in glioblastoma tissue compared to contralateral healthy tissue of 6.42±0.55 µm vs. 2.81±0.44 µm (n=7, p=0.011).

Conclusion: The obtained vessel radius maps can be used to evaluate capillary networks in healthy and pathological brain tissue.

References:

1 Bauer WR et al. Magn Reson Med 1999;41:51–62.

2 Dickson JD et al. J Magn Reson 2011;212:17–25.

3 von Baumgarten L et al. Clin Cancer Res 2011;17:1692–6205.

Diagnostic Neuroradiology: Vessel Wall

202

Contrast Enhancement Following Coiling of Intracranial Aneurysms in 3T MRI and its Relationship to Aneurysm Recurrence Following Endovascular Treatment: A Feasibility Study

Samer Elsheikh^{*1}, Stephan Meckel², Horst Urbach¹

¹Universitätsklinikum Freiburg, Klinik für Neuroradiologie, Freiburg, Deutschland

²Klinik für Neuroradiologie, Freiburg, Deutschland

Purpose: Coiling of cerebral aneurysms aims at preventing aneurysm rupture due to endothelialisation of the aneurysm neck. Contrast enhanced, high resolution black blood MRI facilitates imaging of the vessel walls but also of the sac contents and is therefore suited to study the healing process.

Methods: This is a non-randomized prospective feasibility study. Patients, presenting for the follow-up MRI/MRA examination were considered for inclusion. Pre- and postcontrast axial T1 and sagittal 3D T1-space black blood sequences were acquired. Outcomes included: time elapsed since coiling, frequency and pattern of aneurysmal enhancement, image quality and degradation due to implants and patient compliance.

Results: A total of 31 patients were included (1 Patient interrupted the examination). Time elapsed since treatment was 87–5318 days (median: 417). Enhancement was seen in 24/30 aneurysms in multiple locations (n=31). Enhancement inside the aneurysm (n=17), of the wall (n=7)/dome (n=1) or at the base (n=6). In 28/30 patients the images were of adequate diagnostic quality. Stent implants caused negligible image artefacts.

Conclusion: Aneurysm enhancement following coiling is a common finding. We are running a long term study to examine changes occurring over time and their association with aneurysm recurrence.

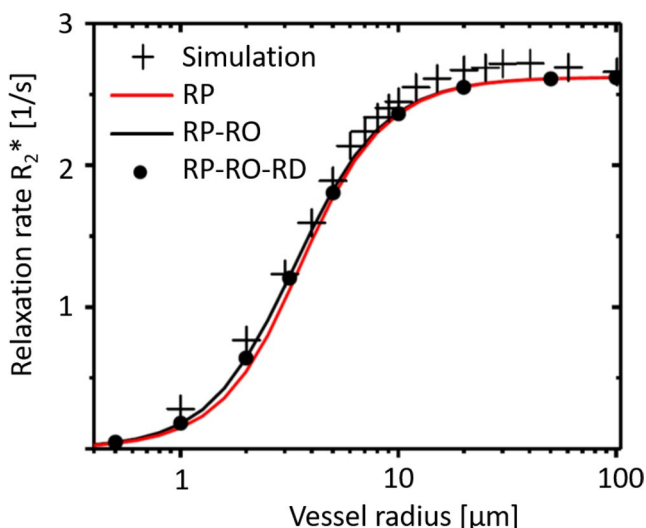


Fig. 1 Relaxation rate R_2^* vs. vessel radius. Simulation data from ² for randomly positioned and oriented radii are shown against model results for randomly positioned (RP) vessels, including random vessel orientation (RP-RO), and including a random distribution of vessel radii (RP-RO-RD) with a coefficient of variation of 0.15. Simulation results best coincide with the RP-RO model, indicating a stronger influence of mean radii over radius distributions within one voxel on the signal decay. (Simulation parameters: blood volume fraction=0.03, diffusion constant = $1 \mu\text{m}^2/\text{ms}$, TE=30ms, $B_0=3\text{T}$.)

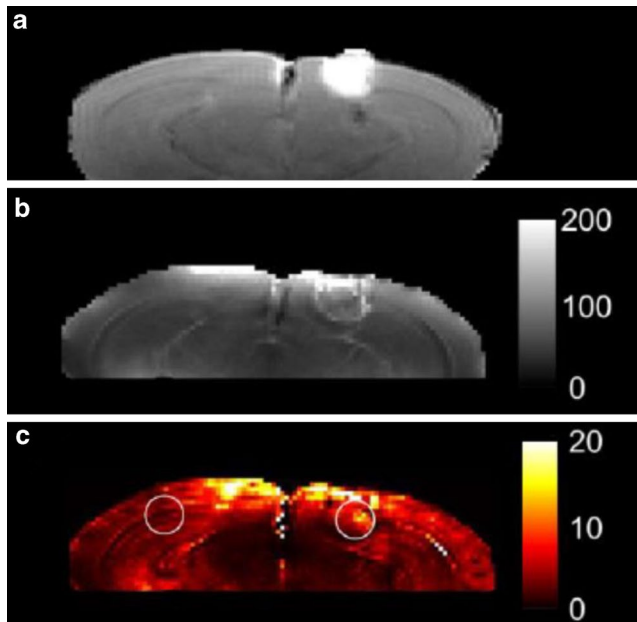


Fig. 2 Vessel radius mapping for mouse glioblastoma. **a** T1w contrast-enhanced image of left-hemispheric cortically injected U87-glioblastoma cells in 8–10 week-old male NMRI nude mice. **b** R_2^* map (units: $1/\text{s}$; based on a multigradient-echo sequence with TE=3.5, 8.5, 13.5, ... 38.5 ms, TR=800 ms). **c** Vessel radius map (units: μm , resolution: $200 \times 200 \mu\text{m}^2$). Radii are increased in the tumor region (encircled, left hemisphere) compared to the contralateral side.

257

Contrast enhanced 3T -MRI as potential predictor of aneurysm recurrence after endovascular treatment

Caroline Molavi Tabrizi^{*1}, Gerrit Schubert², Rea Rodriguez-Raecke³, Arno Reich⁴, Martin Wiesmann⁵, Marguerite Müller⁶

¹Klinik für Neuroradiologie der Uniklinik RWTH Aachen, Deutschland

²Universitätsklinikum der RWTH Aachen, Neurochirurgische Klinik, Aachen, Deutschland

³Universitätsklinikum RWTH Aachen

⁴Universitätsklinikum Aachen, Neurologie, Klinik für Neurologie, Aachen, Deutschland

⁵Klinik für Diagnostische und Interventionelle Neuroradiologie, Aachen, Deutschland

⁶Klinik für Diagnostische und Interventionelle Neuroradiologie, RWTH Aachen University, Aachen, Deutschland

Purpose: Recurrence of intracranial aneurysm after endovascular treatment occurs in up to 33,6% (Raymond et al. Stroke 2003). Therefore follow-up is required. For the individual patient it is not possible to predict if or when recurrence occurs. By comparing MRI -data of patients with and without recurrence we intended to find correlations to help select patients that are prone to develop aneurysm recurrence.

Methods: We investigated $n=108$ patients with a total amount of $n=124$ intracranial aneurysms with 3T -MRI at different times after endovascular treatment. $N=189$ MRI -studies were analyzed concerning the presence of contrast enhancement of the thrombus as well as the wall of the aneurysm. Results were compared between aneurysms with ($n=50$) and without recurrence ($n=139$).

Results: Aneurysms with recurrence after endovascular treatment ($n=50$) had a significantly higher prevalence of contrast enhancement of the intraluminal thrombus ($p<0.05$). In most cases this contrast enhancement was detected early (0–3 months) after treatment. Over time (>3 months after treatment) MRI -data of patients with and without recurrence assimilated. We did not find a correlation between contrast enhancement of the aneurysm wall and recurrence.

Conclusion: Early contrast enhancement of the intraluminal thrombus after endovascular treatment of intracranial aneurysms seems to be prognostic for aneurysm recurrence. This finding may correspond to a lower packing volume of the implanted coils.

Reference

1. Raymond et al. Stroke 2003

314

Characteristics of lobulated unruptured intracranial aneurysms as seen on digital subtraction angiography

Lukas Görtz^{*1}, Christoph Kabbasch², Jan Borggrefe³, Christina A. Hamisch⁴, Gerrit Brinker⁵, Roland Goldbrunner⁶, Anastasios Mpotsaris⁷, Boris Krischek⁸

¹Universitätsklinikum Köln, Zentrum für Neurochirurgie, Köln, Deutschland

²Uniklinik Köln, Abteilung für Radiologie und Neuroradiologie, Institut für Diagnostische und Interventionelle Radiologie, Köln, Deutschland

³Universität zu Köln, Institut für Diagnostische und Interventionelle Radiologie, Köln, Deutschland

⁴Klinik und Poliklinik für Allgemeine Neurochirurgie, Zentrum für Neurochirurgie, Uniklinik Köln, Köln, Deutschland

⁵Klinikum der Universität zu Köln; Zentrum für Neurochirurgie; Klinik für Allgemeine Neurochirurgie, Köln, Deutschland

⁶Klinikum der Universität zu Köln, Zentrum für Neurochirurgie, Klinik für Allgemeine Neurochirurgie, Köln, Deutschland

⁷Klinik für Diagnostische und Interventionelle Neuroradiologie, Aachen, Deutschland

⁸Zentrum für Neurochirurgie, Universitätsklinikum Köln

Purpose: Previous studies confirmed that lobulated aneurysms carry a higher risk of rupture than single-sac aneurysms. We aimed to determine the angiographic characteristics of lobulated aneurysms that may help identify aneurysms at risk for rupture at an early stage of aneurysm generation.

Methods: We retrospectively analyzed consecutive patients that underwent digital subtraction angiography between 2010 and 2017. Aneurysm morphology, vessel geometry and treatment indications were compared between lobulated and regular single-sac aneurysms.

Results: A total of 143 patients with 82 lobulated and 121 regular aneurysms were enrolled. In univariate analysis, lobulated shape was significantly related to anterior communicating artery location (26.8% vs. 2.5%; $p < 0.001$), bifurcation location (69.5% vs. 27.3%; $p < 0.001$), aneurysm size (8.1 ± 3.2 mm vs. 4.9 ± 3.0 mm; $p < 0.001$), inflow angle ($144.6 \pm 26.1^\circ$ vs. $113.6 \pm 26.6^\circ$; $p < 0.001$) and aneurysm treatment (86.6% vs. 60.3%; $p < 0.001$). In multivariate analysis, lobulated aneurysms were independently associated with bifurcation location (OR: 3.0, 95% CI: 1.2–7.5; $p = 0.019$), larger aneurysm size (> 5.5 mm; OR: 5.4, 95% CI: 1.7–17.8; $p = 0.005$) and increased inflow angle ($> 125^\circ$; OR: 2.8, 95% CI: 1.1–7.2; $p = 0.031$).

Conclusion: Bifurcation location and a straighter aneurysm inflow angle are independent factors related to aneurysm growth and formation of lobulated aneurysms, and may therefore lead to an increased risk of rupture.

341

The value of dedicated contrast-enhanced MR angiography regarding follow-up imaging of intracranial aneurysms treated by coil embolization

Maximilian Patzig^{*1}, Gruber Margareta², Robert Forbrig³, Franziska Dorn⁴

¹Klinikum der Universität München, Institut für Neuroradiologie, München, Deutschland

²Klinikum der Universität München, Institut für Neuroradiologie

³University Hospital, Institute of Neuroradiology, Munich, Deutschland

⁴Klinikum der Universität München—Campus Großhadern, Institut für Klinische Radiologie, Abteilung für Neuroradiologie, München, Deutschland

Purpose: Aneurysm recurrence after coil embolization is reported in about 20% of cases and is regarded as the major drawback of endovascular therapy in comparison to neurosurgical clipping. Thus, high quality follow-up imaging after coiling is crucial. We aimed to assess the value of dedicated contrast-enhanced MR angiography (ceMRA) in this setting.

Methods: We identified all patients with intracranial aneurysms who were treated by coil embolization at our institution since 2011. Of these, all patients who had at least one follow-up visit with both DSA and 3T-MRI with first-pass arterial ceMRA were included in this study. DSA and MRI exams were separately graded by two blinded readers using the modified Raymond-Roy-Score (mRRS, grades 1–4). The diagnostic accuracy of ceMRA was calculated with DSA serving as a reference standard. For the purpose of this study, “relevant” aneurysm remnants were defined as mRR grades 3 and 4.

Results: The study comprised 114 comparable pairs of ceMRA and DSA. Forty-three of these pairs regarded aneurysms treated by stent-assisted coiling. A relevant aneurysm remnant was detected in 19

cases (16.7%) on DSA and in 24 cases (21.0%) on ceMRA. Sensitivity and specificity of ceMRA for the detection of relevant aneurysm remnants were 94.7% and 93.7%, respectively. In the subgroup of aneurysms treated by stent-assisted coiling, sensitivity and specificity were each 100%.

Conclusion: CeMRA is a highly accurate follow-up imaging tool for coiled aneurysms. The use of stents does not affect the assessability of the treated aneurysm. In our study, ceMRA detected more potentially relevant aneurysm remnants than DSA, raising the question whether DSA can still be considered the gold standard in this setting.

383

Preventing (re-)rupture of both ruptured and unruptured aneurysms treated with coiling: A follow-up algorithm using MR angiography

Ben Gold^{*1}, Joachim Berkefeld², Eva Hermann³, Marlies Wagner⁴

¹Universitätsklinikum Frankfurt, Institut für Neuroradiologie, Frankfurt

²Neuroradiologie, Kelkheim, Deutschland

³Universitätsklinikum Frankfurt

⁴Universitätsklinikum Frankfurt, Institut für Neuroradiologie, Frankfurt, D

Purpose: We analysed our single-center collective of patients with coiled aneurysms, who received follow-up MR angiographies (MRA), to create an algorithm how to monitor coiled aneurysms regarding reperfusion and to prevent (re-)rupture.

Methods: We retrospectively included 206 adult patients with 249 coiled aneurysms from 2003 to 2016. Of those, 166 aneurysms were initially ruptured. Data included localization of the aneurysm (anterior or posterior circulation), rupture yes/no, dates of follow-up MRA, (re-)rupture, and patient characteristics (age, gender). Survival analysis by Kaplan-Meier estimator (each all aneurysms, ruptured and unruptured aneurysms) was performed using the endpoints reperfusion or (re)rupture.

Results: For patient characteristics and aneurysm subgroups see table 1. None of the patients experienced (re-)rupture. Kaplan-Meier-plots suggest highest frequency of reperfusion during the first year after coiling. After four years, reperfusion is rare, and no reperfusion occurred after 5 years (see figures 1 and 2). Further correlation analysis (patient data, extend of aneurysm occlusion etc.) is in progress.

Conclusion: Rupture after aneurysm coiling is extremely rare if follow-up MRA is performed. Our preliminary data suggest the urgent need of follow-up MRA during the first year after coiling. However, in case of stable aneurysms, follow-up MRA after coiling can be suspended. Further correlation analysis regarding patient data and aneurysm characteristics is currently in progress.

Table 1

characteristic	result
age	56,75+/- 10,51
gender	
• f	151/249 (60,64%)
• m	99/249 (39,76%)
Initially ruptured	166/249 (66,66%)
Aneurysm of posterior circulation	116/250 (46,58%)

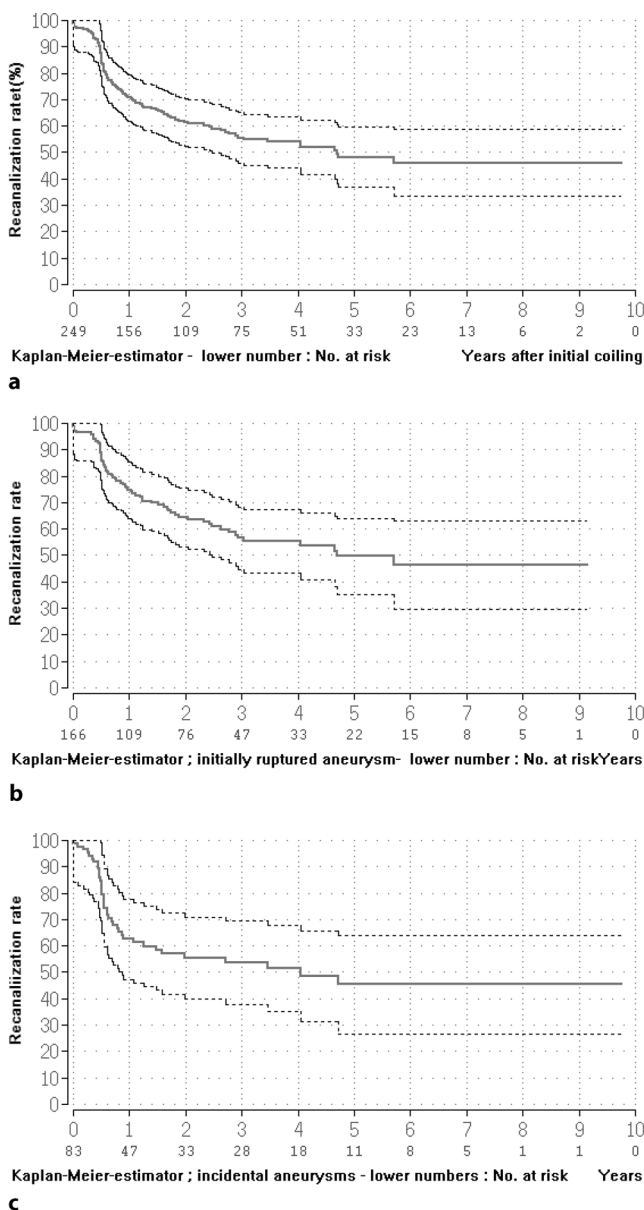


Fig. 1 Arrow indicates acute left thalamic LI in DW-MRI **a**, NCCT **b**, window-optimized NCCT **c** and Best Contrast (BC)

Diagnostic Neuroradiology: Others

119

Triage of Four Noncontrast CT Markers and Spot Sign for Outcome Prediction after Intracerebral Hemorrhage

Peter Sporns^{*1}, Andre Kemmling², Jens Fiehler³, Walter Heindel¹, Uta Hanning⁴

¹Institut für Klinische Radiologie, Institut für Klinische Radiologie, Münster, Deutschland

²Institut für Klinische Radiologie, Universitätsklinikum Münster, UKSH Lübeck, Hamburg, Deutschland

³Diagnostikzentrum Univ.-Klinikum Hamburg-Eppendorf, Klinik und Poliklinik für Neuroradiologische Diagnostik und Intervention, Hamburg, Deutschland

⁴Institut für Diagnostische und Interventionelle Neuroradiologie, Hamburg, Deutschland

Purpose: Besides the established spot sign (SS) in CT angiography (CTA), there is growing evidence that different imaging markers in noncontrast CT (NCCT) offer great value for outcome prediction in patients with intracerebral hemorrhage (ICH). However, it is unclear how the concurrent presence of each sign independently contributes to the predictive power of poor outcome. We therefore aimed to clarify the predictive value of four recently published NCCT parameters (blend sign (BS), black hole sign (BHS), island sign (IS) and hypodensities) and the established SS in one large series of patients with ICH.

Methods: Retrospective study of the stroke database at two tertiary stroke centers; inclusion criteria were: 1) spontaneous ICH and 2) NCCT and CTA performed on admission within 6 hours after onset of symptoms. We defined a binary outcome (good outcome (mRS ≤ 3) versus poor outcome (mRS > 3)) at discharge. The predictive value of each sign was assessed in univariate and multivariable logistic regression models.

Results: Of 201 patients with spontaneous ICH, 28 (13.9%) presented with BHS, 38 (18.9%) with BS, 120 (59.7%) with hypodensities, 53 with IS (26.4%) and 45 (22.4%) with SS. Multivariable logistic regression analysis identified baseline hematoma volume (odds ratio, 1.02 per ml; $P < 0.001$), the presence of intraventricular hemorrhage (odds ratio 2.50; $P = 0.02$) and the presence of the imaging signs hypodensities (odds ratio, 2.47; $P = 0.018$) and SS (odds ratio 11.43; $P < 0.001$) on baseline CT scan as independent predictors of poor outcome.

Conclusion: All NCCT imaging markers show a high correlation with the CTA SS and are reliable predictors of poor outcome in patients with ICH. SS and hypodensities were the most reliable outcome predictors.

124

Age and sex influence mouse brain stiffness

Katharina Schregel^{*1}, Miklos Palotai², Navid Nazari³, Julie P. Merchant⁴, Walter M. Taylor⁴, Charles R. G. Guttmann², Ralph Sinkus⁵, Tracy L. Young-Pearse⁶, Samuel Patz²

¹Department of Radiology, Brigham and Women's Hospital, Harvard Medical School, Institute of Neuroradiology, University Medical Center Goettingen, Goettingen, Deutschland

²Department of Radiology, Brigham and Women's Hospital, Harvard Medical School, Boston, United States

³Department of Biomedical Engineering, Boston University, Boston, United States

⁴Ann Romney Center for Neurologic Diseases, Brigham and Women's Hospital, Boston, United States

⁵Department of Radiological Imaging, Imaging Sciences & Biomedical Engineering Division, King's College London, London, United Kingdom

⁶Ann Romney Center for Neurologic Diseases, Brigham and Women's Hospital, Harvard Medical School, Boston, United States

Purpose: Normal aging is accompanied by neurodegeneration, which influences the cerebral biomechanics. A softening of the human brain with age has been reported¹⁻³ the wave patterns detected by MRE are affected by atrophic changes in brain geometry occurring in an individual's life span. Moreover, regional variability in MRE-detected age effects is expected corresponding to the regional variation in atrophy. Therefore, the sensitivity of brain MRE to brain volume and aging was investigated in 66 healthy volunteers aged 18–72. A linear decline in whole-brain elasticity was observed ($-0.75\%/year$, $R\text{-square}=0.59$, $p < 0.001$). Findings on the impact of sex on human brain stiffness are controversial^{2,3}

constitution of soft biological tissue and is increasingly used as a diagnostic marker, e. g. in staging liver fibrosis or characterizing breast tumors. In this study, multifrequency magnetic resonance elastography was used to investigate the in vivo viscoelasticity of healthy human brain in 55 volunteers (23 females). We investigated the impact of age and sex on mouse brain biomechanics using magnetic resonance elastography (MRE).

Methods: Ten healthy C57BL/6 mice (5f/5 m) underwent repeated MRI and MRE scans at 7T over 14 months. Biomechanical properties were assessed in the following regions: whole brain, corpus callosum, cortex and deep grey matter. Regional differences in brain stiffness over time across the whole cohort and between sexes were evaluated.

Results: Brain stiffness decreased over time. This was observable for both, grey and white matter. Grey and white matter exhibited relevant differences in the biomechanical properties. When comparing male and female mice, the cortical stiffness of female mice was significantly higher than in male animals at an age of 11 months. All other structures had similar stiffness values in males and females.

Conclusion: Physiological aging impacts mouse brain stiffness. The differences in cortical stiffness in males and females might hint at a sexually dimorphic pattern of neurodegeneration. These findings are of interest for future cerebral MRE studies in mice.

References

1. Sack I, et al. The influence of physiological aging and atrophy on brain viscoelastic properties in humans. *PloS One*. 2011;6:e23451.
2. Arani A, et al. Measuring the effects of aging and sex on regional brain stiffness with MR elastography in healthy older adults. *NeuroImage*. 2015;111:59–64.
3. Sack I, et al. The impact of aging and gender on brain viscoelasticity. *NeuroImage*. 2009;46:652–7.

131

First evaluation of a novel method for a single run 3D Angiography (3DA)

Stefan Lang^{*1}, Philip Hölter², Manuel Schmidt³, Hannes Lücking⁴, Christian Kaethner⁵, Markus Kowarschik⁵, Arnd Dörfler⁶

¹Universitätsklinikum Erlangen, Abteilung Neuroradiologie, Erlangen, Deutschland

²Abteilung Neuroradiologie, Erlangen, D

³Universitätsklinikum Erlangen, Neuroradiologische Abteilung, Erlangen, Deutschland

⁴Universitätsklinikum Erlangen, Deutschland

⁵Siemens Healthineers AG

⁶Universitätsklinikum Erlangen, Abteilung für Neuroradiologie, Erlangen, Deutschland

Purpose: 3D DSA consists of mask and fill runs for generating subtracted 3D images. To save patient dose (PD), a novel AI-based method for single run 3D Angiography (3DA) has been developed that generates DSA-like 3D images based on fill runs only. Our aim was an initial evaluation of 3DA.

Methods: 3D DSA datasets of cerebral aneurysms were reconstructed using conventional and prototype software (Siemens Healthineers AG, Erlangen, Germany). Corresponding reconstructions have been analyzed by 2 neuroradiologists in consensus reading in terms of quantitative (aneurysm size AS in mm, parent vessel's diameter VD in mm) and qualitative parameters (image quality IQ, localization, aneurysmal configuration, neck width).

Results: In total 10 datasets ($n_{\text{male}}=6; n_{\text{female}}=4; \text{age}_{\text{mean}}=62.8$ years) have been successfully reconstructed using both conventional and prototype software. In all cases corresponding reconstructions demonstrated complete congruency in terms of IQ ($\text{IQ}_{3\text{D DSA}/3\text{DA}}=4$), local-

ization ($n_{\text{ACA}}=2; n_{\text{ACI}}=4; n_{\text{BA}}=2; n_{\text{MCA}}=2$), aneurysmal configuration (saccular_{3D DSA/3DA}=10) and neck width (narrow_{3D DSA/3DA}=2; medium_{3D DSA/3DA}=2; wide_{3D DSA/3DA}=6). Analysis of the aneurysm size ($\text{AS}_{3\text{D DSA}}=5.2 \pm 3.2$ mm; $\text{AS}_{3\text{DA}}=5.2 \pm 3.1$ mm) and the parent vessel's diameter ($\text{VD}_{3\text{D DSA}}=3.6 \pm 0.8$ mm; $\text{VD}_{3\text{DA}}=3.7 \pm 0.8$ mm) did not show significant differences ($p < 0.05$) between both reconstructions.

Conclusion: 3DA is a promising method and shows comparable results to 3D DSA in terms of quantitative and qualitative parameters and might help to reduce PD.

164

Geschosse in der MRT: bildmorphologische und histologische Auswirkungen/Projectiles in MRI: behavior, image quality and histologic changes

Carsten Hackenbroch^{*1}, Melanie Wafa², Stefanie Kling², Uwe-Max Mauer²

¹Bwk Ulm, Blaustein, Deutschland

²Bwk Ulm

Purpose: Gunshot injuries are rare in Germany, but important in military and police incidents. Thereby MRI is in most cases contraindicated up to now, whereas its information, especially in case of spinal cord injuries or brain injuries, is very important for the outcome of the patient and further rehabilitation. The goal of our study is a better understanding of the behavior of bullets and their fragments in a magnetic field and the histologic changes induced by them.

Methods: Projectiles with ferromagnetic ($n=2$) and non-ferromagnetic ($n=5$) properties were tested in a soft tissue model (M. masseter of a pig). Standard protocols at 1, 1.5 and 3 Tesla were examined. Before and after every MR-scan a CT-Scan was performed. Images were assessed for artifacts, overall quality and motion/torque. Additionally, histology was performed at the contact surfaces between bullets/fragments and soft tissue.

Results: Ferromag. projectiles showed a decreased image quality and strong artifacts, compared to non-ferromag. projectiles, thus having no benefit for clinical use at all. Additionally, there is danger of movement/torque in the magnetic field. Non-ferromag. projectiles showed a very heterogeneous image quality, depending on the material composition. Histology showed no signs of cell death along the fragments.

Conclusion: Non-ferromag. projectiles should be no contraindication for an MRI-scan. But image quality and artifacts are strongly dependent on the material composition. Ferromag. projectiles are contraindicated in a magnetic field due to movement/torque, but no histologic changes (heat-exposure, i. e.) were found. The knowledge of the incorporated projectile is essential for further planning if a patient is suitable for MRI or not.

215

Do we still need contrast agent to maximize sensitivity for new lesions in Multiple Sclerosis?

Paul Eichinger^{*1}, Simon Schön², Hanni Wiestler³, Haike Zhang⁴, Viola Pongratz⁵, Jan Kirschke⁶, Claus Zimmer⁷, Mark Mühlau⁸, Benedikt Wiestler⁹

¹Abteilung für Diagnostische und Interventionelle Neuroradiologie, Klinikum Rechts der Isar, TU München, München, D

²Abteilung für Diagnostische und Interventionelle Neuroradiologie, Klinikum Rechts der Isar, TU München, Germany, München, D

³Kbo Isar-Amper-Klinikum, München, Deutschland

⁴Abteilung für Neuroradiologie, Klinikum Rechts der Isar, TU München, München, Deutschland

⁵Abteilung für Neurologie, Klinikum Rechts der Isar

⁶Abteilung für Diagnostische und Interventionelle Neuroradiologie, München, Deutschland

⁷Klinikum Rechts der Isar der TUM, Technische Universität München, Abteilung für Diagnostische und Interventionelle Neuroradiologie, München, Deutschland

⁸Klinikum Rechts der Isar, Neurologie, München, Deutschland

⁹Neuroradiologie, TU München, München, D

Purpose: The routine administration of contrast agent in follow up MRI of patients with multiple sclerosis (MS) is considered necessary to maximize sensitivity for new lesions. We hypothesized that this does not longer hold true if 3D images and sophisticated image post-processing are used.

Methods: We analyzed 507 MS follow-up scans including 3D FLAIR, 3D T2, 3D Double inversion recovery (DIR) and 3D T1 +/- gadolinium. Additionally, we calculated a longitudinal subtraction map for the DIR images. The non-enhanced images were analyzed for new or enlarging lesions. In an independent read, the contrast-enhanced T1 was analyzed for contrast enhancing lesions (CEL).

Results: In 264 of 507 scans new lesions were detected (total: 1992 new lesions). 207 CEL were detected in 69 of 507 scans. Four of those CEL (0.20% of all new lesions) were missed in the non-enhanced images and only retrospectively identified as new lesions. However, the three patients in whom these CEL were missed showed a high number of both CEL and new lesions that had been correctly detected. Hence, evaluation of the general presence of new lesions did not depend on contrast administration in a single scan.

Conclusion: Contrast agent may be considered dispensable for detecting new lesions. In light of growing concerns regarding intracranial

gadolinium depositions our data question the routine use of contrast agent in follow-up scans of patients with multiple sclerosis.

216

Compressed Sense in MRI of Multiple Sclerosis: Halving scan time without quality loss

Paul Eichinger^{*1}, Andreas Hock², Jan Kirschke³, Claus Zimmer⁴, Mark Mühlau⁵, Benedikt Wiestler⁶

¹Abteilung für Diagnostische und Interventionelle Neuroradiologie, Klinikum Rechts der Isar, TU München, München, D

²Philips GmbH Market Dach

³Abteilung für Diagnostische und Interventionelle Neuroradiologie, München, Deutschland

⁴Klinikum Rechts der Isar der TUM, Technische Universität München, Abteilung für Diagnostische und Interventionelle Neuroradiologie, München, Deutschland

⁵Klinikum Rechts der Isar, Neurologie, München, Deutschland

⁶Neuroradiologie, TU München, München, D

Purpose: Compressed sense (CS) is a method of sparsely undersampling the k-space, thus requiring less readout measurements for a MRI scan. Its introduction into clinical practice allows for reduced scan times. We evaluated CS for double inversion recovery (DIR) sequences in Multiple Sclerosis (MS), where preserving sensitivity for small lesions is particularly important.

Methods: We included 109 MRI scans of patients with MS in which—besides FLAIR, T1 and T2—a standard 3D DIR (scan time 6.30 min)

Fig. 1 Example of a lesion missed in the CS DIR

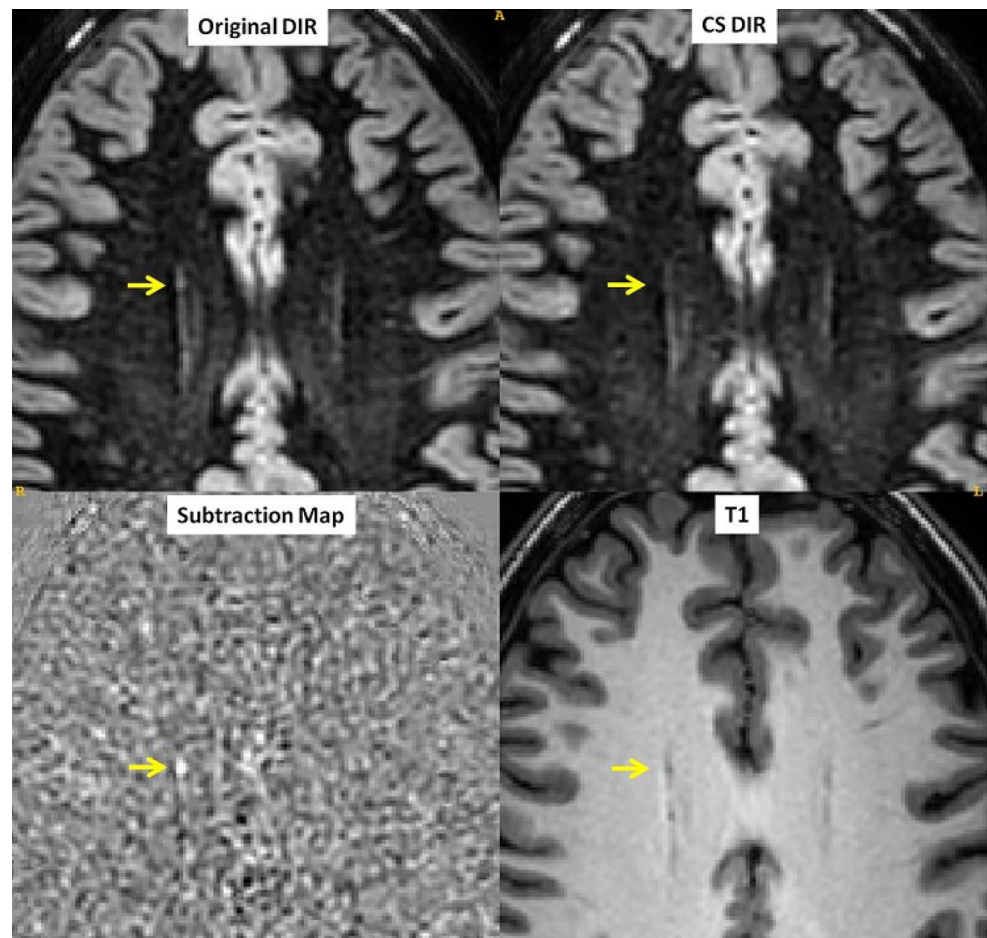
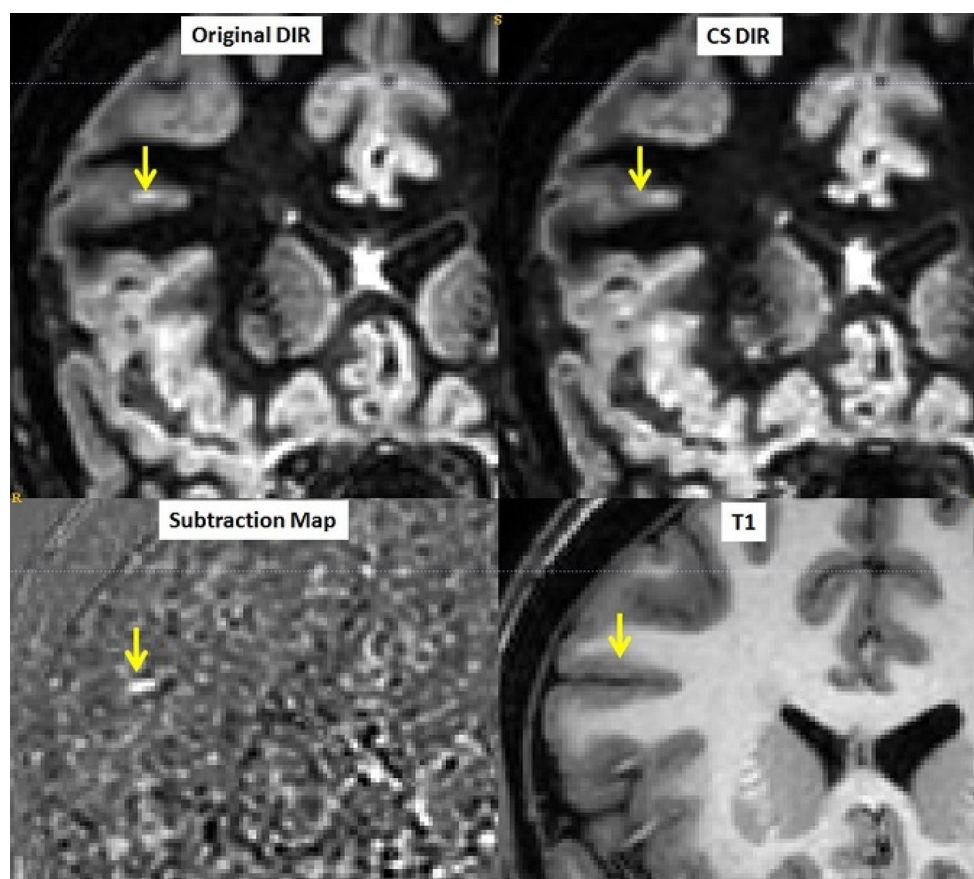


Fig. 2 Example of a cortical artifact in the original DIR: While the original DIR shows a hyperintensity on the cortex/sulcal interface, the T1 image demonstrates the lack of a corresponding lesion, thus revealing it as an imaging artifact



and a DIR with CS (scan time 3.12 min) were acquired. Apart from CS, these sequences shared the same scan parameters. Subtraction images of the two sequences were generated to visualize intensity differences. These subtraction maps were analyzed by two neuroradiologists for discrepant hyperintensities between the DIR sequences.

Results: In total, there were two lesions detected in the original DIR but not in the CS DIR, and one lesion only in the CS-DIR. An example of a lesion not visible in the CS DIR is shown in Fig. 1. With a total lesion count of approx. 8000, these discrepant lesions are negligible. Of note, in 16 scans there were cortical artifacts in the original DIR, not visible in the CS DIR (Fig. 2). Some of these may be mistaken for cortical lesion if not cross checked in other sequences.

Conclusion: With CS, scantime can be reduced up to 50% without compromising sensitivity for lesions. Moreover, CS imaging appears to be less prone to certain imaging artifacts.

222

Leakage of Gadolinium based contrast Agent in the subarachnoid space after intraoperative MRI

Monika Müller-Eschner^{*1}, Martin Voss², Marlies Wagner³

¹Universitätsklinikum Frankfurt, Institut für Neuroradiologie, Frankfurt am Main, D

²Universitätsklinikum Frankfurt, Klinik für Neurologie, Frankfurt am Main, Deutschland

³Universitätsklinikum Frankfurt, Institut für Neuroradiologie, Frankfurt, D

Purpose: Intraoperative MRI improves the extent of resection of malignant brain tumors. Signal changes of CSF due to GBCA leakage in

the subarachnoid space have been reported. Though GBCA potentially exhibits neurotoxic effects, usually no associated complications are observed.

Methods: Patients with signal changes of CSF in the postoperative MRI after intraoperative MRI, were identified in retrospect and included. A matching control cohort was generated. Both groups were analyzed for duration of intensive care stay and presence of systemic or focal seizures. A subgroup with newly diagnosed malignant glioma was additionally analyzed for initiation of adjuvant treatment and overall survival.

Results: Seven patients with postoperative GBCA accumulation in the subarachnoid space were identified, five presenting with focal seizures and altered mental status, symptoms that can be interpreted as neurotoxic manifestations. Poor patient condition led to extended intensive care stay and prolonged initiation of adjuvant treatment in patients with newly diagnosed malignant glioma. Overall survival was reduced compared to the matched control group.

Conclusion: Though intraoperative MRI leads to improved extend of resection and overall survival, in very rare cases GBCA accumulates in the subarachnoid space and leads to neurotoxic manifestations, which should be considered in patients, presenting with seizures and delayed awakening after intraoperative MRI.

238

Increased water content in periventricular caps in patients without acute hydrocephalus

Thorsten Sichtermann^{*1}, Johanna Kornelia Furtmann¹, Garret Gilmour¹, Jan Philipp Bach², Ana-Maria Oros-Peusquens³, Martin Wiesmann¹, Nadim-Joni Shah³, Omid Nikoubashman¹

¹Department of Diagnostic and Interventional Neuroradiology, RWTH University Hospital Aachen, Aachen, Deutschland

²Department of Neurology, University Hospital RWTH Aachen

³Institut für Neurowissenschaften und Medizin (INM-4), Forschungszentrum Jülich

Purpose: Periventricular caps (PVC) are a common finding on MR imaging. It is not fully understood to what extent PVC are caused by transependymal edema or gliosis. To understand the underlying pathophysiology, we compared the quantitative water content of PVC and gliotic white matter lesions (WML), hypothesizing that periventricular caps are caused by transependymal edema rather than gliosis.

Methods: In a prospective study, we compared the water content of PVC and WML in 50 patients, using a quantitative multiple-echo gradient-echo MR water mapping sequence.

Results: Compared to normal white matter, the water content of PVC was significantly higher than that of WML ($p = .002$) with an average increase of $17 \pm 5\%$ in PVC and $11 \pm 4\%$ in WML. ROC analysis revealed that a relative increase of water content of $\geq 15\%$ rather corresponds to PVC than WML with a specificity of 93% and a sensitivity of 60% ($p < .001$).

Conclusion: Our results, which show that the water content of PVC was significantly higher than that in WML, imply a differing pathophysiology of these lesions. Quantifying the water content of T2-hyperintensities may be a useful additional tool for the characterization and differentiation of T2-hyperintensities in diseases such as idiopathic normal pressure hydrocephalus.

260

MRI in patients with hearing implants—feasibility report for routine clinical practice

Johann-Martin Hempel^{*1}, Benjamin Bender², Anke Tropitzsch³, Hubert Löwenheim³, Ulrike Ernemann²

¹Uniklinik Tübingen, Abteilung für Diagnostische und Interventionelle Neuroradiologie, Tübingen, Deutschland

²Universitätsklinikum Tübingen, Radiologische Klinik, Abteilung für Diagnostische und Interventionelle Neuroradiologie, Tübingen, Deutschland

³Klinik für Hno

Purpose: Performing an MRI in patients with hearing implants is technically feasible in most instances. Nonetheless, the vendor-specific limitations and technical conditions vary markedly and thus hamper routine applicability. Especially in ambulatory patient care, this constellation often prevents an MRI scan from patients with hearing implants. However, those patients may also need further MR examinations for follow-up or because of other conditions.

Therefore, we sought to define a robust and feasible algorithm for facilitating the feasibility of MR examinations in patients with hearing implants and harmonizing safety precautions.

Methods: We performed a thorough literature analysis and gathered all relevant technical and safety specifications as well as MR-related limitations of recent inner ear, middle ear, and brain stem implants from the four leading international manufacturers.

Results: We provide a systematic overview of the recent hearing implant models containing its MR-related specifications and safety precautions. Furthermore, we present a standard operating procedure (SOP) to ensure safe and straightforward MR imaging in patients with hearing implants. This robust workflow algorithm represents the “least common denominator” of all available and relevant safety instructions as well as MR-specific limitations.

Conclusion: A standardized and simple algorithm allows for optimal care of patients with hearing implant undergoing an MR examination. It may also help to facilitate and “de-taboo” MR imaging of this specific patient cohort in ambulatory radiologic patient care.

263

Does cerebral bloodflow change during MRI?—Unexpected findings of an Arterial Spin Labeling study

Robin Lüddecke¹, Julia Forstenpointner¹, Ralf Baron¹, Janne Giertmühlen¹, Olav Jansen², Thomas Lindner^{*3}

¹Sektion für Schmerzforschung² Klinik für Neurologie, Universitätsklinikum Schleswig-Holstein Campus Kiel

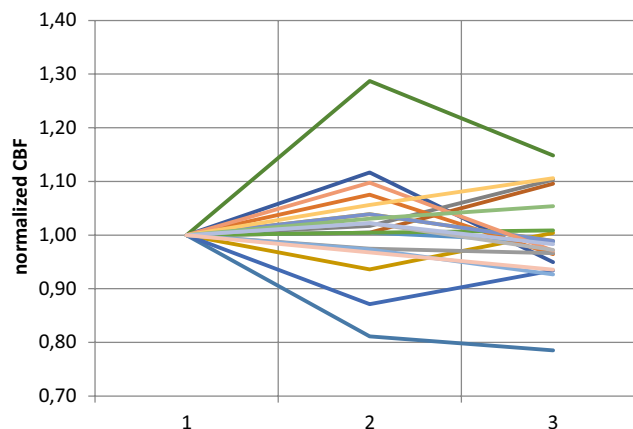
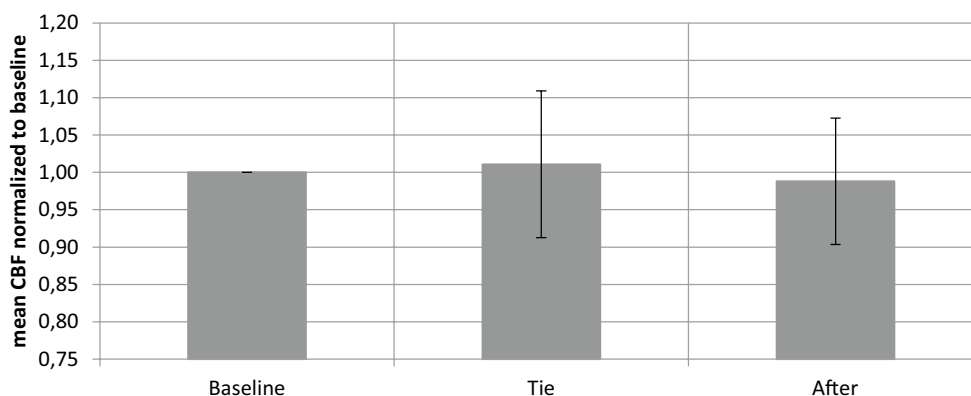


Fig. 1 Normalized CBF of each volunteer during the three scans

Fig. 2 Mean normalized CBF of all volunteers



²Direktor des Instituts für Neuroradiologie, Klinik für Radiologie und Neuroradiologie, Kiel, Deutschland

³Klinik für Radiologie und Neuroradiologie, Universitätsklinikum Schleswig-Holstein, Kiel, Deutschland

Purpose: Arterial Spin Labeling (ASL) methods allow for the non-invasive acquisition of cerebral blood flow (CBF). Thereby studies on healthy volunteers can be conducted. As part of a study of compressing extracranial arteries (and veins) we conducted ASL scans on an experimental (with compression) and a control (without compression) group. Here we present the results of the non-compression group.

Methods: In this study 15 volunteers with and without compression of extracranial vessels ASL scans have been conducted before during and after compression. The control group received the same scans but without compression at the same timepoints (15 minutes between ASL scans). All scans have been conducted using a Philips 3T Achieva MRI and perfusion imaging was acquired using pseudo-continuous ASL.

Results: The healthy group showed no mean change of CBF in the three scans. However, looking at the individual results changes of up to 30% in both directions were visible.

Conclusion: These unexpected findings raise questions regarding reproducibility of data and reasons for changes in CBF during MRI acquisitions. There might be effects of first changing and then getting used to the horizontal position in MRI. The reasons for these changes should be investigated further and in future studies used for correction of acquired data.

264

Permute Arterial Spin Labeling for the non-invasive time-resolved acquisition of cerebral blood flow

Thomas Lindner^{*1}, Olav Jansen², Michael Helle³

¹Klinik für Radiologie und Neuroradiologie, Universitätsklinikum Schleswig-Holstein, Kiel, Deutschland

²Direktor des Instituts für Neuroradiologie, Klinik für Radiologie und Neuroradiologie, Kiel, Deutschland

³Philips GmbH Innovative Technologies, Research Laboratories, Hamburg, Deutschland

Purpose: Arterial Spin Labeling (ASL) methods allow for the non-invasive acquisition of cerebral blood flow¹. The technique relies on the repeated acquisition of the same data to achieve sufficient signal. Thereby, the method is generally not time-resolved.

Methods: In this study the acquisition order of the slices is changed during each repetition of the scan instead of having the same order for each scan. The order we propose equals a permutation (i. e. each slice is on each position but only acquired once per repetition). Following this, each slice is read out equally often at each time-point. The experiments have been conducted on a Philips 3T Achieva MRI scanner.

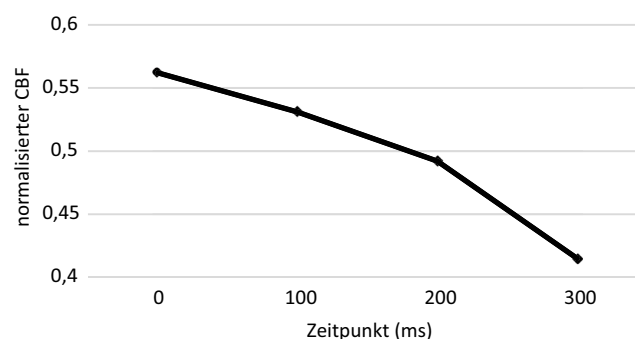
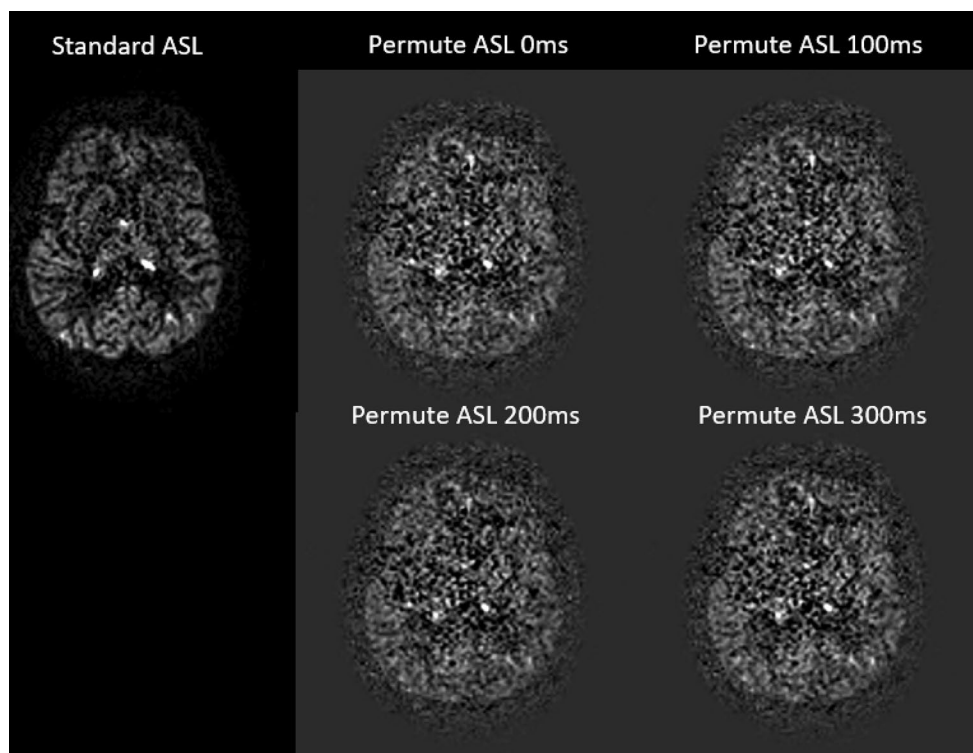


Fig. 1 Relative CBF of a healthy volunteer over a course of 300ms (with 100ms temporal resolution)

Fig. 2 Comparison of standard ASL (one time-point) and time-resolved ASL perfusion



Results: The initial results of the study appear promising to acquire time-resolved ASL perfusion data. The image quality however needs to be increased to be comparable to the standard acquisition.

Conclusion: By re-ordering the Slices during acquisition it is possible to obtain time-resolved ASL perfusion data with freely chosen time intervals. In future studies the influence of physiological parameters like heartbeat should be further investigated as the temporal resolution can be as low as 15ms.

Reference

1 Alsop D, et al. Magn Reson Med 2015

287

Improved Automatic Planning for Superselective Arterial Spin Labeling

Michael Helle^{*1}, Fabian Wenzel², Kim van de Ven³, Peter Börner²

¹Philips GmbH Innovative Technologies, Research Laboratories, Hamburg, Deutschland

²Philips GmbH Innovative Technologies

³Philips Healthcare

Purpose: Super-Selective Arterial Spin Labeling proved to be an efficient method for selective labeling of individual blood vessels and has been applied in various patient studies. This study presents an advanced fully automated approach based on vessel detection and analysis. It is completely integrated in the scanner console and allows labeling of the major brain feeding vessels in an efficient and robust way.

Methods: Measurements were performed in 6 healthy volunteers on a 1.5T Ingenia Scanner (Philips, Best, The Netherlands). Automatic planning of labeling spots was performed on the basis of a TOF scan of the arteries in the neck. The automated planning consists of several image processing steps. Parameters with impact on the final labeling spot of a particular vessel are based on 3 rejection criteria: 1. angular deviation from the z-direction of the magnet. 2. extent of the labeling plane into which the course of a vessel should not re-enter after labeling. 3. maximum length of a vessel part inside the labeling plane. Image acquisition for flow territory mapping was performed based on the automatic positioning of the labeling spots onto both internal carotid (ICA) and vertebral arteries (VA).

Results: Successful flow territory mapping was performed and similar labeling efficiency was achieved when compared to non-selective ASL. However, labeling efficiency decreased in VAs possibly due to mixing of blood in the posterior circulation. Average processing time in each volunteer to find optimal labeling positions for all major brain feeding arteries was approx. 12s.

Conclusion: Fully automatic positioning of the labeling spot can be helpful in clinical routine scan protocols to overcome user-dependent and time-consuming planning.

307

Diagnostic Value of Low Dose CT to detect Ventriculoperitoneal Shunt Complications: A Retrospective Analysis

Saif Afat^{*1}, Georg Bier², Konstantin Nikolaou³, Marc A. Brockmann⁴, Hans Clusmann⁵, Hussam Aldin Hamou⁶, Martin Wiesmann⁷, Ahmed Othman⁸

¹Klinik für Diagnostische und Interventionelle Radiologie, Tübingen, Deutschland

²Diagnostische und Interventionelle Neuroradiologie- Uni-Klinik Tübingen, Deutschland

³Diagnostische und Interventionelle Radio, Diagnostische und Interventionelle Radiologie, Tübingen, Deutschland

⁴Universitätsmedizin Mainz, Klinik und Poliklinik für Neuroradiologie, Mainz, Deutschland

⁵Klinik für Neurochirurgie—Uniklinik Aachen, Deutschland

⁶Klinik für Neurochirurgie—Uniklinik Aachen

⁷Klinik für Diagnostische und Interventionelle Neuroradiologie, Aachen, Deutschland

⁸Diagnostische und Interventionelle Radiologie, Deutschland

Purpose: The aim of this study is to investigate the diagnostic performance of Whole body Low-Dose CT (LD-CT) for detecting mechanical ventriculoperitoneal shunt complications.

Methods: This retrospective study included 100 patients (mean age: 56.1 ± 18.8 years, 51 female) with suspected VP-Shunt complication who underwent whole Body LD-CT (tube voltage, 100 kVp; tube current-time product, 10 mAs). The CT images were independently reviewed by three radiologists for presence/absence of mechanical VP-shunt complications, overall image quality and diagnostic confidence. On a five-point Likert scale the readers scored the image quality (1=very low, 5 very high) and the diagnostic confidence (1=low confidence, 5=high confidence). ROC analysis and the area under the curve (AUC) were used to assess the patient based diagnostic accuracy with final clinical diagnosis and intra-operative findings serving as reference standard.

Results: Image quality was rated very good (median score, 5; range, 4–5). Diagnostic confidence was rated very high (median score, 5; range, 4–5). Interobserver agreement was almost perfect for image quality ($\kappa=0.810$) and for diagnostic confidence ($\kappa=0.808$). Twenty-two out of the 100 included patients had confirmed mechanical VP-Shunt complications. Twenty-one positive patients were correctly identified on LD-CT by all 3 readers, no false positive cases were recorded by any of the readers, yielding a sensitivity of 95.5%, a specificity of 100% (95% CI, 0.926–1) and a perfect agreement ($\kappa=1$).

Conclusion: Whole-body LD-CT allows detection of VP-Shunt complication with excellent diagnostic accuracy and very high diagnostic confidence.

338

Quantitative Lesion Water Uptake Predicts Malignant Cerebellar Edema in Acute Ischemic Stroke

Gabriel Brooks^{*1}, Fabian Flottmann², Andre Kemmling³, Jawed Nawabi¹, Peter Sporns⁴, Hannes Leischner⁵, Susanne Siemonsen⁶, Jens Fiehler⁷, Uta Hanning⁸

¹Klinik und Poliklinik für Neuroradiologische Diagnostik und Intervention, Universitätsklinikum Hamburg-Eppendorf, Hamburg, Deutschland

²Universitätsklinikum Hamburg-Eppendorf, Klinik und Poliklinik für Neuroradiologische Diagnostik und Intervention, Klinik und Poliklinik für Neuroradiologische Diagnostik und Intervention, Hamburg, Deutschland

³Institut für Klinische Radiologie, Universitätsklinikum Münster, UKSH Lübeck, Hamburg, Deutschland

⁴Institut für Klinische Radiologie, Institut für Klinische Radiologie, Münster, Deutschland

⁵Universitätsklinikum Hamburg-Eppendorf, Klinik und Poliklinik für Neuroradiologische Diagnostik und Intervention, Hamburg, Deutschland

⁶Klinik und Poliklinik für Neuroradiologische Diagnostik und Intervention, Universitätsklinikum Hamburg-Eppendorf, Hamburg, D

⁷Diagnostikzentrum Univ.-Klinikum Hamburg-Eppendorf, Klinik und Poliklinik für Neuroradiologische Diagnostik und Intervention, Hamburg, Deutschland

⁸Klinik und Poliklinik für Neuroradiologische Diagnostik und Intervention, Universitätsklinikum Hamburg-Eppendorf, Institut für Klinische Radiologie, Uniklinikum Münster, Hamburg, Deutschland

Purpose: Malignant cerebellar edema is a life-threatening complication of acute stroke that requires timely diagnosis and management.

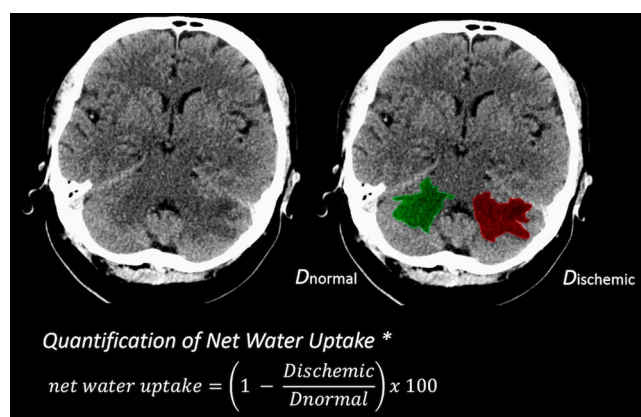


Fig. 1

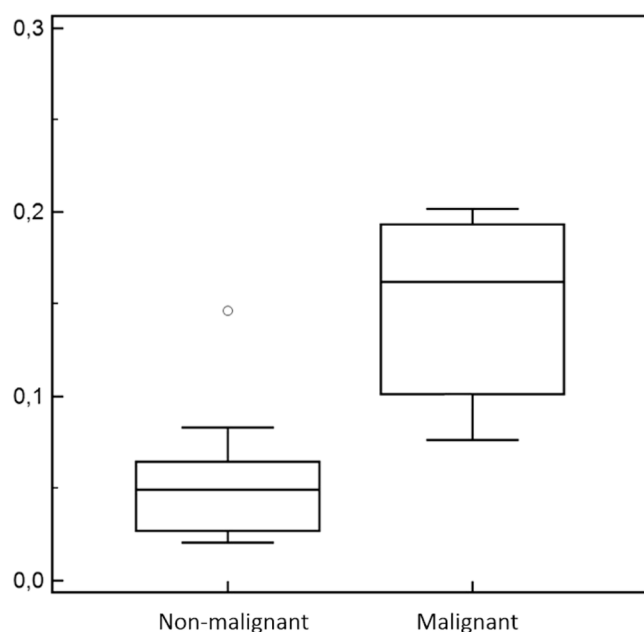


Fig. 2 Net water update at admission

Net water uptake (NWU) per brain volume is a new quantitative imaging biomarker of space-occupying ischemic edema, which can be measured in computed tomography (CT). We hypothesize that NWU in early posterior circulation stroke lesions can predict malignant cerebellar edema.

Methods: In this pilot study, 22 acute posterior circulation stroke patients with CT imaging at admission and follow-up (FUCT) were included. 10 patients developed malignant cerebellar edema defined by using an established 10-point scale in FUCT, of which >3 are considered malignant. NWU was quantified in admission CT and FUCT based on CT-densitometry and compared with pc-ASPECTS.

Results: The mean pc-ASPECTS score at admission was 7 (SD \pm 3; 5.4 [\pm 3] for malignant and 8.5 [\pm 1.7] for non-malignant infarctions; $p=0.01$). Edematous tissue expansion by NWU within the early infarct lesion was 14.9% (\pm 3.7) for malignant and 5.3% (\pm 2.3) for non-malignant infarctions, respectively ($p<0.0001$). Based on univariate ROC curve analysis, NWU above 7.2% accurately identified all malignant infarctions (AUC 0.95, specificity 83.3%, 95%CI: 0.77–0.99). In multivariate regression analysis, NWU at admission was superior to pc-ASPECTS in predicting malignant edema.

Conclusion: CT-based quantitative NWU in early posterior circulation infarct lesions is a promising surrogate marker for developing malignant edema. Besides pc-ASPECTS, the measurement of lesion water uptake may further support identifying patients at risk for malignant infarction.

339

Fluid attenuated inversion recovery vascular hyperintensities indicate slow poststenotic arterial blood flow in internal carotid artery stenosis

Alex Förster^{*1}, Holger Wenz², Matthias Gawlitza³, Christoph Groden², Angelika Alonso⁴

¹Abteilung für Neuroradiologie, Universitätsmedizin Mannheim, Mannheim, Deutschland

²Abteilung für Neuroradiologie, Universitätsmedizin Mannheim

³Service de Neuroradiologie, Hôpital Maison Blanche, Chu de Reims

⁴Neurologische Klinik, Universitätsmedizin Mannheim

Purpose: Stenosis of the internal carotid artery (ICA) is commonly associated with a poststenotic decrease in blood flow velocity. Fluid attenuated inversion recovery (FLAIR) vascular hyperintensities (FVH) are a phenomenon that represents a slow arterial blood flow. In this study, we investigated the frequency and extent of FVH in the distal ICA in patients with proximal ICA stenosis.

Methods: We analyzed the MRI findings in 51 patients with a total of 60 ACI stenoses with special focus on the frequency and extent of FVH in the petrous segment of the ICA on FLAIR images and correlated these with Doppler/duplex sonography results.

Results: In 46 (76.7%) patients with ICA stenosis, FVH could be detected in the petrous segment of the ICA: in 19 (44.9%) a thin hyperintense rim near the vessel wall (grade 1), in 24 (40.8%) a strong hyperintense rim near the vessel wall (grade 2), and in 3 (14.3%) a hyperintense filling of the entire lumen (grade 3). For examples see Fig. 1. The median degree of stenosis was significantly higher in grade 2 (80%) and 3 (90%) compared to grade 1 FVH (60%; $p=0.002$). The median poststenotic flow velocity was significantly lower in grade 2 (35 cm/s) and 3 (20 cm/s) than in grade 1 FVH (65 cm/s; $p<0.001$).

Conclusion: In proximal ICA stenosis FVH in the petrous segment of the ICA is a common finding reflecting the decreased poststenotic blood flow and could be useful to recognize a proximal ICA stenosis already on FLAIR images.

345

Gd-contrast administration is dispensable in multiple sclerosis patients without new T2/FLAIR lesions on follow-up MRI

Kianush Karimian-Jazi^{*1}, Brigitte Wildemann², Ricarda Diem², Thomas Hielscher³, Martin Bendszus⁴, Michael Breckwoldt⁵

¹Abteilung Neuroradiologie, Klinische Kooperationsseinheit Experimentelle Neuroonkologie (Dkfz), Heidelberg, D

²Abteilung Neurologie, Universitätsklinikum Heidelberg/Kopfclinik

³Dkfz, Deutsches Krebs Forschungszentrum

⁴Abteilung Neuroradiologie, Universitätsklinikum Heidelberg/Kopfclinik

⁵Abteilung Neuroradiologie, Universitätsklinikum Heidelberg/Kopfclinik, Dkfz, Deutsches Krebsforschungszentrum

Purpose: Magnetic resonance imaging (MRI) is the most important paraclinical parameter for diagnosis and monitoring of multiple sclerosis (MS) patients. Blood-brain barrier breakdown indicated by gadolinium (Gd)-contrast enhancement of the MS plaque is the hallmark of lesion activity. Recently, there have been major safety concerns regard-

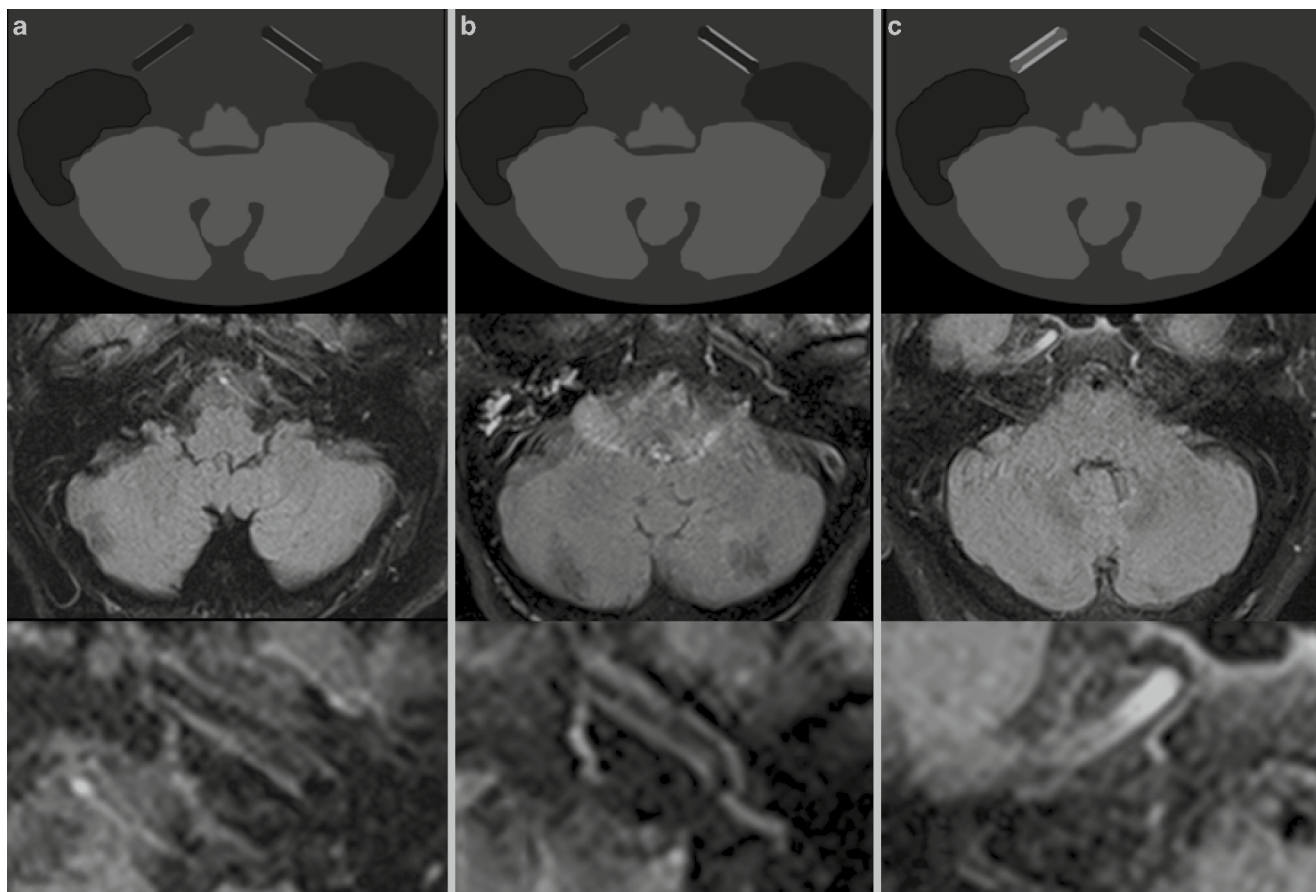


Fig. 1

ing linear Gd-contrast administration. Here, we assessed the diagnostic relevance of Gd-administration in MRI follow-up examinations if the T2 lesion load is unchanged.

Methods: We included 100 MS patients with at least 2 cMRI follow-up examinations in our department. MRI was performed at 3 Tesla with a standardized protocol including T2-w, FLAIR and T1-w contrast enhanced sequences. Images were analyzed for overall lesion load and the occurrence of new lesions. Isolated Gd-enhancing lesions without correlate in T2/FLAIR images and reactivated lesions were further assessed for size and signal intensity.

Results: We identified a total of 343 new T2 lesions and 152 contrast-enhancing lesions in a total of 559 MRI follow-up examinations. Of the Gd-enhancing lesions 145/152 (95.4%) showed a correlate as a new T2/FLAIR lesion. There were just 3 enhancing lesions without T2/FLAIR correlate and only 4 lesions that exhibited lesion reactivation. As a predictive factor of enhancement we found that enhancing lesions had a higher T2 signal ratio.

Conclusion: The likelihood of missing “active lesions” is overall small (1.7%) if T2 lesions are stable compared to the previous examination. Lesion reactivation is overall rare. Our study indicates that Gd-contrast administration might be dispensable in follow-up MRI of MS patients if no new T2/FLAIR lesions and no new neurological symptoms are present.

355

Age- and gender effects on brainstem MR-planimetry

Stephanie Mangesius^{*1}, Anna Hussl², Susanne Tagwercher², Eva Reiter², Christoph Müller², Florian Krismer², Philipp Mähknecht², Michael Schocke³, Elke R. Gizewski³, Werner Poewe⁴, Klaus Seppi⁴

¹Department of Neuroradiology, Innsbruck Medical University, Innsbruck, Austria, Innsbruck, Austria

²Department of Neurology, Innsbruck Medical University, Innsbruck, Austria

³Department of Neuroradiology, Innsbruck Medical University, Innsbruck, Austria, Neuroimaging Core Facility, Innsbruck Medical University, Innsbruck, Austria

⁴Department of Neurology, Innsbruck Medical University, Innsbruck, Austria, Neuroimaging Core Facility, Innsbruck Medical University, Innsbruck, Austria

Purpose: MR planimetry of brainstem structures can be helpful for the discrimination of parkinsonian syndromes. It has been suggested that ageing might influence brainstem MR measurements assessed by MR planimetry. Gender-effects on planimetric measurements have never been investigated so far. The aim of this study was to evaluate age- and gender effects on brainstem MR-planimetric measures.

Methods: Brainstem MR-planimetric measures including brainstem diameters (midbrain, pons, middle and superior cerebellar peduncle) and areas (pontine and midbrain), the ratios derived from both midbrain-to-pons diameters and areas as well as the Magnetic Resonance

Parkinson Index (MRPI) were assessed on 1.5 Tesla weighted MR images in a large cohort of 97 healthy controls.

Results: Effects of gender were observed on both pontine measurements (diameter and area). Effects of age were shown on midbrain measurements (area and diameter), as well as on combined planimetric measurements (MRPI and ratios derived from both midbrain-to-pons diameters and areas). There were neither gender nor age effects on combined measurements nor midbrain diameter in the population aged 50 to 80 years, the age-range relevant for the differential diagnosis of neurodegenerative parkinsonism.

Conclusion: Although age and gender might influence single brain-stem planimetric MR measures, our results indicate that there is no need for age- or gender-specific cut-offs for the relevant age group.

359

Improved Detection of Acute Lacunar Infarcts on Non-Contrast CT Using a Multiband-Filter

Felix Schön^{*1}, Daniel Kaiser¹, Hannes Wahl¹, Dirk Daubner¹, Volker Pütz², Jennifer Linn¹

¹University Hospital- TU Dresden, Institute for Diagnostic and Interventional Neuroradiology, Dresden, Deutschland

²University Hospital- TU Dresden, Clinic and Polyclinic for Neurology, Dresden, Deutschland

Purpose: Lacunar infarcts (LI) are difficult to detect by computed tomography (CT) within the first hours of stroke onset. We postulate that non-contrast CT (NCCT) post-processing using a multiband filter ("BestContrast"/BC) improves diagnostic accuracy.

Methods: We retrospectively analysed NCCT of 34 patients with acute thalamic LI, not initially detected in NCCT but by diffusion-weighted magnetic resonance imaging (DW-MRI). We examined CT densities of LI based on corresponding DW-MRI lesion using a semi-automatic workflow of brain extraction, coregistration and segmentation. We also analysed densities of unaffected contralateral thalamus and old thalamic LI ($n=22$). Unprocessed, window- and BC-optimized NCCT images of thalamic LI, LI in other regions and healthy age matched patients were reviewed by a blinded neuroradiologist in 3 sessions to evaluate the benefit of post-processing.

Results: On NCCT, Hounsfield Units (HU) of acute thalamic LI were significantly reduced compared to corresponding contralateral tissue (29.6 ± 3.1 HU vs. 33.3 ± 2.6 HU; $p < 0.001$). Old LI had significantly reduced HU (16.6 ± 4.1 HU; $p < 0.001$). Therefore, window-optimized level/width to detect LI on NCCT are 30/6 HU and on optimized BC a center/delta of 30/6 HU at a slope of 5 (Fig. 1). Sensitivity for thalamic

LI was 82% (95% CI 64–92) in window optimized and 86% (95% CI 69–94) in BC-optimized NCCT. Specificity was 70% (95% CI 48–85) and 75% (95% CI 53–88).

Conclusion: NCCT post-processing with BC could increase the accuracy in detecting thalamic lacunar infarction.

363

Signal variance-based Collateral Index in DSC perfusion: a novel method to assess leptomeningeal collateralization in acute ischemic stroke

Alexander Seiler^{*1}, Arne Lauer², Ralf Deichmann², Ulrike Noeth³, Eva Herrmann⁴, Joachim Berkefeld⁴, Oliver C. Singer², Johannes C. Klein², Waltraud Pfeilschifter², Marlies Wagner²

¹Universitätsklinikum Frankfurt, Johann-Wolfgang-Goethe-Universität, Klinik für Neurologie, Frankfurt, Deutschland

²Schleusenweg 2_16 60528 Frankfurt

³Sc

⁴S

Purpose: Assessment of leptomeningeal collateralization is of major importance in acute large vessel stroke as it is a determinant of the amount of salvageable tissue, the progression rate of the ischemic process and a predictor of the clinical outcome after reperfusion therapy. However, evidence of collateral scores obtained from clinical imaging data is limited. We introduce a quantitative and observer-independent collateral index based on MR-perfusion-weighted imaging (PWI) data. **Methods:** 55 patients with internal carotid and/or middle cerebral artery occlusion were included. Coefficient of signal variation maps were calculated from the PWI raw data time series. An intra-individual collateral vessel index (CVI_{PWI}) was calculated. Initial ischemic core volume was determined from diffusion-weighted imaging (DWI). Time-to-peak maps were used to delineate areas of hypoperfusion and to determine the PWI/DWI mismatch.

Results: CVI_{PWI} correlated significantly with the initial ischemic core volume ($\rho = -0.459$, $p = 0.0001$) and the PWI/DWI mismatch ratio ($\rho = 0.494$, $p = 0.0001$). Significant correlations of CVI_{PWI} were found with NIHSS and mRS at discharge ($\rho = -0.341$, $p = 0.015$ and $\rho = -0.305$, $p = 0.023$). In multivariate logistic regression, CVI_{PWI} was an independent predictor of favourable outcome ($p = 0.017$).

Conclusion: Signal variance-based CVI_{PWI} provides rater-independent information on the collateral supply and is suitable to assess leptomeningeal collateralization in acute stroke.

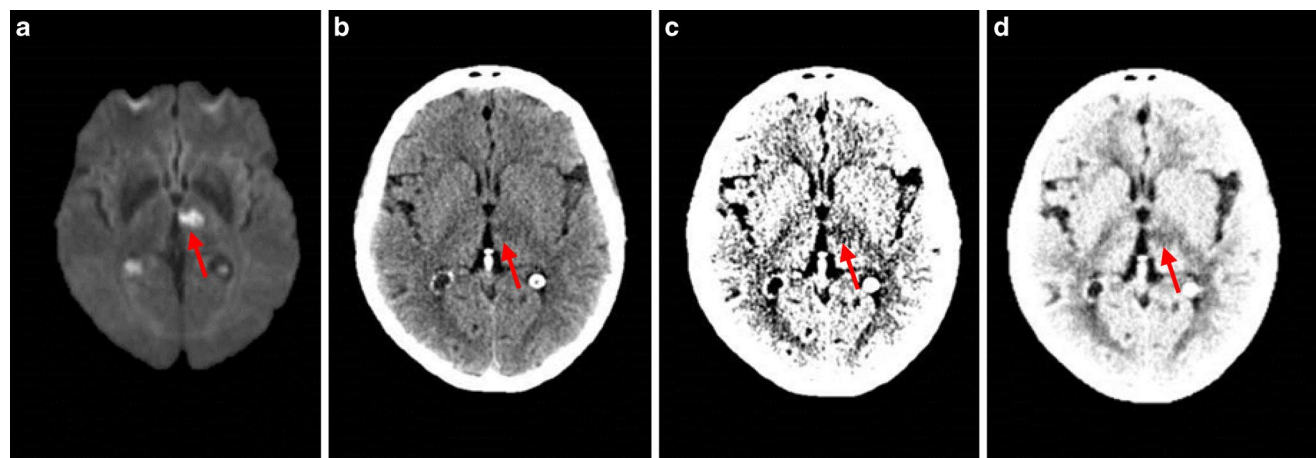


Fig. 1 Arrow indicates acute left thalamic LI in DW-MRI (a), NCCT (b), window-optimized NCCT (c) and Best Contrast (BC)

Extent of microstructural tissue damage correlates with hemodynamic failure in high-grade carotid occlusive disease: An MRI study using quantitative T2 and DSC perfusion.

Alexander Seiler^{*1}, Ralf Deichmann², Ulrike Nöth³, Waltraud Pfeilschifter⁴, Arne Lauer⁵, Oliver C. Singer⁶, Marlies Wagner⁷

¹Universitätsklinikum Frankfurt, Johann-Wolfgang-Goethe-Universität, Klinik für Neurologie, Frankfurt, Deutschland

²Goethe Universität Frankfurt, Universitätsklinikum Frankfurt, Brain Imaging Center, Frankfurt/Main, Deutschland

³Universitätsklinikum Frankfurt, Brain Imaging Center, Frankfurt, Deutschland

⁴Universitätsklinikum Frankfurt, Klinik für Neurologie, Zentrum der Neurologie und Neurochirurgie, Frankfurt/Main, Deutschland

⁵Goethe Universität Ffm, Neurologie, Frankfurt/M., Deutschland

⁶Universitätsklinikum Frankfurt

⁷Universitätsklinikum Frankfurt, Institut für Neuroradiologie, Frankfurt, D

Purpose: Chronic hemodynamic impairment in high-grade carotid occlusive disease causes microstructural abnormalities. Quantitative MR imaging allows assessing pathologic structural changes beyond macroscopically visible tissue damage. In this study, quantitative T2 mapping with DSC-based PWI was used to investigate quantitative T2 changes as a marker of microstructural damage in relation to hemodynamic impairment in patients with unilateral high-grade carotid occlusive disease.

Methods: Eighteen patients with unilateral high-grade ICA or MCA stenosis/occlusion were included. qT2 and perfusion parameters (rCBF, rCBV, rCBF/rCBV) were determined within areas with delayed TTP and compared with values from contralateral unaffected areas after segmentation of normal-appearing hypoperfused WM and cortical regions. Hemispheric asymmetry indices were calculated for all parameters.

Results: qT2 was significantly prolonged ($P < .01$) in hypoperfused tissue and correlated significantly ($P < .01$) with TTP delay and rCBF/rCBV reduction in WM. Significant correlations ($P < .001$) between TTP delay and the relative CBF/relative CBV ratio were found both in WM and in cortical areas.

Conclusion: qT2 can be used as a marker of microstructural tissue damage even in normal-appearing GM and WM within a vascular territory affected by high-grade carotid occlusive disease. The extent of damage correlates with the degree of hemodynamic failure measured by DSC perfusion.

Reference

1 AJNR Am J Neuroradiol. 2018 May 10. <https://doi.org/10.3174/ajnr.A5666>. [Epub ahead of print]

390

Splenial lesion pattern on diffusion-weighted imaging: A comparison of Marchiafava–Bignami syndrome, reversible splenium lesion, and ischemic infarction

Alex Förster^{*1}, Mansour Al-Zghoul², Holger Wenz², Johannes Böhme², Philipp Eisele³, Angelika Alonso³, Christoph Groden²

¹Abteilung für Neuroradiologie, Universitätsmedizin Mannheim, Mannheim, Deutschland

²Abteilung für Neuroradiologie, Universitätsmedizin Mannheim

³Neurologische Klinik, Universitätsmedizin Mannheim

Purpose: Various neurological disorders are associated with lesions predominantly or exclusively affecting the splenium of the corpus callosum, e.g. Marchiafava–Bignami syndrome (MBS), reversible splenium lesion (RSL), and ischemic stroke (IS). Clinical presentations may be indistinguishable. In the present study, we sought to examine the possibility of distinguishing these disorders by means of MRI.

Methods: A total of 4 patients with MBS, 8 patients with RSL and 9 patients with isolated IS in the splenium were identified from an MRI report database (2002–2017) and analyzed with focus on lesion localization, shape and size, as well as relative ADC reduction on diffusion-weighted imaging.

Results: In MBS, symmetrical boomerang-shaped lesions (see Fig. 1A), in RSL central oval or round lesions (see Fig. 1B) and in IS eccentric irregular lesions in the splenium (see Fig. 1C) were found. The median lesion size in MBS (6.25 [IQR 2.04–8.62] ml) was significantly larger than in RSL (0.28 [IQR 0.09–1.15] ml, $p=0.01$) and IS (0.09 [IQR 0.05–0.94] ml; $p=0.01$). RSL showed a more pronounced

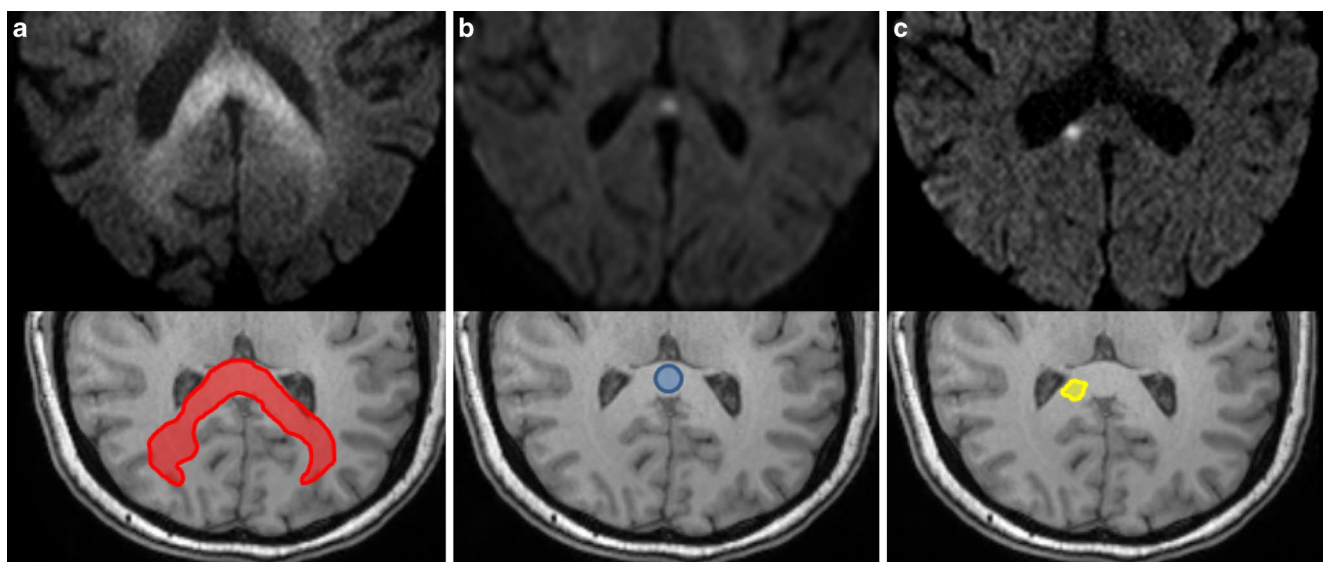


Fig. 1

ADC reduction (0.19 [IQR 0.14–0.26]) compared to IS (0.27 [IQR 0.20–0.19]) but this did not reach statistical significance ($p=0.051$).

Conclusion: Lesions of the splenium are best classified by form and localization. Larger boomerang-shaped lesions are typical for MBS, whereas smaller lesions may be categorized in central oval/round, typical for RLS, and eccentric irregular, typical for IS.

418

Diagnostic and Prognostic Value of the Entorhinal Cortex Atrophy (ERICA) Score in MCI

Jonas Enkirch^{*1}, Andreas Traschütz², Hans Heinz Schild³, Michael Heneka⁴, Elke Hattingen⁵

¹Radiologie, Uniklinikum Bonn, Neuroradiologie, Bonn, Deutschland

²Uniklinik Bonn, Neurologie, Bonn, Deutschland

³Radiologische Klinik, Bonn, Deutschland

⁴Universitätsklinikum Bonn, Klinik für Neurodegenerative Erkrankungen und Gerontoneurologie, Bonn, Deutschland

⁵Institut für Neuroradiologie, Frankfurt/Main, Deutschland

Purpose: To validate the entorhinal cortex atrophy (ERICA) MRI rating scale regarding diagnosis, biomarker status, neuropsychological data and dementia risk in subjects with mild cognitive impairment (MCI).

Methods: ERICA scores (Fig. 1) were retrospectively compared regarding their discrimination of MCI ($n=80$) from subjective cognitive decline (SCD; $n=60$) and their sensitivity, specificity and predictive values for cerebrospinal fluid amyloid/tau status as well as conversion to dementia due to Alzheimer's disease were evaluated (median follow-up 28 months). Associations with neuropsychological tests were explored by correlation and multivariable linear regression analysis.

Results: ERICA score significantly distinguished subjects with MCI from SCD (AUC=0.74, 95% CI 0.66–0.82). The ERICA score achieved 97% positive predictive value for the presence of MCI. It was specifically associated with measures of verbal learning and memory after adjusting for age, sex, education and global cognitive level. Sensitivity to predicting conversion to Alzheimer's disease dementia was 53% and specificity was 83%. The ERICA score achieved 90% positive and 100% negative predictive value when combined with tau status and verbal recall, respectively.

Conclusion: The ERICA score is a valuable tool to establish clinical diagnosis and prognosis in patients with MCI.

Reference

- 1 Enkirch SJ, Traschütz A, Müller A, Widmann CN, Gielen GH, Heneka MT, Jurcoane A, Schild HH, Hattingen E. The ERICA Score: An MR Imaging-based Visual Scoring System for the Assessment of Entorhinal Cortex Atrophy in Alzheimer Disease. Radiology. 2018 [Epub ahead of print]

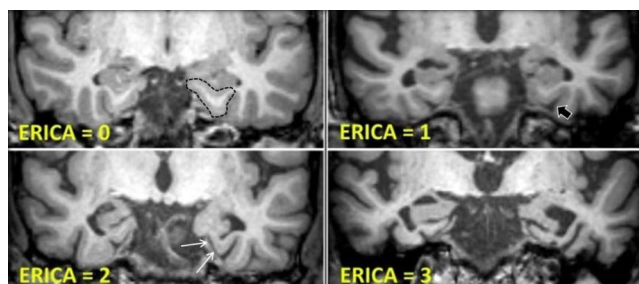


Fig. 1

419

Comparison of fat-saturated Turbo-Spin-Echo versus Short-Tau-Inversion-Recovery sequences in the diagnostic work-up of optic nerve neuritis

Tobias D. Faizy^{*1}, Gabriel Broocks², Isabelle Frischmuth³, Fabian Flottmann⁴, Hannes Leischner⁵, Jan-Patrick Stellmann⁶, Christoph Heesen⁷, Jens Fiehler⁸, Susanne Siemonsen⁹

¹Universitätskrankenhaus Hamburg-Eppendorf, Klinik und Poliklinik für Interventionell und, Diagnostische Neuroradiologie, Hamburg, Deutschland

²Klinik und Poliklinik für Neuroradiologische Diagnostik und Intervention, Universitätsklinikum Hamburg-Eppendorf, Hamburg, Deutschland

³Klinik und Poliklinik für Diagnostische und Interventionelle Neuroradiologie, Hamburg

⁴Universitätsklinikum Hamburg-Eppendorf, Klinik und Poliklinik für Neuroradiologische Diagnostik und Intervention, Klinik und Poliklinik für Neuroradiologische Diagnostik und Intervention, Hamburg, Deutschland

⁵Universitätsklinikum Hamburg-Eppendorf, Klinik und Poliklinik für Neuroradiologische Diagnostik und Intervention, Hamburg, Deutschland

⁶Universitätsklinikum Hamburg-Eppendorf, Klinik und Poliklinik für Neurologie, Klinik für Neurologie, Hamburg, Deutschland

⁷Universitätsklinikum Hamburg-Eppendorf, Institut für Neuroimmunologie und Multiple Sklerose, Klinik für Neurologie, Hamburg, Deutschland

⁸Diagnostikzentrum Univ.-Klinikum Hamburg-Eppendorf, Klinik und Poliklinik für Neuroradiologische Diagnostik und Intervention, Hamburg, Deutschland

⁹Universitätsklinikum Hamburg-Eppendorf, Hamburg

Purpose: Coronary fat-saturated (fs) T2 Short-Tau-Inversion-Recovery (STIR) sequences are broadly used to evaluate optic nerve morphology in patients with clinical suspicion of e.g. neuroinflammatory diseases. Our purpose was to evaluate the diagnostic value of a new coronary Turbo-Spin-Echo (TSE) MRI sequence for the assessment of optic nerve neuritis.

Methods: 53 patients underwent 3T MRI examination including coronary fs STIR and TSE sequences. Images were assessed by two neuro-radiologists in random order on diagnostic workstations. Number and extent of optical lesions (OL) as well as their localization (retroorbital, passage of canalis opticus and involvement of chiasma) and brightness were assessed. Moreover, a “security rating” was established and raters had to indicate, whether they felt “sure”, “pretty certain” or “unsure” about their rating and the accessibility of the sequences.

Results: No difference in lesion numbers was detected between the two sequences ($p=0.9$). OLs appeared brighter on TSE sequences ($p=0.02$). Lesions located retroorbitally ($p=0.03$), in the passage of canalis opticus ($p=0.01$) and chiasma ($p=0.001$) appeared hyperintense in more consecutive slices and thus suspicious to indicate a more extensive inflammatory involvement of optic nerve on TSE sequences. Overall reader security was superior for the TSE sequence ($p=0.01$).

Conclusion: TSE sequences may add substantially to multimodal imaging approaches in the diagnostic workup of optic nerve neuritis.

432

Identifying pathological brain volume loss in individual patients with early stage MS

Lothar Spies^{*1}, Roland Opfer², Ann-Christin Ostwaldt¹, Christine Egger³, Praveena Manogaran⁴, Sven Schippling⁴

¹Jung Diagnostics GmbH, Research, Hamburg, Deutschland

²Jung Diagnostics GmbH, ., Hamburg, Deutschland

³University Hospital Zurich and University of Zurich, Neurology, Neuroimmunology and Multiple Sclerosis Research, Zürich, Switzerland

⁴University Hospital Zurich and University of Zurich, Department of Neurology, Neuroimmunology and Multiple Sclerosis Research, Zürich, Switzerland

Purpose: Measurements of brain volume loss (BVL) in individual multiple sclerosis (MS) patients is a controversial issue. Recently, age-dependent cutoffs for BVL per year (BVL/year) have been suggested to help identify pathological BVL in patients, with an error rate of 20% ("elevated BVL") or 5% ("pathological BVL"). Furthermore, an intra-patient fluctuation range accounting for the measurement error and potential short-term biological confounders has been determined.

Methods: A cohort of 78 early relapsing MS patients (median age 34.3 years, median disease duration 0.7 years) received two standardized MRI examinations with an average interval of 2.4 years. BVL was determined with SIENA from the FMRIB Software Library. The number of patients featuring a BVL/year higher than the 20% and 5% age-dependent cut-offs after subtracting the fluctuation range of 0.54/(length of scan interval)% was assessed.

Results: The median BVL/year in the cohort was 0.35%. Considering both intra-patient fluctuation and patient age, 19 (24%) patients showed elevated BVL/year, while 13 (16%) patients showed pathological BVL/year. From 10 patients with a scan interval shorter than 1.5 years, 2 featured elevated BVL/year and 1 showed pathological BVL/year. Out of the 68 patients with scan intervals longer than 1.5 years, 17 showed elevated BVL/year and 12 showed pathological BVL/year.

Conclusion: We found that in a subset of patients, pathological BVL can be detected with a high degree of certainty, even in an early MS cohort. With increasing scan interval lengths, pathological BVL/year can be detected in a higher proportion of patients. In individual patients, intra-patient fluctuation and age effects need to be considered to interpret BVL values.

448

Quantitative measurements of relative FLAIR signal intensities in brainstem stroke for estimation of lesion age

Johannes Böhme^{*1}, Holger Wenz², Mansour Al-Zghloul³, Máté Maros⁴, Angelika Alonso⁵, Christoph Groden⁶, Alex Förster⁷

¹Universitätsmedizin Mannheim, Neuroradiologie, Mannheim, D

²Universitätsmedizin Mannheim, Abteilung für Neuroradiologie, Abteilung für Neuroradiologie, Mannheim, Deutschland

³Abteilung für Neuroradiologie, Mannheim, Deutschland

⁴Universitätsklinikum Mannheim, Fakultät der Universität Heidelberg, Abteilung für Neuroradiologie, Mannheim, Deutschland

⁵Universitätsmedizin Mannheim, Neurologische Klinik, Mannheim, Deutschland

⁶Universitätsmedizin Mannheim, Abteilung für Neuroradiologie, Mannheim, Deutschland

⁷Abteilung für Neuroradiologie, Abteilung Neuroradiologie, Mannheim, Deutschland

Purpose: A mismatch between DWI and FLAIR lesion may be useful to identify acute ischemic stroke patients within a 4.5 hour time win-

dow. Recently, relative signal intensity (rSI) on FLAIR has been proposed for quantitative measurement. In the present study we sought to evaluate the value of rSI for onset determination in hyperacute brainstem infarction (BI).

Methods: In 50 patients (median age of 71 years; 29 (58%) male) with hyperacute BI (within 24 hours after symptom onset), MRI findings were analyzed with emphasis on rSI on FLAIR by use of Signal Processing In NMR-Software.

Results: A BI in the mesencephalon was observed in 4 (8%), in the pons in 38 (76%), and in the medulla oblongata in 8 (16%) patients. Patients had a median time from symptom onset to MRI of 196 (IQR 119–409.5) minutes. On DWI, BI had a median volume of 0.26 (IQR 0.15–0.38) ml. The rSI in the BI on FLAIR showed no significant correlation with time from symptom onset ($r=0.216$, $P=0.132$), nor lesion volume ($r=-0.077$, $p=0.59$). Regarding BI location no differences in the rSI in the BI on FLAIR were observed ($p=0.46$). The ROC analysis identified an rSI in the BI on FLAIR of 1.10 (sensitivity 51.7%, specificity 42.9%) as the best cutoff values for predicting the symptom onset ≤ 4.5 hours.

Conclusion: Quantitative rSI on FLAIR do not reliably identify patients within 4.5 h of symptom onset in acute BI. Consequently, therapeutic decisions should not be based on quantitative rSI measurements in patients with BI.

464

Is there evidence for a size threshold of single white matter lesions in the diagnosis of multiple sclerosis?

Sophia Grahl¹, Viola Pongratz¹, Paul Schmidt¹, Christina Engl¹, Matthias Bussas¹, Angela Radez², Gabriel Escamilla-Gonzalez², Frauke Zipp², Sergiu Groppa², Carsten Lukas³, Jan Kirschke^{*4}, Claus Zimmer⁵, Muna Hoshi¹, Achim Berthele¹, Bernhard Hemmer¹, Mark Mühlau¹

¹Klinikum Rechts der Isar, Tum

²Uniklinik Mainz

³St Josef Hospital, Ruhr University Bochum

⁴Abteilung für Diagnostische und Interventionelle Neuroradiologie, München, Deutschland

⁵Klinikum Rechts der Isar der Tum, Technische Universität München, Abteilung für Diagnostische und Interventionelle Neuroradiologie, München, Deutschland

Purpose: White matter lesions (WML) in cMRI are essential for diagnosis and follow-up assessment of multiple sclerosis (MS). The aim of the study was to provide evidence for a WML size threshold for three-dimensional (3D) MRI sequences at 3 Tesla.

Methods: Included were healthy controls (HC) and patients at two centers with 3D FLAIR and T1w sequences. A total of 269 patients with clinically isolated syndrome (CIS) or recurrent MS (expanded disability status scale: 1.5 \pm 1.1; age: 36y \pm 10) and 136 age-matched and sex-matched HC were examined. The WML size threshold that best distinguished between patients and HC was estimated using ROC analysis and Youden-J.

Results: In both cohorts, independent of the MR scanner, the discriminative power was highest at a WML size threshold of 3 mm diameter.

Conclusion: The WML size threshold of 3 mm in diameter, previously proposed without scientific evidence(1) for the diagnostic criteria of MS seems to be a good choice for 3D MRI sequences at 3 Tesla.

Reference

- Swanton JK, Rovira A, Tintore M, et al. MRI criteria for multiple sclerosis in patients presenting with clinically isolated syndromes: a multicentre retrospective study. *The Lancet Neurology* 2007;6:677–86.

Spine

121

Clinical improvement and cost-effectiveness of CT-guided radiofrequency sacroplasty (RFS) and cement sacroplasty (CSP)—a prospective randomised comparison of methodsReimer Andresen^{*1}, Sebastian Radmer², Julian Ramin Andresen³, Mathias Wollny⁴, Urs Nissen⁵, Hans-Christof Schober⁶¹Institute of Diagnostic and Interventional Radiology/Neuroradiology, Department of Neurosurgery and Spine Surgery, Westkuestenlinikum Heide, Academic Teaching Hospital of the Universities of Kiel, Luebeck and Hamburg, Heide, Deutschland²Centre of Orthopaedics, Berlin, Berlin, Deutschland³Medical School, Sigmund Freud University, Vienna, Austria⁴Medimbursement, Tarmstedt⁵Institute of Diagnostic and Interventional Radiology/Neuroradiology, Department of Neurosurgery and Spine Surgery, Westkuestenlinikum Heide, Academic Teaching Hospital of the Universities of Kiel, Luebeck and Hamburg, Heide, Deutschland⁶Department of Internal Medicine I, Municipal Hospital Suedstadt Rostock, Academic Teaching Hospital of the University of Rostock**Purpose:** The objective of this study was a comparative analysis of cement augmentation by means of RFS and CSP with regard to outcome and cost-effectiveness.**Methods:** CT-guided cement augmentation was performed on 100 pat. with insufficiency fractures, 50 pat. being treated with RFS and 50 pat. with CSP. Leakages were detected by CT. Pain intensity was determined on a VAS before and after the intervention. The pat.s' self-sufficiency was assessed using the Barthel index. Pat. were asked about any complications and their level of satisfaction. Costs incurred for carrying out the procedure were compared with the respective reimbursements received.**Results:** Both procedures were technically fully feasible in all pat.. No leakages were found in the RFS group, as opposed to 8.1% asymptomatic leakages in the CSP group. The mean value for pain before intervention was 8.8 in the RFS- and 8.7 in the CSP group. On the 2nd postoperative day, there was a significant pain reduction with an average value of 2.4 for both groups, which remained more or less

constant over the follow-up period. The Barthel index increased significantly from an average of 30 before the intervention to 80 on the 4th postoperative day and 70 after 24 months. No differences were found between the two procedures with regard to pain, improvement in functional status and satisfaction. Taking into account the state-wide base rate used for calculating reimbursement, 3,834.75 € remained for RFS and 5,084.32 € for CSP.

Conclusion: RFS and CSP showed equally good clinical outcomes, and both procedures were profitable.

170

Relationship of paraspinal muscle DTI metrics to isometric strength measurements in healthy subjectsElisabeth Klupp^{*1}, Barbara Cervantes², Sarah Schlaeger³, Stephanie Inhuber⁴, Michael Dieckmeyer², Claus Zimmer⁵, Jan Kirschke⁶, Dimitrios Karampinos⁷, Thomas Baum⁸¹Rechts der Isar, TU München, Neuroradiologie, München, D²Abteilung für Diagnostische und Interventionelle Radiologie, Klinikum Rechts der Isar, Technische Universität München³Neuroradiologie, Klinikum Rechts der Isar, TU München, München, Deutschland⁴Department of Sport and Health Sciences, Technische Universität München⁵Klinikum Rechts der Isar der Tum, Technische Universität München, Abteilung für Diagnostische und Interventionelle Neuroradiologie, München, Deutschland⁶Abteilung für Diagnostische und Interventionelle Neuroradiologie, München, Deutschland⁷Institut für Diagnostische und Interventionelle Radiologie, Klinikum Rechts der Isar, Technische Universität München, München⁸Abteilung für Neuroradiologie, Klinikum Rechts der Isar, München, Deutschland**Purpose:** Diffusion Tensor Imaging (DTI) enables the microstructural examination of muscle tissue and its pathological changes. Little is known about associations between muscular DTI parameters and corresponding muscle strength measurements. This study investigated associations of DTI parameters of paraspinal muscles with isometric strength measurements.**Fig. 1** Pearson correlation coefficients r for muscle strength measurements versus DTI parameters of the erector spinae muscle. Bold denotes $p < 0.05$ (statistical significance), italic denotes $p < 0.1$ (statistical trend).

	Relative flexion muscle strength	Relative extension muscle strength	Ratio relative extension / flexion
MD	n.s.	0.439 ($p=0.047^*$)	0.527 ($p=0.014^*$)
FA	n.s.	n.s.	n.s.
λ_1	n.s.	<i>0.426</i> ($p=0.054$)	0.519 ($p=0.016^*$)
λ_2	n.s.	<i>0.429</i> ($p=0.053$)	<i>0.431</i> ($p=0.051$)
λ_3	n.s.	<i>0.390</i> ($p=0.080$)	0.518 ($p=0.016^*$)
RD	n.s.	<i>0.417</i> ($p=0.060$)	0.483 ($p=0.026^*$)

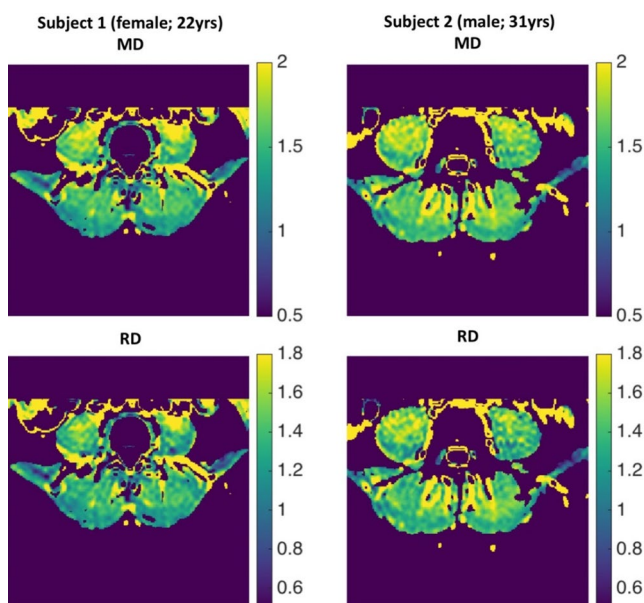


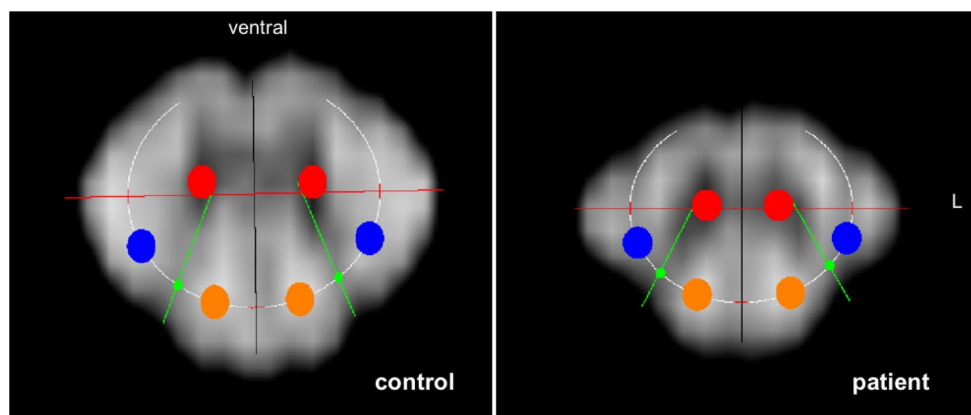
Fig. 2 Representative MD- and RD-maps of two subjects. MD and RD maps are shown in units of $10^{-9}\text{m}^2/\text{s}$

Methods: 21 healthy subjects (30 ± 5 yrs) were scanned on a 3T scanner. DTI (24 directions) was performed using a single-shot echo planar imaging sequence with a conjunction of SPAIR and slice-selection gradient reversal for fat suppression. Erector spinae muscles were segmented manually. Eigenvalues (λ_1 , λ_2 , λ_3), mean diffusivity (MD), radial diffusivity (RD) and fractional anisotropy (FA) were calculated. Absolute flexion (F) and extension (E) back muscle strength, measured with a rotational dynamometer, were adjusted for BMI to obtain relative (R) strength values and placed in relation (E/F).

Results: MD correlated significantly with RE and the ratio E/F; λ_1 , λ_3 and RD showed significant correlations with the ratio E/F and statistical trends when correlated with RE (Fig. 1). See Fig. 2 for representative MD- and RD-maps.

Conclusion: DTI seems to enable not only the characterization of back muscle fiber architecture but also the probing of microstructure differences related to muscle function. Thus, DTI may track slight changes of back muscle tissue composition and may be useful in the early diagnosis of back muscle diseases or back pain.

Fig. 1 Spinal DTI at the height of cervical vertebra 2 in a representative patient and control. The measured ROIs are displayed on fractional anisotropy maps, blue (PT), orange (DC), and red (AH)



Fractional anisotropy estimation of the pyramidal tracts, dorsal columns and anterior horns in normal ageing and pathologic conditions in the cervical spinal cord

Tobias Lindig^{*1}, Benjamin Bender², Tim W. Rattay³, Ludger Schöls⁴, Thomas Nägele⁵, Ulrike Ernemann², Uwe Klose⁶

¹Radiologische Klinik, Abteilung für Diagnostische und Interventionelle Neuroradiologie, Tübingen, Deutschland

²Universitätsklinikum Tübingen, Radiologische Klinik, Abteilung für Diagnostische und Interventionelle Neuroradiologie, Tübingen, Deutschland

³Zentrum für Neurologie—Abteilung für Neurodegenerative Erkrankungen, Hertie-Institut für Klinische Hirnforschung, Deutsches Zentrum für Neurodegenerative Erkrankungen (Dzne), Tübingen, Deutschland

⁴Universitätsklinikum Tübingen, Hertie-Institut für Klinische Hirnforschung; Deutsches Zentrum für Neurodegenerative Erkrankungen (Dzne), Sektion Klinische Neurogenetik, Klinik für Neurologie, Tübingen, Deutschland

⁵Abteilung Diagnostische und Interventionelle Neuroradiologie, Department Radiologie, Abteilung für Diagnostische und Interventionelle Neuroradiologie, Freiburg/N., Deutschland

⁶Universitätsklinik Tübingen, Department Radiologie, Abteilung für Diagnostische und Interventionelle Neuroradiologie, Tübingen, Deutschland

Purpose: To quantify white matter anisotropy of the human cervical spinal cord is still a challenge. The purpose of this work is to develop a standardized evaluation method for a robust FA estimation of the pyramidal tracts (PT), dorsal columns (DC) and anterior horns (AH) in normal ageing and pathologic conditions.

Methods: A monopolar EPI sequence with double spin-echo diffusion preparation optimized for both a high SNR and a high axial in-plane resolution of 0.8 mm^2 was used. Impairment of the upper spinal cord was assessed in cross sectional images of 77 healthy subjects and 30 patients with hereditary spastic paraplegia (HSP) at 3T. To allow a semi-automated, bilateral ROI evaluation of the PT, DC and AH an ellipsoid was adjusted onto the individual FA image of each subject's spinal cord (Fig. 1).

Results: Fig. 2 shows stable FA values from 18 years to the age of 65 for the PT (0.56, SD 0.03), DC (0.57, SD 0.03) and AH (0.38, SD 0.04). No decline of FA values can be demonstrated in normal ageing, at least until the age of 65.

Fig. 3 shows a significant ($p < .001$) reduction in mean FA values of the pyramidal tracts of spastic paraplegia patients compared to controls. As HSP is the prototype disease of the degenerating first motor neuron, the measured decline in FA reflects well this pathologic condition.

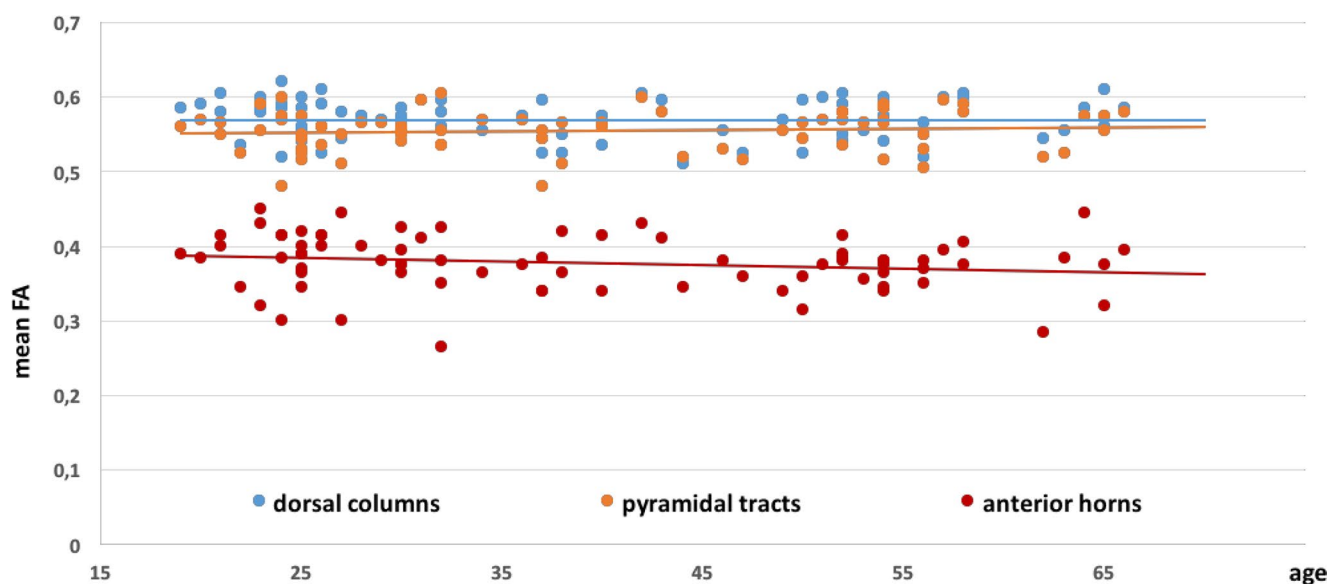


Fig. 2 Mean fractional anisotropy of the DC, PT and AH are plotted against age in healthy controls. Linear correlation lines are provided

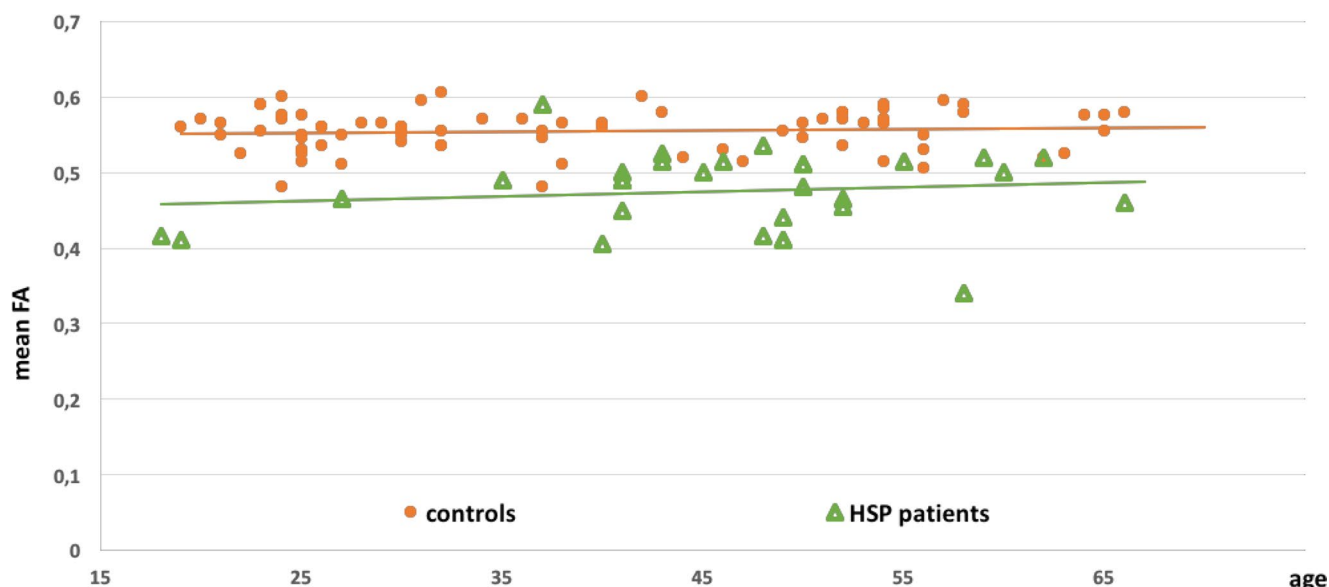


Fig. 3 Mean fractional anisotropy of PT are plotted against age in healthy controls and spastic paraplegia patients. Linear correlation lines are provided

Conclusion: Spinal DTI of the upper cervical cord is clinically feasible at 3T, enabling robust FA measurements of PT, DC and AH in normal ageing and pathologic conditions.

188

MDCT-based finite element analysis of vertebral fracture risk: how much dose is needed?

Nico Sollmann^{*1}, D Anitha², Kai Mei³, Michael Dieckmeyer⁴, Felix K. Kopp³, Claus Zimmer¹, Jan S. Kirschke¹, Peter B. Noel³, Karupppasamy Subburaj², Thomas Baum¹

¹Abteilung für Neuroradiologie, Klinikum Rechts der Isar, Technische Universität München, München, Deutschland

²Engineering Product Development (Epd) Pillar, Singapore University of Technology and Design (Sutd), Singapur

³Institut für Diagnostische und Interventionelle Radiologie, Klinikum Rechts der Isar, Technische Universität München, München, Deutschland

⁴Abteilung für Neuroradiologie & Institut für Diagnostische und Interventionelle Radiologie, Klinikum Rechts der Isar, Technische Universität München, München, Deutschland

Purpose: The purpose of this work was to compare vertebral failure loads, predicted from finite element (FE) analysis of patients with and without osteoporotic vertebral fractures (OVFs) at virtually reduced dose levels, compared to standard-dose exposure from multi-detector computed tomography (MDCT) imaging and evaluate whether ultra-low dose derived FE analysis can still differentiate patient groups.

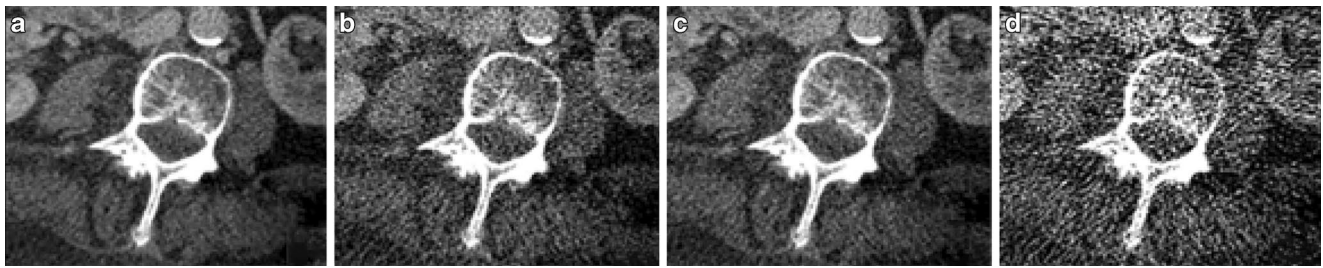


Fig. 1 MOCT images illustrating changes in image quality with dose reduction from standard **a** to half **b** to quarter **c** to tenth dose **d**

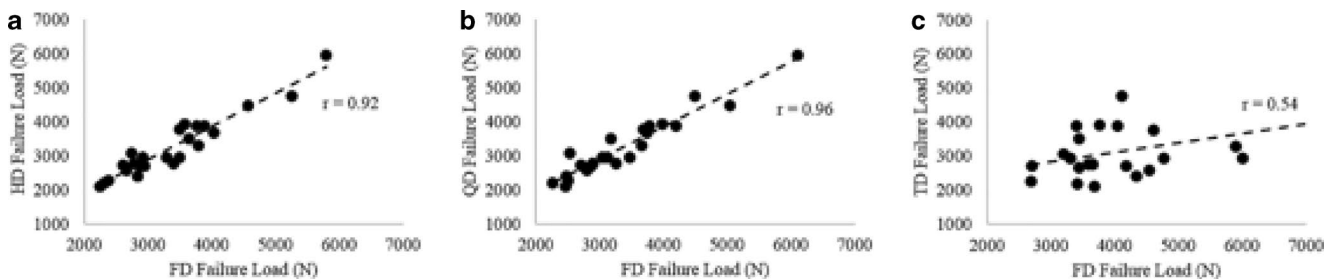


Fig. 2 Correlation between FE-predicted failure loads for each individual dose, half dose (HD) **a**, quarter dose (QD) **b** & tenth dose (TD) **c** as a function of full dose (FD) for fracture group

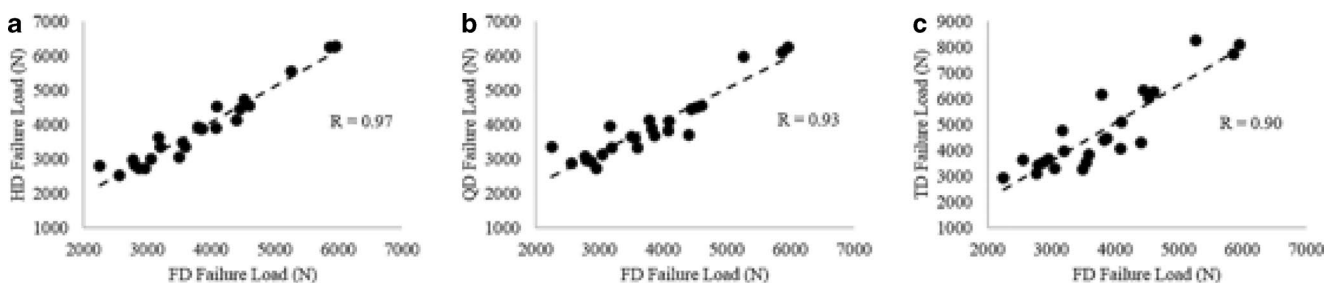


Fig. 3 Correlation between FE-predicted failure loads for each individual dose, half dose (HD) **a**, quarter dose (QD) **b** & tenth dose (TD) **c** as a function of full dose (FD) for control group

Methods: 16 patients were evaluated at standard-dose MDCT (8 with and 8 without OVFs). Images were reconstructed at virtually reduced dose levels (i.e. half, quarter and tenth of standard dose; Fig. 1). Failure load was determined at L1-3 from FE analysis and compared between standard, half, quarter, and tenth doses and used to differentiate between fractures and controls.

Results: Failure load derived at standard dose (3254 ± 909 and 3794 ± 984 N) did not significantly differ from half (3390 ± 890 and 3860 ± 1063 N) and quarter dose (3375 ± 915 and 3925 ± 990 N) but was significantly higher in the tenth dose (4513 ± 1762 and 4766 ± 1628 N). Failure load differed significantly between patients with OVFs and controls at standard, half and quarter doses, but not at tenth dose (Figs. 2 & 3).

Conclusion: MDCT allows a dose reduction of at least 75% compared to standard-dose for an adequate prediction of vertebral failure load based on non-invasive FE analysis.

197

Spinal CSF leaks: Diagnosis and treatment

Horst Urbach^{*1}, Emre Kaya², Ulrich Hubbe³, Jürgen Beck⁴

¹Universitätsklinikum Freiburg, Klinik für Neuroradiologie, Freiburg, Deutschland

²Freiburg, DE, Faculty of Medicine, University of Freiburg, Germany, Dept. of Neuroradiology, Medical Center—University of Freiburg

³Klinik für Neurochirurgie, Freiburg, Deutschland

⁴Department of Neurosurgery, Medical Center, University of Freiburg, Deutschland

Purpose: In patients with spontaneous intracranial hypotension clinical symptoms are caused by spinal CSF leaks. It is still a matter of debate how so called fast leaks are diagnosed and treated (Schievink et al. 2016).

Methods: Within 5 years 50 consecutive patients with suspected intracranial hypotension were studied with various imaging modalities. (Dynamic) myelography, (dynamic) CT-myelography, and digital subtraction myelography were compared. Patients with proven CSF leaks

were treated with high volume epidural blood patches (30–70 ml) and if those were not successful finally operated.

Results: CT-myelography ($n=50$) showed distant epidural contrast medium in 22 patients and in 1–12 levels. With dynamic CT-myelography ($n=5$) dural tears were incorrectly localized in 3 patients. Dynamic myelography ($n=12$) correctly localized a dural tear in 4 surgically treated patients, however, in 2 patients additional focussed dynamic CT-myelography was applied. 8 of 22 patients got free of symptoms following high volume epidural blood patches, 8 patients were operated, in 6 patients follow-up-data are lacking

Conclusion: We propose a diagnosis and treatment algorithm for patients with spontaneous intracranial hypotension.

199

Traumatic extracranial arteriovenous fistulas—a very unusual reason for intraspinal venous congestion

Franziska Dorn¹, Philipp Mennemeyer^{*2}

¹Klinikum der Universität München—Campus Großhadern, Institut für Klinische Radiologie, Abteilung für Neuroradiologie, München, Deutschland

²Abteilung für Neuroradiologie, Campus Großhadern, LMU München, München, Deutschland

Purpose: Venous congestion of the cervical spine is rare and usually associated with intraspinal/-cranial dural arteriovenous fistulas (dAVF). AVFs arising from the subclavian artery and/or its branches can occur after trauma or central venous puncture; they typically present with a pulsatile bruit, whereas symptoms due to venous reflux into spinal and/or intracranial veins are not described yet.

Methods: We present 2 patients with acquired thyrocervical AVFs and signs of venous spinal and/or intracranial congestion.

Results: Pat. 1 (37, m) had a pulsatile bruit after gun-shooting at the age of 10y and now presented with chemosis/proptosis of his right eye. CTA showed cervical/intraspinal venous engorgement, DSA proofed AVF between the thyrocervical trunk and the jugular vein. Symptoms resolved within 2 days after coilocclusion of the AVF.

Pat. 2 (54, f) rapidly developed instability and gait disturbance 1.5y after central venous puncture. There was no subclavicular swelling or bruit. MRI showed cervical venous engorgement and craniocervical edema, DSA revealed AVF between the thyrocervical trunk and the jugular vein. After coilocclusion of the AVF, symptoms improved, and the edema decreased.

Conclusion: Extracranial AVFs are a potential cause of intraspinal and/or intracranial venous congestion. Therefore, DSA should include the subclavian artery in patients suspected for dAVF, in particular if there is a history of trauma or venous puncture.

319

Iodine density thresholds for the separation of vertebral bone metastases from healthy appearing trabecular bone in spectral detector computed tomography

Jan Borggrefe¹, Victor Neuhaus², Markus Le Blanc³, Nils Große Hokamp⁴, Volker Maus⁵, Anastasios Mpotsaris⁶, Simon Lennartz⁷, Daniel Pinto dos Santos⁸, David Maintz⁹, Nuran Abdullayev^{*10}

¹Universität zu Köln, Institut für Diagnostische und Interventionelle Radiologie, Köln, Deutschland

²Uniklinik Köln, Institut für Diagnostische und Interventionelle Radiologie, Institut für Diagnostische und Interventionelle Radiologie, Köln, Deutschland

³Universitätsklinik Köln, Institut für Diagnostische und Interventionelle Radiologie, Köln, Deutschland

⁴Uniklinik Köln, Institut für Diagnostische und Interventionelle Radiologie, Köln, Deutschland

⁵University Hospital of Göttingen, Institute for Neuroradiology, Göttingen, Deutschland

⁶Klinik für Diagnostische und Interventionelle Neuroradiologie, Aachen, Deutschland

⁷Institut für Diagnostische und Interventionelle Radiologie, Deutschland

⁸Institut für Diagnostische und Interventionelle Radiologie, Department of Radiology, Köln, Deutschland

⁹Institut F. Diagnos. U. Interv. Radiologie, Köln, Deutschland

¹⁰Inst. F. Diagn. U. Interv. Radiologie, Inst. F. Diagn. U. Interv. Radiologie, Köln, Deutschland

Purpose: To evaluate quantitative iodine density mapping (IDM) from spectral detector computed tomography (SDCT) as a quantitative parameter for the separation of vertebral trabecular bone metastases (BM) and healthy trabecular bone (HTB).

Methods: This retrospective study includes portal venous SDCT datasets of cancer patients with and without known bone metastasis ($n=43$ and $n=40$, respectively). Target lesions as well as non-affected control vertebrae were defined by two radiologists in consensus using follow-up CT imaging, MRI and/or bone scintigraphy. IDM and its standard deviation (SD) were determined based on ROI measurements in BM and HTB of patients with and in HTB of patients without bone metastasis, and various reference tissues/vessels in both. Phantomless bone mineral density (vBMD) measurements of the lumbar spine were conducted.

Results: We found a significant difference between IDM of BM and HTB (mean 5.55 ± 0.98 vs. 3.57 ± 0.96) ($p < 0.0001$); however, there was a considerable overlap and a vBMD bias. A trivariate analysis including IDM, the inhomogeneity of the IDM as determined by the SD, and the normalization to the vertebral venous sinus improved the statistical separation of metastasis to a specificity of 100.0% and a sensitivity of 95.4% (AUC 0.98, $\Delta p < 0.05$ compared to univariate models).

Conclusion: SDCT allows for quantification of iodine in bone lesions which appears promising to serve as a parameter for the detection of bone metastases.

322

Superior Prediction of Incident Vertebral Fractures by Opportunistic Quantitative CT compared to Dual-Energy X-ray Absorptiometry

Maximilian Löffler^{*1}, Alina Jacob¹, Anna Rienmüller², Thomas Baum¹, Claus Zimmer³, Yu-Mi Ryang⁴, Jan Kirschke⁵

¹Abteilung für Neuroradiologie, Klinikum Rechts der Isar, München, Deutschland

²Neurochirurgie Klinikum Rechts der Isar Tübingen, Orthopädie Medizinische Universität Wien, München, Deutschland

³Klinikum Rechts der Isar der TUM, Technische Universität München, Abteilung für Diagnostische und Interventionelle Neuroradiologie, München, Deutschland

⁴Neurochirurgische Klinik und Poliklinik, München, Deutschland

⁵Abteilung für Diagnostische und Interventionelle Neuroradiologie, München, Deutschland

Purpose: Osteoporosis manifests in low-energy fractures with severe health consequences. Accurate screening enables effective prevention. Opportunistic osteoporosis screening in routine clinical CT (QCT) is a promising alternative to dual-energy X-ray absorptiometry (DXA). The aim of this study was to compare central DXA with opportunistic QCT of lumbar vertebra in their ability to predict incident osteoporotic vertebral compression fractures (VCF).

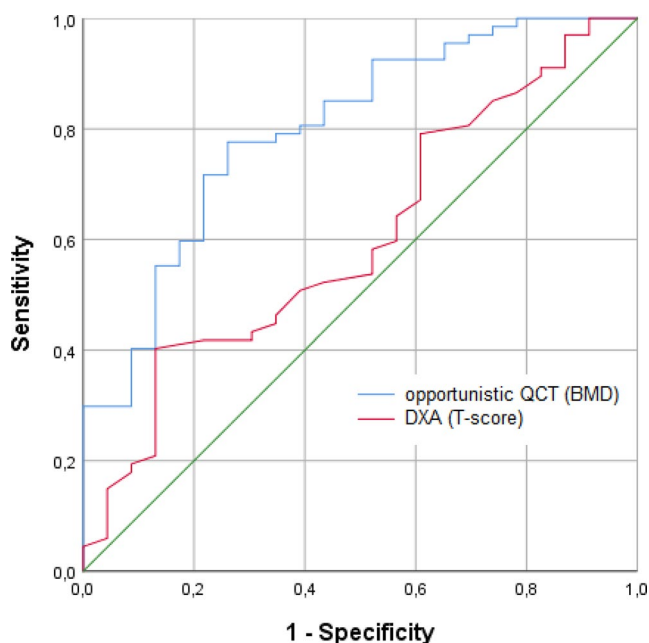


Fig. 1 Receiver-operating characteristics curves for predicting incident vertebral compression fractures by opportunistic QCT (BMD) and DXA (T-score)

Methods: We reviewed 327 consecutive patients, aged 50 years and older, who had lumbar CT (baseline) and DXA within a 12-month period. Of those, 90 patients were identified with follow-up imaging after at least 12 months or who sustained an incident or progressive VCF documented in earlier imaging. Fracture status and volumetric bone mineral density (BMD) were retrospectively evaluated in baseline CT and fracture status was reassessed at follow-up. BMD was obtained through asynchronously calibrated QCT. Area under the ROC curve (AUC) for BMD by QCT and T-scores by DXA was calculated for the incidence of VCF at follow-up.

Results: Twenty-three patients had a progressive or new VCF at follow-up. The predictive performance for incident VCF was far superior for BMD by QCT (AUC=0.800, 95% confidence interval [CI]=0.696–0.904) compared to T-scores by DXA (AUC=0.603, CI=0.471–0.735; Fig. 1).

Conclusion: In the prediction of incident VCF, opportunistic BMD measurements in routine CT outperformed T-scores of reference DXA.

Spinal cord atrophy evaluation with mean upper cervical cord area—height and intracranial volumes as important covariates

Claudia Chien^{*1}, Graham Cooper¹, Friedemann Paul², Michael Scheel³

¹Charité-Universitätsmedizin Berlin, Neurocure Clinical Research Center, Berlin, Deutschland

²Charité-Universitätsmedizin Berlin, Neurocure Clinical Research Center, Department of Neurology, Berlin, Deutschland

³Charité-Universitätsmedizin Berlin, Neurocure Clinical Research Center, Department of Neuroradiology, Berlin, Deutschland

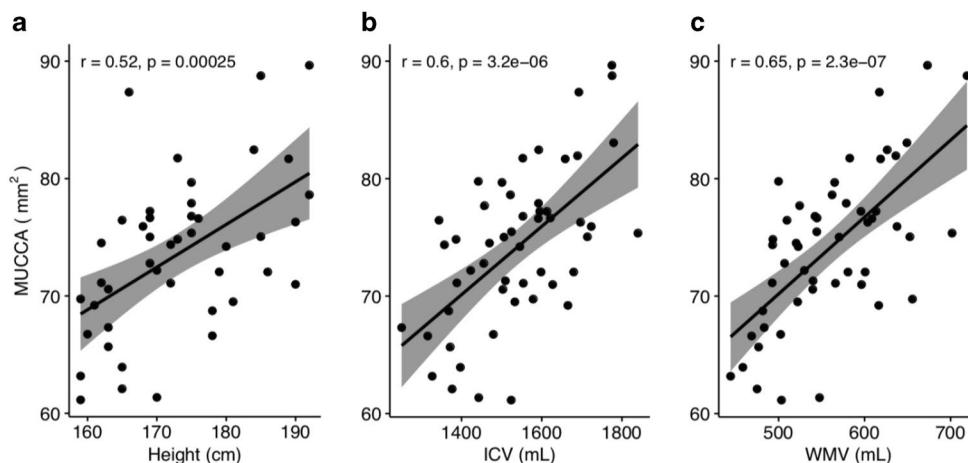
Purpose: Spinal cord atrophy (SCA) is an important outcome parameter in neuroinflammatory disorders, e.g. multiple sclerosis and neuromyelitis optica. The mean upper cervical cord area (MUCCA) has been proposed as a biomarker for SCA evaluation. This study investigates associations and interdependencies of several factors (age, sex, weight, height, intracranial volume) with MUCCA.

Methods: A cohort of healthy control subjects ($n=52$, F/M=36/16, age mean \pm sd=35.6 \pm 12.3 years) was investigated (MPRAGE brain with cervical spine, 1 mm isotropic resolution, TR/TE=1900/3.03 ms). MUCCA was measured with a semiautomatic approach (JIM Software). Intracranial volume (ICV) and estimates of gray matter (GMV), white matter (WMV) and CSF were calculated using SIENAX (FSL). Correlational analysis and stepwise linear regression models were used to identify the most important MUCCA covariates.

Results: Independent correlational analysis showed all factors besides age as significantly associated with MUCCA: age ($r=0.1$, $p=0.49$), sex ($r=0.32$, $p=0.02$), height ($r=0.52$, $p<0.001$), weight ($r=0.28$, $p=0.05$), ICV ($r=0.6$, $p<0.001$). In a stepwise linear regression model (including age, sex, weight, height, ICV) only two factors remained significantly associated with MUCCA: height ($p=0.004$) and ICV ($p<0.001$). In a separate analysis of ICV components (i.e. GMV, WMV and CSF) WMV ($p<0.001$) was identified as the only influencing factor for MUCCA measures.

Conclusion: SCA analysis using MUCCA measurements need to take ICV and height into account as important covariates. With respect to ICV components, WMV is the main influencing factor and should be, depending on the research hypothesis, considered as an important covariate.

Fig. 1 Association of MUCCA with **a** height, **b** intracranial volume, and **c** white matter volume as the major influencing factors of MUCCA in a cohort of healthy control subjects



Pediatric Neuroradiology

108

CNS Imaging and Long-Term Effects of Whole Brain Irradiation in Pediatric Cancer Patients

Luciana Porto^{*1}, Sarah Kammerer²¹Neuroradiologie, Frankfurt am Main, Deutschland²Uniklinikum Frankfurt

Purpose: To evaluate the central nervous system post irradiation changes on MRI in children.

Methods: We retrospectively reviewed the MR images of children with primary brain tumors treated with whole brain irradiation (RT) during the last 10 years. Variables such as age at the time of irradiation, total radiation dose and time interval between radiation and MR changes were evaluated. A total of 15 children (11 male and 4 female) were included. Mean age at time of RT was 10,53 years. Median dose: 29,13 Gy (range 23,4–54 Gy)

Results: All patients revealed abnormalities in the imaging studies. Seven patients developed these CNS abnormalities within a few months after irradiation (mean 4.86 months), in eight patients CNS abnormalities occurred after one year interval post-treatment (mean 52.63 months). In almost all patients, a T2-increase of supra- and infratentorial white matter could be observed. Nine patients showed cerebellar atrophy during follow up.

Conclusion: At this small sample of pediatric patients who underwent RT, a correlation between the age of the child or the radiation dose and the extent of the changes could not be confirmed. However, we observed a trend towards stronger brain parenchymal degeneration with cystic changes in the younger age group of children. Older children

and adolescents seem to be more susceptible to vascular dysplasia with cavernous hemangiomas and microbleedings. Future studies are needed to evaluate whether MRI changes can predict neurological outcome.

128

Regionally higher gyrification index correlates with gestational age and full-scale IQ in prematurely born adults.

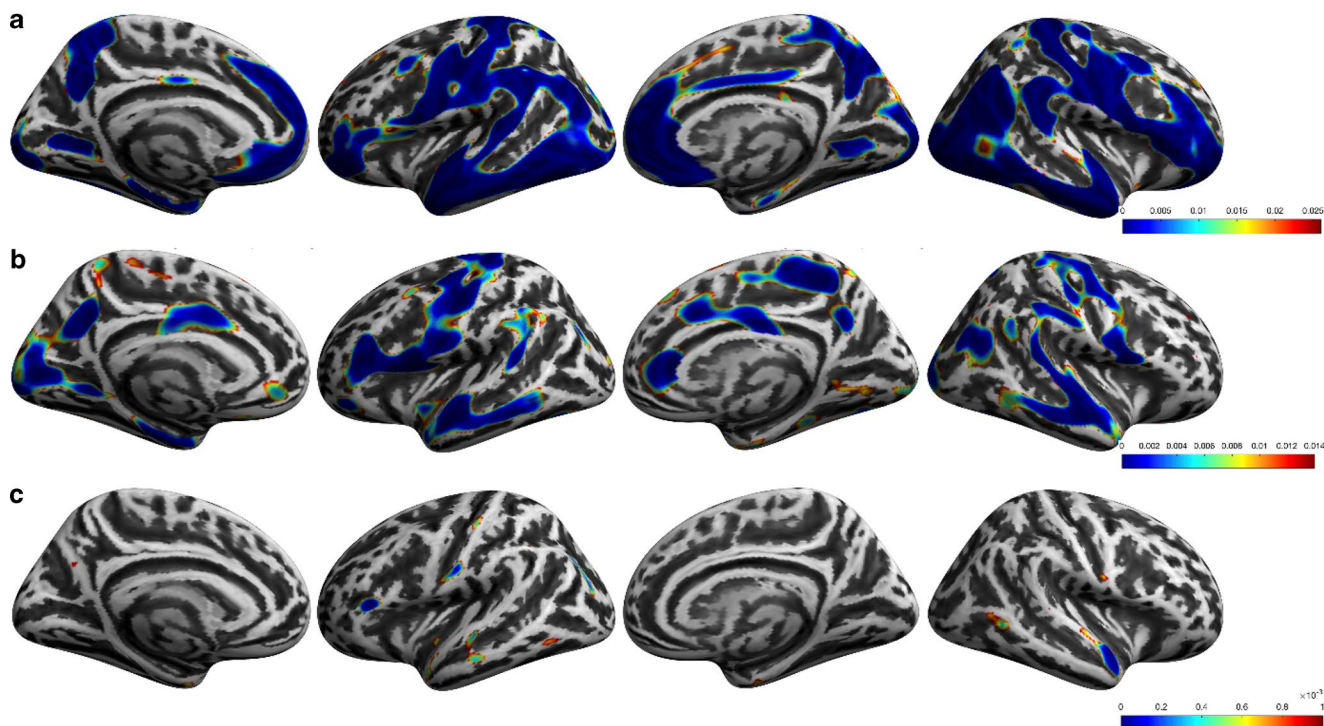
Dennis Hedderich^{*1}, Maria Berndt², Aurore Menegaux³, Lukas Scheef⁴, Marcel Daamen⁵, Peter Bartmann⁶, Claus Zimmer⁷, Henning Boecker⁸, Dieter Wolke⁹, Christian Sorg¹⁰, Josef Bäuml²¹Abteilung für Diagnostische und Interventionelle Neuroradiologie, Klinikum Rechts der Isar der TU München, München, D²Klinikum Rechts der Isar, Technische Universität München, Abteilung für Diagnostische und Interventionelle Neuroradiologie, München, Deutschland³Abteilung für Diagnostische und Interventionelle Neuroradiologie, Klinikum Rechts der Isar, TU München⁴Functional Neuroimaging Group, Department of Radiology, University Hospital Bonn, Bonn, Germany, Deutschland⁵Functional Neuroimaging Group, Department of Radiology, University Hospital Bonn, Bonn, Germany, Department of Neonatology, University Hospital Bonn, Bonn, Germany⁶Uni-Kinderklinik Bonn, University Hospital Bonn, Department of Neonatology, Bonn, Deutschland⁷Klinikum Rechts der Isar der TUM, Technische Universität München, Abteilung für Diagnostische und Interventionelle Neuroradiologie, München, Deutschland⁸University Hospital Bonn, Department of Radiology, Functional Neuroimaging Group, Bonn, Deutschland

Fig. 1 a–c Left medial, left lateral, right medial and right lateral inflated surface views are shown. **a** Increased gyrification index in preterm subjects compared to term subjects in large frontotemporoparietal cortex areas with a slight predominance of right hemispheric differences. Corrected for sex and scanner $p < 0.05$, FDR corrected. **b** Negative correlation of gestational age and GI in preterm subjects after correction for SGA, sex, and scanner. $p < 0.05$, FDR corrected. **c** Negative correlation of GI in preterm subjects with full scale IQ after correction for sex and scanner. $p < 0.001$, uncorrected

⁹University of Warwick, Warwick Medical School, Coventry, United Kingdom

¹⁰Abteilung für Neuroradiologie, Klinikum Rechts der Isar, TU München, Deutschland

Purpose: Cortical folding is a mainstay of human brain development and predominantly takes place in the last trimester. Thus, this developmental process may be disrupted by preterm birth with persisting changes until adulthood. The goal of this study is to investigate differences in gyrification index (GI) between preterm (PT) and term born (TB) adults and whether gestational age (GA) and full-scale IQ (IQ) is linked with GI in PT subjects.

Methods: 212 subjects (101 PT, 111 TB, mean age 26.8 years, 58.5% males) were included. Gyrification index was calculated based on 3D T1 sequences using the Cat12 toolbox and SPM12[1]. Two-sample t-tests and multiple regression were used to assess GI differences between PT and TB subjects and whether GA and IQ predict GI in PT subjects. Statistical significance was set at $p < 0.05$, FDR-corrected.

Results: We found widespread GI increases in PT subjects in fronto-temporoparietal cortices. Lower GA was linked with a higher GI mostly in frontotemporal cortices after correction for smallness for gestational age (SGA) and neonatal treatment index (INTI). Higher GI in the right superior temporal gyrus and the left inferior frontal gyrus was associated with reduced IQ. See Fig. 1.

Conclusion: GI is increased in PT adults, likely reflecting disrupted brain development in the third trimester. Additionally, regionally increased GI is associated with lower full IQ, linking brain structure with intellectual performance after premature birth.

Reference

1. Luders E, Thompson PM, Narr KL, et al. A curvature-based approach to estimate local gyrification on the cortical surface. *Neuroimage* 2006;29:1224–30.

156

Linking infant regulatory problems, adult behavior problems, and the allostatic-interoceptive-system by altered structural connectivity

Maria Berndt^{*1}, Josef Bäuml¹, Johanna Seitz², Aurore Menegaux², Nicole Baumann³, Mihai Avram⁴, Satja Mulej Bratec⁴, Linda Breeman⁵, Claus Zimmer⁶, Dieter Wolke⁷, Christian Sorg⁸

¹Klinikum Rechts der Isar, Technische Universität München, Abteilung für Diagnostische und Interventionelle Neuroradiologie, München, Deutschland

²Abteilung für Diagnostische und Interventionelle Neuroradiologie, Klinikum Rechts der Isar, TU München

³University of Warwick, Department of Psychology, Coventry, United Kingdom

⁴Klinikum Rechts der Isar TU München

⁵University of Warwick

⁶Klinikum Rechts der Isar der Tum, Technische Universität München, Abteilung für Diagnostische und Interventionelle Neuroradiologie, München, Deutschland

⁷University of Warwick, Warwick Medical School, Coventry, United Kingdom

⁸Abteilung für Neuroradiologie, Klinikum Rechts der Isar, TU München, Deutschland

Purpose: Infant regulatory problems (iRP) (i.e. crying, feeding, sleeping) are associated with behavior problems lasting into adulthood (e.g. withdrawn behavior and avoidant personality traits). These are mediated by decreases of intrinsic functional connectivity within the allostatic-interoceptive system (AIS)—a system comprising mainly the default mode (DMN) and salience network (SN), linked in the temporoparietal junction (TPJ). It is unknown, however, whether structural alterations in the AIS occur in iRP. We hypothesized changed structural connectivity of the TPJ within the AIS to be relevant for adult behavioral problems.

Methods: As part of the Bavarian Longitudinal Study 90 adults with ($n=23$) and without ($n=67$) iRP were assessed by behavioral testing and diffusion tensor imaging. Probabilistic tractography was used to measure structural connectivity between TPJ and DMN/SN. Group differences were associated with behavioral problems via Spearman rank bivariate correlation.

Results: Adults with iRP showed reduced structural connectivity between right anterior TPJ and SN ($p < 0.05$ FWE-corrected, see fig.). Aberrant structural connectivity was associated with withdrawn behavior ($r=0.45$, $p=0.04$) and avoidant personality ($r=0.57$, $p=0.007$).

Conclusion: We provide evidence for long-term effects of iRP on adult structural connectivity of the TPJ within the AIS, and for structural changes being associated with adult social-emotional problems. Data suggest a possible link between infant regulatory and adult behavioral problems via AIS.

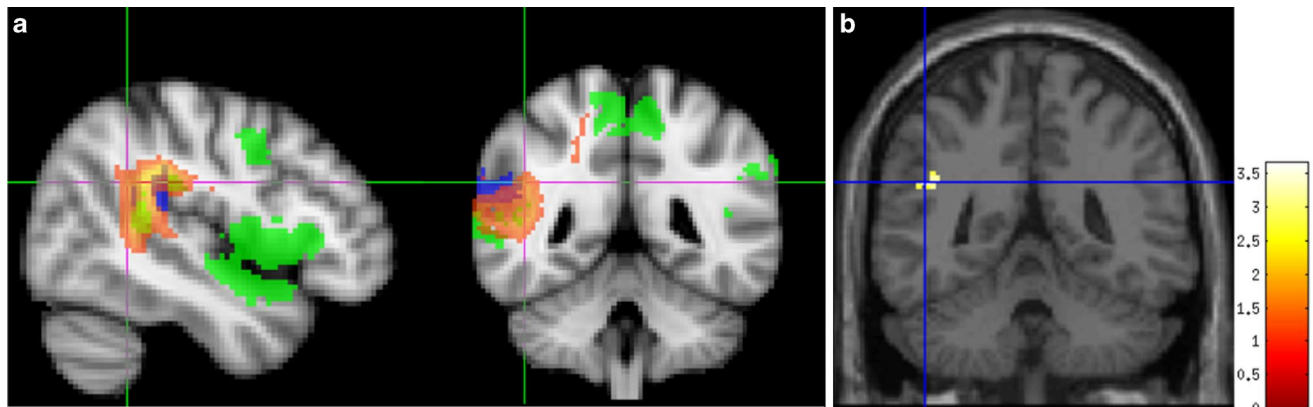


Fig. 1 **a** Example of probabilistic fibertracking (red/yellow) between right anterior temporoparietal junction (in blue) and salience network (in green). **b** Voxels of reduced structural connectivity for iRP-adults in comparison to adults without preceding iRP (voxel-wise t-test, $p < 0.05$, FWE corrected)

Neuroimaging findings in children with hereditary hemophagocytic lymphohistiocytosis—a report from the German reference center

Ulrike Löbel^{*1}, Katharina Wustrau², Gritta Janka³, Ingo Müller⁴, Jens Fiehler¹, Kai Lehmberg⁴

¹Department of Diagnostic and Interventional Neuroradiology, Hamburg, Deutschland

²Division of Pediatric Stem Cell Transplantation and Immunology, Department of Pediatric Hematology and Oncology, Hamburg, Deutschland

³Department of Pediatric Hematology and Oncology, Hamburg, Deutschland

⁴Division of Pediatric Stem Cell Transplantation and Immunology, Hamburg, Deutschland

Introduction: Hemophagocytic lymphohistiocytosis (HLH) is a life-threatening hyperinflammatory syndrome characterised by prolonged fever, hepatosplenomegaly and pancytopenia. Patients may develop inflammatory CNS involvement, presenting with meningism, cranial nerve palsies and seizures, resulting in pathological neuroimaging.

Methods: We aimed to identify the most common neuroimaging findings in patients with hereditary HLH, recruited from the HLH 94 and HLH2004 studies in Germany, Switzerland, and Austria.

Results: MRI was available for 37 patients (20 female, 17 male; median age, 1.5 years [min, 0.1; max, 17.8 years]). In patients with more than one MRI, the scan with most pathological changes was selected for cross-sectional analysis. Bilateral symmetric cerebellar lesions were most common (41%, A), followed by diffuse central (38%, B), diffuse subcortical (36%) as well as diffuse periventricular (31%), cortical (31%, C) and focal subcortical (28%, D) lesions. Contrast enhancement (19%, E) and restricted diffusion (15%) were recorded. Two patients presented with imaging findings of “PRES”. Brain at-

rophy (F) and abnormal myelination were frequently identified and may be treatment-related. Imaging of the spine (5 patients) showed focal hyperintensity on T2-wweighted imaging and focal contrast enhancement.

Conclusion: Neuroimaging in patients with familial HLH is variable and non-specific, but bilateral symmetric cerebellar lesions, if present, are typical in the clinical context of HLH.

206

Thrombectomy in Childhood Stroke

Peter Sporns^{*1}, Andre Kemmling², Uta Hanning³, Walter Heindel¹, Moritz Wildgruber⁴

¹Institut für Klinische Radiologie, Institut für Klinische Radiologie, Münster, Deutschland

²Institut für Klinische Radiologie, Universitätsklinikum Münster, UKSH Lübeck, Hamburg, Deutschland

³Universitätsklinikum Eppendorf, Institut für Neuroradiologie

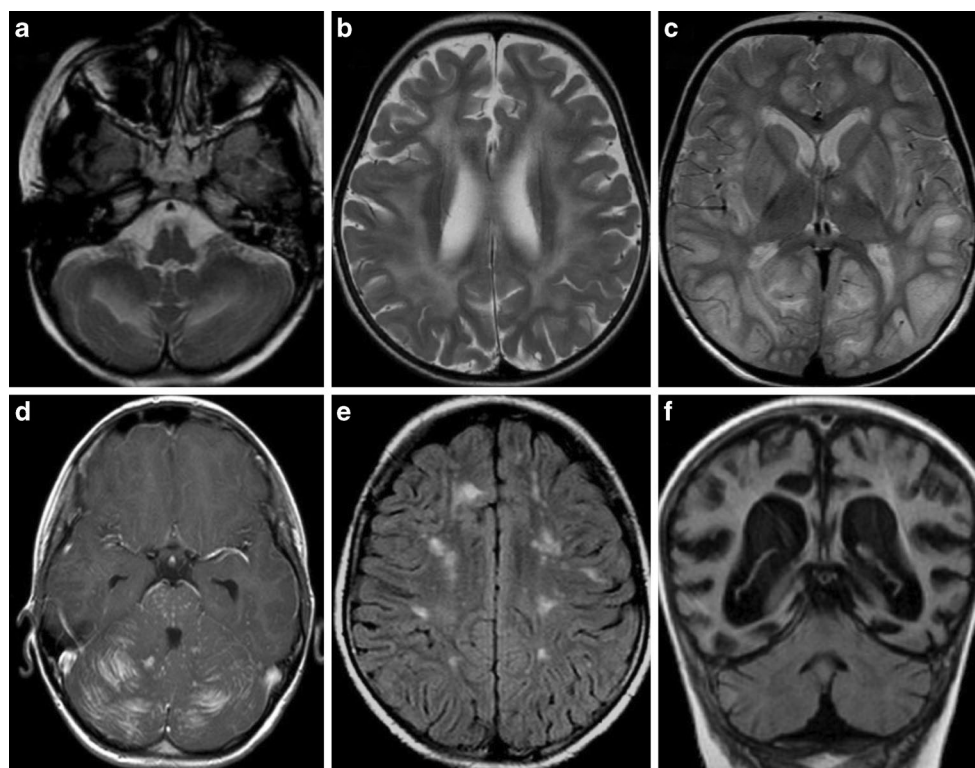
⁴Institut für Klinische Radiologie, Münster, Deutschland

Purpose: Childhood stroke is a rare clinical event with potentially severe outcome. Several randomized trials have shown the efficacy of thrombectomy for large intracranial vessel occlusions in adults. However, the safety and efficacy of thrombectomy in children is unknown. We aimed to investigate the feasibility and outcome of thrombectomy in pediatric patients.

Methods: We performed a retrospective analysis of all patients aged between 29 days and 18 years admitted for mechanical thrombectomy at three tertiary care stroke centers presenting with a pediatric NIHSS (PedNIHSS) ≥ 4 . Interventional results and clinical outcomes were assessed at day 7 after thrombectomy (PedNIHSS) as well as after three months (mRS=modified Ranking Scale).

Results: Overall 12 children were included. Median PedNIHSS on admission was 12.5 (IQR 8.0–21.5). Angiographic outcomes for thrombectomy were good in all patients (6×mTICI 3, 6×mTICI 2b).

Fig. 1



Moreover, most patients showed a remarkable improvement of neurological outcome after thrombectomy with a median PedNIHSS of 3.5 (IQR 1–8) at day 7 and a mRS of 1.0 (IQR 0–2.0) at 3 months. No major periprocedural complications were observed.

Conclusion: Thrombectomy is effective and safe not only in adults but also in childhood ischemic stroke.

308

Persistent notochordal canal of cervical, thoracic and lumbar spine, MRI findings in premature baby

Hadi Nasri^{*1}, Michael Mull², Jan Patrick Alt³, Martin Wiesmann⁴, Anastasios Mpotsaris⁵

¹Uniklinik Aachen, Aachen, Deutschland

²Uniklinik Aachen, Neuroradiologie, Aachen, Deutschland

³Department of Diagnostic and Interventional Neuroradiology, RWTH Aachen University, Aachen, Deutschland

⁴Klinik für Diagnostische und Interventionelle Neuroradiologie, Aachen, Deutschland

⁵Klinik für Diagnostische und Interventionelle Neuroradiologie, Aachen, Deutschland

Purpose: The Persistence of notochordal canal is a rare and asymptomatic developmental anomaly of spine. This anomaly is usually discovered incidentally with imaging.

Methods: A baby was born prematurely in 36+1 weeks of gestation with caesarian section due to fetal tachycardia. At six months of age, the abdominal ultrasound was performed as follow-up examination. Accessory spleen and mild dilation of right renal pelvis were found

on ultrasound examination. However, these findings were not detected after one year-old. At 18 months of age, this baby suffering from motor developmental disorder was admitted to our hospital for further MRI examination of brain and spine.

Results: On MRI images of the brain, age-appropriate myelination without any other pathologic lesions was observed. Also, MRI findings of spine showed a vertically oriented canal spanning the third posterior of C3-L5. On T1 image, the signal intensity of notochord canal was similar to normal vertebral bone marrow (Fig. 1a). However, on T2-weighted image, this signal intensity of the canal was hyperintense (Fig. 1b).

Conclusion: Our clinical case is the first reported case with this anomaly involved all three cervical, thoracic and lumbar sections of spine. It is anticipated that follow-up examination in near future can give us information on the physiological process of notochordal canal regression and the rate of canal remnants in adulthood.

367

Imaging characteristics of WNT-subgroup medulloblastomas—cohort of the German HIT-trials

Annika Stock^{*1}, Martin Mynarek², Torsten Pietsch³, Stefan M. Pfister⁴, Dominik Sturm⁵, Steve Clifford⁶, Stefan Rutkowski⁷, Brigitte Bison⁸, Monika Warmuth-Metz⁸

¹Department of Neuroradiology, University Hospital Wuerzburg, Reference Center for Neuroradiology, University Hospital of Wuerzburg, Würzburg, Deutschland

²Department of Pediatric Haematology and Oncology, University Medical Center Hamburg-Eppendorf

Fig. 1 Persistence of notochordal canal, sagittal view. **a** T1-weighted image shows the hypointense canal along C3-L5 (black arrows), **b** In T2-weighted image, the signal of the canal is hyperintense (white arrows), **c** the notochordal canal begins from C3 in T2-weighted image (white arrow)



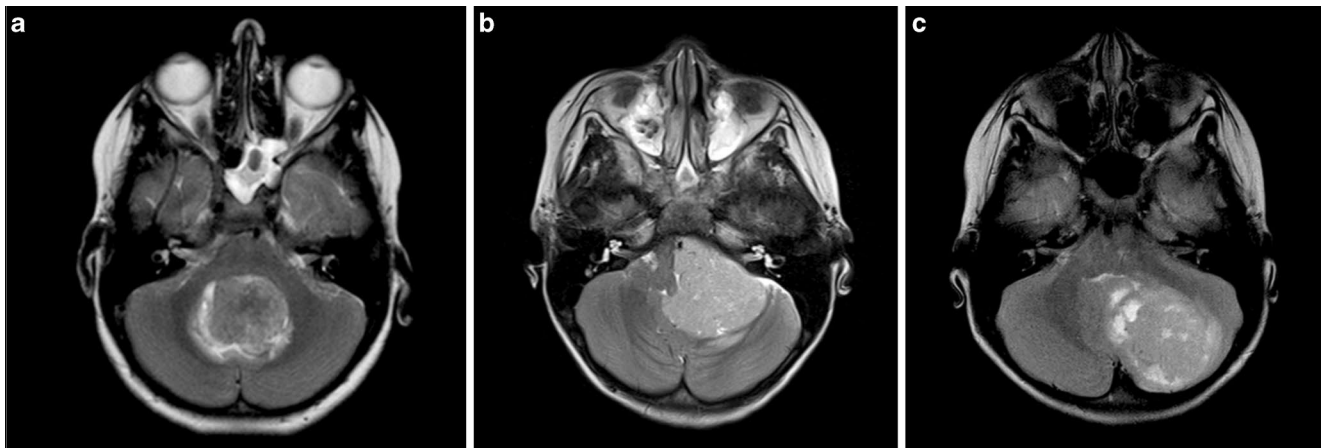


Fig. 1 Localization **a)** midline, **b)** cerebellopontine angle, **c)** cerebellar hemisphere

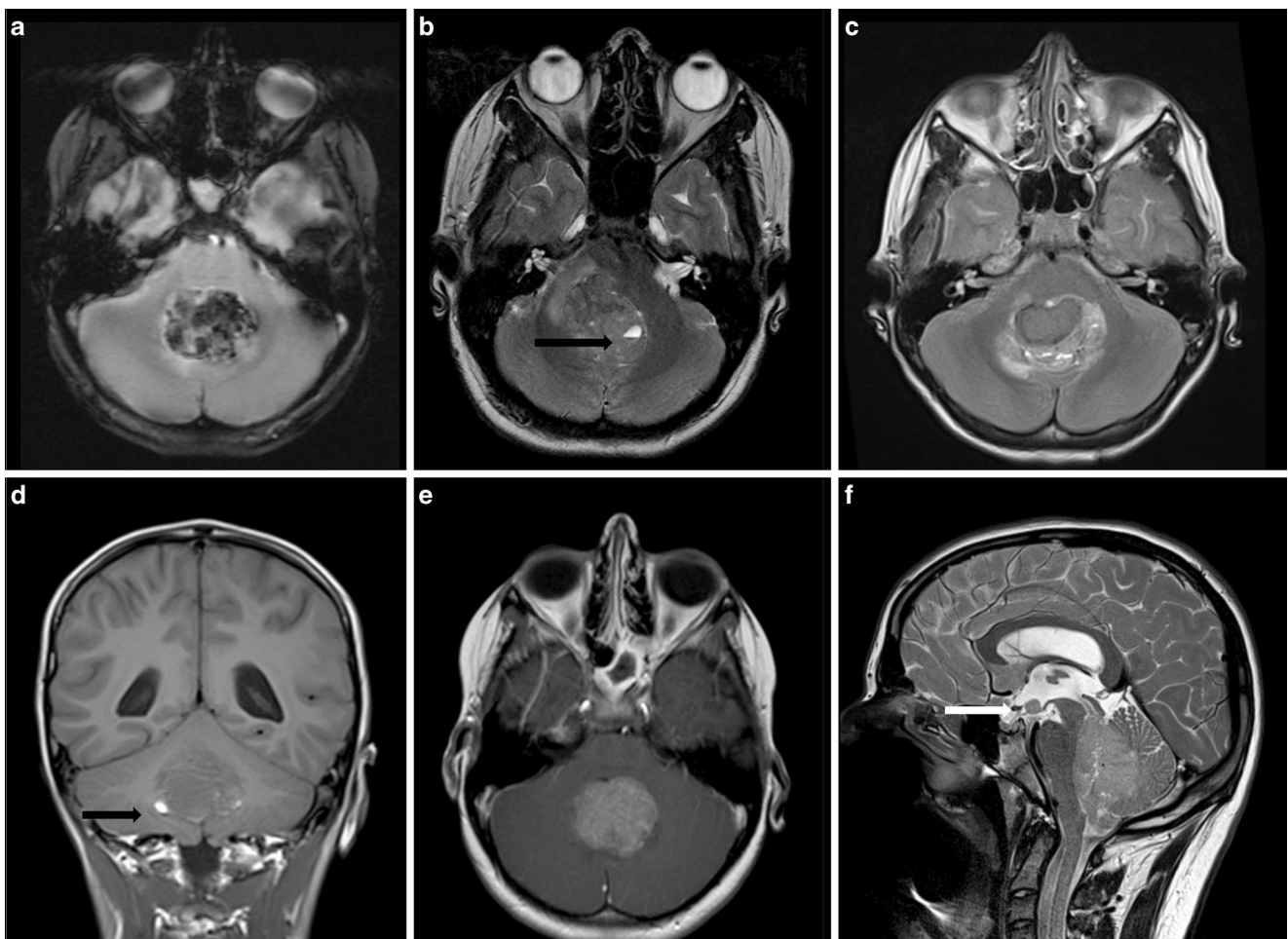


Fig. 2 **a** Deoxygenated blood in T2*WI. **b** Cyst with blood contents (→). **c** Inhomogeneous signal in T2WI. **d** Hypointense signal in T1WI and small bleeding (→). **e** 100% contrast enhancement. **f** Leptomeningeal dissemination (→)

³Institute of Neuropathology, University of Bonn Medical Center

⁴Division of Pediatric Neurooncology, German Cancer Research Center (Dkfz)

⁵Division of Pediatric Neurooncology, German Consortium for Translational Cancer Research (Dtkf), German Cancer Research Center (Dkfz)

⁶Northern Institute for Cancer Research, Newcastle University, United Kingdom

⁷Department of Pediatric Hematology and Oncology, University Medical Center Hamburg-Eppendorf

⁸Reference Center for Neuroradiology, University Hospital of Würzburg

Purpose: Medulloblastomas (MBs) are the most common malignant brain tumors in childhood. In addition to the known five histopathological variants, four distinct molecular genetic subgroups have been identified. The rarest subgroup is the wingless pathway activated medulloblastoma (WNT-MB). So far, this is the largest pediatric cohort systematically examined for MR imaging features.

Methods: WNT-MB cases were obtained from the database of the German multicenter HIT trials. This study includes pediatric patients with complete histological and molecular genetic data. Images were rated by standardized reference imaging criteria. Rating was performed in 40 pediatric patients by two neuroradiologists.

Results: In our cohort 92.5% are histologically classic MBs. 80% are localized in the midline, 15% in the cerebellopontine angle and 5% in the cerebellar hemisphere. Leptomeningeal dissemination is rare (17.5%). In 57.5% intratumoral blood products were found and 10 MB showed cysts with blood contents. T1- and T2-signal intensity is iso- to hypointense and tumor structure is inhomogeneous in T2-weighted images. Contrast enhancement is moderate to strong predominantly in 76–100% of the tumor volume. In our cohort we found a female predominance (1.86:1 ratio).

Conclusion: Our cohort especially shows that WNT-MBs are not preferentially off-midline tumors as postulated in previous studies with small case numbers.

371

Pediatric Brain AVM: Results of Interdisciplinary Management

Marcel Alfter¹, Marta Aguilar Perez², Markus Blankenburg³, Oliver Ganslandt⁴, Dietmar Kühne⁵, Hans Henkes⁶

¹Neuroradiologische Klinik, Stuttgart, Deutschland

²Neuroradiologie, Neuroradiologische Klinik, Stuttgart, Deutschland

³Klinikum Stuttgart, Stuttgart, Deutschland

⁴Klinikum Stuttgart, Neurochirurgische Klinik, Stuttgart, Deutschland

⁵Alfried-Krupp-Krankenhaus

⁶Klinik für Neuroradiologie, Neuroradiologische Klinik, Stuttgart, Deutschland

Purpose: The results of the interdisciplinary management of brain AVMs in children and adolescents were evaluated.

Methods: The following data of 116 patients treated between 1990 and 2018 was evaluated in retrospect: initial clinical presentation, mode of treatment, result of treatment, complications and their sequelae.

Results: Initial presentation: 9× incidental, 62× hemorrhage, 21× seizure(s), 6× progressive neurological deficit, 10× headache, 3× cognitive disorder, 1× cardiac failure, 1× hydrocephalus, 1× exophthalmos, 2× visual disturbance. Treatment: 5× microsurgery, 30× embolisation, 1× radiosurgery, 46× embolization and microsurgery, 33× embolization and radiosurgery, 1× conservative management. Results: 16× AVM not obliterated, 72× obliteration confirmed by DSA, 9× obliteration suspected but no DSA, 19× treatment underway. Complications: 58× none, 10× hemorrhage, 36× ischemia, 12× hemorrhage and ischemia. Sequelae: 7× none, 32× transient deficit, 19× permanent defi-

cit. Outcome: 52× mRS 0, 37× mRS 1, 18× mRS 2, 4× mRS 3, 1× mRS 4, 1× mRS 5, 1× missing, 2× mRS 6—their AVMs were not obliterated and they died during the following course from AVM hemorrhages.

Conclusion: The treatment of pediatric brain AVMs follows individualized concepts. The treatment of macrofistulas is straightforward. For large plexiform AVMs a combination of different treatment modalities is used. The complication rate is mainly determined by the localization of the AVM nidus.

Artificial Intelligence/Radiomics

132

Classification of Glioma Subtypes in ADC-map based diffusion MRI—a faster diagnostic approach?

Nils Christoph Nüßle^{*1}, Johann Hempel², Jens Schittenhelm³, Ulrike Ernemann⁴, Uwe Klose⁵

¹Universitätsklinik Tübingen; Department Radiologie; Abteilung für Diagnostische und Interventionelle Neuroradiologie, Tübingen, Deutschland, Tübingen, Deutschland

²Universitätsklinikum Tübingen, Tübingen

³Universitätsklinik Tübingen, Institut für Neuropathologie, Tübingen, Deutschland

⁴Universitätsklinikum Tübingen, Radiologische Klinik, Abteilung für Diagnostische und Interventionelle Neuroradiologie, Tübingen, Deutschland

⁵Universitätsklinik Tübingen, Department Radiologie, Abteilung für Diagnostische und Interventionelle Neuroradiologie, Tübingen, Deutschland

Purpose: Gliomas are the most common primary cerebral tumors. Fast diagnoses including accurate grading are important for the decision on appropriate therapies. The purpose was to assess the diagnostic performance of ADC-values from two high-b-value measurements in the pre-operative *in vivo* assessment of gliomas.

Methods: 97 patients with suspected glioma underwent pre-operative MRI including DWI with 6 b-values up to 2500 s/mm², 2 averages, 6 directions. Signals were averaged over all directions. 9 different ADC-maps from pairs of two b-values were calculated (Five using b0 and four using b500 as a reference). Mean Kurtosis (MK)- and Mean Diffusivity (MD)-maps were calculated from all acquired data. Entire tumor volume was manually delineated on the FLAIR-images on multiple slices. These VOIs were transferred to the ADC-, MK- and MD-maps and mean values of the tumor subtypes were compared.

Results: MK-analysis delivered best results using all six measured b-values ($p \leq 0.001$).

Results of the MD evaluation were significant, when leaving out the b-value of 0 s/mm² ($p \leq 0.01$).

Two b-value dependent ADC-map based evaluation showed great potential in separating the three diagnosis groups and statistically highly significant differences between the groups were demonstrated ($p \leq 0.001$).

Conclusion: Using only two b-values, the acquisition time can be reduced by 66%, while results remain comparable to MK-evaluation.

Findings underline the hypothesis, that different glioma subtypes seem to show differences in DWI.

ADC-map based evaluation of glioma in DWI provides great potential in pre-interventional diagnosing of glioma subtypes. Further investigations, using higher b-values, may provide even higher diagnostic accuracy.

Fig. 1 FLAIR- and DW-Images of histopathologically confirmed GBM-patient. Unmodified FLAIR, FLAIR with drawn in tumor region and ADC-map (based on b0 and b2500), reshaped to the matrix of the FLAIR-images, with transferred tumor region

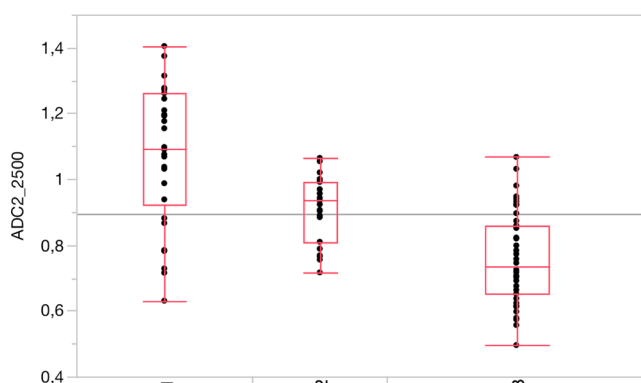
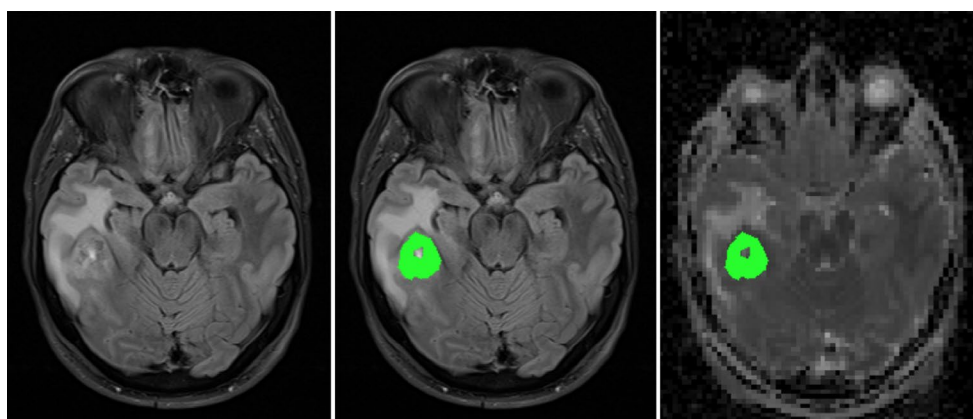


Fig. 2 Distribution of the mean ADC-values using b500 and b2500, classified to the three groups (1=Astrocytoma, 2=Oligodendroglioma, 3=GBM)

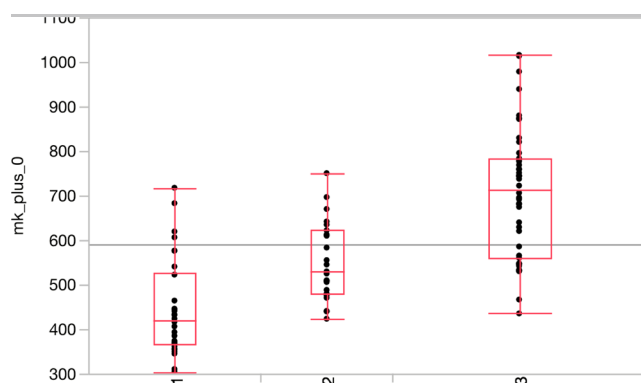


Fig. 3 Distribution of the mean kurtosis using all measured b-values from 0 s/mm² to 2500 s/mm², classified to the three groups (1=Astrocytoma, 2=Oligodendroglioma, 3=GBM)

162

Performance of a state-of-the art deep learning model for automated detection and segmentation of biopsy-proven meningiomas using multiparametric MRI

Kai Roman Laukamp^{*1}, Frank Thiele², Georgy Shakirin³, David Zopfs⁴, Marco Timmer⁵, Andrea Faymonville⁶, David Maintz⁷, Michael Perkuhn⁸, Jan Borggrefe⁹

¹University Hospitals Cleveland Medical Center, Department of Radiology, Cleveland, Oh, USA, Case Western Reserve University, Department of Radiology, Cleveland, Oh, USA, Department of Radiology, University of Cologne, Cologne, Germany, Cleveland, United States

²Institute for Diagnostic and Interventional Radiology, Cologne, Deutschland

³Institute for Diagnostic and Interventional Radiology, Research Aachen, Cologne, Deutschland

⁴Uniklinik Köln; Abteilung für Radiologie und Neuroradiologie; Institut für Diagnostische und Interventionelle Radiologie, Köln, Deutschland, Köln, Deutschland

⁵Allgemeine Neurochirurgie, Uniklinik Köln, Klinikum der Universität zu Köln; Zentrum für Neurochirurgie; Klinik für Allgemeine Neurochirurgie, Köln, Deutschland

⁶Neurochirurgie

⁷Institut F. Diagnos. U. Intervent. Radiologie, Köln, Deutschland

⁸Institute for Diagnostic and Interventional Radiology, Philips Research Aachen, Cologne, Deutschland

⁹Universität zu Köln, Institut für Diagnostische und Interventionelle Radiologie, Köln, Deutschland

Purpose: Volumetric assessment of meningiomas is highly relevant for therapy planning and monitoring. We used a multiparametric deep-learning-model on routine MR data including images from referring institutions to investigate performance in automated detection and segmentation of meningiomas in comparison to manual segmentations.

Methods: 56 of 136 consecutive preoperative MR datasets (T1-/T2-weighted, T1-weighted contrast-enhanced [T1CE], FLAIR) of meningiomas treated surgically at the University Hospital Cologne and graded histologically as tumor grade I ($n=38$) or II ($n=18$) were included. The DLM was trained on an independent dataset of 249 glioma cases and segments different tumor parts as defined in the brain tumor image segmentation-benchmark (BRATS-benchmark). The DLM was based on DeepMedic-architecture. Results were compared to manual segmentations by two radiologists in a consensus reading in FLAIR and T1CE. **Results:** The DLM detected meningiomas in 55 of 56 cases. Further, automated segmentations correlated strongly with manual segmentations: average Dice-coefficients were 0.81 ± 0.10 (range: 0.46–0.93) for the total tumor volume (union of tumor volume in FLAIR and T1CE) and 0.78 ± 0.19 (range: 0.27–0.95) for contrast enhancing tumor volume in T1CE.

Conclusion: The DLM yielded accurate automated detection and segmentation of meningiomas despite diverse scanner data and thereby may improve and facilitate therapy planning and monitoring of this highly frequent tumor entity.

Predicting Conversion from Clinically Isolated Syndrome to Multiple Sclerosis—A MRI Feature Based Machine Learning Approach

Haike Zhang^{*1}, Claus Zimmer², Mark Mühlau³, Esther Alberts⁴, Viola Pongratz⁵, Benedikt Wiestler⁶, Paul Eichinger⁷

¹Abteilung für Neuroradiologie, Klinikum Rechts der Isar, TU München, München, Deutschland

²Klinikum Rechts der Isar der TUM, Technische Universität München, Abteilung für Diagnostische und Interventionelle Neuroradiologie, München, Deutschland

³Klinikum Rechts der Isar, Neurologie, München, Deutschland

⁴Klinikum Rechts der Isar, Technische Universität München, Abteilung für Diagnostische und Interventionelle Neuroradiologie, München, Deutschland

⁵Abteilung für Neurologie, Klinikum Rechts der Isar

⁶Neuroradiologie, TU München, München, D

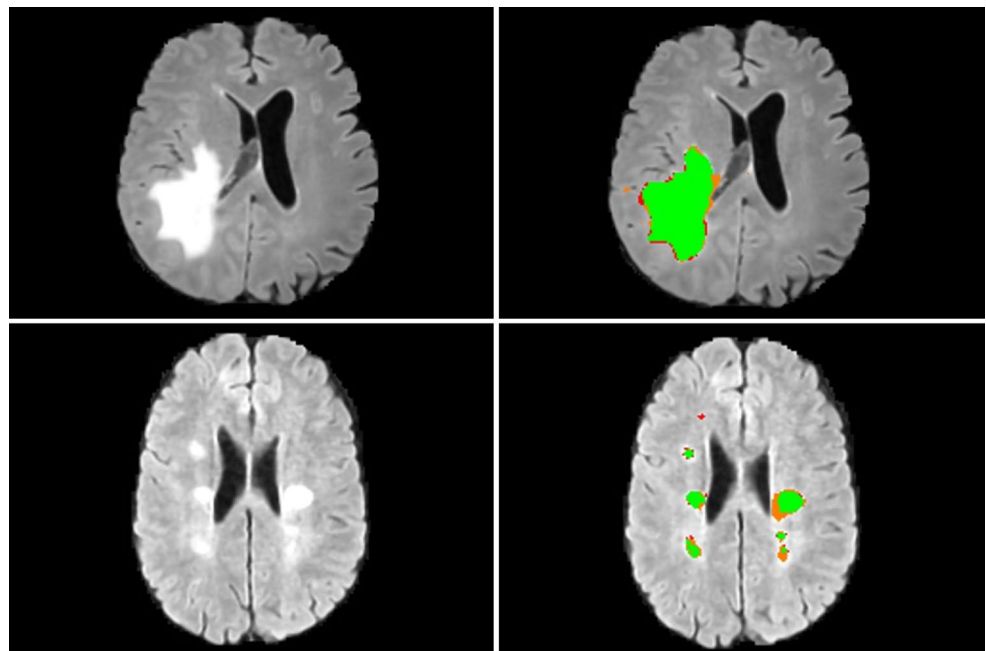
⁷Abteilung für Diagnostische und Interventionelle Neuroradiologie, Klinikum Rechts der Isar, TU München, München, Deutschland

Purpose: MRI plays a central role in establishing the diagnosis of Multiple Sclerosis (MS). We hypothesized that studying MRI features of the lesions such as shape and brightness in the baseline scan of patients with a Clinically Isolated Syndrome (CIS) may predict conversion into MS.

Methods: We performed a single centre analysis of a prospective cohort of 84 CIS patients, who were followed-up for at least 3 years. Conversion into definite MS was defined according to the 2010 McDonald criteria, i. e. encompassed clinical and radiological criteria. Lesions in 3D FLAIR and 3D T1 images were segmented semi-automatically. Shape and brightness features were automatically calculated from these masks and input into an oblique random forest machine learning model (RFM). Prediction accuracies were validated through a three-fold cross-validation.

Results: 66 patients converted to MS and prediction of (non-)conversion was correctly in 71 patients in an RFM based on shape features. Brightness features did not improve the model's performance. This predictor was significantly more accurate than predicting with Barkhof's criteria ($p < 0.001$, McNemar's test) with a sensitivity of 94% and specificity of 50% (85% and 28% respectively for Barkhof's criteria).

Fig. 1 Example of a glioblastoma (top) and MS segmentation (bottom). Green delineates a “true positive” segmentation, orange is “false positive” and red is “false negative”



Conclusion: Our study shows that MRI shape parameters of lesions can contribute to predicting the future course of CIS patients more accurately.

Learning what's normal: Deep-learning human brain anatomy for unsupervised anomaly delineation in MR images

Christoph Baur¹, Nassir Navab¹, Claus Zimmer², Shadi Albarqouni¹, Benedikt Wiestler^{*3}

¹Camp, TU München

²Neuroradiologie, TU München

³Neuroradiologie, TU München, München, D

Purpose: Truly unsupervised image analysis (i. e. without human input) is an exciting field of research in modern (neuro)radiology. To this end, reliable detection of pathological findings is a pivotal, yet until now unreached first step.

Methods: We leveraged recent Unsupervised Deep Learning techniques, i. e. Variational Autoencoders (AE) and adversarial training, to learn to compress and faithfully reconstruct 3D-FLAIR images of healthy human brain anatomy. When feeding the trained model with an image containing pathologies, it reconstructs a healthy version of the image, such that anomalies can be detected by subtracting the reconstruction from the input. To test this pipeline, we analyzed images of patients with Multiple Sclerosis (typically many small lesions) and Glioblastoma (large lesions with mass effect), diseases the network has never seen during training.

Results: Mean Dice scores for both diseases were in the range of state-of-the-art unsupervised segmentation strategies: 0.68966 for Multiple Sclerosis and 0.67679 for Glioblastoma (examples in **Fig. 1**). For the different diseases, different levels of compression were found to significantly influence the segmentation scores.

Conclusion: The network architecture we present is capable of faithfully reconstructing “normal” brain anatomy and thereby detecting pathologies the network has never seen before. This approach has great potential to advance the field of machine-driven, unsupervised image analysis.

Impact of Different Reconstruction Algorithms and Different Slice Thickness on Automated Stroke Software Tool to Detect Early Ischemic Changes

Friederike Austein^{*1}, Nora Jürgensen¹, Thomas Lindner¹, Olav Jansen²

¹Klinik für Radiologie und Neuroradiologie, Universitätsklinikum Schleswig-Holstein, Kiel, Deutschland

²Direktor des Instituts für Neuroradiologie, Klinik für Radiologie und Neuroradiologie, Kiel, Deutschland

Purpose: Identifying differences of evaluation of the established 10-point quantitative topographic CT scan score (Alberta Stroke Program Early CT-Score (ASPECTS)) for the detection of early ischemic changes by an automated computational software tool using different advanced reconstruction algorithms for brain CT (knowledge-based iterative algorithm (IMR) and standard iterative reconstruction (IR)) with different slice thicknesses.

Methods: We enrolled 50 patients with advanced CT (including native CT, CT-angiography and CT-perfusion) indicated by suspected acute stroke in the anterior circulation. We reconstructed axial images with IR and IMR using different slice thicknesses. CT-perfusion, follow-up

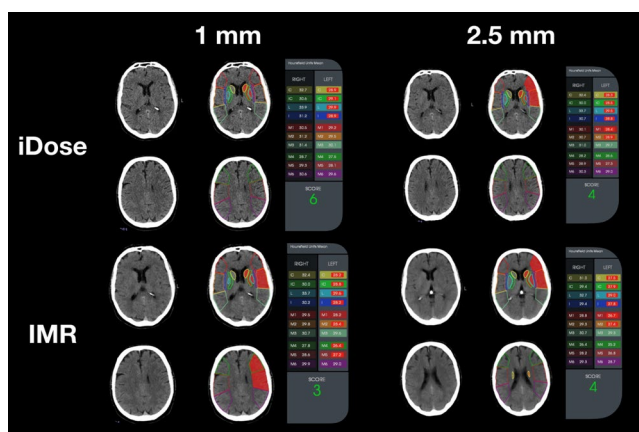


Fig. 1

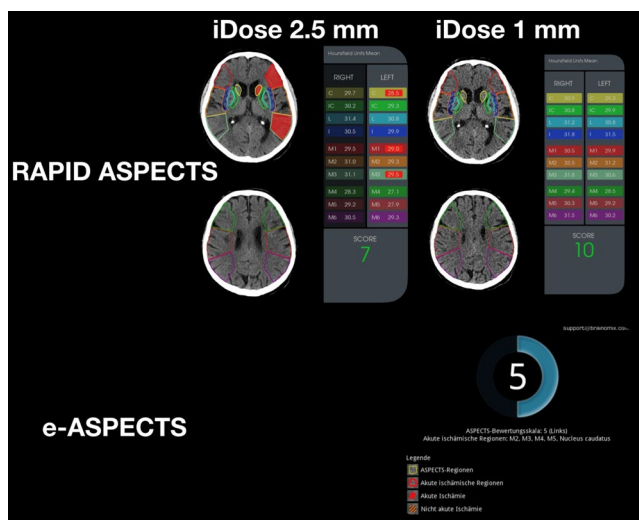


Fig. 2

scans and the evaluation of the radiologists served as ground truth to determine the definite infarct area. This retrospective study was approved by our ethics committee.

Results: The preliminary results showed that the automated ASPECT results were significantly influenced by reconstruction algorithms and slice thicknesses (Figures).

Conclusion: Automated stroke CT evaluation appears to be significantly influenced by the reconstruction algorithm and slice thickness which could lead to differences in therapeutic decision-making. Further research is necessary for standardization of reconstruction and optimal slice thickness to apply the automated stroke CT in more daily clinical use.

234

Automated brain extraction of multi-sequence MRI in brain tumor patients using artificial neural networks

Irada Tursunova^{*1}, Marianne Schell¹, Fabian Isensee², Antje Wick³, Wolfgang Wick³, Martin Bendszus¹, Klaus Maier-Hein², Philipp Kickingereder⁴

¹University Hospital Heidelberg- Dep. of Neuroradiology

²German Cancer Research Center (Dkfz)—Division of Medical Image Computing

³University Hospital Heidelberg- Dep. of Neurology

⁴University Hospital Heidelberg- Dep. of Neuroradiology, Heidelberg, Deutschland

IT, MS and FI contributed equally

Purpose: To develop an artificial neural network (ANN) that allows automated brain extraction from multi-sequence MRI in patients with brain tumors.

Methods: We used MRI data of patients with recurrent glioblastoma from a prospective randomized phase II and III trial (EORTC 26101 study) with 2495 examinations of 590 patients from 37 centers in Europe. Data included pre- and postcontrast T1 (T1/cT1), FLAIR and T2-weighted images ($n=10005$ individual sequences) and ground-truth brain mask segmentations. The developed ANN was trained with all MRI sequences using 2/3 of the data in a 5-fold cross-validation and tested on the remaining data. We report averages of evaluation metrics for each sequence (Hausdorff distance and DICE scores) for the test set and compared the performance (only for the T1 sequence) with standard brain extraction algorithms including 3dSkullStrip, BEaST, BSE, OptiBET and ROBEX.

Results: Wilcoxon signed-rank tests on T1 revealed significant higher performance of our ANN (medians: HD, 2.76; DICE, 0.98) on brain extraction over all competing common software packages (medians: HD, 5.43–24.38; DICE, 0.89–0.95; $p<0.001$, each). Moreover, quantitative metrics demonstrate excellent performance of the brain extraction across all MRI sequences (medians: HD, 2.74–4.38; DICE, 0.96–0.98) (see Fig. 1).

Conclusion: The developed ANN allows reliable and automated brain extraction and overcomes limitations of existing brain extraction algorithms since it is applicable to all standard anatomical sequences and acts robust in the presence of pathological alterations.

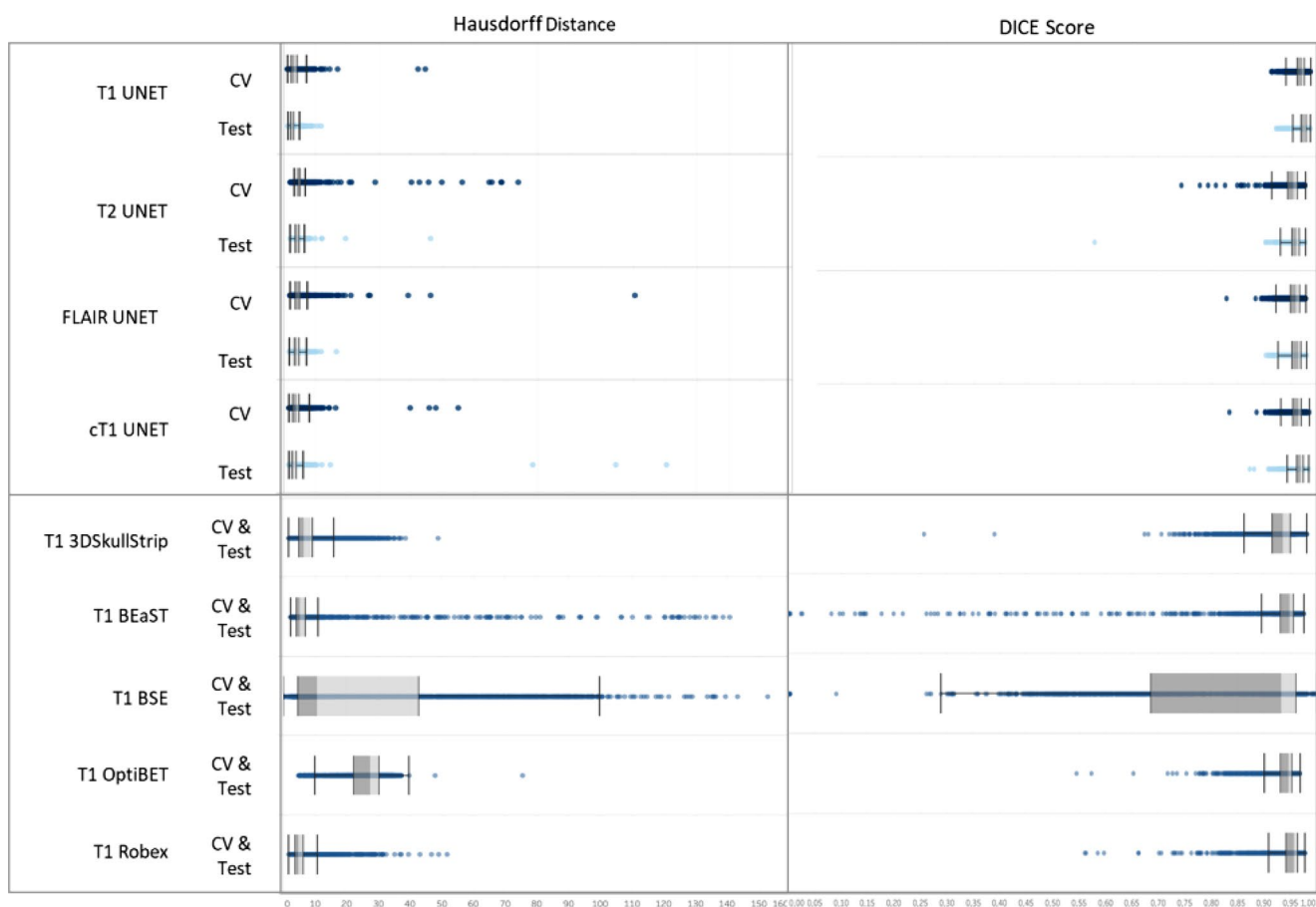


Fig. 1

237

Performance of a deep learning algorithm for automated detection of intracranial aneurysms from non-invasive brain imaging

Thorsten Sichtermann^{*1}, Anton Faron², Rik Sijben¹, Nikolas Teichert³, Jessica Freiherr¹, Martin Wiesmann¹

¹Department of Diagnostic and Interventional Neuroradiology, RWTH University Hospital Aachen, Aachen, Deutschland

²Department of Diagnostic and Interventional Neuroradiology, RWTH University Hospital Aachen, Department of Radiology, University Hospital Bonn, Aachen, Deutschland

³Department of Diagnostic and Interventional Neuroradiology, Moorenstr. 5, 40225 Düsseldorf, Germany, Deutschland

Purpose: Rupture of an intracranial aneurysm is a serious incident causing subarachnoid hemorrhage associated with high fatality and morbidity rates. Detection of an intracranial aneurysm is a challenging task even for experienced radiologists. Therefore, a sufficient system for automated detection of intracranial aneurysms may be expedient.

Methods: Within a retrospective study, we established a pipeline, based on a neural network, for the detection of intracranial aneurysms from 3D time-of-flight (TOF) MRI data. Eighty-five datasets of patients with a total of 115 intracranial aneurysms were obtained to train, validate and test the performance of the model via fivefold cross-validation. Sensitivity and false positives per case were determined for different pre- and postprocessing.

Results: The highest mean sensitivity of our system for the detection of intracranial aneurysms was 90% with a sensitivity of 94% for aneurysms with a diameter larger than 3 mm and 97% for aneurysms larger than 5 mm. Best location-dependent performance was measured for aneurysms located in the posterior circulation. By integrating a detection threshold, a distinct reduction of false positives could be achieved. Our findings further suggest that skull stripping and N4 bias correction contribute to the performance of the system.

Conclusion: Our system based on a deep-learning convolutional network can detect intracranial aneurysms with a high sensitivity from 3D TOF MRI data.

241

Automatic detection of Focal Cortical Dysplasias (FCD) by morphometric MRI analysis and supervised machine learning

Horst Urbach^{*1}, Linda Rubensdörfer², Hansjörg Mast³, Shan Yang⁴, Ralf Schwarzwald⁵, Judith Kröll-Seger⁶, Hans-Jürgen Huppertz⁷

¹Universitätsklinikum Freiburg, Klinik für Neuroradiologie, Freiburg, Deutschland

²Department of Neuroradiology, Medical Center—University of Freiburg, Faculty of Medicine, University of Freiburg, Germany, Freiburg, Deutschland

³Universitätsklinikum Freiburg, Klinik für Neuroradiologie, Freiburg Im Breisgau, D

⁴Universitätsklinikum Freiburg, Klinik für Neuroradiologie, Freiburg, D

⁵Universitätsklinikum Freiburg, Freiburg

⁶Swiss Epilepsy Clinic, Klinik Lengg AG, Zürich, Ch

⁷Schweizerische Epilepsie-Klinik, Medizinische Bildverarbeitung, Zürich, Switzerland

Purpose: Focal cortical dysplasias (FCD) as the most common resected epileptogenic lesions in children and the third most common lesions in adults are often subtle and overlooked on MRI. Purpose of this study was to evaluate whether these lesions can be fully automatically detected.

Methods: A convolutional neuronal network (CNN) with 1 hidden layer and 5 neurons was fed with 15 input maps resulting from segmentation and morphometric analysis of an MPRAGE sequence with 1 mm³ isotropic voxels. MRI data of 97 patients with manually segmented FCDs and 363 healthy controls were cross-validated to train and test the CNN. The algorithm was applied to a series of 25 patients with FCD type 2.

Results: 22 of 25 FCDs were fully automatically detected (sensitivity, 88%). In three false-negative patients, the FCDs were visualized on the junction and FLAIR images, however one FCD was overlooked on the FLAIR sequence. False positive findings required a careful correlation of FLAIR and output maps of the CNN

Conclusion: A simple convolutional neuronal network aids in the detection of FCD. Further refinements to reduce false positive findings would be beneficial.

243

Automatic detection of FCDs by morphometric analysis and supervised machine learning: Comparison of MPRAGE and MP2RAGE-based analysis

Horst Urbach^{*1}, Linda Rubensdörfer², Hansjörg Mast³, Shan Yang⁴, Ralf Schwarzwald⁵, Hans-Jürgen Huppertz⁶

¹Universitätsklinikum Freiburg, Klinik für Neuroradiologie, Freiburg, Deutschland

²Department of Neuroradiology, Medical Center—University of Freiburg, Faculty of Medicine, University of Freiburg, Germany, Freiburg, Deutschland

³Universitätsklinikum Freiburg, Klinik für Neuroradiologie, Freiburg Im Breisgau, D

⁴Universitätsklinikum Freiburg, Klinik für Neuroradiologie, Freiburg, D

⁵Universitätsklinikum Freiburg, Freiburg

⁶Schweizerische Epilepsie-Klinik, Medizinische Bildverarbeitung, Zürich, Switzerland

Purpose: Focal cortical dysplasias (FCD) as the most common resected epileptogenic lesions in children and the third most common lesions in adults are often subtle and overlooked on MRI. Purpose of this study was to evaluate whether the fully automatic detection can be improved using MP2RAGE sequences enabling an intrinsic correction of B1-inhomogeneities.

Methods: MPRAGE and MP2RAGE data sets were acquired in a consecutive series of 212 epilepsy patients. A supervised convolutional neuronal network (CNN) with 1 hidden layer and 5 neurons was fed with 15 input maps resulting from segmentation and morphometric analysis of MPRAGE or MP2RAGE sequences. Output maps were compared with respect to the size of true positives and the number and size of false positives

Results: 8 FCDs were fully automatically detected. In all cases, the size of true positives in the CNN output maps was larger on the MP2RAGE- compared to the MPRAGE-based analysis.

Conclusion: MP2RAGE-based analysis creates clearer output maps than MPRAGE-based analysis. This might be the result of better inhomogeneity correction.

301

Supervised ensemble classifier of preoperative network characteristics predicts postoperative visual field deficit after selective amygdalahippocampectomy

Theodor Rüber^{*1}, Bastian David², Jasmine Salomé Eberle³, Daniel Delev⁴, Jennifer Gaubatz⁵, Conrad Prillwitz⁵, Bernd Weber¹, Bettina Wabbels⁶, Johannes Schramm⁷, Christian Elger⁵, Elke Hattingen⁸

¹Universitätsklinikum Bonn, Klinik für Epileptologie, Bonn, Deutschland

²Universitätsklinikum Bonn, Epileptologie, Klinik für Epileptologie, Bonn, Deutschland

³Universitätsklinik Bonn, Klinik für Epileptologie, Bonn, Deutschland

⁴Universitätsklinik Bonn, Klinik für Neurochirurgie, Deutschland

⁵Universitätsklinik Bonn, Klinik für Epileptologie

⁶Universitätsklinik Bonn, Universitätsaugenklinik

⁷Universitätsklinikum Bonn, Klinik für Neurochirurgie, Bonn, Deutschland

⁸Institut für Neuroradiologie, Frankfurt/Main, Deutschland

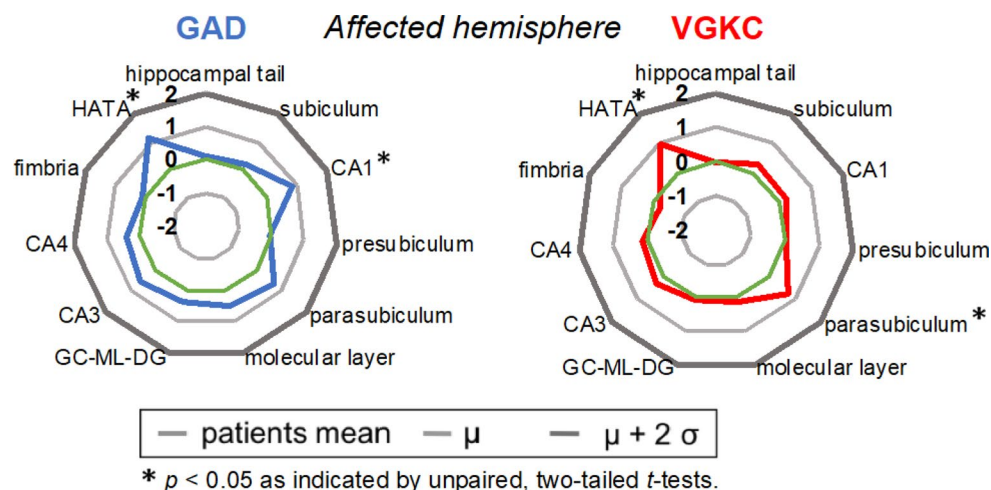
Purpose: Selective amygdalahippocampectomy (sAH) is an effective treatment for patients with therapy-refractory temporal lobe epilepsy, but may cause contralateral superior visual field defect (VFD) in more than half of the cases. Whereas Diffusion Tensor Imaging (DTI) studies have demonstrated postoperative correlates of VFD, preoperative imaging predictors of VFD have not yet been found. Here, we aimed to predict postoperative VFD using ensemble machine learning on preoperative brain graphs (1) and to determine neuronal correlates of VFD severity (2).

Methods: 28 patients (15 females, mean age \pm SD: 38.8 \pm 12.8) with therapy-refractory temporal lobe epilepsy underwent Goldmann perimetry as well as MRI including T1-MPRAGE and DTI prior to and after (2–21 months) sAH. To predict postoperative VFD (1), we inserted a preoperative DTI-based subnetwork of the lesioned hemisphere into a supervised ensemble learning technique combining tree-based classifiers with an artificial neural network. Neuronal correlates of the VFD were analyzed (2) employing a tractography-based region of interest analysis.

Results: (1) Using preoperative network characteristics only, the ensemble classifier was able to predict postoperative VFD (Precision = 95.45%, Recall = 95.45%, Accuracy = 93.10%). (2) Tractography-based analysis of the optic radiation yielded a significant correlation between diffusivity parameters of the ipsilesional sagittal stratum and VFD severity.

Conclusion: We demonstrated that the postoperative VFD after sAH can be reliably predicted based on preoperative imaging data only. The regional postoperative correlate of VFD severity in the optic radiation may emphasize the functional importance of this region.

Fig. 1



303

Volume alterations of hippocampus subfields in patients with antibody-associated limbic encephalitis may be used to predict serogroup

Theodor Rüber^{*1}, Leon Ernst², Bastian David³, Irene Domínguez⁴, Jennifer Gaubatz², Bernd Weber¹, Albert J. Becker⁵, Christian Elger², Elke Hattingen⁶

¹Universitätsklinikum Bonn, Klinik für Epileptologie, Bonn, Deutschland

²Universitätsklinikum Bonn, Klinik für Epileptologie

³Universitätsklinikum Bonn, Epileptologie, Klinik für Epileptologie, Bonn, Deutschland

⁴Uniklinik Bonn, Klinik für Epileptologie, Klinik für Epileptologie, Bonn, Deutschland

⁵Universitätsklinikum Bonn, Institut für Neuropathologie, Sektion für Translationale Epilepsieforschung, Bonn, Deutschland

⁶Institut für Neuroradiologie, Frankfurt/Main, Deutschland

Purpose: Limbic encephalitis (LE) is an autoimmune syndrome defined by clinical, pathological and radiological criteria and often involves temporal lobe epilepsy. We hypothesized to find serospecific volume alterations of hippocampal subfields and aimed to build a machine learning classifier which could differentiate between serogroups. **Methods:** T1-MPRAGE scans of 23 patients with GAD-associated LE (mean age: 34.2 y), of 25 patients with VGKC-complex-associated LE (mean age: 59.5 y), both within two years after seizure onset, and of 48 matched healthy controls were retrospectively collected and parcellation of hippocampal subfields was performed using FreeSurfer. Volumes of hippocampal subfields were inserted into a decision tree classifier.

Results: Serospecific volume alterations of hippocampal subfield were found in the affected hemisphere after data was regrouped according to the lateralization in EEG (see figure 1). Using imaging data only, the decision tree classifier was able to differentiate between the two serogroups (sensitivity >80%, specificity >80%).

Conclusion: Since several studies indicate a direct link between the CA1 area in the human hippocampus and remote autobiographical memory retrieval, the predominant affection of CA1 found may constitute the structural correlate of autobiographical memory deficits often associated with GAD-autoantibody positive LE. The configuration of hippocampal subfields may be employed as a serospecific imaging biomarker of LE.

306

Evaluation of Conventional Automated and Volume Weighted ASPECTS vs CT Perfusion Core Volume to Predict the Final Infarct Volume after Successful Thrombectomy

Friederike Austein¹, Antonia Carlotta Fischer^{*2}, Nora Jürgensen¹, Olav Jansen³

¹Klinik für Radiologie und Neuroradiologie, Universitätsklinikum Schleswig-Holstein, Kiel, Deutschland

²Klinik für Radiologie und Neuroradiologie, Universitätsklinikum Schleswig-Holstein, Deutschland

³Direktor des Instituts für Neuroradiologie, Klinik für Radiologie und Neuroradiologie, Kiel, Deutschland

Purpose: Comparing automated conventional and volume weighted Alberta Stroke Program Early CT score (ASPECTS) to CT perfusion core volume in order to predict the final infarct volume (FIV) in acute ischemic stroke (AIS) patients after successful thrombectomy.

Methods: Patients with AIS and large vessel occlusion who achieved TIC1 2b or 3 reperfusion grade were included. Automated conventional and volume weighted ASPECT scores of the baseline CT were determined with e-ASPECTS software (Brainomix, Oxford, UK). Additionally, we used RAPID software (iSchemaView, Stanford, USA) to analyze the CT perfusion core volume.

Results: We included 119 patients. Mean \pm SD values for automated conventional ASPECTS, volume weighted ASPECTS, CT perfusion core volume and FIV were 6.4 ± 2.6 , $16.4 \text{ mL} \pm 15.4$, $18.3 \text{ mL} \pm 24.6$ and 70.0 ± 99.6 . CTP core showed a higher correlation with FIV $r=0.4$ (CI 95% 0.293; 0.497, $P<0.0001$) than automated conventional ASPECTS ($r=-0.209$, CI 95% -0.323 ; -0.089 , $P=0.002$) and volume weighted ASPECTS ($r=0.185$ CI 95% 0.065; 0.300, $P=0.003$).

Conclusion: In the setting of successful thrombectomy, CTP core volume is a better predictor of FIV than either automated conventional or volume weighted ASPECTS.

Discordant and converting receptor expressions in brain metastases from breast cancer: Radiomics based non-invasive receptor status prediction

Helge Kniep^{*1}, Frederic Madesta², Tanja Schneider³, Jens Fiehler⁴, Matthias Bechstein¹, Tobias Gauer², René Werner⁵, Susanne Gellissen¹

¹Klinik und Poliklinik für Neuroradiologische Diagnostik und Intervention, Universitätsklinikum Hamburg-Eppendorf, Hamburg, Deutschland

²Klinik für Strahlentherapie und Radioonkologie, Universitätsklinikum Hamburg-Eppendorf, Hamburg, Deutschland

³-, -, Hamburg, Deutschland

⁴Diagnostikzentrum Univ.-Klinikum Hamburg-Eppendorf, Klinik und Poliklinik für Neuroradiologische Diagnostik und Intervention, Hamburg, Deutschland

⁵Institut für Computational Neuroscience, Universitätsklinikum Hamburg-Eppendorf, Hamburg, Deutschland

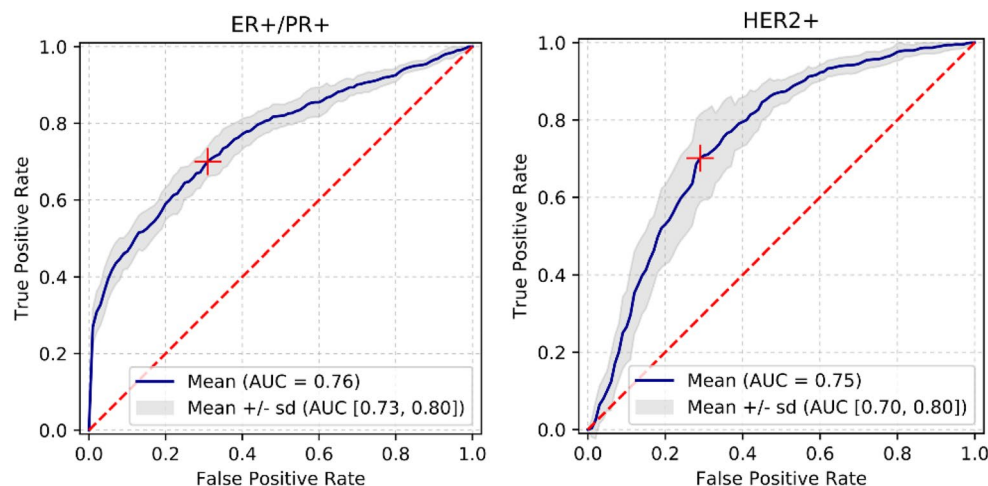
Purpose: Discordance and conversion of receptor expressions in metastatic lesions and primary tumors is often observed in patients with brain metastases from breast cancer. Therefore, personalized therapy requires continuous monitoring of receptor expressions and dynamic adaptation of applied targeted treatment options. Radiological in-vivo techniques may allow receptor status tracking at high sampling rates, low risk and cost. The present study investigates the potential of receptor status prediction in a machine learning approach. We hypothesized that radiomic features of standard of care MR images can be used to predict the receptor status of brain metastases.

Methods: The analysis includes 143 brain metastases from 37 patients with breast cancer (Fig. 1). 1423 quantitative features of T1 contrast-enhanced, T1 native and FLAIR images and basic clinical data

Receptor status	# of metastases
PR+ and/or ER+	20
HER2+	22
PR+ and/or ER+ and HER2+	62
Tripple negative	39
Total	143

Fig. 1 Histologically confirmed receptor expression in the study cohort

Fig. 2 ROC AUCs of validation data sets for **a** ER+ and/or PR+ metastases and **b** HER2+ metastases



(age, sex) were evaluated utilizing random forest algorithms with 5-fold model-external cross-validation.

Results: ROC AUCs of the validation sets were 0.76 for PR+/ER+ and 0.75 for HER2+, all P-values <0.001 (Fig. 2). Sensitivities and specificities reached 70% for both receptor expressions.

Conclusion: Quantitative features of standard of care MR images provided high discriminatory accuracy in predicting the receptor status of brain metastases from breast cancer. The approach could allow receptor expression tracking at high sampling rates and may support agile treatment optimization for more effective therapies.

Assessment of intracranial collaterals on CT-angiography: comparison of human readers versus a fully automated computer-based algorithm

Johannes Pfaff^{*1}, Fatih Seker², Simon Nagel³, Peter Arthur Ringleb⁴, Martin Bendszus⁵, Christian Herweh⁶

¹Universitätsklinikum Heidelberg, Abteilung für Neuroradiologie, Abteilung für Neuroradiologie, Heidelberg, Deutschland

²Universitätsklinikum Heidelberg, Neuroradiologie, Heidelberg, Deutschland

³Universitätsklinikum Heidelberg, Neurologische Klinik, Neurologie, Heidelberg, Deutschland

⁴Universitätsklinikum Heidelberg, Neurologische Klinik, Sektion Vaskuläre Neurologie, Heidelberg, Deutschland

⁵Universitätsklinikum Heidelberg, Abteilung für Neuroradiologie, Heidelberg, Deutschland

⁶Neurologische Klinik/Abteilung für Neuroradiologie, Abteilung für Neuroradiologie, Heidelberg, Deutschland

Purpose: Assessment of intracranial collaterals is prone to interrater variability. We compared the performance of a computer-based algorithm with those of experienced neuroradiologists.

Methods: Single-phase CT angiography scans of acute stroke patients were retrospectively scored by the algorithm, two blinded neuroradiologists and two expert readers with full access to clinical and additional imaging information, providing the ground truth. Collaterals were scored according to Tan et al. and additionally for each cortical ASPECTS region (M1-6 & insula) on a three-point scale: no collaterals (=0) vs. 0–50% (=1) vs. >50% (=2), compared to the contralateral side, respectively, resulting in a score between 0 and 14 (“full collaterals”). We also derived a two-point scale by merging previous categories 0 and 1 resulting in a 7-point score (“good collaterals”). Intra-class-correlation-coefficients (ICC) were calculated.

Results: 235 patients with Carotid-T, M1- or M2-occlusion were analyzed. Median Tan score was 2 for all raters and ICC values between the algorithm and readers vs. ground truth were 0.793 (0.73–0.84), 0.829 (0.78–0.87) and 0.798 (0.74–0.84) (all $p < 0.001$). Median “full collateral” and “good collateral” scores were similar among human readers and the algorithm (11, 8 and 9, respectively 4, 2 and 3). ICC between readers and the algorithm vs. ground truth were 0.859 (0.82–0.89), 0.868 (0.83–0.9) and 0.819 (0.76–0.86) for “full collaterals” and 0.853 (0.81–0.87), 0.824 (0.77–0.86) and 0.826 (0.77–0.87) for “good collaterals” (all $p < 0.001$).

Conclusion: Fully automated evaluation of intracranial collaterals in acute ischemic stroke patients was in excellent agreement with human readers and the ground truth.

388

Development and multi-center validation of an automated MS reporting software

Benedikt Wiestler^{*1}, Benjamin Bender², Ulrike Ernemann², Claus Zimmer³, Jan Kirschke³, Paul Eichinger³

¹Neuroradiologie, TU München, München, D

²Neuroradiologie, Tübingen

³Neuroradiologie, TU München

Purpose: To facilitate assessment of MS follow-up examinations, we developed a tool for user-independent identification and classification of new or enlarged MS lesions in subtraction images over time.

Methods: To overcome the susceptibility of previous lesion detection approaches to artifacts and misregistrations, our software exploits multi-modal (FLAIR and T1) subtraction images based on non-line-

ar deformable SyN transforms. Lesion classification (periventricular, (juxta)cortical, subcortical, infratentorial) uses the SRI24 atlas which is adapted to the individual patient anatomy using ANTs Atropos. The software was compared in two cohorts from TU Munich (Philips 3T, 33 patients) and Tuebingen (Siemens 1.5 and 3T, 10 patients) against the clinical report.

Results: In the Munich cohort, the software correctly identified 151/164 lesions (92% accuracy), as opposed to a lesion detection accuracy of 72.5% for the clinical report (119/164 lesions). In the second cohort from Tuebingen, 14/15 new or enlarged lesions were detected (93.3% accuracy). The overall false positive rate was 19.5%, mostly easily identifiable artefacts close to the base of the skull. Classification accuracy was high (78.5%, **Fig. 1**).

Conclusion: In a multicenter setting across different MR scanners, our software consistently displays a very high detection and classification accuracy of new/enlarged MS lesions, highlighting the future potential of computer-assisted imaging. To further lessen the false-positive rate, we are currently developing an additional filter using a shape- and location-driven random forest classifier.

397

Fully automated brain segmentation from T1-weighted isotropic MRI scans using deep convolutional neural nets

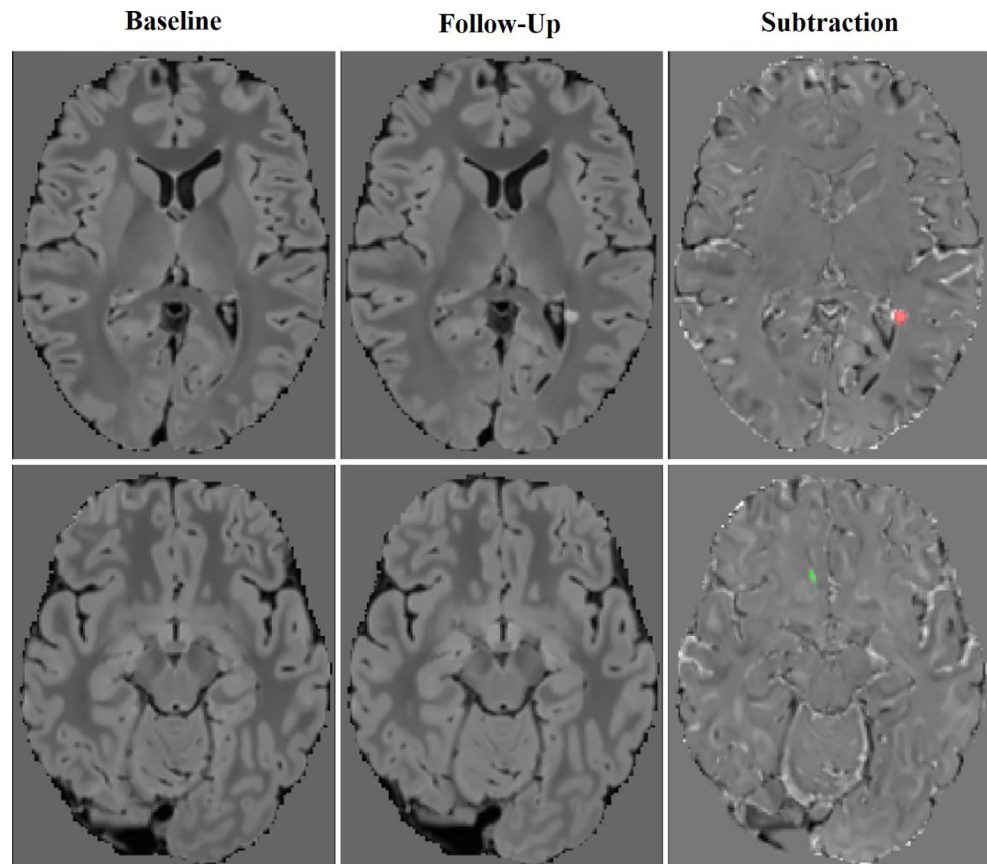
Kirsten Thünemann^{*1}, Olav Jansen², Christian Riedel³

¹UKSH Kiel, Klinik für Radiologie und Neuroradiologie

²Direktor des Instituts für Neuroradiologie, Klinik für Radiologie und Neuroradiologie, Kiel, Deutschland

³University Medical Center Schleswig-Holstein, Department of Neuroradiology, Kiel, Deutschland

Fig. 1 Examples of two lesions identified by the software, and their location-based color-coding. Top row a left periventricular lesion (red), Bottom row, a right (juxta)cortical lesion (green)



Purpose: To investigate, if deep convolutional neural networks can be used to automatically segment brain structures efficiently and accurately enough to be useful for clinical practice.

Methods: 272 T1-weighted isotropic MRI datasets from patients with an age range between 10 and 69 years were collected from our clinical PACS system. Inclusion criteria were high image quality and imaging reported as normal. All isotropic datasets were completely segmented using FreeSurfer. A deep convolutional neural networks with 5 convolutional layers followed by fully connected layers was trained to outline 25 brain structures using FreeSurfer results on 200 MRI datasets. Segmentation quality was subsequently tested using the remaining 72 MRI scans and measured using the Dice overlap score.

Results: While training the deep net required an overall computing time of 8 days, segmentation of the testing MRI scans took an average time of 5 minutes. The median Dice score for all test sets was 0.93 (SD: 0.05). In all 72 datasets, all 25 segmented brain structures were detected with close correlation compared to the reference segmentation using FreeSurfer.

Conclusion: Deep convolutional neural networks can be trained to efficiently and accurately segment brain structures for further volumetric analysis or as a coordinate system for subsequent lesion localization. They segment volumetric MRI scans quickly enough to incorporate them into clinical workflow.

398

Performance of a Deep-Learning Neural Network in Detection of Intracranial Aneurysms from 3D Time-of-flight Magnetic Resonance Angiography Compared to Human Readers

Anton Faron^{*1}, Thorsten Sichtermann², Nikolas Teichert³, Jessica Freiherr², Anastasios Mpotsaris², Martin Wiesmann²

¹Radiologische Universitätsklinik Bonn, Bonn, Deutschland

²Klinik für Diagnostische und Interventionelle Neuroradiologie, Uniklinik RWTH Aachen

³Institut für Diagnostische und Interventionelle Radiologie, Universitätsklinikum Düsseldorf

Purpose: Aneurysm detection might be challenging even for experienced radiologists. We aimed to study the performance of a deep-learning model for detection of aneurysms from cranial imaging compared to that of human readers.

Methods: After approval of the retrospective study by the institutional review board a pipeline for automated aneurysm detection from 3D time-of-flight magnetic resonance angiographies (TOF-MRA) based on the framework DeepMedic was established. Datasets of 85 consecutive patients acquired during clinical routine were obtained to train, validate and test the model via cross-validation. Manual voxel-wise segmentation, based on radiological reports and critical image revision, served as groundtruth. In order to compare the sensitivity to that of human readers, the dataset without annotation was presented to two blinded readers with different levels of experience in the field of diagnostic imaging (2 years, 12 years). Values were compared using Kruskal-Wallis-Test.

Results: Groundtruth consisted of 115 aneurysms with a mean diameter of 7 mm (range: 2–37 mm) and a mean volume of 215 mm³ (range: 6–4518 mm³). Mean overall sensitivities were 88% for the model, 95% for reader 1, and 94% for reader 2. Statistical analysis revealed no significant differences between the model and the readers ($P(\text{all})=0.1$; $P(\text{diameter}>3\text{ mm})=0.94$; $P(\text{diameter}>5\text{ mm})=0.59$).

Conclusion: A deep-learning model can detect aneurysms from TOF-MRA imaging with a sensitivity comparable to that of experienced human readers.

399

Automatic clot detection in NECT images of acute ischemic stroke patients using a convolutional neural network

Paula Kettenberger^{*1}, Olav Jansen², Christian Riedel³

¹UKSH Kiel, Klinik für Radiologie und Neuroradiologie

²Direktor des Instituts für Neuroradiologie, Klinik für Radiologie und Neuroradiologie, Kiel, Deutschland

³University Medical Center Schleswig-Holstein, Department of Neuroradiology, Kiel, Deutschland

Purpose: To investigate, if clots in proximal cerebral arteries can be automatically detected in non-enhanced cranial CT (NECT) images using a deep learning approach.

Methods: Thin slice NECT images of 185 patients with acute ischemic strokes were registered with the CT angiography (CTA) images scanned immediately after the NECT scans. On the CTA images, the contrast gap at the site of occlusion was identified and marked with a 3D region of interest (ROI) ending at the proximal and distal end of the occlusion. A deep convolutional neural network with 3 layers of convolutional filters followed by totally connected layers was trained to identify the region of interest for every patient as copied into the registered NECT images for a total of 150 stroke cases and 100 patients scanned for other reasons and without a predefined ROI. Using the remaining 35 stroke patients and 30 NECT scans taken from non-stroke patients, we measured ROC curves for correct occlusion identification.

Results: The training time for the convolutional neural network was 7 days and 3.5 hours on a standard workstation with a modern high performance graphic card. The average time for a single inference case was 3 minutes and 35 seconds (+/- 45 seconds). The area under the curve for the identification of an occlusion site and its correct position in the test set was found to be 0.893.

Conclusion: Proximal cerebral artery occlusions can be identified on NECT images with high reliability using a pretrained deep convolutional neural network. The fact that the AUC for clot detection does not exceed 0.9 might be explained by the fact that in rather rare cases of intracranial stenoses, a hyperdense artery sign might not be detectable.

412

Identification of acute ischemic stroke patients from NECT images using a capsular network approach

Christian Riedel^{*1}

¹University Medical Center Schleswig-Holstein, Department of Neuroradiology, Kiel, Deutschland

Purpose: To evaluate if a hybrid approach of a convolutional neural network with a shallow capsular network can be trained to reach super-human performance in recognizing early signs of infarction in NECT images of acute ischemic stroke patients.

Methods: We trained a shallow capsular neural network which received inputs from 5 convolutional layers with NECT images of 150 patients with an acute stroke and 150 patients with a different pathological condition. The training used labeling for early signs of infarction derived from CTA-, CTP and subsequent NECT imaging. After training, the ROC curves for correct identification of patients with early signs of infarction were compared to those found by three expert reviewers blinded with respect to the clinical situation for a total of 80 test NECT sets.

Results: The ROC curve for the correct identification of more than one early sign of infarction was found to have an area under the curve of 0.894, whereas the expert reviewers had an AUC between 0.783 and 0.854.

Conclusion: Using the capsular network approach, complex spatial hierarchies in 3D medical images can be used in order to recognize early signs of infarction even with a super-human performance.

425

Deep learning-based imaging classifier for improving differential diagnosis between primary and metastatic brain tumors

Máté Maros^{*1}, Chang Gyu Cho², Alex Förster³, Johannes Böhme⁴, Mohamad Mansour Al-Zghloul⁵, Eva Neumaier Probst⁶, Andreas von Deimling⁷, Miriam Ratliff⁸, Marcel Seiz-Rosenhagen⁹, Daniel Hänggi¹⁰, Christoph Groden¹¹, Holger Wenz¹²

¹Universitätsklinikum Mannheim, Fakultät der Universität Heidelberg, Abteilung für Neuroradiologie, Mannheim, Deutschland

²Abteilung für Neuroradiologie, Universitätsklinikum Mannheim, Med. Fakultät Mannheim der Universität Heidelberg, Mannheim, Deutschland

³Abteilung für Neuroradiologie, Abteilung Neuroradiologie, Mannheim, Deutschland

⁴Universität Heidelberg, Universitätsklinikum Mannheim, Neuroradiologie, Mannheim, Deutschland

⁵Abteilung für Neuroradiologie, Universitätsklinikum Mannheim, Mannheim, Deutschland

⁶Universität Heidelberg, Universitätsmedizin Mannheim, Neuroradiologie, Mannheim, Deutschland

⁷Universitätsklinikum Heidelberg, Neuropathologie, Heidelberg, Deutschland

⁸Universitätsklinikum Mannheim; Neurochirurgische Klinik; Universitätsmedizin Mannheim, Medizinischen Fakultät Mannheim der Universität Heidelberg, Clinical Cooperation Unit Neurooncology, German Cancer Consortium (Dtk), German Cancer Research Center (Dkfz), Mannheim, Deutschland

⁹Neurochirurgische Klinik, Universitätsmedizin Mannheim, Medizinische Fakultät Mannheim, Universität Heidelberg, Mannheim, Deutschland

¹⁰Universitätsklinikum Mannheim, Neurochirurgische Klinik, Universitätsmedizin Mannheim, Medizinischen Fakultät Mannheim der Universität Heidelberg, Mannheim, Deutschland

¹¹Universitätsmedizin Mannheim, Abteilung für Neuroradiologie, Mannheim, Deutschland

¹²Universitätsmedizin Mannheim, Abteilung für Neuroradiologie, Abteilung für Neuroradiologie, Mannheim, Deutschland

Purpose: The solely radiological differentiation between glioblastoma multiforme (GBM) and metastases (META) at the initial diagnosis can be extremely challenging, due to similar imaging morphology and scarce clinical data regarding primary tumor. Here, we investigated the applicability of deep learning-based image classifiers to improve this distinction.

Methods: We retrieved a retrospective cohort of 430 patients including 212 GBMs (119M/93F, mean age 63.8 years, range: 2–92 yrs) and 218 METAs (122M/96F, mean age 61.8 years, range: 23–86 yrs) undergoing cranial magnetic resonance imaging (cMRI) using institutional tumor protocol. MRIs were reassessed by two independent blinded readers. The single most representative transversal FLAIR, DWI, contrast enhanced T1-weighted images were selected and categorized based on histopathological findings ($n=493$, $n_{\text{GBM}}/n_{\text{META}}=216/277$). The cohort was randomly splitted into training- (~75%), validation- (~18%) and test sets (~8%). We used data augmentation techniques and custom modified and fitted a deep convolutional neural networks (CNN)¹ and built an ensemble model using these CNN classifiers.

Results: Despite our lean approach and comparably small data sets the regularized sequence-specific CNNs achieved a training accuracy

of between ~70–90% with a corresponding validation accuracy of 70–75% while the ensemble model provided a test accuracy of ~83%.

Conclusion: Deep learning-based GBM and META differentiation using expert-guided MR-image selection can support neuroradiologists to increase initial diagnostic accuracy.

Reference

1. Simonyan, Karen, and Andrew Zisserman. “Very deep convolutional networks for large-scale image recognition.” arXiv (2014)

437

Radiomics-based shape and texture analyses on multiparametric MR imaging data for grading of biopsy-proven meningiomas

Kai Roman Laukamp^{*1}, Georgy Shakirin², Frank Thiele³, Bettina Baeßler⁴, David Zopfs⁵, Marco Timmer⁶, Andrea Faymonville⁷, Michael Perkuhn⁸, Jan Borggrefe⁹

¹University Hospitals Cleveland Medical Center, Department of Radiology, Cleveland, Oh, USA, Case Western Reserve University, Department of Radiology, Cleveland, Oh, USA, Department of Radiology, University of Cologne, Cologne, Germany, Cleveland, United States

²Institute for Diagnostic and Interventional Radiology, Research Aachen, Cologne, Deutschland

³Institute for Diagnostic and Interventional Radiology, Cologne, Deutschland

⁴Institut für Diagnostische und Interventionelle Radiologie, Köln, Deutschland

⁵Uniklinik Köln; Abteilung für Radiologie und Neuroradiologie; Institut für Diagnostische und Interventionelle Radiologie, Köln, Deutschland, Köln, Deutschland

⁶Allgemeine Neurochirurgie, Uniklinik Köln, Klinikum der Universität zu Köln; Zentrum für Neurochirurgie; Klinik für Allgemeine Neurochirurgie, Köln, Deutschland

⁷Neurochirurgie

⁸Institute for Diagnostic and Interventional Radiology, Philips Research Aachen, Cologne, Deutschland

⁹Universität zu Köln, Institut für Diagnostische und Interventionelle Radiologie, Köln, Deutschland

Purpose: Higher meningioma grades are associated with tumor growth and recurrence. Especially differentiation of low and intermediate grades is challenging, and reliable grading is not established. We applied radiomics-based shape and texture analyses on routine MRI for grading.

Methods: MRI (T1/T2, T1 contrast-enhanced [T1CE], FLAIR, DWI, ADC) of $n=46$ grade I and $n=25$ II non-treated meningiomas with histological work-up were included. Manual segmentations were performed on FLAIR, T1CE and ADC by two radiologists in a consensus reading. Imaging data was preprocessed. Pyradiomics-package (vanGriethuysen2017) generated 815 radiomics features. Step-wise dimension reduction and feature selection were performed. Biopsy results were used as reference.

Results: Four independent radiomics features were identified showing the strongest predictive values for higher tumor grades: roundness-FLAIR-shape (area-under-curve [AUC]: 0.80), cluster-shades-FLAIR/T1CE (0.80), DWI/ADC-variability (0.72), FLAIR/T1CE-energy (0.76, $p<0.001$ each). These features led in a multivariate regression model to an AUC of 0.91 for differentiation of grade I and II meningiomas.

Conclusion: Radiomics applied on routine MRI is feasible for differentiation between low and intermediate meningiomas and a multivariate regression model yielded very good classification performance. In line with previous studies, higher meningioma grades were associated with shape parameters, contrast-enhancement and DWI/ADC-variability.

Automated voxel- and region-based analysis of gray matter and cerebrospinal fluid space in primary dementia disorders using machine-learning

Karl Egger^{*1}, Shan Yang², Marco Reiser³, Ahmed Abdulkadir⁴, Marc Hohenhaus⁵, Elias Kellner⁶, Horst Urbach⁷

¹Department of Neuroradiologie, Freiburg University Medical Center, Freiburg, Deutschland

²Universitätsklinikum Freiburg, Klinik für Neuroradiologie, Freiburg, D

³University Medical Center Freiburg, Freiburg

⁴Freiburg Brain Imaging Center, Freiburg

⁵Klinik für Neurochirurgie, Neurozentrum, Universitätsklinikum Freiburg, Freiburg, Deutschland

⁶Uniklinik Freiburg, Abteilung Mr-Physik der Abteilung Klinik für Radiologie, Freiburg

⁷Universitätsklinikum Freiburg, Klinik für Neuroradiologie, Freiburg, Deutschland

Purpose: Previous studies showed voxel-based volumetry as a helpful tool in detecting pathologic brain atrophy. Aim of this study was to investigate whether the inclusion of cerebro-spinal fluid (CSF) volume improves the imaging based diagnostic accuracy by using an automated machine-learning algorithm.

Methods: 30 healthy elderly, 30 frontotemporal dementia (FTD), 30 Alzheimer's dementia (AD), 30 Lewy body dementia (LBD) patients, and 30 Normal Pressure Hydrocephalus (NPH) patients were analyzed with voxel-based morphometry and compared with a reference group of 360 healthy elderly controls. Abnormal GM and CSF volumes were visualized via z-scores. Volumetric results were finally evaluated by Support-Vector-Machine and Receiver Operator Characteristics (ROC) analyses.

Results: Based on the volume of abnormal GM and CSF voxels high accuracy was shown in separating dementia from normal ageing (AUC 0.93 and 0.91, respectively) within 5 different brain regions per hemisphere (frontal, medial temporal, temporal, parietal, occipital). Accuracy for separating FTD and AD was higher based on CSF volume (FTD: AUC 0.80 vs. 0.75 in frontal regions; AD: AUC 0.78 vs. 0.68 in parietal regions based on CSF and GM respectively). Highest Accuracy was achieved in separating NPH-patients based on whole brain voxel-wise analyses (AUC 0.98.)

Conclusion: Differentiation of NPH patients and primary dementia patients from normal ageing persons shows high accuracy when based on an automated machine learning algorithm and is therefore ready for implementation into diagnostic routine.

Computational Neuroscience/Functional Imaging

An integrated workflow for automated age-dependent regional brain atrophy estimation

Julian Caspers^{*1}, Bernd Turowski², Christian Rubbert³

¹Universitätsklinikum Düsseldorf, Institut für Diagnostische und Interventionelle Radiologie, Institute of Neuroscience and Medicine (INM-1), Research Centre Jülich, Düsseldorf, Deutschland

²Universitätsklinikum Düsseldorf, Institut für Diagnostische und Interventionelle Radiologie, Düsseldorf, Deutschland

³Universitätsklinikum Düsseldorf, Institut für Diagnostische und Interventionelle Radiologie, Düsseldorf, Deutschland

Purpose: Estimating regional deviations of brain volume from a patient's normative age cohort is challenging and entails immense in-

ter-reader variation. We propose an automated workflow for age-dependent estimation of brain volume changes relative to a standard population.

Methods: 3D T1w MRIs of 693 healthy subjects aged between 16 and 77 years from the publicly available enhanced Nathan Kline Institute—Rockland Sample were preprocessed to generate sex- and age-dependent gray-matter (GM) templates. Preprocessing comprises GM segmentation, normalization to MNI152 and 8 mm smoothing as implemented in CAT12 for SPM12. For each age between 18 and 75, voxel-wise mean and standard deviation (SD) template maps were generated across subjects with the respective age ± 2 years.

To estimate volume changes of an out-of-sample subject, a 3D T1w scan is preprocessed in the same way and a voxel-wise z-value map is generated from the resulting normalized GM map using the age-specific mean and SD templates. The z-map is transformed into subject space, color coded and fused with the structural MRI.

Results: The proposed workflow can be implemented on a server communicating with the PACS for automated and parallelized atrophy map generation. Processing of one subject is performed in less than 10 minutes on a state-of-the-art server.

Conclusion: Automated brain volume change estimation as implemented in the proposed framework could significantly facilitate radiologic workflows and improve regional brain atrophy evaluation.

Sex differences in white matter alterations following repetitive subconcussive head impacts in collegiate ice hockey players

Nico Sollmann^{*1}, Paul S. Echlin², Vivian Schultz³, Alexander P. Lin³, Martha E. Shenton³, Inga K. Koerte³

¹Abteilung für Neuroradiologie, Klinikum Rechts der Isar, Technische Universität München, München, Deutschland

²Elliott Sports Medicine Clinic, Burlington, ON, Canada

³Psychiatry Neuroimaging Laboratory, Brigham and Women's Hospital, Harvard Medical School, Boston, MA, USA

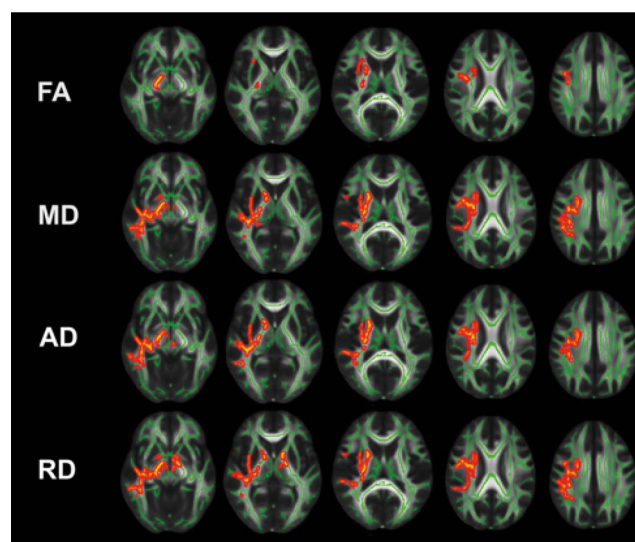
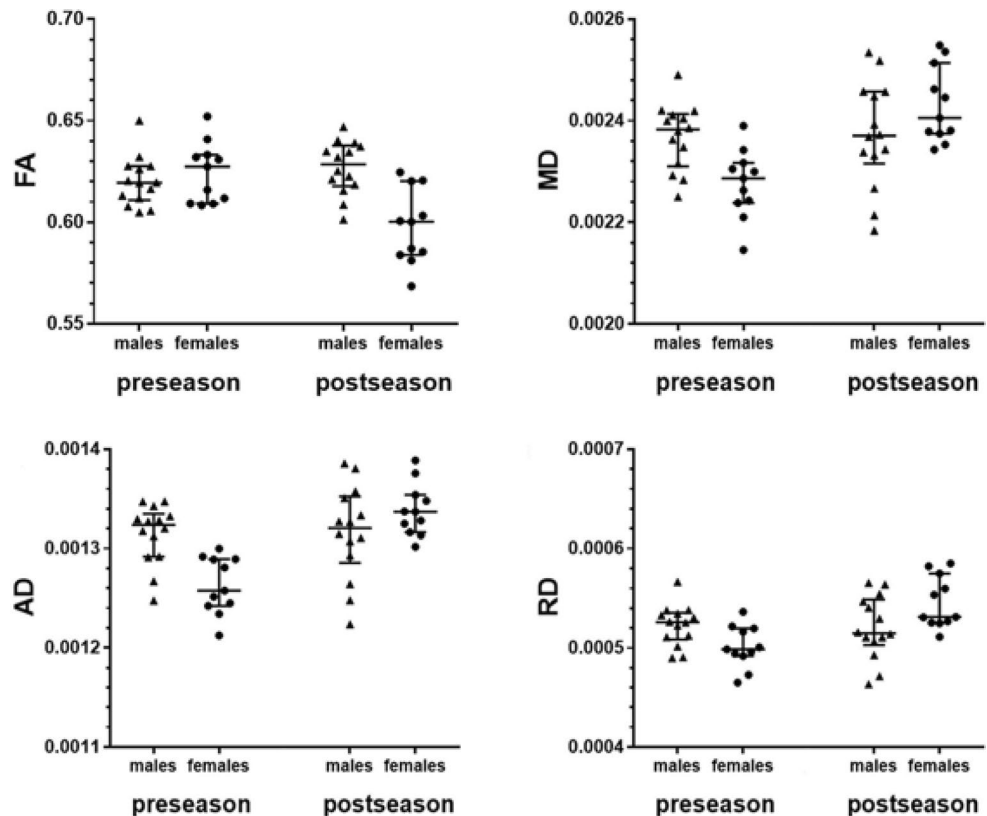


Fig. 1 This figure illustrates the results of the tract-based analysis for fractional anisotropy (FA), mean diffusivity (MD), axial diffusivity (AD), and radial diffusivity (RD). Voxel clusters with statistically significant differences ($p < 0.05$) in change over time (postseason minus preseason data sets) between male and female participants are highlighted in red to yellow

Fig. 2 This figure depicts scatter plots of average values in the voxel clusters with statistically significant group differences ($p < 0.05$) for fractional anisotropy (FA), mean diffusivity (MD), axial diffusivity (AD), and radial diffusivity (RD)



Purpose: Repetitive subconcussive head impacts (RSHI) may lead to structural alterations of the brain. While differences between males and females have already been suggested following a concussion, whether there are sex differences following exposure to RSHI remains unknown.

Methods: 25 collegiate ice hockey players (20.6 ± 2.0 years) underwent diffusion-weighted magnetic resonance imaging (dMRI) before and after the ice hockey season and did not experience a concussion during the season. Whole-brain tract-based spatial statistics were used to compare pre- and postseason dMRI. Pre- and postseason cognitive performance were assessed by the Immediate Post-Concussion Assessment and Cognitive Test.

Results: Significant differences between the sexes were primarily located within the superior longitudinal fasciculus, the internal capsule, and the corona radiata of the right hemisphere (Fig. 1). In significant voxel clusters ($p < 0.05$), decreases in fractional anisotropy (absolute difference pre- vs. postseason: 0.0268) and increases in mean diffusivity (0.0002), axial diffusivity (0.00008), and radial diffusivity (0.00005) were observed in females whereas males showed no significant changes (Fig. 2). There was no significant correlation between the change in dMRI and cognitive performance.

Conclusion: The results of this study suggest sex differences in structural alterations following exposure to RSHI. Future studies need to investigate the underlying associations with exposure.

196

Language function shows similar cortical patterns by functional MRI and repetitive nTMS in healthy volunteers

Monika Probst^{*1}, Theresa Hauck², Claus Zimmer³, Florian Ringel⁴, Bernhard Meyer⁵, Afra Wohlschläger⁶, Sandro Krieg⁷

¹Abteilung für Diagnostische und Interventionelle Neuroradiologie, Klinikum Rechts der Isar, Technische Universität München, München, D

²Plastische Chirurgie, Erlangen, Deutschland

³Klinikum Rechts der Isar der TUM, Technische Universität München, Abteilung für Diagnostische und Interventionelle Neuroradiologie, München, Deutschland

⁴Universitätsmedizin der Johannes Gutenberg-Universität Mainz, Mainz, Deutschland

⁵Klinikum Rechts der Isar, Technische Universität München, Neurochirurgische Klinik und Poliklinik, München, Deutschland

⁶Klinikum Rechts der Isar, Technische Universität München, Abteilung für Diagnostische und Interventionelle Neuroradiologie, München, Deutschland

⁷Neurochirurgische Klinik und Poliklinik, Klinikum Rechts der Isar, Technische Universität München, Deutschland

Purpose: fMRI and navigated transcranial magnetic stimulation (nTMS) are both modalities used in preoperative tumor resection planning. In tumor patients fMRI and nTMS revealed differences in the detected language sites, which might be attributed to tumor-induced oxygenation changes impairing the accuracy of fMRI. We compared the accordance of both techniques in healthy subjects using exactly the same tasks during investigations.

Methods: 19 healthy right-handed subjects performed object naming, pseudoword reading, verb generation, and action naming during fMRI at 3 T and nTMS. For nTMS language mapping, we stimulated 46

cortical spots over the left hemisphere; each site was stimulated for 3 times. Language positive points during nTMS for 1, 2, or 3 errors out the 3 stimulations per spot (1/3, 2/3, 3/3) were compared to the positive fMRI clusters.

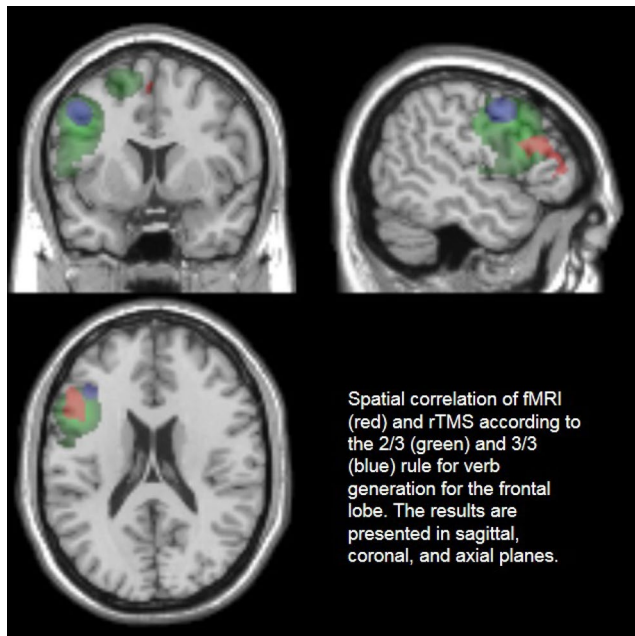
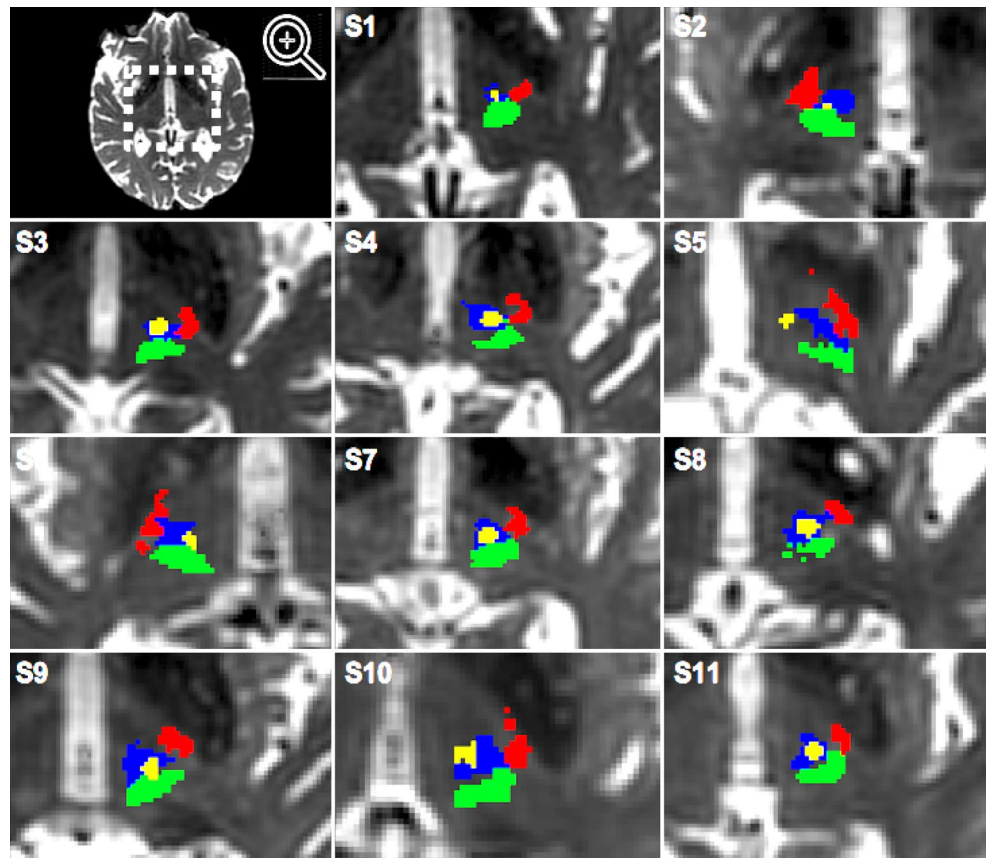


Fig. 1

Fig. 1 Example of fiber tracts (PT=red, ML=green, DTCT=blue) and lesion (yellow) location and overlap on post-treatment b0 images



Results: There was a increasing trend in pseudoword reading as well as verb generation with t-values for 3/3 errors corresponding to $p_a < 0.001$, uncorrected for multiple comparisons, on average across the whole nTMS-spot map. We found a close spatial agreement between several nTMS-spots and fMRI clusters accentuated in the frontal lobe. Compared to the fMRI clusters, there was a higher congruence for 2/3 and 3/3 errors than for 1/3 errors.

Conclusion: Results of language mapping in healthy subjects by fMRI and rTMS correspond well depending on the different language task.

209

Diffusion parameter changes in the cerebello-thalamo-cortical network after MR imaging-guided focused ultrasound thalamotomy

Christian Thaler^{*1}, Qiyuan Tian², Max Wintermark³, Pejman Ghanouni³, Casey H. Halpern⁴, Jaimie M. Henderson⁴, Jens Fiehler⁵, Kim Butts Pauly², Jennifer McNab³

¹Diagnostikzentrum Univ.-Klinikum Hamburg-Eppendorf, Department of Radiology, Stanford University, Hamburg, Deutschland

²Department of Radiology, Department of Electrical Engineering

³Department of Radiology

⁴Department of Neurosurgery

⁵Diagnostikzentrum Univ.-Klinikum Hamburg-Eppendorf, Klinik und Poliklinik für Neuroradiologische Diagnostik und Intervention, Hamburg, Deutschland

Purpose: The objective of this study was to use diffusion MRI to segment and detect changes in white matter tracts in essential tremor pa-

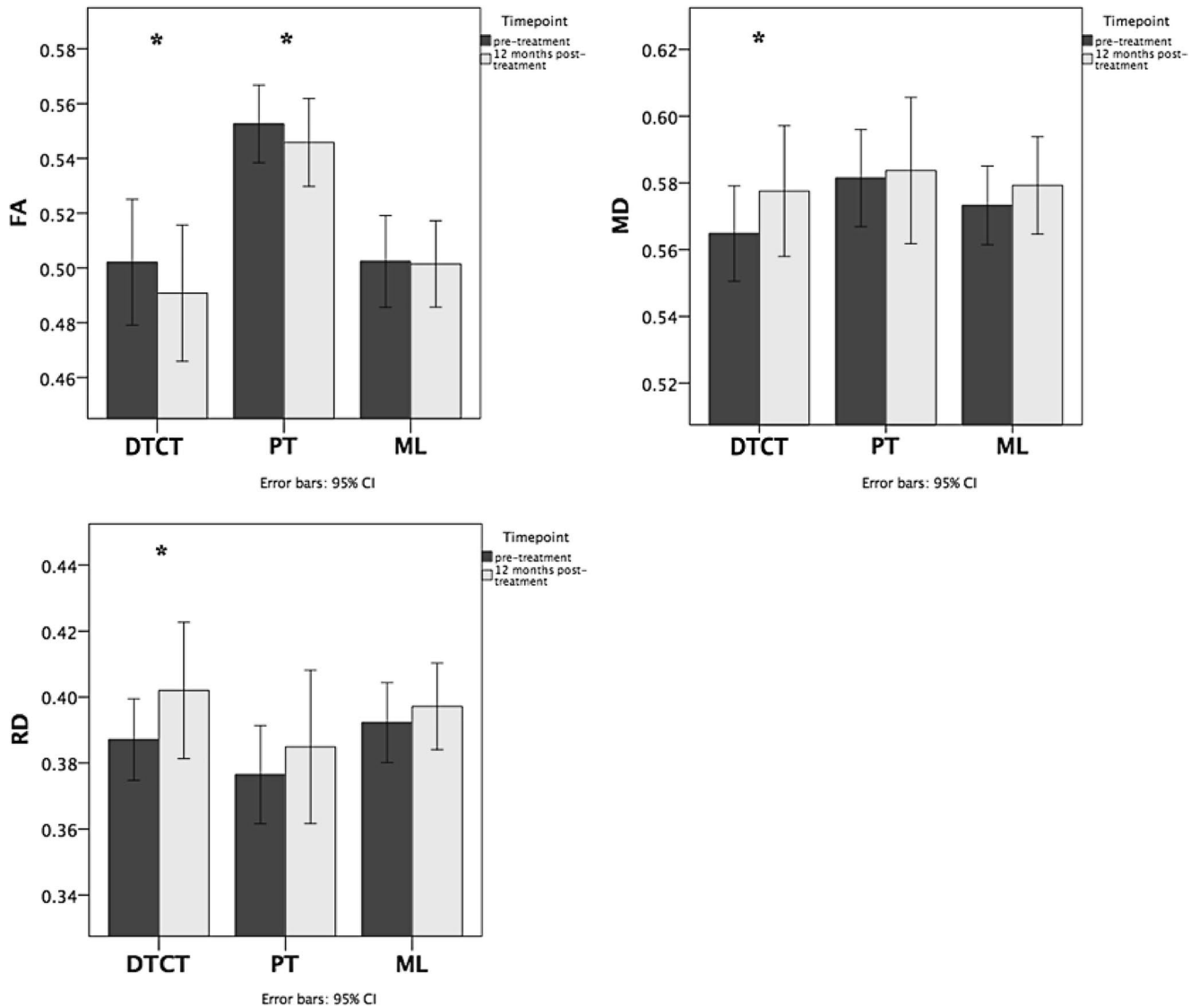


Fig. 2 Diffusion parameter changes within the fiber tracts. *Indicates significant difference ($p < 0.05$)

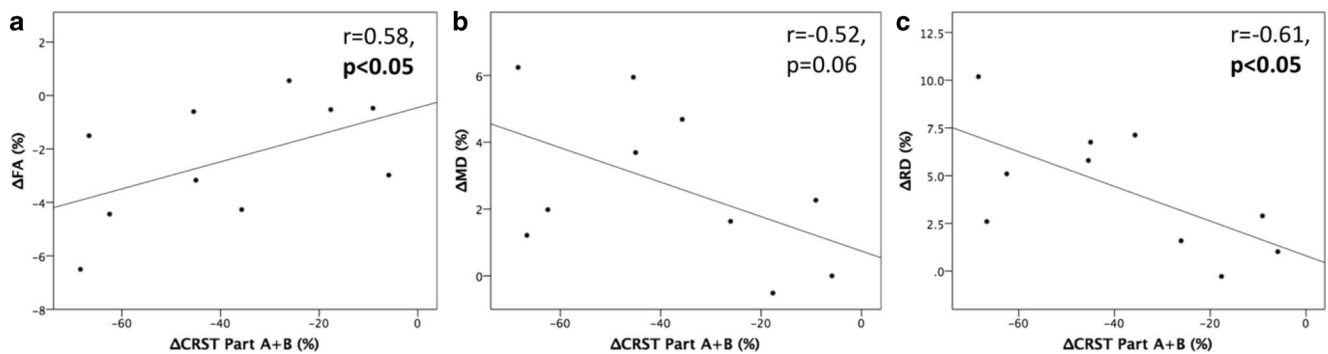


Fig. 3 Significant correlations between the FA and RD changes within the DTCT and clinical improvement

tients treated with MRI-guided focused ultrasound (MRgFUS) thalamotomy.

Methods: MRgFUS thalamotomy was performed in 11 patients with essential tremor. All patients received 3T MRI, including structural and diffusion scans, prior to the procedure as well as 1 year after the treatment. At each time point, clinical status was assessed using the Clinical Rating Scale for Tremor (CRST). Tractography was performed for the dentato-thalamic-cortical tract (DTCT), the medial lemniscus (ML) and the pyramidal tract (PT) and diffusion parameters (fractional anisotropy (FA), mean diffusivity (MD), radial diffusivity (RD)) were obtained within the tracts in the pre- and post-treatment data.

Results: All diffusion parameters changed significantly within the lesion as well as in the DTCT on the treated side ($p < 0.05$). FA and RD changes within the DTCT correlated significantly with clinical outcome ($r = 0.58$ and $r = -0.61$, $p < 0.05$).

Conclusion: Diffusion parameters changed significantly within the DTCT after MRgFUS and changes correlated well with clinical outcome. This study demonstrates that diffusion MRI can detect the microstructural effects of MRgFUS, thereby helping to elucidate the treatment mechanism and ultimately improve targeting prospectively.

280

Cerebral activation during the visual presentation of aversive and neutral stimuli in Takotsubo-Cardiomyopathie (TTC) female patients

Ruth Steiger^{*1}, Fabian Barbieri², Andreas Rietzler³, Michael Verius⁴, Christian Siedentopf³, Astrid Grams³, Elke Gizewski³, Wolfgang Dichtl²

¹University Clinic of Neuroradiology, Neuroimaging Research Core Facility, Medical University of Innsbruck, Innsbruck, Austria

²University Clinic of Internal Medicine III

³University Clinic of Neuroradiology

⁴University Clinic of Radiology

Purpose: Nearly 10% of all heart attacks in postmenopausal female patients are caused by the Takotsubo Cardiomyopathie (TTC). Acute emotional stress is considered to be the trigger in the majority of cases. Examination of the human brain via fMRI (3T) enables the investigation of the activation of decisive brain areas which might be correlated with emotional stress processing. It was shown that subarachnoid haemorrhage and stroke in the left-hemispheric insula are often accompanied by a TTC (so-called “neurogenic stunned myocardium”). Hence the assumption exists that female patients with acute TTC will manifest an increased activation within this region.

Methods: To detect the emotion-related brain activation we implemented an event-related fMRI setting with conditions of alternating aversive- and neutral images (IAPS) and images of fixation. fMRI Data was analyzed with SPM12 and for the statistical group analysis we assume a normal distribution and performed two-sample t-tests.

Results: After analysis of 20 female TTC patients our study shows that the amygdala, gyrus fusiform and insula are activated and play an important role during visual presentation of aversive and neutral stimuli in TTC. In other neuroimaging studies it could also be shown that the amygdala is reacting on fear-inducing and threatening visual stimuli.

Conclusion: We therefore conclude that in correlation with visual presentation of aversive images these 3 brain regions are essentially involved in stimuli-processing.

288

Noise Reduction in Perfusion Imaging using Data-driven Prior Knowledge

Sebastian Bannasch¹, Christina Eckel², Robert Fryscht³, Oliver Beuing⁴, Gerald Warnecke⁵, Georg Rose⁶

¹Stimulate, Magdeburg, D

²Otto-von-Guericke Universität, Deutschland

³Otto-von-Guericke-Universität Magdeburg, Institut für Medizintechnik, Forschungscampus Stimulate, Magdeburg, Deutschland

⁴Institut für Neuroradiologie, Institut für Neuroradiologie, Institut für Neuroradiologie, Magdeburg, Deutschland

⁵Institut für Analysis und Numerik

⁶Institut für Medizintechnik, Otto-von-Guericke-Universität Magdeburg, Forschungscampus Stimulate, Magdeburg, D

Purpose: Model-based CT reconstruction (MBCT) by incorporating prior knowledge, are investigated in order to provide a C-arm-based perfusion imaging. The study addresses the issue of temporal under-sampled dynamic C-arm CT data. We demonstrate that MBCT is beneficial for dynamic conventional CT data as well.

Methods: In order to create a compact data set that encodes prior knowledge, we have evaluated and statistically analyzed various clinical perfusion CT data.

Results: The performance of our MBCT is shown on a noisy data set that was not part of our prior knowledge data base. The left side depicts the original and on the right side the MBCT image is shown. Both are CT slices of a single time frame at the arterial-input-peak in ΔHU . Finally, an exemplary time attenuation curve of an artery voxel and its regularized version is shown.

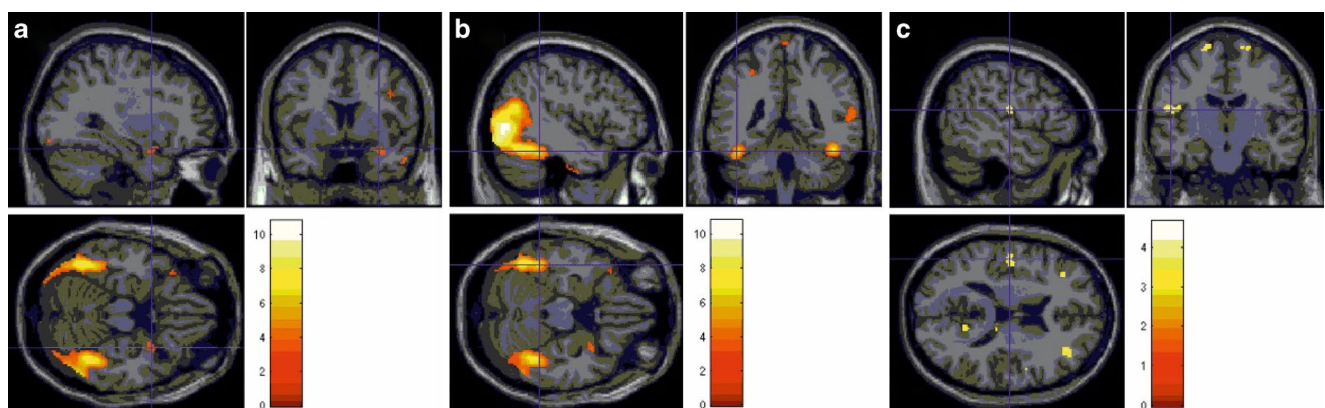


Fig. 1 Activated brain areas during visual presentation of aversive and non-aversive stimuli, **a** Amygdala (Av. vs. Neutr.), **b** Gyrus fusiform (Av. vs. Neutr.), **c** Insula (Neutr. vs. Av.)

Fig. 1

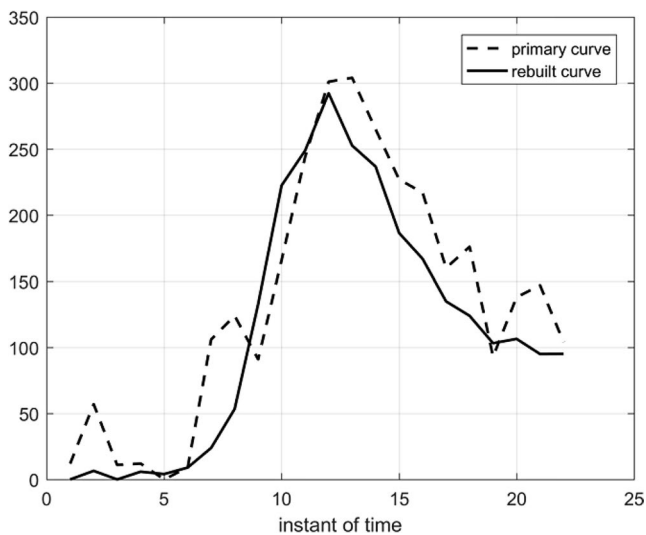
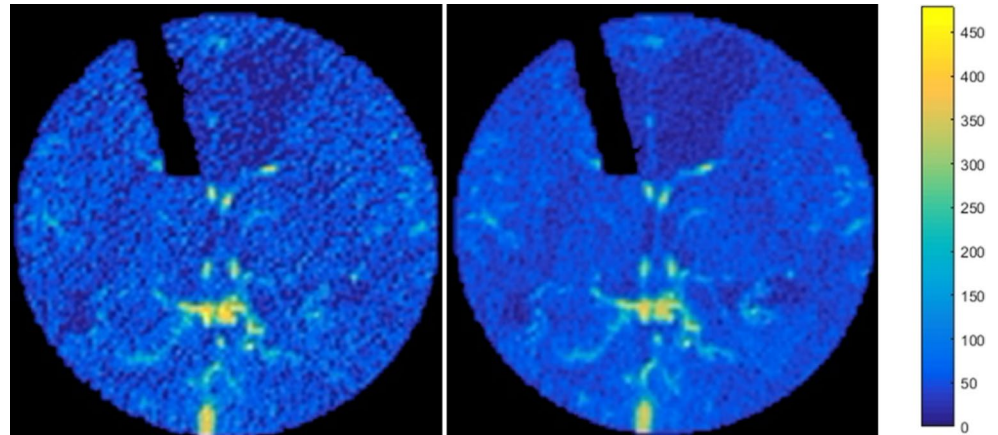


Fig. 2

Conclusion: The signal-to-noise ratio is drastically improved in the MBCT reconstructions. This method will be used in the future in order to improve the quality of perfusion maps.

Acknowledgement: This abstract is funded by the BMBF within the Forschungscampus *STIMULATE* under grant number ‘13GW0095A’ and within the context of the project ‘Graduate School MEMoRIAL’ funded by the ESF under grant number ‘ZS/2016/08/80646’. Additionally, the authors thank Professor Dr. Thomas Henzler and the M²OLIE Forschungscampus for providing further CT data set.

300

Imaging glioma biology: spatial comparison of APT, CBV, DTI and FET

Simon Schön^{*1}, Jorge Cabello², Igor Yakoushev², M. Molina Romero³, Marie Metz⁴, Ilham Karimov², Thomas Pyka⁴, Andreas Hock⁵, Friederike Liesche⁶, Jens Gempt⁷, Christine Preibisch⁴, Claus Zimmer⁴, Wolfgang Weber², Benedikt Wiestler⁴

¹Abteilung für Diagnostische und Interventionelle Neuroradiologie, Klinikum Rechts der Isar, TU München, Germany, München, D

²Klinik für Nuklearmedizin, Klinikum Rechts der Isar, TU München, Germany

³Zentralinstitut für Medizintechnik (Imetum), TU München, Germany

⁴Abteilung für Diagnostische und Interventionelle Neuroradiologie, Klinikum Rechts der Isar, TU München, Germany

⁵Philips Healthcare

⁶Institut für Allgemeine Pathologie, Klinikum Rechts der Isar, TU München, Germany

⁷Neurochirurgische Klinik und Poliklinik, Klinikum Rechts der Isar, TU München, Germany

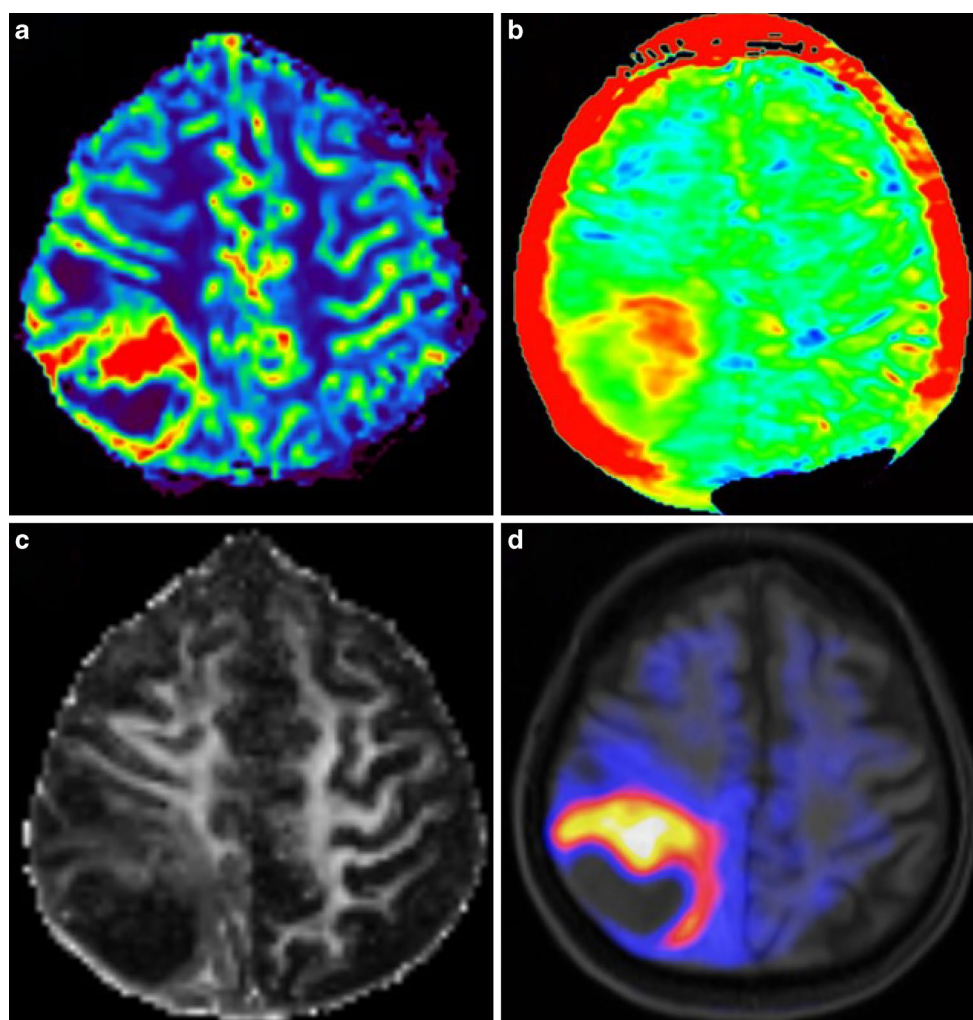
Purpose: Multimodal imaging bears great potential to advance our understanding of glioma biology. Here, we investigate spatial correlation of novel and established imaging techniques.

Methods: We examined 18 glioma patients with amide proton transfer (APT), 32-direction diffusion-tensor (DTI) and perfusion-weighted imaging (PWI; **Fig. 1**). In addition, patients underwent static FET-PET imaging. Post-processing encompassed calculating cerebral blood volume (nCBV) maps using AUC-based leakage correction and free-water & tissue volume estimation from DTI data using a deep net for signal deconvolution. Tumors were segmented semi-automatically and images were linearly co-registered using ANTs.

Results: We observed highly significant voxel-wise intensity correlations between APT and FET (Spearman’s $\rho=0.374$, adj. $p<0.0001$) as well as between CBV and the tissue volume fraction (Spearman’s $\rho=0.313$, adj. $p=0.0002$) in the FLAIR-hyperintense peritumoral area. FET and CBV were also positively correlated (Spearman’s $\rho=0.309$, adj. $p=0.0006$). Interestingly, APT and tissue volume fraction were negatively correlated in contrast-enhancing tumor (Spearman’s $\rho=0.238$, adj. $p=0.009$).

Conclusion: Among three MRI sequences, PET signal was most strongly correlated with APT. Nonetheless, each imaging modality depicts unique areas within the tumor, as expected from the different biological processes they capture. This and further spatial analyses will be discussed in detail.

Fig. 1 Example of imaging sequences studies: **a** nCBV, **b** APT, **c** fractional anisotropy (FA) from DTI data, **d** FET-PET



343

Assessment of the disease-specificity of morphometric findings: examples from chronic musculoskeletal pain

Benedikt Sundermann^{*1}, Mahboobeh Dehghan Nayyeri², Bettina Pfeleiderer¹, Kim Stahlberg³, Leonie Jünke³, Lara Baie³, Ralf Dieckmann⁴, Dennis Liem⁴, Thomas Happe⁵, Markus Burgmer³

¹Universitätsklinikum Münster, Institut für Klinische Radiologie, Münster, Deutschland

²Heinrich-Heine-University Düsseldorf, Department of Psychosomatic Medicine and Psychotherapy, Lvr Clinic, Düsseldorf

³Universitätsklinikum Münster, Klinik für Psychosomatik und Psychotherapie, Münster

⁴Universitätsklinikum Münster, Klinik für Allgemeine Orthopädie und Tumororthopädie, Münster

⁵Praxis, Münster

Purpose: Neuroimaging studies have provided evidence of altered gray matter volume (GMV) in chronic pain conditions such as fibromyalgia syndrome (FMS). Such studies usually compare one specific patient group with healthy controls. The purpose of this study was to evaluate whether GMV alterations are specific to a single disease entity such as FMS or rather reflect less specific changes in chronic pain in general.

Methods: We carried out voxel-based morphometry (T1 MPRAGE acquired at 3T) in FMS ($n=27$) and included a second control group with chronic pain in osteoarthritis ($n=26$) in addition to a healthy control group ($n=22$). Global and regional GMVs were compared between the three groups.

Results: While both pain groups exhibited locally altered GMV compared to healthy controls, no differences between these two pain groups were evident.

Conclusion: GMV changes in FMS reflect changes related to chronic pain in general rather than highly disease-specific effects. Inclusion of carefully selected control groups beyond healthy controls should be considered in VBM and similar neuroimaging studies in order to avoid overinterpretations regarding disease-specificity.

357

Effect of thalamic GABA on cognitive control in patients with restless leg Syndrome (RLS) using 1H MR-spectroscopy

Annett Werner^{*1}, Rui Zhang², Jennifer Linn³, Christian Beste⁴, Ann-Kathrin Stock⁴

¹Clinic and Institute for Diagnostic and Interventional Neuroradiology, University Hospital Carl Gustav Cars Dresden, Dresden, Deutschland

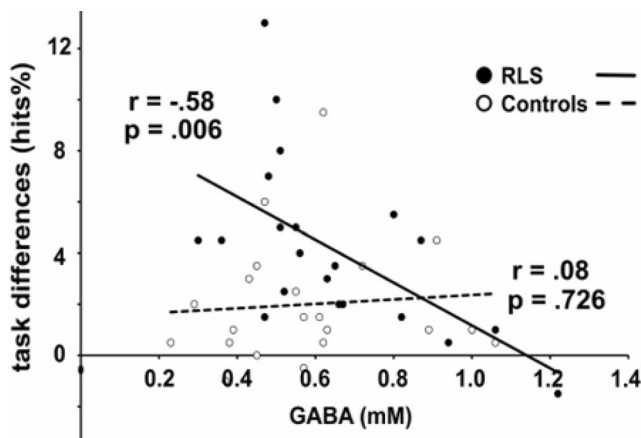


Fig. 1

²Cognitive Neurophysiology, Department of Child and Adolescent Psychiatry, Faculty of Medicine, TU Dresden

³Clinic and Institute for Diagnostic and Interventional Neuroradiology, University Hospital Carl Gustav Cars Dresden

⁴Cognitive Neurophysiology, Department of Child and Adolescent Psychiatry, Faculty of Medicine, TU Dresden, Germany

Purpose: To investigate the potential relationship between thalamic GABA concentrations and cognitive control in RLS patients, a neuropsychological experimental paradigm was used in combination with ¹H-Magnetic Resonance Spectroscopy.

RLS is a sensory-motor disorder, characterized by an urge to move the legs and arms during rest and patients have been shown to experience changes in cognitive control functions such as decision making or working memory. Neuronal changes are most commonly found in cortical-basal gangliathalamic loops and characterized by changes in GABAergic signaling.

If RLS patients display impairments in working memory and cognitive control, they should show larger task differences than healthy controls due to their control constraints.

Methods: Patients: 30 RLS patients & 30 age matched controls (mean age: 60.2 years)

Neuropsychological testing: experimental paradigm consisting of a high and a low demand task

MRI & MRS: 3T Siemens “Verio”; single-voxel localized ¹H MRS (adapted PRESS- sequence, voxel located in the left thalamus); metabolite quantitation using LC-Model and an adapted MATLAB-script (C.Choi, USA [1])

Results:

- Performance differences between two tasks are larger in RLS-patients than in healthy controls
- GABA is significantly correlated with behavioral performance (figure).

Conclusion: Compared to healthy controls, RLS patients displayed reduced cognitive control capacities which were most likely based on working memory deficits.

362

Model-based analysis of resting-state between-network functional connectivity to identify Parkinson's disease patients

Christian Rubbert^{*1}, Christian Mathys², Simon Eickhoff³, Felix Hoffstaedter³, Benjamin Sigl⁴, Nikolas Teichert⁵, Martin Südmeyer⁶, Christian Hartmann⁷, Bernd Turowski⁸, Alfons Schnitzler⁹, Julian Caspers¹⁰

¹Universitätsklinikum Düsseldorf, Institut für Diagnostische und Interventionelle Radiologie, Düsseldorf, Deutschland

²Institute of Radiology and Neuroradiology, Evangelisches Krankenhaus, University of Oldenburg, Department of Diagnostic and Interventional Radiology, University Dusseldorf, Medical Faculty, Düsseldorf, Deutschland

³Heinrich-Heine-Universität Düsseldorf, Institut für Klinische Neurowissenschaften und Medizinische Psychologie, Forschungszentrum Jülich, Institut für Neurowissenschaften und Medizin (INM-¹), Düsseldorf, Deutschland

⁴Institut für Diagnostische und Interventionelle Radiologie, Düsseldorf, Deutschland

⁵Department of Diagnostic and Interventional Radiology, University Dusseldorf, Medical Faculty

⁶Klinikum Ernst von Bergmann, Klinik für Neurologie, Potsdam, Deutschland

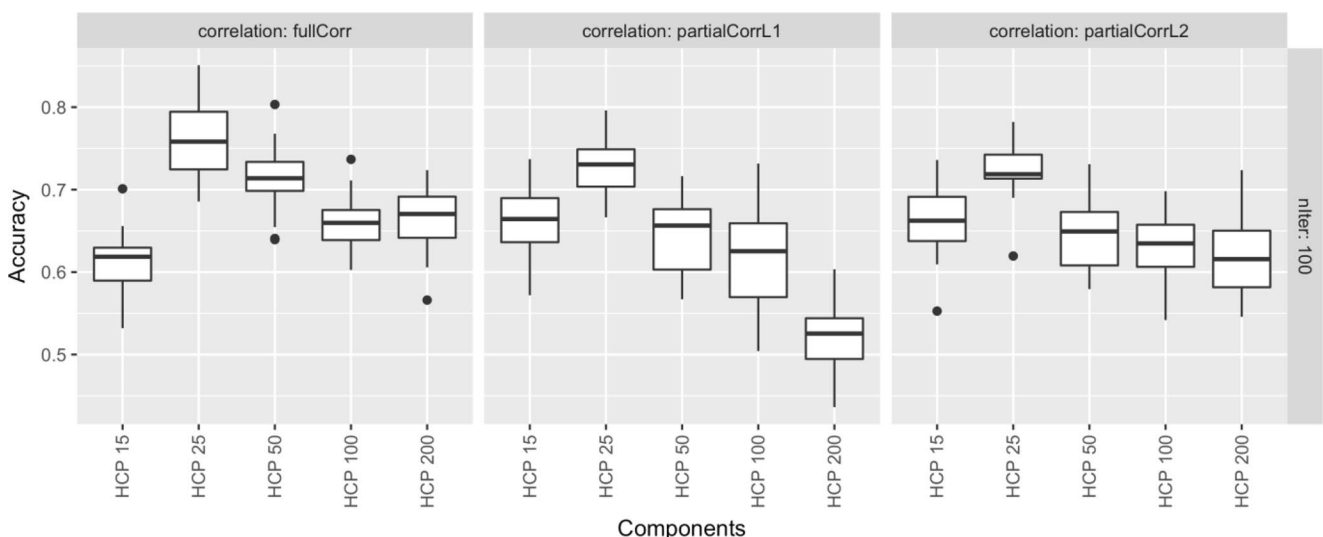


Fig. 1

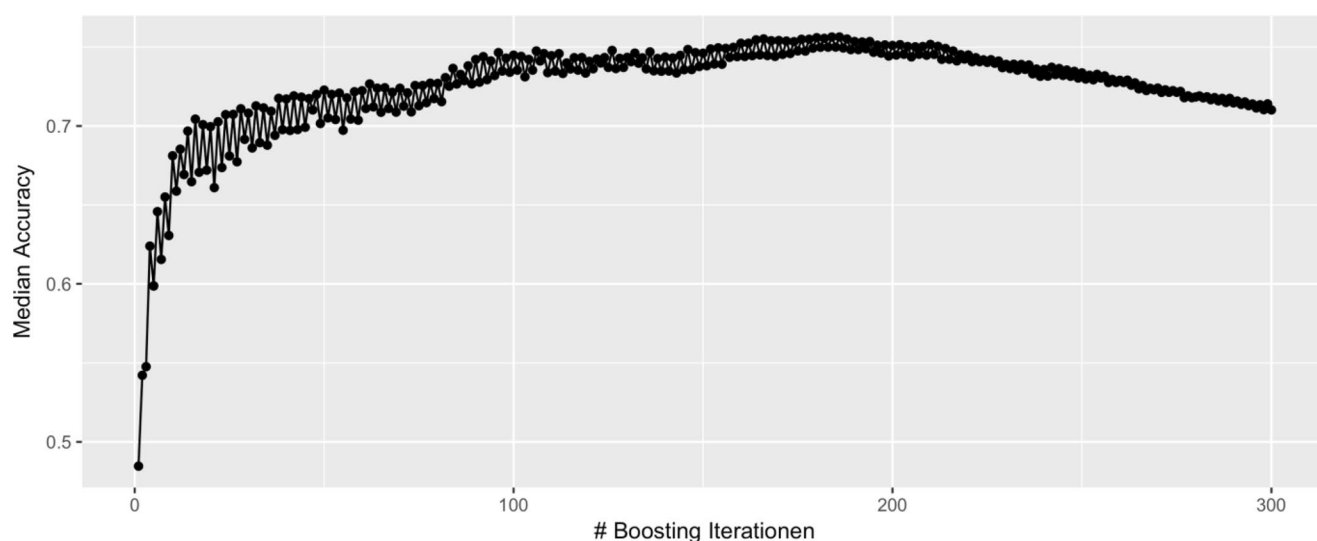


Fig. 2

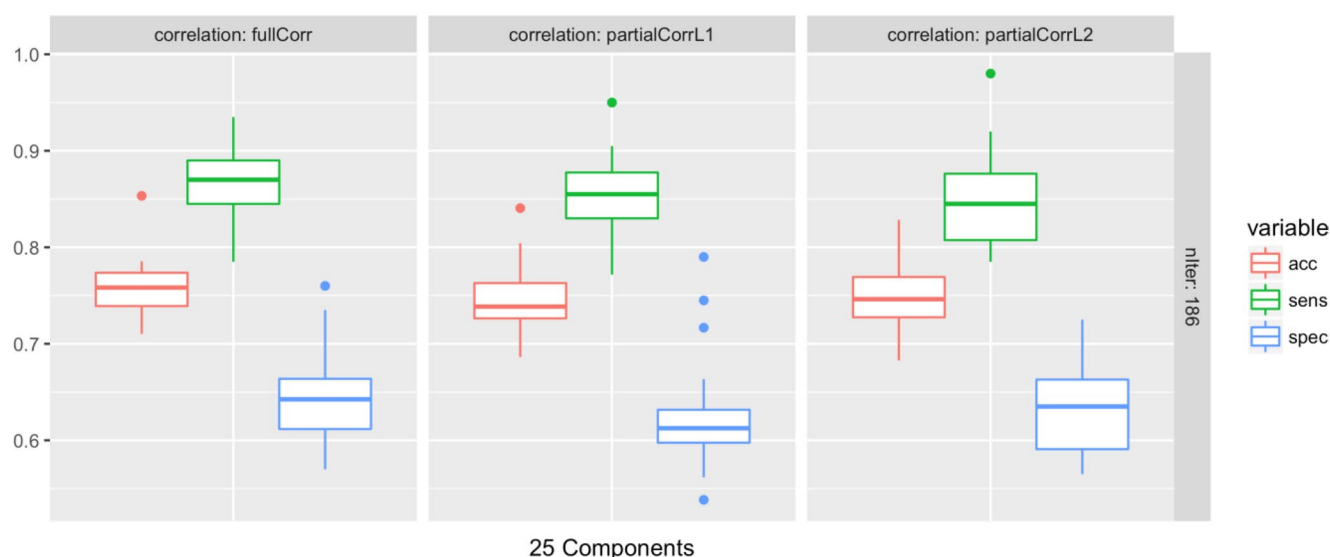


Fig. 3

⁷Universitätsklinikum Düsseldorf, Zentrum für Bewegungsstörungen und Neuromodulation der Klinik für Neurologie, Heinrich-Heine-Universität Düsseldorf, Institut für Klinische Neurowissenschaften und Medizinische Psychologie, Düsseldorf, Deutschland

⁸Universitätsklinikum Düsseldorf, Institut für Diagnostische und Interventionelle Radiologie, Düsseldorf, Deutschland

⁹Universitätsklinikum Düsseldorf, Klinik für Neurologie, Institut für Klinische Neurowissenschaften, Düsseldorf, Deutschland

¹⁰Universitätsklinikum Düsseldorf, Institut für Diagnostische und Interventionelle Radiologie, Institute of Neuroscience and Medicine (INM-1), Research Centre Jülich, Düsseldorf, Deutschland

Purpose: Parkinson's disease (PD) is a clinical diagnosis without a test for definite diagnosis. Resting-state functional connectivity shows alterations in PD and may be a valuable biomarker. We evaluated between-network connectivity in resting-state fMRI (rsfMRI) in a data-driven approach to identify PD patients.

Methods: Whole-brain rsfMRI (Siemens Trio 3T, EPI, TR 2.2 s, TE 30 ms, flip 90°, resolution 3.1³ mm, 11 min) of 42 PD patients (med-

ical OFF) and 47 healthy controls matched for age and gender were analysed.

Between-network connectivity (full and partial correlations with L1/L2 regularization) were computed for each subject based on canonical functional network architecture at different levels of granularity (HCP1200, recon2). A Boosted Logistic Regression model (100 iterations) was trained on the correlation matrices using 20 repeats of 10-fold cross-validation. The number of iterations was optimized for the best models. Performance metrics were averaged over the validation folds.

Results: Median accuracies over different granularities are shown in Fig 1. The models with 25 components performed best across correlation methods: 75.8% (full), 73.1% (partial, L1) and 71.9% (partial, L2). The optimal number of iterations was 186 (Fig 2). No significant difference in accuracy, sensitivity or specificity were found between the optimized models (Fig 3) according to an unpaired t-test ($p > 0.05$). There were less outliers after L2 regularization (median acc. 74.6%, sens. 84.5%, spec. 63.5%).

Conclusion: Accuracy for predicting PD in rsfMRI is overall acceptable. Aligning the rsfMRI pre-processing pipeline with the HCP1200 dataset should be evaluated to boost performance.

364

Uncertainty Quantification for Patient-Specific Blood Flow Simulation in Brain Aneurysms

Julien Abinahed^{*1}, Sarada Dakua¹, Georges Younes¹, Abdulla Al-Ansari¹, Ayman Zakaria¹, Pablo Bermejo¹, Peter Coveney², Robin Richardson², Derek Groen², Abbes Amira³, Faycal Bensaali³, Xiaojun Zhai³

¹Hmc, Doha, Qatar

²Ucl, United Kingdom

³Qu, Qatar

Purpose: Clinical decision-making in the area of cerebral cardiovascular health currently benefits from a diverse range of data obtained from scans and other physical measurements. Computational Fluid Dynamics (CFD) simulations provide a way to enhance the interpretation and predictive power of this already-available data. We discuss the difficulties and successes encountered in the development of an automated and entirely patient-specific pipeline to predict the effects of flow diverter introduction in the treatment of aneurysms. In particular, we focus on the challenges of uncertainty quantification, given the sensitivity of models to the input data.

Methods: Using medical imaging data, we reconstruct the anatomy including uncertainty measures for each patient. We then generate the necessary input for CFD simulation algorithm (HemeLB¹) deployed on large High-Performance Computing platforms. The effect of uncertainty on CFD results is then analyzed.

Results: Quantification of uncertainty during geometric reconstruction stage for patient-specific CFD simulations provides further insights into the clinical reliability of CFD for brain aneurysms.

Conclusion: Uncertainty quantification for patient-specific blood flow simulations is an important steps towards effective translation to clinical decisions support systems.

Reference

1. Mazzeo MD, Coveney PV. HemeLB: A high performance parallel lattice-Boltzmann code for large scale fluid flow in complex geometries. *Comput. Phys. Commun.* 2008;178:894–914

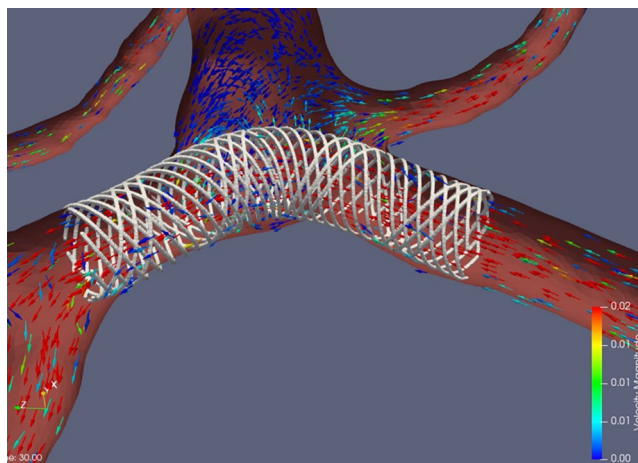


Fig. 1 Example of blood flow simulation

372

Anisotropy and diffusion effects in myelin water imaging

Felix Tobias Kurz^{*1}, Lukas R Buschle², Artur Hahn³, Martin Bendszus³, Sabine Heiland³, Christian Ziener³, Johann Jende³

¹Universitätsklinik Heidelberg, Uniklinikum Heidelberg, Neuroradiologie, Heidelberg, Deutschland

²DfKz Heidelberg

³Universitätsklinikum Heidelberg

Purpose: To develop a diffusion-sensitive model that describes magnetization decay in the myelin sheath with structural and inherent anisotropic magnetic susceptibility properties.

Methods: The model provides a numerical solution of the Bloch-Torrey equation that determines magnetization decay in the presence of diffusion effects and local field perturbations induced by differences in tissue magnetic susceptibilities. It is based on a multi-compartment cylindric myelin sheath (Fig. 1) with anisotropic magnetic susceptibility and characteristic frequency shift ¹.

Results: The myelin sheath magnetization decay, $M(t)$, is dependent on the inherent magnetic susceptibility anisotropy, $\Delta\chi$, in the myelin phospholipid bilayers (Fig. 2). For increasing diffusion effects with a diffusion constant $D \approx 100 \mu\text{m}^2/\text{ms}$, the signal decay approaches the limit of fast diffusion effects (FD, from [1]), and for negligible diffusion ($D=0 \mu\text{m}^2/\text{ms}$) the limit of static dephasing (Fig. 3).

Conclusion: The model provides a robust framework for the study of MR signal decay in white matter which may be particularly helpful for the study of changes in myelin integrity in neurological diseases such as multiple sclerosis or hypomyelinating diseases ²⁻⁴.

Reference

- 1 Sukstanskii AL et al. *Magn Reson Med.* 2014;71:345–53.
- 2 Kitzler HH et al. *Neuroimage.* 2012;59:2670–7.
- 3 MacKay et al. *Brain Plast.* 2016;2:71–91.
- 4 Deoni SC et al. *Neuroimage.* 2012;63:1038–53.

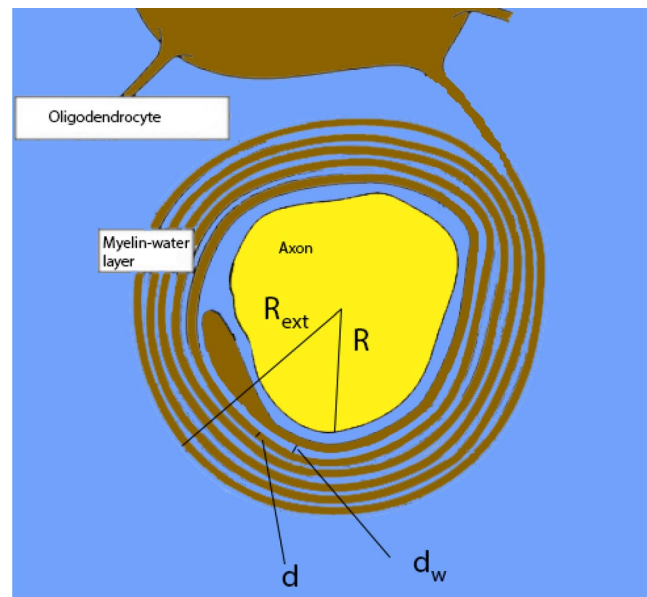


Fig. 1 Schematic model of the myelin sheath structure. The axon with radius R is surrounded by alternating phospholipid bilayers (brown, thickness d) and aqueous layers (blue, thickness d_w). The model assumes a concentric layer arrangement around the cylindric axon

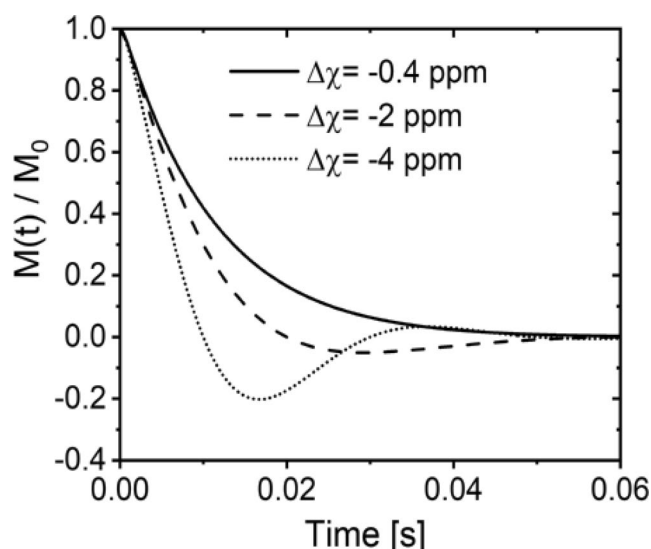


Fig. 2 MR signal decay $M(t)$ in the myelin sheath. For increasing values of magnetic susceptibility anisotropy in the phospholipid bilayers, $\Delta\chi$, the signal decay features a slow oscillatory component ($M_0 = M(0)$)

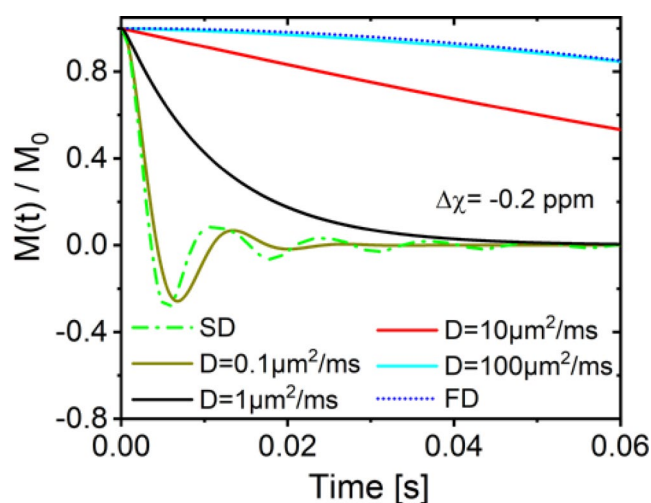


Fig. 3 MR signal decay in the myelin sheath for different values of the diffusion constant D . SD: regime of static dephasing (negligible diffusion effects) FD regime of fast diffusion [1]

381

Tractography in use: Fiber-tracts involved in the improvement of bradykinesia in deep brain stimulation for Parkinson's disease

Quirin Strotzer^{*1}, Judith Anthofer¹, Alexander Brawanski¹, Claudia Fellner¹, Rupert Faltermeier¹, Jürgen Schlaier¹

¹Universitätsklinikum Regensburg, Regensburg, Deutschland

Purpose: Deep brain stimulation becomes increasingly important in treating the motor symptoms of Parkinson's disease. To improve target planning, we investigated the connectivity between the stimulated volume and cerebral fiber-tracts using probabilistic tractography to find out which tracts have a positive effect on bradykinesia.

Methods: 18 patients with Parkinson's disease who received bilateral deep brain stimulation in the subthalamic nucleus were included. Bradykinesia was existing in 31 hemibodies. The effectiveness in reducing bradykinesia was individually assessed for every of the 124 contacts (4 per electrode) in the associated contralateral brain hemispheres. We performed probabilistic tractography using diffusion weighted magnetic resonance imaging (64 gradient directions, 12-channel head-coil) to create a connectivity profile for the stimulated volume of every contact.

Results: 92 contacts (74.2%) were clinically effective. Effective and ineffective contacts were compared for their connectivity patterns. Effective contacts were significantly ($p < 0.05$) more often associated with the ipsilateral superior cerebellar peduncle and the ipsilateral dentate nucleus, which partly define the ascending cerebello-thalamo-cortical pathway. Significant negative correlations existed with the contralateral medial cerebellar peduncle, the central pons and the motor cortex representing the descending cortico-ponto-cerebellar pathway.

Conclusion: A connectivity-based approach may improve target planning in deep brain stimulation. Considering bradykinesia in Parkinson's disease, the cortico-cerebellar loop seems to play a key role.

391

Exploring Individual Multiple Sclerosis Lesions Development and Volume Change for Therapy Monitoring

Caroline Koehler¹, Hannes Wahl¹, Tjalf Ziemssen², Jennifer Linn³, Hagen H. Kitzler^{*4}

¹Institut und Poliklinik für Diagnostische und Interventionelle Neuroradiologie, Universitätsklinikum Carl Gustav Carus, Dresden, Deutschland

²Zentrum für Klinische Neurowissenschaften, Klinik für Neurologie, Universitätsklinikum Carl Gustav Carus, Dresden, Deutschland

³Universitätsklinikum Carl Gustav Carus an der TU Dresden, Institut und Poliklinik für Diagnostische und Interventionelle Neuroradiologie, Dresden, Deutschland

⁴Institut und Poliklinik für Diagnostische und Interventionelle Neuroradiologie, Dresden, Deutschland

Purpose: Magnetic resonance imaging (MRI) is used to follow-up multiple sclerosis (MS) and evaluate disease progression and therapy response via lesion quantification. Conventional MRI data post-processing analysis research in the recent past focused on reliable, precise and reproducible automated MS lesion segmentation and the measurement of total brain lesion volume¹.

Methods: An *Automatic Follow-up of Individual Lesions* (AFIL) algorithm was developed beyond this standard to process time series of binary lesion masks. The labelled masks allowed the evaluation of individual lesion volume courses. Algorithm performance testing was executed in early MS with four MRI visits, and MS experienced readers verified the accuracy.

Results: AFIL distinguished 328 individual lesion courses with 0.9% error rate. A total of 121 new lesions evolved within the observed time period. The proportional courses of 69.1% lesions in the persistent lesion population exhibited varying volume, 16.9% exhibited stable volume, 3.4% exhibiting continuously increasing, and 0.5% exhibited continuously decreasing volume.

Conclusion: The algorithm tracked individual lesions and observed different MS lesion courses. This may facilitate the concept of *No Evidence of Disease Activity* (NEDA) monitoring that incorporated newly appearing or enlarging T2 lesions as indicators of sub-clinical disease progression².

References

1. Llado, X et al. Automated detection of multiple sclerosis lesions in serial brain MRI. *Neuroradiology*, 2012;54(8):787–807.
2. Stangel, M et al. Towards the implementation of ‘no evidence of disease activity’ in multiple sclerosis treatment: the multiple sclerosis decision model. *Ther Adv Neurol Disord*. 2015;8(1):3–13.

408

Regional and Gender Differences of Cerebral Energy Metabolism Measured by 31P Magnetic Resonance Spectroscopy

Andreas Rietzler^{*1}, Ruth Steiger², Lisa Maria Walchhofer³, Raffaella Matteucci Gothe⁴, Bernhard Glodny³, Michael Schocke⁵, Elke Ruth Gizewski², Astrid Ellen Grams²

¹Medizinische Universität Innsbruck, Department Radiologie, Universitätsklinik für Neuroradiologie, Innsbruck, Austria

²Univ.Klinik für Neuroradiologie

³Univ.Klinik für Radiologie

⁴Private Universität für Gesundheitswissenschaften, Medizinische Informatik und Technik, Hall

⁵Universitäts- und Rehabilitationskliniken Ulm

Purpose: Phosphorous magnetic resonance spectroscopy (31P-MRS) allows the analysis of various energy metabolites in vivo. The aim of the present study was to investigate the influence of brain region, hemisphere, age and gender on the 31P-MRS metabolism.

Methods: 125 healthy volunteers (64 women, 61 men; between 20 and 85 years) were examined with a 3 Tesla three-dimensional 31P-MRS sequence of the supratentorial brain. Data post-processing was performed with the AMARES algorithm of the software jMRUI. The metabolite ratios PCr/ATP, Pi/ATP and PCr/Pi from the brain areas frontal lobe, parietal lobe, occipital lobe, temporal lobe and basal ganglia of both hemispheres were generated and compared.

Results: For all metabolite ratios significant regional differences and in several regions gender differences were found. In some brain regions and for some metabolites hemispheric differences were detected. In addition chances with ageing were found, which differed between women and men.

Conclusion: The present results indicate that the 31P-MRS metabolism varies throughout the brain, with age and between genders. This study displays an important foundation for the design and the interpretation of future 31P-MRS studies under physiological conditions or on patients with various cerebral diseases.

452

Multiple Aneurysms AnaTomy CHallenge 2018 (MATCH)—State-of-the-art segmentation and hemodynamic simulation

Philipp Berg^{*1}, Samuel Voß², Sylvia Saalfeld³, Gábor Janiga², Oliver Beuing⁴

¹Department of Fluid Dynamics and Technical Flows, University of Magdeburg, Forschungscampus Stimulate, Magdeburg, Magdeburg, Deutschland

²Department of Fluid Dynamics and Technical Flows, University of Magdeburg, Deutschland

³Department of Simulation and Graphics, University of Magdeburg, Deutschland

⁴Institute of Neuroradiology, University Hospital Magdeburg, Deutschland

Purpose: Blood flow simulations are increasingly used to assess the rupture risk of intracranial aneurysms (IAs). However, due to differ-

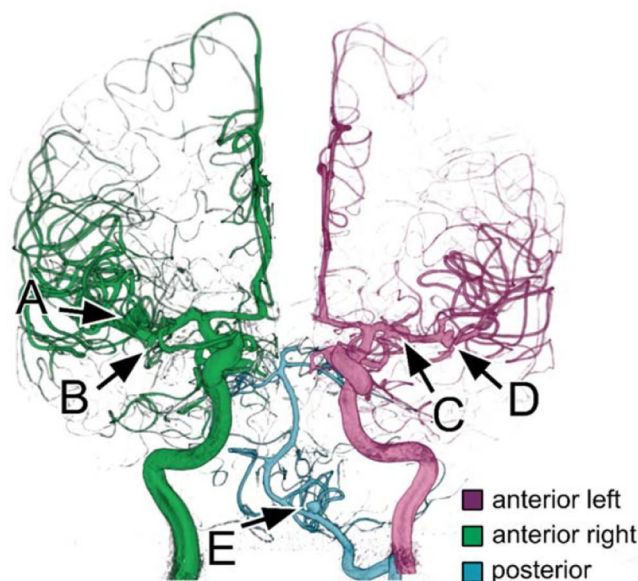


Fig. 1 MATCH case with 5 IAs

ences in segmentation and simulation techniques and also model simplifications, the acceptance among physicians is still limited.

Methods: To evaluate variations in 3D vessel reconstruction and flow simulations, an international competition was held. Two tasks were requested: Phase I) Participants should segment surface models from the same clinical data set containing five IAs; phase II) Then, flow simulations should be performed with the aim of identifying the ruptured aneurysm.

Results: 26 international research groups participated in phase I and 17 of these in phase II. Relevant differences of up to 50% were observed with respect to the 3D segmentations. This concerns vessel diameter, aneurysm size, inflow areas and number of outlet branches. As a result, only 4 groups (24%) correctly identified the ruptured aneurysm. All these groups were very experienced and used up to 16 morphological and hemodynamic parameters for assessment.

Conclusion: The challenge reveals that the combination of experienced technicians, precise segmentation, and advanced rupture risk assessment models lead to a correct prediction of the ruptured IA. If confirmed by further studies, this may become clinically relevant. However, the effect of uncertainties in the vessel reconstruction on the evaluation of hemodynamic parameters is underrated.

Head and Neck

117

The Dilemma of Antiplatelet-Therapy in Stent-Grafting of Carotid-Blowout-Patients

Kornelia Kreiser^{*1}, Isabell Gröber¹, Claus Zimmer², Katharina Storck³

¹Abteilung für Diagnostische und Interventionelle Neuroradiologie, Klinikum Rechts der Isar, München, Deutschland

²Klinikum Rechts der Isar der TUM, Technische Universität München, Abteilung für Diagnostische und Interventionelle Neuroradiologie, München, Deutschland

³Klinik und Poliklinik für Hals-, Nasen- und Ohrenheilkunde, Klinikum Rechts der Isar, München, Deutschland

Purpose: Patients with head and neck cancer are at risk of developing a carotid blowout syndrome (CBS) not only due to tumor infiltration, but also due to fistulas and therapy-related necrosis occurring as late as years after surgery or the last radiation therapy.

Reporting our experiences with preventive and acute treatment of CBS with stentgrafts and discussing different ways of running antiplatelet therapy (APT).

Methods: We reviewed all patients between 2010–2016 who underwent stentgraft-placement and analyzed the outcome, the complications and the antiplatelet regime.

Results: 17 patients were treated in 24 sessions due to threatened ($n=7$), imminent ($n=5$) or acute bleeding ($n=12$). The median survival was higher for patients suffering from radiogenic fistulas or soft tissue infections than it was for those with tumor bulk. The antiplatelet regime covered the entire range from administering aspirin only, started during the procedure, to loading doses of aspirin and clopidogrel, perioperative heparin and aspirin/clopidogrel for 12 months followed by a lifelong aspirin subscription. Rare complications were not associated with the pre- or periprocedural, but with the postprocedural antiplatelet regime.

Conclusion: Even in patients with head and neck cancer a carotid blow-out does include a heterogeneous group of clinical constellations. The pre- and periprocedural antiplatelet regime has to be adapted to every single case. Most complications occur post-procedural: rare thrombotic events are closely linked to not taking a medication, therefore the drug compliance should be taken in greater account. Frequent rebleedings may be reduced by an earlier reduction of dual- to mono-antiplatelet therapy.

165

Associations between ADC histogram Analysis and complex PET Parameters in head and neck cancer.

Hans-Jonas Meyer^{*1}, Alexey Surov², Osama Sabri³, Sandra Purz⁴

¹Klinik für Diagnostische und Interventionelle Radiologie, Leipzig, Deutschland

²Klinik für Diagn. und Interv. Radiologie, Klinik für Diagn. und Interv. Radiologie, Diagnostische und Interventionen Radiologie, Leipzig, Deutschland

³Klinik und Poliklinik für Nuklearmedizin, Department of Nuclear Medicine, Leipzig, Deutschland

⁴Universitätsklinikum Leipzig AöR, Klinik und Poliklinik für Nuklearmedizin, Klinik und Poliklinik für Nuklearmedizin, Leipzig, Deutschland

Purpose: Histogram analysis is an emergent imaging technique to further analyze radiological images. The exact associations between functional imaging modalities, namely Diffusion-weighted imaging, quantified by apparent diffusion coefficients, and FDG-PET images, quantified by SUV. The aim of this study was to use histogram analysis parameters derived from ADC maps and to correlate them with several FDG-PET derived parameters in head and neck squamous cell carcinoma.

Methods: 34 patients (26% female) with a mean age of 56.7 ± 10.2 years were prospectively included in the present study with histopathologically primary head and neck squamous cell cancer. ADC histogram parameters were calculated by an inhouse made matlab software using a whole lesion measurement. PET parameters were estimated with routinely used approach. Spearman's correlation analysis was used for statistically analysis.

Results: The correlation analysis in the whole tumor group revealed a statistically significant correlation between entropy and MTV as well as TLG ($p=0.67$, $P<0.0001$ and $p=0.61$, $P=0.0002$ respectively). In well differentiated tumors alone, these correlations were even stronger with the correlation coefficient between entropy and MTV ($p=0.79$, $P=0.002$) and TLG ($p=0.66$, $P=0.01$). For poor differentiated tumors the correlations were weaker, namely between entropy and MTV ($p=0.55$, $P=0.01$) and TLG ($p=0.56$, $P=0.01$).

Conclusion: This study identified that entropy derived from ADC maps is strongly associated with MTV and TLG in head neck cancer. This correlation was even stronger in well differentiated tumors.

201

ADC-histogram Analysis in head and neck squamous cell carcinoma. Associations with different histopathological Features including Expression of EGFR, VEGF, Hif-1alpha, Her-2 and p53.

Hans-Jonas Meyer^{*1}, Gordian Hamerla², Anne Kathrin Höhn³, Alexey Surov⁴

¹Klinik für Diagnostische und Interventionelle Radiologie, Leipzig, Deutschland

²Universitätsklinikum Leipzig, Abteilung für Neuroradiologie

³Institut für Pathologie Ukl, Deutschland

⁴Klinik für Diagn. und Interv. Radiologie, Klinik für Diagn. und Interv. Radiologie, Diagnostische und Interventionen Radiologie, Leipzig, Deutschland

Purpose: Apparent diffusion coefficient (ADC) values derived from Diffusion-weighted images are able to reflect microstructure in tumors, such as cellularity, extracellular matrix or proliferation potential. This present study sought to correlate prognostic relevant histopathologic parameters with ADC values derived from a whole lesion measurement in head and neck cancers.

Methods: Thirty-four patients with histological proven primary HNSCC were prospectively acquired. Histogram analysis was derived from ADC maps. In all cases, expression of Hif1-alpha, VEGF, EGFR, p53, p16, Her 2 were analyzed.

Results: In the overall patient sample ADCmax correlated with p53 expression ($p=-0.446$, $P=0.009$) and ADCmode correlated with Her2-expression ($p=-0.354$, $P=0.047$). In the p16 positive group there were several correlations. P25, P90 and entropy correlated with Hif1-alpha ($p=-0.423$, $P=0.05$, $p=-0.494$, $P=0.019$, $p=0.479$, $P=0.024$, respectively). Kurtosis correlated with P53 expression ($p=-0.466$, $P=0.029$).

For p16 negative carcinomas the following associations could be identified. Mode correlated with VEGF-expression inversely ($p=-0.657$, $P=0.039$). ADCmax, P75, P90, and Std correlated with p53-expression ($p=-0.827$, $P=0.002$, $p=-0.736$, $P=0.01$, $p=-0.836$, $P=0.001$ and $p=-0.70$, $P=0.016$, respectively). There were no statistically differences regarding ADC histogram parameters between p16 positive and p16 negative carcinomas.

Conclusion: Correlations between prognostic relevant histopathologic parameters and ADC histogram values could be identified in HNSCC, which differed significantly according to p16 status.

246

Visualization of traumatic neuropathies of the trigeminal nerve

Egon Burian^{*1}, Dominik Weidlich², Claus Zimmer³, Monika Probst⁴

¹Abteilung für Diagnostische und Interventionelle Neuroradiologie, Klinikum Rechts der Isar, München, Deutschland

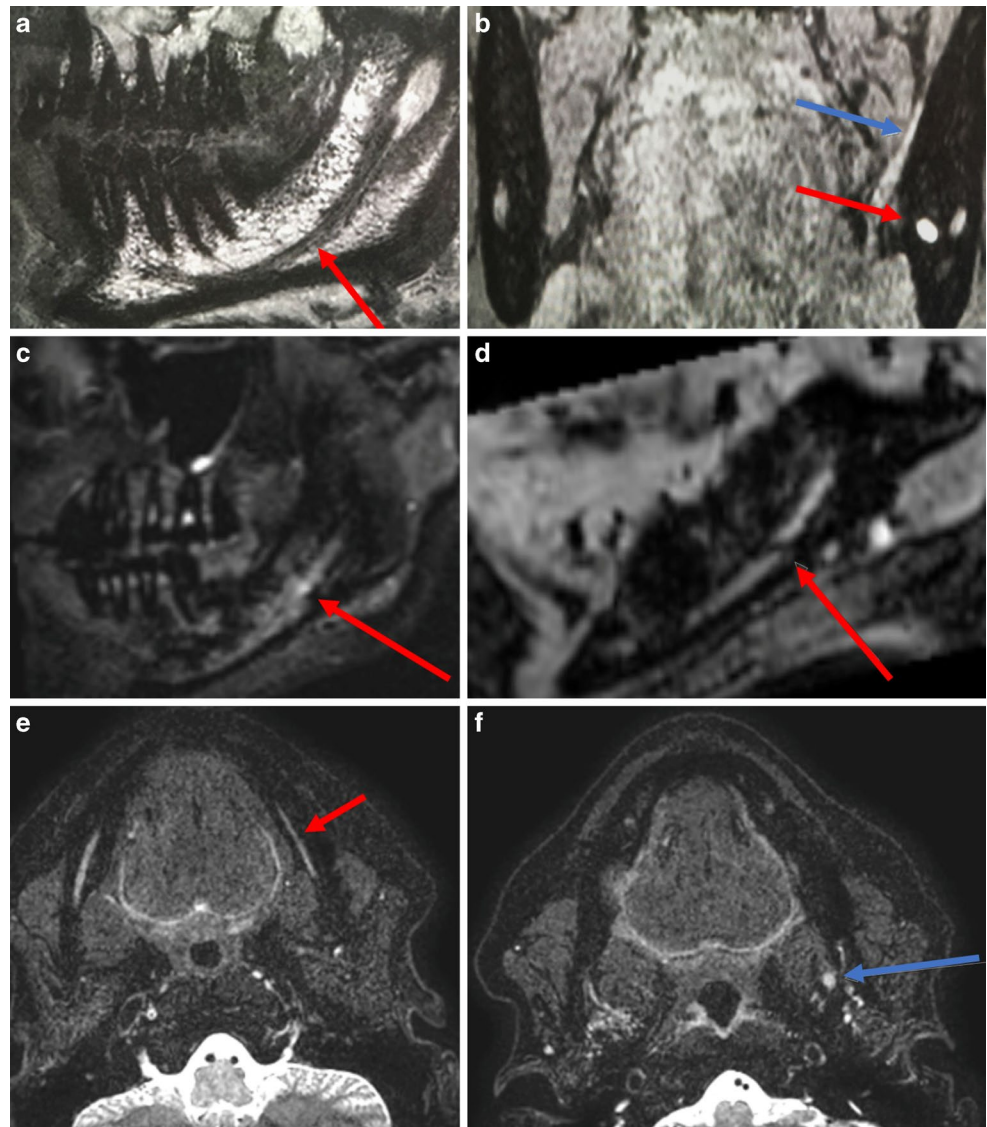
²Institut für Diagnostische und Interventionelle Radiologie, Klinikum Rechts der Isar, Technische Universität München

³Klinikum Rechts der Isar der Tum, Technische Universität München, Abteilung für Diagnostische und Interventionelle Neuroradiologie, München, Deutschland

⁴Abteilung für Diagnostische und Interventionelle Neuroradiologie, Klinikum Rechts der Isar, Technische Universität München, München, D

Purpose: Clinical neurosensory testing currently is the reference standard for diagnosis of traumatic peripheral trigeminal neuropathies.

Fig. 1 **a** IAN (red arrow), **b** IAN (red arrow), LN (blue arrow), **c** Neurapraxia IAN, **d** Neurotmesis IAN, **e** Wallerian degeneration left IAN, **f** Traumatic neuroma LN



Despite the high rate of false-positive and false-negative results leading to low reliability no other diagnostic modality evolved constituting to accuracy of diagnosis finding. MRI using dedicated imaging sequences showed promising results in early clinical testing. In this study we investigate on the direct visualization of traumatic neuropathies of the inferior alveolar nerve (IAN) and lingual nerve (LN) with MRI and try to differentiate between neurapraxia (nerve compression or traction) and neurotmesis (transection of axon and myelin sheath).

Methods: 4 healthy volunteers and 6 patients suffering from a traumatic injury during operative wisdom tooth removal were examined on a 3T Ingenia scanner (Philips). The patients clinically showed trigeminal sensory deficiencies, ranging from hypaesthesia to anaesthesia. The conducted sequence protocol consisted of a 3D SPIR, 3D WATS, 3D WATS/DESS and a “black bone”-sequence.

Results: In this study we show the feasibility of a direct visualization of proximal and peripheral traumatic neuropathies of the IAN and the proximal LN. The sequences allowed for differentiation between neurapraxia and neurotmesis including the subsequent Wallerian degeneration.

Conclusion: In cases of clinical evidence for traumatic trigeminal neuropathies MRI allows for diagnosis confirmation and accurate defect determination and localization.

334

Radiation dose and image quality in intraoperative CT (iCT) angiography of the brain with stereotactic head frames

Robert Forbrig^{*1}, Moritz Herzberg¹, Maximilian Patzig², Robert Stahl³, Lucas Geyer⁴, Jun Thorsteinsdottir⁵, Christian Schichor⁶, Friedrich-Wilhelm Kreth⁷, Thomas Liebig⁸, Franziska Dorn⁹, Christoph Trumm¹⁰

¹University Hospital, Institute of Neuroradiology, Munich, Deutschland

²Klinikum der Universität München, Institut für Neuroradiologie, München, Deutschland

³University Hospital, Department of Radiology

⁴Center of Radiology and Neuroradiology, Ingolstadt, Deutschland

⁵University Hospital, Department of Neurosurgery, Deutschland

⁶University Hospital, Department of Neurosurgery, Munich, Deutschland

⁷Neurochirurgische Klinik, Klinikum der Ludwig-Maximilians-Universität München, München, Deutschland

⁸Ludwig-Maximilians-Universität München, University Hospital, Institute of Neuroradiology, München, Deutschland

⁹Klinikum der Universität München—Campus Großhadern, Institut für Klinische Radiologie, Abteilung für Neuroradiologie, München, Deutschland

¹⁰Institute for Diagnostic and Interventional Radiology, Neuroradiology and Nuclear Medicine

Purpose: Cerebral intraoperative computed tomography (iCT) angiography with stereotactic frames is an integral part of navigated neurosurgery. In this context, CT scanners must offer maximal diagnostic accuracy and reasonable radiation dose. We report on our experience.

Methods: Retrospective analysis of patients, who received a cerebral stereotactic iCT angiography on a 128 slice CT scanner (SOMATOM Definition AS+, Siemens Healthineers) between February 2016 and December 2017. In group A, automated tube current modulation (ATCM, CARE Dose 4D; reference value 410 mAs) and automated tube voltage selection (CARE kV, reference value 120 kV) were enabled, and only examinations with a selected voltage of 120 kV were included. In group B, fixed tube parameters were applied (300 mAs, 120 kV). Sinogram

Affirmed Iterative Reconstruction (SAFIRE; strength 3) was used in both groups. Radiation dose was calculated for normalized 16-cm scan length. Objective and subjective image quality were assessed.

Results: Two-hundred patients ($n=100$ in groups A and B, respectively) were included. In group A, median tube current was 643 mAs (group B, 300 mAs; $p<0.001$). Normalized median values of dose length product and effective dose were 1602 mGy*cm and 3.05 mSv in group A, and 743 mGy*cm and 1.41 mSv in group B, respectively ($p<0.001$). Image quality did not significantly differ between groups.

Conclusion: In cerebral stereotactic iCT angiography, ATCM results in a significantly higher radiation dose due to substantial increment of tube current at the frame level, while image quality is not increased. ATCM should therefore be disabled in these examinations.

382

Evaluation after cochlear implant surgery: correlation of clinical outcome and imaging findings using Flat-Detector CT

Annika Stock^{*1}, Alessandro Bozzato², Victoria Bozzato², Joachim Hornung³, Arnd Dörfler⁴, Tobias Struffert⁵

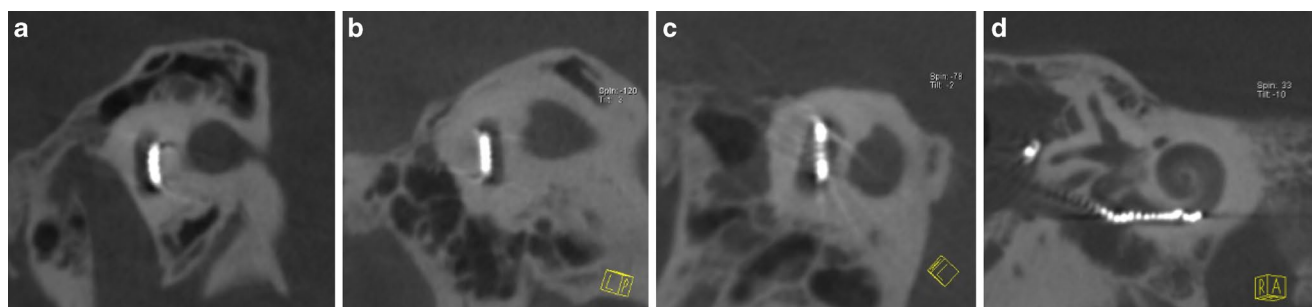
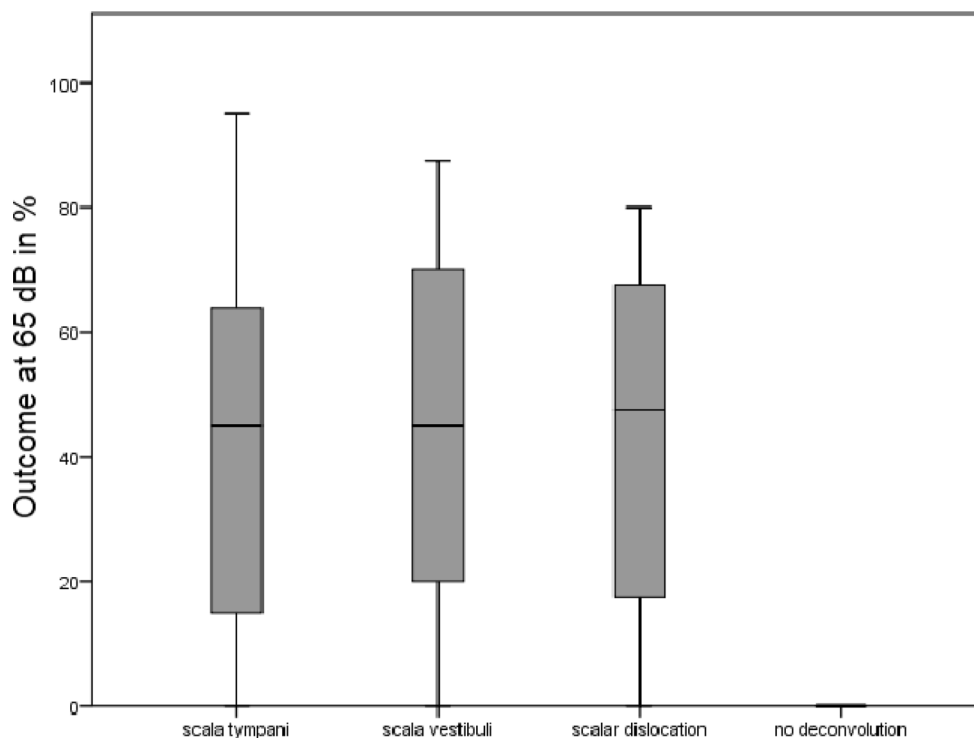


Fig. 1 Electrode position: **a)** scala tympani, **b)** scala vestibuli, **c)** scalar dislocation and **d)** no deconvolution intracochlear

Fig. 2 Outcome (Freiburg monosyllabic test at 65 dB in % in quiet) after 6 month of rehabilitation



¹Department of Neuroradiology, University Hospital Wuerzburg, Reference Center for Neuroradiology, University Hospital of Wuerzburg, Würzburg, Deutschland

²Department of Otorhinolaryngology, Head and Neck Surgery Saarland University Medical Center

³Department of Otorhinolaryngology, Head and Neck Surgery, University Hospital Erlangen

⁴Department of Neuroradiology, University Hospital Erlangen

⁵Department of Neuroradiology, University Hospital Giessen

Purpose: Assessment of cochlear implants (CIs) electrode position using Flat-Detector Computed Tomography (FDCT) to test dependence of the postoperative outcome on intracochlear electrode position.

Methods: 102 patients with 107 CIs underwent FDCT. Electrode position was rated as 1) scala tympani, 2) scala vestibuli, 3) scalar dislocation and 4) no deconvolution. Two independent neuroradiologists rated all image data sets twice and the scalar positioning was verified by a third neuroradiologist to achieve consensus. Preoperative and postoperative speech audiometry by Freiburg monosyllabic test was used to evaluate postoperative outcome after six months of speech rehabilitation.

Results: Electrodes position was assessable by FDCT in all 107 CIs. 60 electrodes were detected in the scala tympani, 21 in the scala vestibuli and 24 electrodes showed scalar dislocation. Two electrodes were not placed intracochlear. Test for dependence showed no significant difference on rehabilitation outcomes between scala tympani and scala

vestibuli insertions. Rehabilitation was also possible in patients with dislocated electrodes.

Conclusion: The superior spatial resolution of the FDCT allows accurate assessment of intracochlear electrode position. In this study cohort the electrode position had no significant impact on postoperative outcome, except of no deconvoluted CIs.

400

The curve matters: 4D Golden Angle Radial Sparse MRI in cervical paragangliomas and schwannomas

Theo Demerath^{*1}, Kristine Blackham², Bram Stieltjes², Tilman Schubert²

¹Klinik für Radiologie und Nuklearmedizin, Basel

²Klinik für Radiologie und Nuklearmedizin

Purpose: As cervical paragangliomas may lack classic imaging features in conventional MRI, dynamic contrast enhanced (DCE)-MRI has been used to improve diagnostic confidence. 4D GRASP MR imaging has so far mainly been used in the evaluation of tissue-specific enhancement dynamics e.g. in cardiac, liver and breast imaging but may also be used in differentiating head & neck paragangliomas from schwannomas, which was the aim of this study.

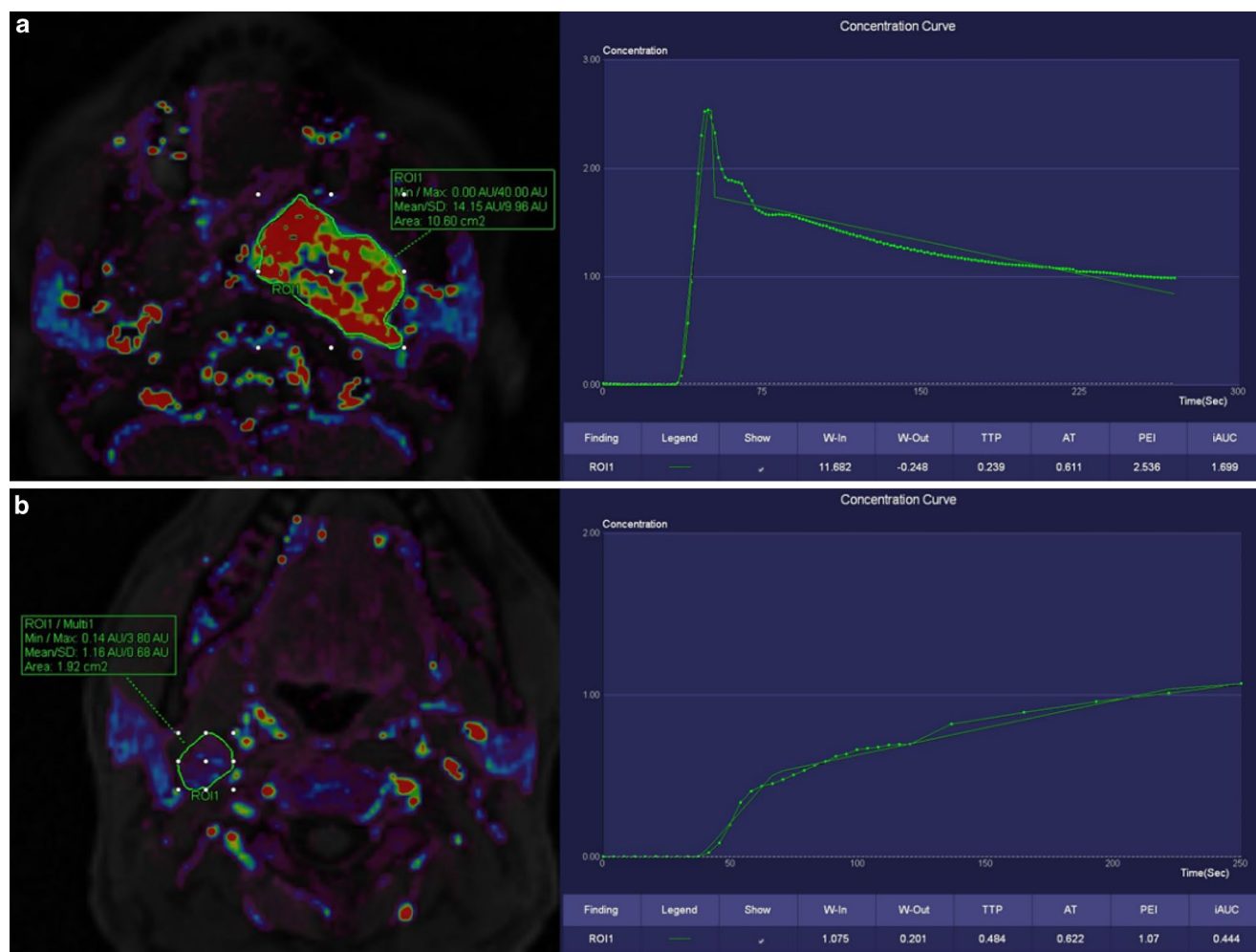


Fig. 1 Wash-In Maps, ROIs and TICs in two cases of **a)** L-carotid paraganglioma and **b)** R-vagal schwannoma

Methods: We visually and semi-quantitatively assessed time-intensity-curves (TICs) in a cohort of 11 cases fulfilling current MRI criteria of cervical paragangliomas ($n=6$) and schwannomas ($n=5$) by using current clinically available postprocessing software.

Results: Paragangliomas were consistently characterized by a Type 3 rapid inflow washout pattern (Fig. 1A), compared to a Type 1/2 inflow pattern in the schwannoma group (Fig. 1B). Mean Time to peak (T_{Peak}) enhancement [paragangliomas] was at 18.9s (SD 2.1), [schwannomas] at 181.5s (SD 28.5).

Conclusion: Visual and semi-quantitative analysis of GRASP-MRI time intensity curves was in this small retrospective series sufficient to differentiate cervical paragangliomas from schwannomas. Benefits in GRASP MRI-based tissue analysis result from technique-specific high spatial and temporal resolution and the ability to retrospectively reconstruct datasets of different temporal resolutions.

416

Diagnostic value of computed tomography of the paranasal sinuses for the evaluation of recurrent or severe Epistaxis

Noel van Horn¹, Tobias D. Faizy^{*2}, Gabriel Broocks³, Michael Schönfeld⁴, Jens Fiehler⁵, Christian Habermann⁶, Murat Karul⁷

¹Institut für Diagnostische und Interventionelle Radiologie, Hamburg, Deutschland

²Universitätskrankenhaus Hamburg-Eppendorf, Klinik und Poliklinik für Interventionell und, Diagnostische Neuroradiologie, Hamburg, Deutschland

³Klinik und Poliklinik für Neuroradiologische Diagnostik und Intervention, Universitätsklinikum Hamburg-Eppendorf, Hamburg, Deutschland

⁴Universitätsklinikum Hamburg-Eppendorf, Klinik und Poliklinik für Neuroradiologische Diagnostik und Intervention, Deutschland

⁵Diagnostikzentrum Univ.-Klinikum Hamburg-Eppendorf, Klinik und Poliklinik für Neuroradiologische Diagnostik und Intervention, Hamburg, Deutschland

⁶Klinik für Diagnostische und Interventionelle Radiologie, Deutschland

⁷Klinik für Diagnostische und Interventionelle Radiologie, Kath. Marienkrankenhaus gGmbH, Hamburg, Deutschland

Purpose: In Germany, no uniform guidelines exist for diagnostic and therapeutic procedures in patients with Epistaxis. However, CT imaging of the paranasal sinuses (CTPS) is regularly performed on patients with recurrent (RE) or severe (SE) Epistaxis to assess the cause of

bleeding. We evaluated the diagnostic efficiency of native CTPS imaging for the assessment of Epistaxis.

Methods: 340 patients (between 2008–2018) were included in our study. Two radiologists re-evaluated CTPS images in order to assess possible causes of SE/RE (e.g. trauma sequelae, tumors, anatomical abnormalities etc.). All patients also underwent subsequent gold-standard endoscopy as a second look/treatment option. Pathological findings detected in CTPS and endoscopy were compared for further analysis.

Results: In 312 out of 340 patients, endoscopy revealed diffuse bleeding of the frontal or posterior nasal septum as a source of bleeding, which was not detectable in CTPS. In 7 patients, nasal or nasopharyngeal tumours caused SE or RE. Due to intractable SE/RE, 21 patients were crossed-over to endovascular particle embolization with CT-angiography prior to treatment necessary.

Conclusion: Early performance of native CTPS prior to endoscopy does not valuable add to the diagnostic workup of SE/RE and is often unnecessary, since causes of SE/RE remain undetectable for the radiologist's eye. CT-angiography of head and neck vessels prior to treatment options such as particle embolization may be a useful diagnostic add-on.

Others

133

Identification of thalamic substructures in high b-value diffusion weighted imaging—a promising tool for DBS-implantation?

Nils Christoph Nüßle^{*1}, Benjamin Bender², Ulrike Ernemann², Uwe Klose³

¹Universitätsklinik Tübingen; Department Radiologie; Abteilung für Diagnostische und Interventionelle Neuroradiologie, Tübingen, Deutschland, Tübingen, Deutschland

²Universitätsklinikum Tübingen, Radiologische Klinik, Abteilung für Diagnostische und Interventionelle Neuroradiologie, Tübingen, Deutschland

³Universitätsklinik Tübingen, Department Radiologie, Abteilung für Diagnostische und Interventionelle Neuroradiologie, Tübingen, Deutschland

Purpose: To evaluate the capability of high b-value diffusion weighted imaging in separating and identifying intrathalamic substructures.

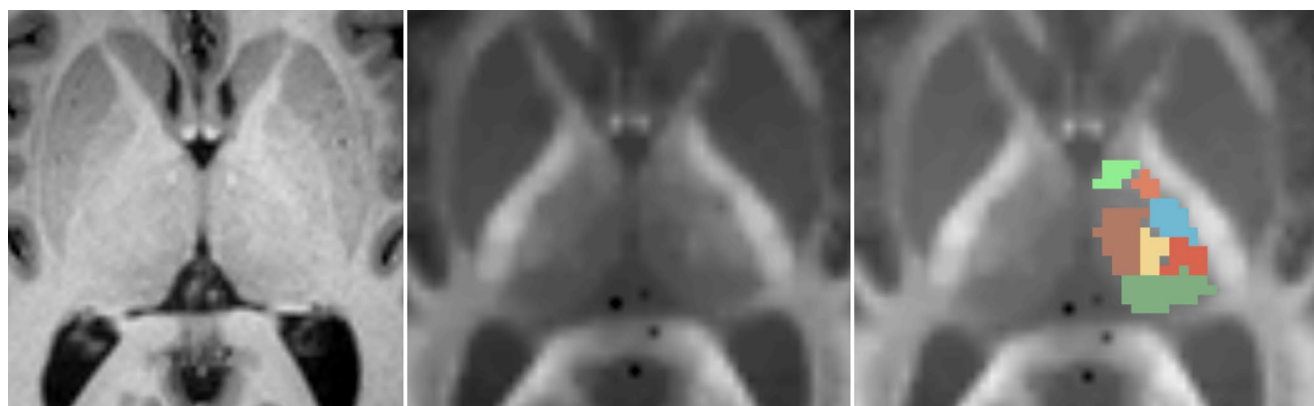


Fig. 1 MRI-scan Qf the thalamic region. T1 MPRAGE, DWI at 5000 s/mm² without and with drawn in nuclei. (Green = pulvinar, light Brown = Nucleus medialis, Brown = Nuclei centrales, Blue = Nuclei ventrointermedii, Red = Nuclei ventrocaudales, Orange = Nuclei ventroorales and light Green = Nucleus lateropolaris thalami)

Methods: 7 healthy subjects (4 male, 3 female) were recruited in a prospective 3T-High-b-value-MRI-study. All subjects were healthy without any cerebral illnesses or injuries. MPAGE 3D sequence was used to acquire anatomically correct images of the brain and to plan acquisition of diffusion-weighted images in AC/PC orientation. Spin-echo echo-planar imaging DWI sequence with b-value of 5000 s/mm² was used and diffusion was encoded in 64 directions. Five averages were measured. 7 intrathalamic substructures (Pulvinar, Nuclei centrales, Nuclei centrales, Nuclei ventrointermedii, Nuclei ventrocaudales, Nuclei ventroorales and Nucleus lateropolaris thalami), defined prior to the evaluation, were identified, drawn in by hand and compared to a histological stereotactical atlas of the brain.

Results: Nuclei, which were drawn in based on diffusion weighted images, corresponded very well with the histological data from the atlases. In all subjects, all substructures could be identified due to different signal variations. No movement artefacts were noted and no noise and vibration problems were reported by the test persons.

Conclusion: High b-value diffusion weighted imaging shows great potential in determining intrathalamic substructures. Therefore, it might lead to better planning of DBS implantation in neurological and psychiatric patients. Further investigations, trying to reduce the needed acquisition time, may provide sequences that are more easily applicable to patients.

143

Reducing systematic bias in MR-based oxygen extraction fraction derived from multi-parametric quantitative assessment of blood oxygenation level dependent signal

Christine Preibisch^{*1}, Stephan Kaczmarz², Jens Götter³, Claus Zimmer⁴

¹Klinikum Rechts der Isar, Technische Universität München, Abteilung für Diagnostische und Interventionelle Neuroradiologie, München, D

²Klinikum Rechts der Isar, Technische Universität München, Abteilung für Diagnostische und Interventionelle Neuroradiologie, München, Deutschland

³Abteilung für Neuroradiologie, Klinikum Rechts der Isar, TU München, München, Deutschland

⁴Klinikum Rechts der Isar der TUM, Technische Universität München, Abteilung für Diagnostische und Interventionelle Neuroradiologie, München, Deutschland

Purpose: Multi-parametric quantitative BOLD (mqBOLD) measurements of relative oxygen extraction fraction (rOEF) may yield relevant information about vascular oxygenation in patients (1–5). We investigated systematic elevations of calculated rOEF values due to T2 measurement and white matter (WM) structure in a multi-parametric MRI study.

Methods: On a clinical 3T MRI scanner, we performed separate measurements of T2, T2*, DSC-based rCBV and DTI. T2 values obtained by 3D vs. 2D GRASE were evaluated in phantoms, healthy volunteers and a patient with internal carotid artery stenosis (ICAS). Tissue orientation effects with respect to B0 were investigated in WM by correlating T2, T2*, R2', rCBV and mq-BOLD-derived rOEF with the DTI-derived main nerve fiber orientation.

Results: With 3D GRASE, we found significantly reduced T2 as well as rOEF values allowing detection of a focal rOEF increase in an ICAS-patient (Fig. 1). With respect to orientation effects, our results confirm a strong dependency of transverse relaxation and rCBV on the main-nerve-fiber orientation towards B0 with anisotropy driven variations up to 37.1%. Comparably weak orientation dependent errors of mq-BOLD derived rOEF (3.8%) demonstrate partially counteracting influences of R2' and rCBV effects.

Conclusion: Reduction of T2-measurement-related bias by 3D GRASE and weak orientation effects of rOEF within WM indicate

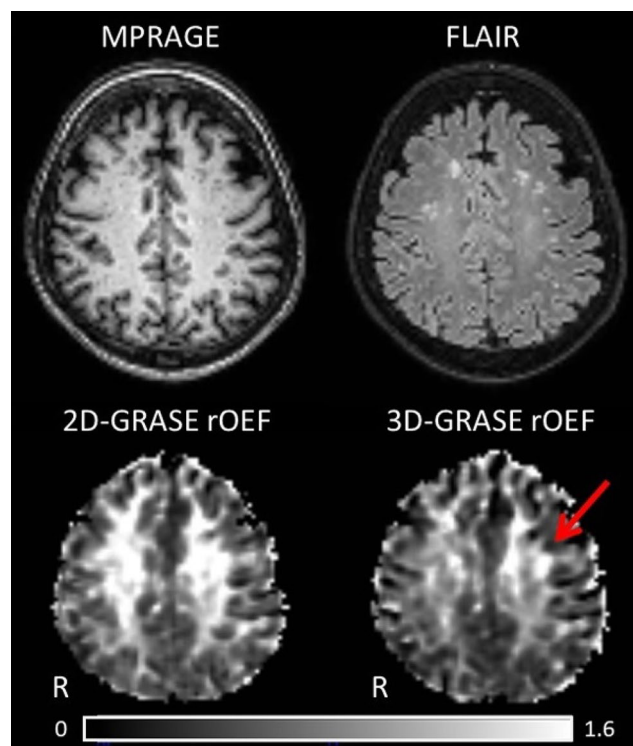


Fig. 1 Exemplary data from a patient with left-sided ICAS. Bottom row: 2D-GrASE (left) vs. 3D-GrASE-derived rOEF maps (right) are compared along with anatomic T1w MPRAGE (top left) and FLAIR (top right) Note a focal rOEF hyperintensity ipsi lateral to the stenosis (red arrow) that is only depicted by 3D-GrASE-based rOEF

good reliability of mqBOLD-derived rOEF values for future studies of brain oxygenation.

References

1. Hirsch et al. NMR Biomed. 2014;27(7):853–62.
2. Tóth et al. J Neurooncol. 2013;115(2):197–207.
3. Wiestler et al. Sci Rep. 2016;6:35142.
4. Preibisch et al. NMR Biomed. 2017;30(11).
5. Götter et al. JCBFM. In press.

169

Association of thigh muscle fat infiltration with isometric strength measurements based on chemical shift encoding-based water-fat MRI

Elisabeth Klupp^{*1}, Sarah Schlaeger², Stephanie Inhuber³, Michael Dieckmeyer⁴, Dominik Weidlich⁵, Claus Zimmer⁶, Jan Kirschke⁷, Dimitrios Karampinos⁸, Thomas Baum⁹

¹Rechts der Isar, TU München, Neuroradiologie, München, D

²Neuroradiologie, Klinikum Rechts der Isar, TU München, München, Deutschland

³Department of Sport and Health Sciences, Technische Universität München

⁴Abteilung für Diagnostische und Interventionelle Radiologie, Klinikum Rechts der Isar, Technische Universität München

⁵Institut für Diagnostische und Interventionelle Radiologie, Klinikum Rechts der Isar, Technische Universität München

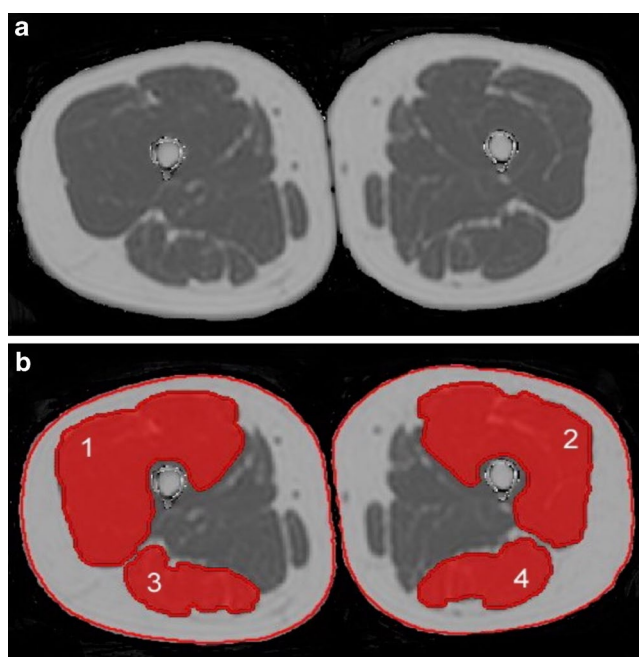


Fig. 1 Representative PDFF map **a** and superimposed manually segmented muscle compartments **b** with 1: right quadriceps muscle, 2: left quadriceps muscle, 3: right ischiocrural muscle, and 4: left ischiocrural muscle. The red lines around the entire thigh contour were used to compute entire thigh CSA

⁶Klinikum Rechts der Isar der TUM, Technische Universität München, Abteilung für Diagnostische und Interventionelle Neuroradiologie, München, Deutschland

⁷Abteilung für Diagnostische und Interventionelle Neuroradiologie, München, Deutschland

⁸Institut für Diagnostische und Interventionelle Radiologie, Klinikum Rechts der Isar, Technische Universität München, München

⁹Abteilung für Neuroradiologie, Klinikum Rechts der Isar, München, Deutschland

Purpose: Chemical shift encoding (CSE)-based water–fat MRI derived proton density fat fraction (PDFF) of the thigh muscles has been proposed as surrogate marker in subjects with neuromuscular disorders. Little is known about the relation of PDFF and corresponding muscle strength measurements, specifically whether PDFF improves the prediction of muscle strength beyond muscle cross-sectional area

(CSA). We investigated associations of thigh muscle PDFF with strength measurements in healthy volunteers.

Methods: Thigh musculature of 20 subjects (29 ± 6 yrs) was scanned on a 3T scanner. A 3D gradient echo sequence was used for CSE-based water–fat separation; PDFF maps were computed as the ratio of fat signal over the sum of fat and water signal. Quadriceps and ischiocrural muscles were segmented manually (Fig. 1). Relative CSA and PDFF were extracted. Absolute flexion and extension strength of the thigh, measured with a rotational dynamometer, were adjusted for BMI to obtain relative strength values.

Results: In contrast to CSA, muscle PDFF correlated significantly with relative muscle strength (Fig. 2). PDFF also was a statistically significant ($p < 0.05$) predictor of relative muscle strength in multi-variate regression models.

Conclusion: Muscle PDFF improves the prediction of thigh muscle strength beyond muscle CSA in healthy subjects. Thus, water–fat MRI can provide clinically important information and may potentially track early changes in muscles that are not severely atrophied or fattily infiltrated.

295

Somatosensory evoked potentials in correlation to whole brain diffusion tensor imaging in patients with multiple sclerosis.

Jan Hamann*, Barbara Ettrich¹, Karl-Titus Hoffmann², Konstantinos Sotiriou¹, Florian Then-Berg¹, Donald Lobsien²

¹Departement of Neurology, Leipzig, Deutschland

²Departement of Neuroradiology, Leipzig, Deutschland

Purpose: This study aimed to evaluate correlations of Somatosensory Evoked Potentials (SSEP) with DTI parameters in white matter tracts in patients with Multiple Sclerosis (MS).

Methods: 46 Patients with MS or clinical isolated syndromes were recruited. Bilateral SSEPs of the Nervus medianus were measured. The mean N20 latencies and Central Conducting Time (CCT) were calculated. MRI scans were made at 3T, DTI acquisition was done with single-shot EPI—technique with 80 diffusion directions. FSL (FMRIB, Oxford, Great Britain) and TBSS were used to process the images and calculate maps of Fractional Anisotropy (FA), Axial Diffusivity (AD) and Radial Diffusivity (RD). The mean N20 and BCT were separately correlated to FA, AD and RD, controlled for age and gender as variables of non-interest. Regions with high correlations ($p \leq 0.05$) were highlighted.

Results: Significant negative correlations with FA and significant positive correlations with RD were measured for mean N20 and CCT in white matter tracts, in the optic tracts, the genu and splenium of the corpus callosum, the deep frontal white matter of both hemispheres. No correlation with AD was found.

Fig. 2 Pearson correlation coefficients r for muscle PDFF and relative CSA versus muscle strength measurements. Bold denotes $p < 0.05$ (statistical significance), Italic denotes $p < 0.1$ (statistical trend)

	relative quadriceps mean CSA		quadriceps PDFF	
	right	left	right	left
relative muscle extension strength	0.314 ($p=0.178$)	0.395 ($p=0.085$)	-0.612 ($p=0.004^*$)	-0.649 ($p=0.002^*$)
	relative ischiocrural CSA		ischiocrural PDFF	
	right	left	right	left
relative muscle flexion strength	0.256 ($p=0.276$)	0.243 ($p=0.301$)	-0.676 ($p=0.001^*$)	-0.446 ($p=0.049^*$)

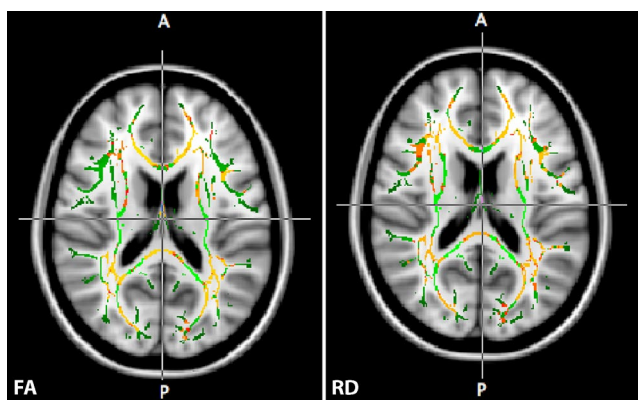


Fig. 1

Conclusion: The widespread correlations of parameters derived from SSEP with microstructural alterations indicates SSEP as a surrogate marker for microstructural damage in multiple sclerosis, that goes beyond the primary sensory functional areas.

298

Low serum cholesterol is associated with peripheral nerve damage in type 2 diabetes: A prospective in vivo study using magnetic resonance neurography

Johann Jende^{*1}, Jan Gröner², Christian Rother³, Tim Hilgenfeld⁴, Alexander Heil⁵, Fabian Preisner⁶, Sabine Heiland⁷, Mirko Pham⁸, Peter Nawroth⁹, Martin Bendszus¹⁰, Felix Tobias Kurz¹¹

¹Universität Heidelberg, Neuroradiologie, Heidelberg, Deutschland

²Universitätsklinik Heidelberg, Endokrinologie, Heidelberg, Deutschland

³Universitätsklinikum Heidelberg

⁴Universitätsklinik Heidelberg, Neuroradiologie, Heidelberg, Deutschland

⁵Universitätsklinikum Heidelberg, Neurologische Klinik, Neuroradiologie, Heidelberg, Deutschland

⁶Universitätsklinikum Heidelberg, Heidelberg, Deutschland

⁷Experimentelle Neuroradiologie, Experimentelle Neuroradiologie, Neuroradiologie, Heidelberg, Deutschland

⁸Universitätsklinikum Würzburg, Institut für Diagnostische und Interventionelle Neuroradiologie, Würzburg, Deutschland

⁹University of Heidelberg, Dept. of Internal Medicine, Heidelberg, Deutschland

¹⁰University Hospital Heidelberg, Department of Neuroradiology, Heidelberg, Deutschland

¹¹Universitätsklinik Heidelberg, Uniklinikum Heidelberg, Neuroradiologie, Heidelberg, Deutschland

Purpose: Several clinical studies have found that dyslipidemia is an important risk factor for the development of distal symmetric diabetic polyneuropathy (DPN) in type 2 diabetes (T2D). The aim of this study was to visualize and quantify the impact of serum cholesterol levels on microstructural nerve remodelling in T2D DPN *in vivo*.

Methods: We prospectively investigated 80 T2D patients suffering from DPN. Clinical, serological and electrophysiological data were acquired. 3T magnetic resonance neurography of the right leg was performed using a T2-weighted, fat-suppressed (T2wFS) turbo-spin-echo sequence. Semi-automated nerve segmentation was performed with a subsequent correlation-analysis of all acquired parameters.

Results: T2wFS-hypointense, lipid equivalent lesion load (LEL) correlated negatively with total serum cholesterol ($r = -0.37; p = 0.001$), HDL

cholesterol ($r = -0.26; p = 0.032$), LDL cholesterol ($r = -0.26; p = 0.037$), and nerve conduction velocities of the tibial ($r = -0.36; p = 0.015$) and peroneal nerve ($r = -0.49; p < 0.001$). Patients under statin treatment showed a higher LEL compared to those without statin treatment ($15.4\% \pm 0.02$ vs. $10.2\% \pm 0.01; p = 0.028$). No correlations were found between LEL and other risk factors for DPN such as patient's age, HbA1c levels or parameters of renal function.

Conclusion: In contrast to previous assumptions, our findings indicate that lowering serum cholesterol in T2D DPN causes an increase in nerve lesions and a decrease in nerve conduction velocities. These findings may be relevant with regards to emerging therapies that promote an aggressive lowering of serum cholesterol in patients with T2D.

373

Does APT-CEST contrast reflects tissue pH: A combined 1H MRI and 31P MRS study

Jan-Rüdiger Schüre^{*1}, Stella Breuer², Manoj Shrestha³, Ralf Deichmann⁴, Marlies Wagner⁵, Ulrich Pilatus⁶

¹Universitätsklinikum Frankfurt Kgu, Frankfurt, D

²Universitätsklinikum Frankfurt

³Brain Imaging Center, Goethe-Universität Frankfurt

⁴Goethe Universität Frankfurt, Universitätsklinikum Frankfurt, Brain Imaging Center, Frankfurt/Main, Deutschland

⁵Universitätsklinikum Frankfurt, Institut für Neuroradiologie, Frankfurt, D

⁶Goethe Universität, Institut für Neuroradiologie, Frankfurt, Deutschland

Purpose: The pH-dependent exchange rate between amides and water protons can be monitored with amide proton transfer-chemical exchange saturation transfer (APT-CEST) MRI thus providing an MRI contrast, which may reflect changed pH values in pathological tissue. However, CEST imaging is challenging because it requires the analysis of the Z spectrum, which depends on various different parameters (e. g. MR pulse sequence, conventional (solid state) magnetization transfer (MT) effects and MT from dissolved proteins, peptides, amino acids and metabolites).

Methods: Several methods were proposed to reduce the ambiguity of the resulting contrast. In this study we employed two different approaches (MTR_{asym} [1], Lorentzian based fitting²), to determine the APT-CEST contrast and compared the results to pH changes determined from the chemical shift of inorganic phosphate from 3D ³¹P magnetic resonance spectroscopic imaging (MRSI). 21 patients with first diagnosis of glioblastoma and 11 healthy controls were included in the study.

Results: Fig.1 illustrates parametrical maps for pH obtained from ³¹P MRSI and APT-CEST contrast based on MTR_{asym} ($\Delta\omega = 3.5$ ppm) as well as APT-CEST contrast based on the Lorentz difference (LD) method. Anatomical (T2w) data are shown in the right column. A ROI-based evaluation was performed in areas of glioblastoma, CNAWM and NAWM for both APT-CEST contrast methods and pH (Fig.2)

Conclusion: The APT-CEST contrast in glioblastoma correlates with increased tissue pH with improved performance for LD ($r = 0.72$).

Reference

1. Zhou et al. Amideprotontransfer (APT) contrast for imaging of brain tumors. In: Magnetic Resonance in Medicine. 2003.
2. Zaiss et al. Quantitative separation of CEST effect from magnetization transfer and spillover effects by Lorentzian-line-fit analysis of z-spectra. In: Journal of Magnetic Resonance. 2011.

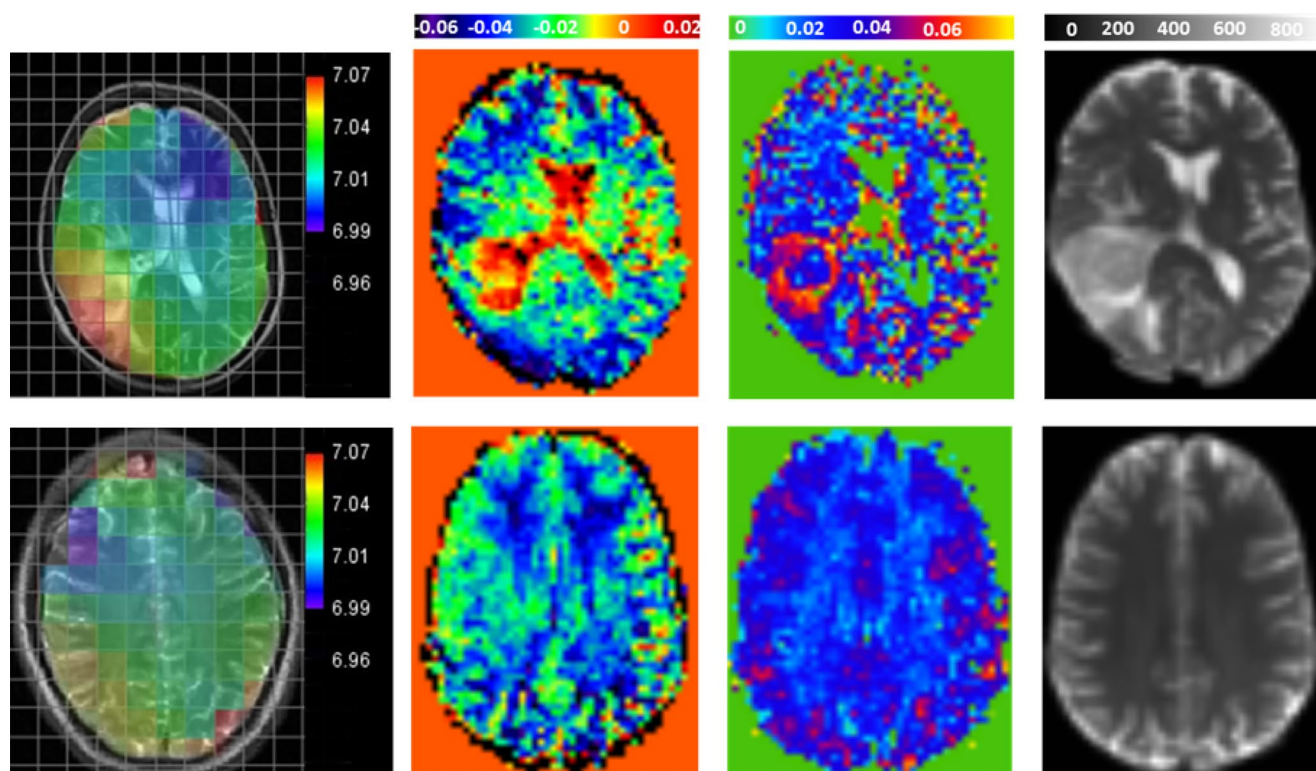
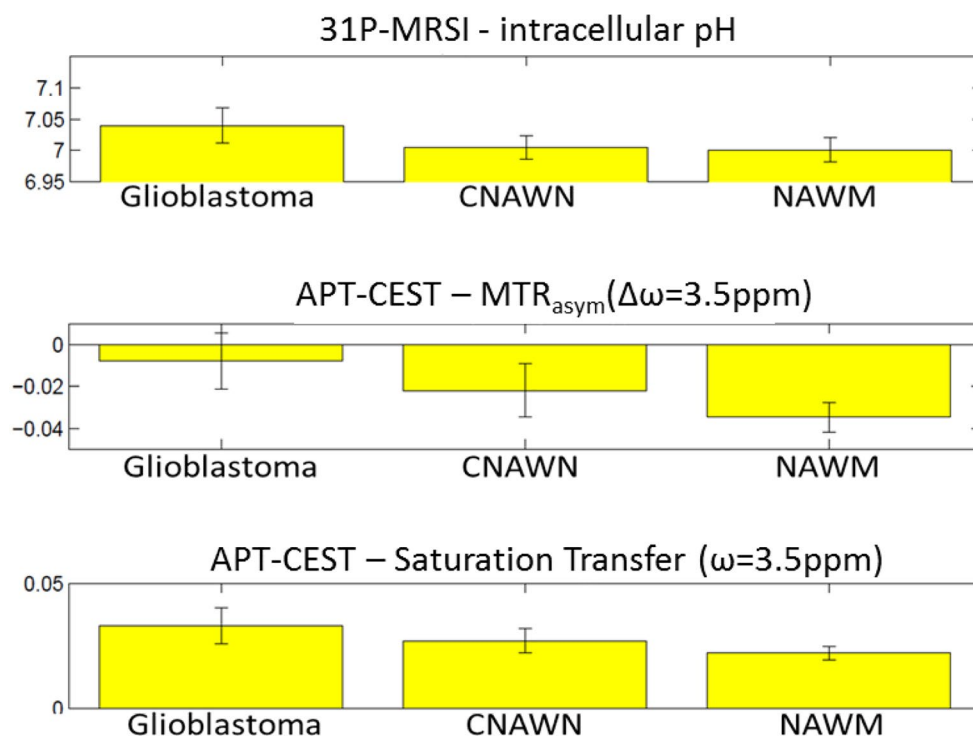


Fig. 1 From left to right – Illustration of contrasts for the intracellular pH via 31P-MRSI, MTR_{asym} ($\Delta\omega=3.5$ ppm), saturation transfer of amides ($\omega=3.5$ ppm) over Lorentzian difference (LD) and a T2 weighting. While the upper row of images shows a patient with glioblastoma, the lower row shows the reference of a healthy subject

Fig. 2 Evaluation of the ROI's (glioblastoma, CNAWM, NAWM) from data of intracellular pH, MTR_{asym} and Saturation transfer of amides over the LD method



Magnetic resonance neurography: Findings in a case with chronic autoimmune brachial radiculoneuritis

Katharina Knaub^{*1}, Tobias Boppel¹, Peter Schramm¹

¹UKSH Campus Lübeck Institut Neuroradiologie, Lübeck, Deutschland

Purpose: The purpose of our case report is to draw attention to chronic changes in radiculoneuritis depicted by magnetic resonance neurography (MRN).

Methods: A 64-year-old man presented the first time in 1998 with a shoulder and upper arm weakness on the left side. A slight pleocytosis and autochthonous IgM-synthesis was found. Electroneurography showed hints for asymmetric polyradiculitis. He was treated with high-dose cortisone and cephalosporins. In 2014 an additional weakness in the left hand occurred. The additional proof of GM1-IgM-antibodies and a blood-brain-barrier disruption led to the diagnosis of autoimmune radiculoneuritis. Eight courses of immunoglobulin therapy followed and in 2018 a treatment with mycophenolate mofetil was established. MRN was performed with 3T Philips Ingenia in a chronic stage of the disease in 2017.

Results: MRN showed impressive signal alterations in the left brachial plexus with increased signal intensity and thickening in the nerve roots C4 till C7 (Fig 1 and 2) and a decreasing diameter and signal intensity in the following peripheral arm nerves. Muscle atrophy and edema in denervated muscles were seen.

Conclusion: To our knowledge there is limited data on MRN findings in autoimmune radiculoneuritis. These findings in chronic stage are suggestive that MRN may be a non-invasive examination applicable to monitor the disease.

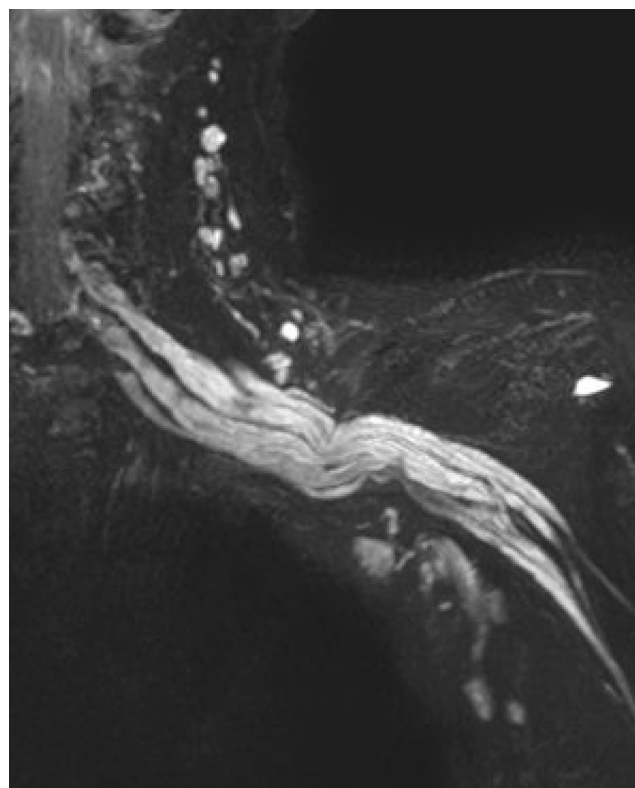


Fig. 1 Coronal MIP of a 3D T2 TSE SPAIR

Multimodal ultra high field magnetic resonance neurography as a novel toolbox for characterization of experimental diabetic neuropathy

Daniel Schwarz^{*1}, Asa S. Hidmark², Manuel Fischer³, Volker Sturm¹, David Milford³, Ingrid Hausser⁴, Michael O. Breckwoldt¹, Nitin Agarwal⁵, Rohini Kuner⁵, Martin Bendszus¹, Peter P. Nawroth⁶, Sabine Heiland¹, Thomas H. Fleming⁶

¹Department of Neuroradiology, Heidelberg University Hospital, Heidelberg, Deutschland

²Department of Medicine I and Clinical Chemistry, Heidelberg University Hospital, Heidelberg, Deutschland

³Department of Neuroradiology, Heidelberg University Hospital, Heidelberg

⁴Institute of Pathology Iph, Heidelberg University Hospital, Heidelberg, Deutschland

⁵Pharmacology Institute, Medical Faculty Heidelberg, Heidelberg University, Heidelberg, Deutschland

⁶Department of Medicine I and Clinical Chemistry, Heidelberg University Hospital, German Center for Diabetes Research (Dzd), Helmholtz-Zentrum, Neuherberg, Heidelberg, Deutschland

Purpose: *In vivo* evaluation of peripheral nerve structure and function in rodent disease models remains a major challenge with current techniques and often provides only restricted information about disease evolution. We implemented a novel multimodal ultra high field magnetic resonance neurography (MRN) approach as an innovative tool for non-invasive nerve assessment and disease monitoring.

Methods: Our dedicated high resolution MRN protocol was performed on a 9.4 T experimental MR-scanner comprising a set of 1) T2-weighted RARE, 2) DTI and 3) MSME sequences. This approach was applied to one of the most widely used animal models in the study

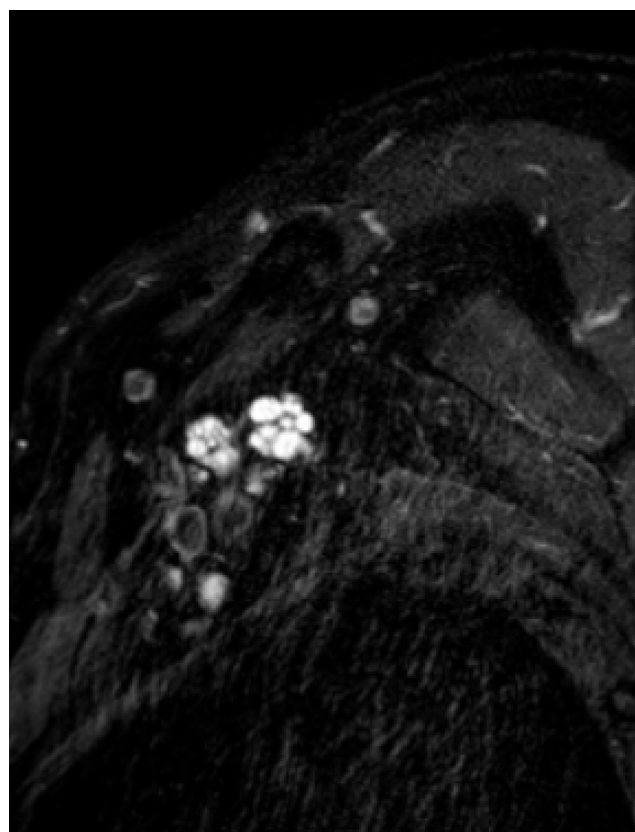


Fig. 2. Parasagittal fatsuppressed T2

of diabetic polyneuropathy (DPN), the streptozotocin (STZ)-induced mouse model of type 1 diabetes ($n=13$), and quantitative results were compared to an age- and sex-matched control group ($n=10$).

Results: In the absence of gross morphologic alterations like axonal fibre loss, a distinct MR-signature was observed in the nerves of STZ-mice which was marked by a significant drop in T2-time and normalized T2w-signal while other parameters such as proton density, fractional anisotropy or apparent diffusion coefficient remained unchanged. These findings differ greatly from the MR-signature previously reported in patients with DPN.

Conclusion: The capacity of our MRN approach to non-invasively assess peripheral nerve structure and function within a given mouse model provides a powerful tool for direct translational comparison to human disease hallmarks not only in diabetes but also in other peripheral neuropathic conditions and may help to highlight exquisite pathophysiological differences and parallels.

447

Using MR-neurography for differential diagnosis of ALS and MMN

Moritz Kronlage^{*1}, Karl Christian Knop², Daniel Schwarz³, Tim Godel⁴, Sabine Heiland⁵, Martin Bendszus⁶, Philipp Bäumer⁷

¹Universitätsklinikum Heidelberg, Abteilung für Neuroradiologie, Heidelberg, D

²Neurologie Neuer Wall, Hamburg

³Department of Neuroradiology, Heidelberg University Hospital, Heidelberg, Deutschland

⁴Uniklinik Heidelberg, Neuroradiologie, Heidelberg, Deutschland

⁵Experimentelle Neuroradiologie, Experimentelle Neuroradiologie, Neuroradiologie, Heidelberg, Deutschland

⁶University Hospital Heidelberg, Department of Neuroradiology, Heidelberg, Deutschland

⁷Universitätsklinikum Heidelberg, Neuroradiologie, und Deutsches Krebsforschungszentrum, Heidelberg, Deutschland

Purpose: Differential diagnosis of amyotrophic lateral sclerosis (ALS) and multifocal motor neuropathy (MMN) is currently based on the clinical presentation in combination with electrophysiological diagnostics. This can be very challenging, since the two diseases clinically often resemble each other. However, they require different therapeutic strategies.

The purpose of this study was to describe the MR-neurographic phenotypes of MMN and ALS and to evaluate high-resolution MR-neurography as a tool for differential diagnosis.

Methods: 22 Patients with ALS and 8 Patients with MMN were examined at a Siemens 3T Skyra using high-resolution MR-neurography Sequences (T2-weighted, fat-saturated). 15 subjects of a healthy collective were matched as controls. Two blinded readers qualitatively rated fascicular hyperintensities and fascicular enlargements as well as signs of muscular denervation. They furthermore classified every subject as having ALS, MMN or being healthy based on imaging findings alone.

Results: Patients with ALS showed prominent muscular signs of denervation and some fascicular hyperintensities but no fascicular enlargements. Patients with MMN showed marked fascicular enlargements and hyperintensities. Correctly classified were 19 of 22 patients with ALS, 7 of 8 patients with MMN and all of the 15 healthy subjects.

Conclusion: MR-neurography may assist in the differential diagnostic workup of patients with ALS and MMN.

473

Endovascular Rescue Treatment for delayed cerebral ischemia following subarachnoid hemorrhage—A single Center analysis

Hani Ridwan^{*1}, Miriam Weiss², Marguerite Müller¹, Alexander Riabikin¹, Martin Wiesmann³, Gerrit A. Schubert²

¹Klinik für Diagnostische und Interventionelle Neuroradiologie, Aachen, Deutschland

²Klinik für Neurochirurgie, Aachen, Deutschland

³Klinik für Diagnostische und Interventionelle Neuroradiologie, Aachen, Deutschland

Purpose: The implementation of rescue efforts for delayed cerebral ischemia (DCI) after aneurysmal SAH remains largely empirical for a lack of supporting evidence, while the associated risk profile is unclear. The present study evaluates the safety and efficacy of endovascular rescue treatment (ERT: continuous intraarterial nimodipine, IAN; transcatheter balloon angioplasty, TBA).

Methods: In this analysis, we assessed periprocedural complications in context of ERT. We evaluated neurological status, multimodal monitoring (ptiO₂; lactate/pyruvate ratio; transcranial doppler) and cranial imaging (CTP, DSA). All parameters were included into multivariate analysis to determine predictors for impending DCI.

Results: 29 consecutive patients were included with 48 ERT (IAN $n=29$; TBA $n=13$; TBA+IAN $n=6$). No serious complications were recorded. Improvement was observed in the majority of patients (neurostatus 63.6%; ptiO₂ 62.5%, $p<0.001$; lactate/pyruvate ratio 47.3%, $p<0.05$; transcranial doppler 53.9%, $p<0.05$; CTP 79.1%; DSA 92.9%). Within the total cohort, DCI related cerebral infarction was noted in $n=7$ cases (14.6%) with favorable outcome in $n=10$ (41.7%) patients.

Conclusion: In highly-selected patients where conservative treatment options are exhausted, ERT is a relatively safe and effective treatment option. Continuous intraarterial treatment in particular may be suitable to surpass DCI resulting in a low rate of DCI related infarction and comparably high percentage of good outcome.

Autorenverzeichnis

A

Abdulkadir, Ahmed 449
 Abdullayev, Nuran 230, 231, 233, 319
 Abinahed, Julien 364
 Abramyuk, Andrij 467
 A. Husain, Bashir 182
 Adeli, Alborz 252
 Afat, Saif 307
 Agarwal, Nitin 414
 Aguilar Perez, Marta 240, 349, 371, 375, 421
 Al-Ansari, Abdulla 364
 Albarqouni, Shadi 208
 Alberts, Esther 205
 Alegiani, Anna Christina 395
 Alexandrou, Maria 286, 316, 336, 403, 466
 Alfter, Marcel 371
 AlMatter, Muhammad 240, 349, 375, 421
 Alonso, Angelika 339, 390, 448
 Alt, Jan Patrick 308
 Altenbernd, Jens 270, 272, 265, 278
 Al-Zghloul, Mansour 390, 425, 448
 Amira, Abbes 364
 Andresen, Julian Ramin 121
 Andresen, Reimer 121, 273
 Anitha, D. 188
 Anthofer, Judith 381
 Arnold, Sebastian 182
 Austein, Friederike 220, 229, 306, 463
 Avram, Mihai 156

B

Bach, Jan Philipp 238
 Baeßler, Bettina 437
 Bähr, Oliver 384
 Baie, Lara 343
 Bannasch, Sebastian 288
 Barbieri, Fabian 280
 Barlinn, Jessica 467
 Barlinn, Kristian 467
 Barnikol, Utako 231
 Baron, Ralf 263
 Bartmann, Peter 128
 Baum, Thomas 169, 170, 188, 322
 Baumann, Nicole 156
 Bäumer, Philipp 447
 Bäuml, Josef 128, 156
 Baur, Christoph 208
 Bätzner, Hansjörg 349, 375, 421
 Bechstein, Matthias 284, 318
 Beck, Christopher 297
 Beck, Jürgen 146
 Becker, Albert J. 303
 Behme, Daniel 141, 230, 233, 321, 350
 Bender, Benjamin 133, 172, 259, 260, 285, 388
 Bendszus, Martin 234, 249, 250, 261, 291, 294, 298, 299, 345, 368, 372, 387, 389, 413, 414, 465, 447
 Bensaali, Faycal 364
 Berg, Philipp 452
 Berghoff, Anna 299
 Berkefeld, Joachim 146, 363, 383
 Berlis, Ansgar 125, 142, 211, 265, 335
 Bermejo, Pablo 364
 Berndt, Maria 128, 156, 175, 181
 Bernhardt, Martina 158
 Berthele, Achim 464
 Beste, Christian 357
 Bester, Maxim 129, 130, 326
 Beuing, Oliver 288, 452
 Beume, Lena-Alexandra 136
 Bhogal, Paul 349
 Bien, Siegfried 146
 Bienias, Tommy 352
 Bier, Georg 259, 307
 Bison, Brigitte 367
 Bittrich, Paul 245
 Blackham, Kristine 114, 400
 Blankenburg, Markus 371
 Bode, Julia 299
 Bode, Markus 125
 Boecker, Henning 128
 Boeckh-Behrens, Tobias 175, 181, 406, 407, 409
 Boeker, Martin 146
 Böhme, Johannes 390, 425, 448
 Bomberg, Hagen 126
 Boogaarts, Jeroen 330
 Boppel, Tobias 213, 404
 Borggrefe, Jan 134, 162, 194, 210, 230, 231, 310, 312, 313, 314, 319, 437, 458
 Börnert, Peter 287
 Boutchakova, Maria 336, 466
 Bozzato, Alessandro 382
 Bozzato, Victoria 382
 Brandt-Wunderlich, Christoph 273
 Brassel, Friedhelm 378
 Brawanski, Alexander 381
 Breckwoldt, Michael 299, 345, 414
 Breeman, Linda 156
 Brehm, Alex 232, 251, 269
 Brehmer, Stefanie 340
 Brekenfeld, Caspar 129, 158, 323, 326, 424
 Brendle, Cornelia 259
 Breuer, Lorenz 139
 Breuer, Stella 373
 Brinker, Gerrit 314
 Brockmann, Marc A. 146, 307
 Brokinkel, Benjamin 252

Broocks, Gabriel 129, 130, 150, 158, 277, 323, 326, 338, 346, 374, 416, 419, 424, 462
 Buchfelder, Michael 146
 Buhk, Jan-Hendrik 129, 284, 315, 326, 353, 358
 Burger, Michael 384
 Burgmer, Markus 343
 Burian, Egon 246
 Buschle, Lukas R 372, 413
 Bussas, Matthias 464
 Butts Pauly, Kim 209

C

Cabello, Jorge 300
 Caspers, Julian 160, 226, 362
 Cervantes, Barbara 170
 Chang, De-Hua 458
 Chien, Claudia 453
 Cho, Chang Gyu 425
 Clifford, Steve 367
 Clusmann, Hans 307
 Coenen, Volker Arnd 290
 Colla, Ruben 321
 Cooper, Graham 453
 Costalat, Vincent 114
 Coveney, Peter 364
 Crossley, Robert 459
 Cryns, Nina 327

D

Daamen, Marcel 128
 Dakua, Sarada 364
 Daubner, Dirk 359
 David, Bastian 301, 303
 Deb-Chatterji, Milani 158, 323, 424
 Degenhart, Christoph 149
 Dehghan Nayyeri, Mahboobeh 343
 Deichmann, Ralf 363, 373, 385
 Delev, Daniel 301
 Demerath, Theo 400
 Deshmane, Anagha 285
 Deuschl, Cornelius 293
 Dichtl, Wolfgang 280
 Dieckmann, Ralf 343
 Dieckmeyer, Michael 169, 170, 188
 Diem, Ricarda 345
 Ditz, Claudia 213
 Dohmen, Christian 231
 Domínguez, Irene 303
 Dörfler, Arnd 131, 139, 146, 382
 Dorn, Franziska 194, 199, 210, 310, 312, 313, 334, 341, 395, 458
 Dörner, Nils 465
 Dovi-Akue, Philippe 203
 Dührsen, Lasse 130

E

Eberle, Jasmine Salomé 301
 Echlin, Paul S. 186
 Eckel, Christina 288
 Eckert, Franziska 259
 Eckey, Thomas 213
 Egger, Christine 432
 Egger, Karl 136, 290, 449
 Eichinger, Paul 205, 215, 216, 388
 Eickhoff, Simon 362
 Eisele, Philipp 390
 Elger, Christian 301, 303
 Elmouden, Rachid 457
 Elsheikh, Samer 202
 Engelhorn, Tobias 139
 Engl, Christina 464
 Enkirch, Jonas 418
 Ernemann, Ulrike 132, 133, 172, 259, 260, 285, 388
 Ernst, Leon 303
 Ernst, Marielle Sophie 130
 Escamilla-Gonzalez, Gabriel 464
 Ettrich, Barbara 295

F

Faizy, Tobias D. 158, 323, 346, 416, 419, 424
 Faltermeier, Rupert 381
 Faron, Anton 237, 398
 Faymonville, Andrea 162, 437
 Fellner, Claudia 381
 Fiebach, Jochen B. 258
 Fiehler, Jens 119, 129, 130, 140, 150, 158, 177, 209, 245, 277, 284, 315, 318, 323, 326, 338, 346, 353, 358, 374, 395, 416, 419, 424
 Fink, Gereon R. 231
 Firsching, Raimund 146
 Fischer, Antonia Carlotta 306
 Fischer, Johanna 181
 Fischer, Manuel 414
 Fischer, Sebastian 265, 270, 272, 278
 Fleming, Thomas H. 414
 Flottmann, Fabian 158, 277, 323, 326, 338, 346, 374, 419, 424
 Forbrig, Robert 313, 334, 341
 Forner, Lisa 136
 Forstenpointner, Julia 263
 Förster, Alex 339, 340, 390, 425, 448
 Forsting, Michael 178, 179, 293, 325
 Freiherr, Jessica 237, 398
 Friedrich, Benjamin 149, 175, 181
 Frischmuth, Isabelle 419
 Frölich, Andreas 129, 130, 315, 326, 353, 358

Frysch, Robert 288
 Fuhrer, Hannah 136
 Furtmann, Johanna Kornelia 238

G

Gallagher, Anthony 459
 Gandhi, Chirayu 285
 Ganeshan, Ramanan 258
 Ganslandt, Oliver 240, 349, 371, 375
 Gascou, Gregory 114
 Gaubatz, Jennifer 301, 303
 Gauer, Tobias 318
 Gawlitza, Matthias 339
 Gellissen, Susanne 318
 Gemes, Blanka 316
 Gempt, Jens 300
 Gepfner-Tuma, Irina 259
 Gera, Roland Gerard 269, 321
 Gerber, Johannes 467
 Gerdsmeyer-Petz, Wolfgang 149
 Gerloff, Christian 424
 Geyer, Lucas 334
 Ghanouni, Pejman 209
 Giertmühlen, Janne 263
 Gilmour, Garret 238
 Giordano, Frank 340
 Gizewski, Elke 235, 280, 355, 408,
 Gliem, Michael 226
 Glodny, Bernhard 235, 408
 Göbel, Juliane 325
 Godel, Tim 447
 Goebel, Einar 284
 Goebel, Juliane 178, 179, 293
 Gold, Ben 383
 Goldbrunner, Roland 314
 Görtz, Lukas 194, 210, 310, 312, 313, 314
 Gothe, Raffaella Matteucci 408
 Göttler, Jens 143
 Grahl, Sophia 464
 Gralla, Jan 140
 Grams, Astrid E. 235, 280, 408
 Greling, Björn 378
 Grieb, Dominik 378
 Grittner, Ulrike 258
 Gröber, Isabell 117
 Groden, Christoph 146, 339, 340, 390, 425, 448
 Groen, Derek 364
 Gröner, Jan 298
 Groppa, Sergiu 464
 Große Hokamp, Nils 319
 Guttman, Charles R.G. 124

H

Haberl, Roman 149
 Habermann, Christian 416
 Hackenbroch, Carsten 164
 Hadler, Felix 329
 Hädrich, Kevin 467
 Haensch, Carl-Albrecht 226
 Hagen, Florian 335

Hahn, Artur 299, 372, 413
 Halpern, Casey H. 209
 Hamann, Jan 295
 Hamerla, Gordian 201
 Hamisch, Christina A. 314
 Hamou, Hussam Aldin 307
 Hänggi, Daniel 146, 425
 Hanning, Uta 119, 129, 130, 150, 206, 277, 326, 338, 346, 374, 424, 462
 Happe, Thomas 343
 Hartmann, Christian 362
 Hattingen, Elke 301, 303, 418
 Hauck, Theresa 196
 Häusler, Karl Georg 258
 Hausser, Ingrid 414
 Haverkamp, Christian 146
 Hedderich, Dennis 128
 Heesen, Christoph 419
 Heil, Alexander 298
 Heiland, Dieter Henrik 271
 Heiland, Sabine 261, 298, 299, 372, 413, 414, 447
 Heindel, Walter 119, 206, 252
 Helbok, Raimund 235
 Helle, Michael 264, 287
 Hellstern, Victoria 240, 349, 375, 421
 Hemmer, Bernhard 464
 Hempel, Johann-Martin 132, 259, 260
 Henderson, Jaimie M. 209
 Heneka, Michael 418
 Henkel, Silja 232, 233
 Henkes, Elina 240, 375
 Henkes, Hans 240, 349, 371, 375, 421
 Henn, Patrick 459
 Herbert, Sebastian 182
 Herold-Mende, Christel 299
 Herrmann, Eva 363, 383
 Herweh, Christian 250, 387
 Herz, Kai 285
 Herzberg, Moritz 334
 Hess, Katharina 252
 Hesse, Amelie 141, 233, 269
 Hidmark, Asa S. 414
 Hielscher, Thomas 345
 Hilgenfeld, Tim 298
 Hock, Andreas 216, 300
 Hoffmann, Angelika 261
 Hoffmann, Karl-Titus 295
 Hoffstaedter, Felix 362
 Hohenhaus, Marc 449
 Höhn, Anne Kathrin 201
 Hölter, Philip 131, 139
 Holtmanspoetter, Markus 459
 Honold, Sarah 235
 Hornung, Joachim 382
 Hoshi, Muna 464
 Hubbe, Ulrich 197
 Hubert, Gordian 149
 Huppertz, Hans-Jürgen 241, 243
 Hussl, Anna 355

I

Ille, Sebastian 187
 Inhuber, Stephanie 169, 170
 Isensee, Fabian 234

J

Jacob, Alina 322
 Jäger, Maike 330, 331
 Jamneala, Gheorghe 271
 Jander, Sebastian 226
 Janiga, Gábor 452
 Janka, Gritta 177
 Jansen, Olav 220, 229, 233, 244, 263, 264, 306, 394, 396, 397, 399
 Jende, Johann 298, 372
 Joachimski, Felix 211
 Jünke, Leonie 343
 Juratli, Tareq 354
 Jürgensen, Nora 220, 229, 306

K

Kabbasch, Christoph 194, 210, 231, 310, 312, 313, 314, 458
 Kaczmarz, Stephan 143
 Kaesmacher, Johannes 406
 Kaethner, Christian 131
 Kaiser, Daniel 359
 Kalkan, Alev 231
 Kallmünzer, Bernd 139
 Kammerer, Sarah 108
 Kampf, Thomas 413
 Karampinos, Dimitrios 169, 170
 Karimian-Jazi, Kianush 345
 Karimov, Ilham 300
 Karul, Murat 416
 Kaschner, Marius 226
 Kastrup, Andreas 286, 316, 336, 466
 Kaya, Emre 197
 Kellner, Elias 449
 Kelm, Anna 187
 Kemmling, Andre 119, 206, 252, 276, 277, 338, 346, 374, 462
 Kettenberger, Paula 399
 Keulers, Annika 428
 Khadhraoui, Eya 251
 Kickingeder, Philipp 234
 Kirschke, Jan 169, 170, 188, 215, 216, 322, 388, 464
 Kitzler, Hagen H. 391
 Hölter, Philip 131, 139
 Klapproth, Susan 396
 Klausner, Fritz 113
 Klein, Johannes C. 363
 Kleinschnitz, Christoph 178, 179
 Kling, Stefanie 164
 Klose, Uwe 132, 133, 172
 Klupp, Elisabeth 169, 170
 Knaub, Katharina 404
 Kniep, Helge 245, 277, 318
 Knop, Karl Christian 447
 Knott, Michael F. X. 139

Koehler, Caroline 391
 Koerte, Inga K. 186
 Köhrmann, Martin 178, 179
 Koller, Kai 389
 Konczalla, Jürgen 146
 Kopetsch, Christoph 273
 Kopp, Felix K. 188
 Körner, Heiko 126
 Kottlors, Jonathan 134
 Kowarschik, Markus 131
 Krafft, Axel 203
 Kramer, Martin 410
 Kraus, Bastian 210, 226, 313
 Kraus, Frank 149
 Kreiser, Kornelia 117, 175
 Kreth, Friedrich-Wilhelm 334
 Krieg, Sandro M. 187, 196
 Krischek, Boris 314
 Krismer, Florian 355
 Kröll-Seger, Judith 241
 Kronlage, Moritz 447
 Küchler, Jan 213
 Kühne, Dietmar 371
 Kuner, Rohini 414
 Kurz, Felix Tobias 298, 299, 372, 413
 Kutschke, Seraphine 405
 Kyselyova, Anna 353, 358

L

Lanfermann, Heinrich 378
 Lang, Stefan 131
 Laschke, Matthias W. 126
 Lauer, Arne 363, 385
 Laukamp, Kai Roman 162, 437
 Lawler, Sean E. 135
 Le Blanc, Markus 319, 458
 Lee, John-Ih 226
 Lehm, Manuel 175, 181, 407, 409
 Lehmborg, Kai 177
 Leinders, Johanna 327
 Leischner, Hannes 158, 245, 277, 323, 338, 346, 374, 419, 424
 Lennartz, Simon 319
 Liebig, Thomas 194, 231, 310, 312, 334, 458, 459
 Liem, Dennis 343
 Liesche, Friederike 300
 Liman, Jan 321
 Lin, Alexander P. 186
 Lindig, Tobias 172, 285
 Lindkvist, Johan 459
 Lindner, Thomas 220, 229, 244, 263, 264
 Linn, Jennifer 146, 354, 357, 359, 391, 467
 Lo, Th 140
 Löbel, Ulrike 177
 Lobsien, Donald 295
 Loebel, Sarah 294
 Loenn, Lars 459
 Löffler, Maximilian 322
 Löwenheim, Hubert 260
 Lücking, Hannes 131

Lüddecke, Robin 263
Lukas, Carsten 464
Lummel, Nina 406

M

Mader, Irina 271
Madesta, Frederic 318
Maegerlein, Christian 149, 175, 181
Mahlknecht, Philipp 355
Maier, Ilko 321
Maier-Hein, Klaus 234
Maintz, David 162, 319
Mangesius, Stephanie 355
Manogaran, Praveena 432
Margareta, Gruber 341
Maros, Máté 425, 448
Mast, Hansjörg 241, 243
Mathys, Christian 362
Mauer, Uwe-Max 164
Maurer, Christoph 125, 142, 211, 335
Maus, Volker 230, 231, 232, 233, 251, 269, 319, 350, 458
Mawrin, Christian 252
May, Rebecca 226
Mc Coy, Mark 113
McNab, Jennifer 209
Meckel, Stephan 136, 146, 202, 203
Mei, Kai 188
Meila, Dan 378
Melber, Katharina 378
Menegaux, Aurore 128, 156
Menger, Michael 126
Menemeyer, Philipp 199
Merchant, Julie P. 124
Mertens, Jessica 327
Metz, Marie 300
Meyer, Bernhard 187, 196
Meyer, Hans-Jonas 165, 201
Meyer, Lukas 286, 316, 336, 466
Michel, Patrik 140
Mildenberger, Iris 340
Milford, David 414
Minnerup, Jens 374
Möhlenbruch, Markus 249, 250, 261, 291, 368, 389, 465
Molavi Tabrizi, Caroline 257
Mönch, Sebastian 175, 181
Mönninghoff, Christoph 178, 179, 293, 325, 442
Mpotsaris, Anastasios 230, 231, 233 308, 314, 319, 350, 398, 405, 428, 458
Mühlau, Mark 205, 215, 216, 464
Mühl-Benninghaus, Ruben 126
Mulej Bratec, Satja 156
Mull, Michael 308
Müller, Angela 467
Müller, Christoph 355
Müller, Ingo 177
Müller, Marguerite 257, 473
Müller, Philipp 123

Müller-Eschner, Monika 222
Mundiyanapurath, Siby 294
Müschenich, Franziska 410
Mutke, Matthias 261
Mynarek, Martin 367

N

Nagel, Simon 249, 250, 387
Nägele, Thomas 172
Nasri, Hadi 308
Navab, Nassir 208
Navia, Pedro 140
Nawabi, Jawed 150, 158, 277, 338
Nawka, Marie Teresa 315
Nawroth, Peter 298, 414
Nazari, Navid 124, 135
Neuberger, Ulf 249, 368
Neuhaus, Victor 319
Neumaier Probst, Eva 425
Neumann, Alexander 213
Niesen, Wolf-Dirk 136, 290
Nikolaou, Konstantin 307
Nikoubashman, Omid 238, 327, 329, 350, 410, 428
Nimsky, Christopher 146
Nissen, Urs 121
Noel, Peter B. 188
Noeth, Ulrike 363
Nolte, Christian H. 395
Nöth, Ulrike 385
Nowicki, Michal O. 135
Nüßle, Nils Christoph 132, 133

O

Opfer, Roland 432
Oros-Peusquens, Ana-Maria 238
Ospel, Johanna 114
Ostwaldt, Ann-Christin 432
Othman, Ahmed 307

P

Paech, Daniel 325
Pallesen, Lars Peder 467
Palotai, Miklos 124, 135
Papa, Rosario 140
Papanagiotou, Panagiotis 286, 316, 336, 403, 466
Patz, Samuel 124, 135
Patzig, Maximilian 334, 341
Paul, Friedemann 453
Paulus, Werner 252
Pereira, Vitor 140
Perkuhn, Michael 162, 437
Peschke, Eva 244
Pfaff, Johannes 249, 250, 261, 294, 368, 387, 389, 465
Pfau, Oskar 276
Pfeilschifter, Waltraud 363, 385
Pfister, Stefan M. 367
Pfleiderer, Bettina 343
Pham, Mirko 261, 298

Pierot, Laurent 140
Pietsch, Torsten 367
Pilatus, Ulrich 373, 384
Pinto dos Santos, Daniel 319
Platen, Sabine 149
Poewe, Werner 355
Pohl, Ewelina 293
Politi, Maria 286, 316, 336, 403, 466
Pongratz, Viola 205, 215, 464
Porto, Luciana 108
Potreck, Arne 261, 294
Prakapenia, Alexandra 467
Pravdivtseva, Mariya 244
Pree, David 406
Preibisch, Christine 143, 300
Prillwitz, Conrad 301
Probst, Monika 196, 246
Prüllage, Pascal 136
Psychogios, Marios-Nikos 141, 232, 233, 251, 269, 321
Puetz, Volker 467
Purz, Sandra 165
Pütz, Volker 359
Pyka, Thomas 300

R

Radbruch, Alexander 178, 179, 293, 294, 325, 442
Radez, Angela 464
Radmer, Sebastian 121
Rajput, Furqan 346
Ratliff, Miriam 425
Rattay, Tim W. 172
Ravindren, Johannes 421
Regelsberger, Jan 130
Reich, Arno 257, 327, 329
Reimann, Gernot 457
Reimold, Matthias 285
Reinacher, Peter 290
Reisert, Marco 449
Reiter, Eva 355
Reith, Wolfgang 126
Riabikin, Alexander 233, 350, 405, 410, 473
Richardson, Robin 364
Richter, Christian 384
Ridwan, Hani 473
Riedel, Christian 233, 394, 396, 397, 399, 412
Rienmüller, Anna 322
Rietzler, Andreas 280, 408
Ringel, Florian 146, 196
Ringleb, Peter Arthur 249, 250, 294, 387, 389
Rodriguez-Raecke, Rea 257
Rohde, Stefan 457
Rölz, Roland 290
Romero, M. Molina 300
Rose, Georg 288
Rostalski, Philipp 276
Roth, Christian 286, 316, 336, 403, 466
Rother, Christian 298
Rubbert, Christian 160, 226, 362
Ruben, Colla 269
Rubensdörfer, Linda 241, 243
Rüber, Theodor 301, 303
Rudahl, David 394
Rüfenacht, Daniel 442
Runck, Frank 125, 142, 211
Rutkowski, Stefan 367
Ryang, Yu-Mi 322

S

Saalfeld, Sylvia 452
Sabri, Osama 165
Sack, Henrik 230
Sahm, Felix 299
Sandmann, Johanna 410
Santalucia, Paola 140
Schacht, Hannes 136
Schackert, Gabriele 146, 354
Scheef, Lukas 128
Scheel, Michael 453
Scheffler, Klaus 285
Scheiwe, Christian 290
Schell, Marianne 234
Schichor, Christian 334
Schieber, Simon 249
Schild, Hans Heinz 418
Schippling, Sven 432
Schittenhelm, Jens 132, 259
Schlaeger, Sarah 169, 170
Schlaier, Jürgen 381
Schlamann, Marc 313
Schlemmer, Heinz-Peter 413
Schlunz-Hendann, Martin 378
Schmidt, Manuel 131, 139
Schmidt, Nils Ole 130
Schmidt, Paul 464
Schmidt, Wolfram 273
Schneider, Alice 258
Schneider, Tanja 150, 245, 318
Schnell, Oliver 203
Schnitzler, Alfons 362
Schober, Hans-Christof 121
Schocke, Michael 355, 408
Schoen, Gerhard 150, 245, 277, 346
Schöls, Ludger 172
Schön, Felix 359
Schön, Simon 215, 255, 300
Schönenberger, Silvia 250
Schönfeld, Michael 129, 130, 326, 416
Schramm, Johannes 301
Schramm, Peter 140, 213, 276, 404, 462
Schregel, Katharina 124, 135, 321
Schubert, Gerrit A. 257, 473
Schubert, Tilman 400
Schultz, Vivian 186
Schuppert, Mark 285
Schüre, Jan-Rüdiger 373
Schwab, Stefan 139
Schwarz, Daniel 414, 447
Schwarzwald, Ralf 241, 243

- Schwenke, Hannes 276, 462
 Seifert, Christian 181
 Seiler, Alexander 363, 385
 Seitz, Johanna 156
 Seiz-Rosenhagen, Marcel 340, 425
 Seker, Fatih 249, 250, 387
 Seppi, Klaus 355
 Shah, Mukesch 146
 Shah, Nadim-Joni 238
 Shah, Yogesh P. 389
 Shakirin, Georgy 162, 437
 Shenton, Martha E. 186
 Shrestha, Manoj 373
 Sichtermann, Thorsten 237, 238, 398
 Siebert, Eberhard 194, 310, 312
 Siedentopf, Christian 235, 280
 Siekmann, Ralf 389
 Siemonsen, Susanne 150, 245, 277, 338, 346, 374, 419
 Sigl, Benjamin 362
 Sijben, Rik 237
 Singen, Andreas 126
 Singer, Oliver C. 363, 385
 Singh, Raveena 327
 Sinkus, Ralph 124, 135
 Skalej, Martin 146
 Skardelly, Marco 259
 Solecki, Gergely 299, 413
 Sollmann, Nico 186, 187, 188
 Sorg, Christian 128, 156
 Sotiriou, Konstantinos 295
 Spallek, Johanna 315, 353
 Spies, Lothar 432
 Spille, Dorothee Cäcilia 252
 Sporns, Peter 119, 206, 252, 338, 346, 374, 462
 Stahl, Robert 334
 Stahlberg, Kim 343
 Steiert, Christine 290
 Steiger, Ruth 235, 280, 408
 Steinbach, Joachim 384
 Steinbacher, Jürgen 113
 Stellmann, Jan-Patrick 419
 Stenzel, Elena 178, 179, 293, 325, 442
 Stetefeld, Henning 231
 Stieltjes, Bram 400
 Stock, Annika 367, 382
 Stock, Ann-Kathrin 357
 Stöckmann, Matthias 130
 Storck, Katharina 117
 Strotzer, Quirin 381
 Struffert, Tobias 382
 Stummer, Walter 252
 Sturm, Dominik 367
 Sturm, Volker 413, 414
 Styczen, Hanna 141
 Subburaj, Karupppasamy 188
 Südmeyer, Martin 362
 Sundermann, Benedikt 343
 Surov, Alexey 165, 201
- T**
- Tabatabai, Ghazaleh 285
 Tagwercher, Susanne 355
 Taschner, Christian 330
 Taylor, Walter M. 124
 Teichert, Nikolas 237, 362, 398
 ten Brinck, Michelle 330
 Tepe, Hans 258
 Tepper, Michael 403
 Tews, Björn 299
 Thaler, Christian 150, 209
 Then-Berg, Florian 295
 Thiele, Frank 162, 437
 Thomalla, Götz 158, 323, 395, 424
 Thorsteinsdottir, Jun 334
 Thünemann, Kirsten 397
 Tian, Qiyuan 209
 Timmer, Marco 162, 437
 Tomori, Toshiaki 112, 126, 248
 Traschütz, Andreas 418
 Tropitzsch, Anke 260
 Trumm, Christoph 334
 Tsogkas, Ioannis 232, 233, 269, 321
 Turowski, Bernd 160, 210, 226, 313, 362
 Tursunova, Irada 234
- U**
- Ulfert, Christian 291, 389
 Urbach, Horst 136, 146, 197, 202, 203, 241, 243, 271, 331, 449
- V**
- van de Ven, Kim 287
 van Horn, Noel 416
 Verius, Michael 280
 Villringer, Kersten 258
 von Deimling, Andreas 425
 Voss, Martin 222
 Voß, Samuel 452
- W**
- Wabbels, Bettina 301
 Wafa, Melanie 164
 Wagner, Marlies 222, 363, 373, 383, 384, 385
 Wahl, Hannes 359, 391
 Walchhofer, Lisa Maria 408
 Wanke, Isabel 178, 179, 293, 325, 442
 Warmuth-Metz, Monika 367
 Warnecke, Gerald 288
 Watkinson, Joe-Iven 463
 Weber, Bernd 301, 303
 Weber, Werner 140, 265, 270, 272, 278
 Weber, Wolfgang 300
 Weidlich, Dominik 169, 246
 Weiß, Daniel 226
- Weiss, Miriam 473
 Weitz, Alejandro Tomasello 140
 Wenger-Alakmeh, Katharina 384
 Wenz, Holger 339, 340, 390, 425, 448
 Wenzel, Fabian 287
 Werner, Annett 354, 357
 Werner, René 318
 Wick, Antje 234
 Wick, Wolfgang 234, 299
 Wiesmann, Martin 233, 237, 238, 257, 307, 308, 327, 329, 350, 398, 405, 410, 428, 473,
 Wiestler, Benedikt 205, 208, 215, 216, 255, 300, 388
 Wiestler, Hanni 215
 Wildemann, Brigitte 345
 Wildgruber, Moritz 206
 Winkler, Frank 299, 413
 Wintermark, Max 209
 Wissgott, Christian 273
 Witton-Davies, Thomas Lyn 149
 Wodarg, Fritz 463
 Wohlschläger, Afra 196
 Wolke, Dieter 128, 156
 Wollenweber, Frank Arne 395
 Wollny, Mathias 121
 Wrede, Karsten H. 293
 Wunderlich, Silke 149, 175, 181, 406, 407, 409
 Würtemberger, Urs 271
 Wustrau, Katharina 177
- Y**
- Yakoushev, Igor 300
 Yang, Shan 241, 243, 449
 Yilmaz, Umut 126
 Younes, Georges 364
 Young-Pearse, Tracy L. 124
- Z**
- Zaiss, Moritz 285
 Zakaria, Ayman 364
 Zamarro Parra, Joaquin 140
 Zane, Rachel 135
 Zhai, Xiaojun 364
 Zhang, Haike 205, 215
 Zhang, Ke 413
 Zhang, Rui 357
 Zickler, Philipp 211
 Ziemssen, Tjalf 391
 Ziener, Christian 372, 413
 Zimmer, Claus 117, 128, 143, 149, 156, 169, 170, 175, 181, 187, 188, 196, 205, 208, 215, 216, 246, 255, 300, 322, 388, 406, 407, 409, 464
 Zipp, Frauke 464
 Zolal, Amir 354
 Zopfs, David 162, 437
 Zülów, Stefan 179
 Zumofen, Daniel 114